ARIZONA GEOLOGICAL SOCIETY
SPRING FIELD TRIP 1988

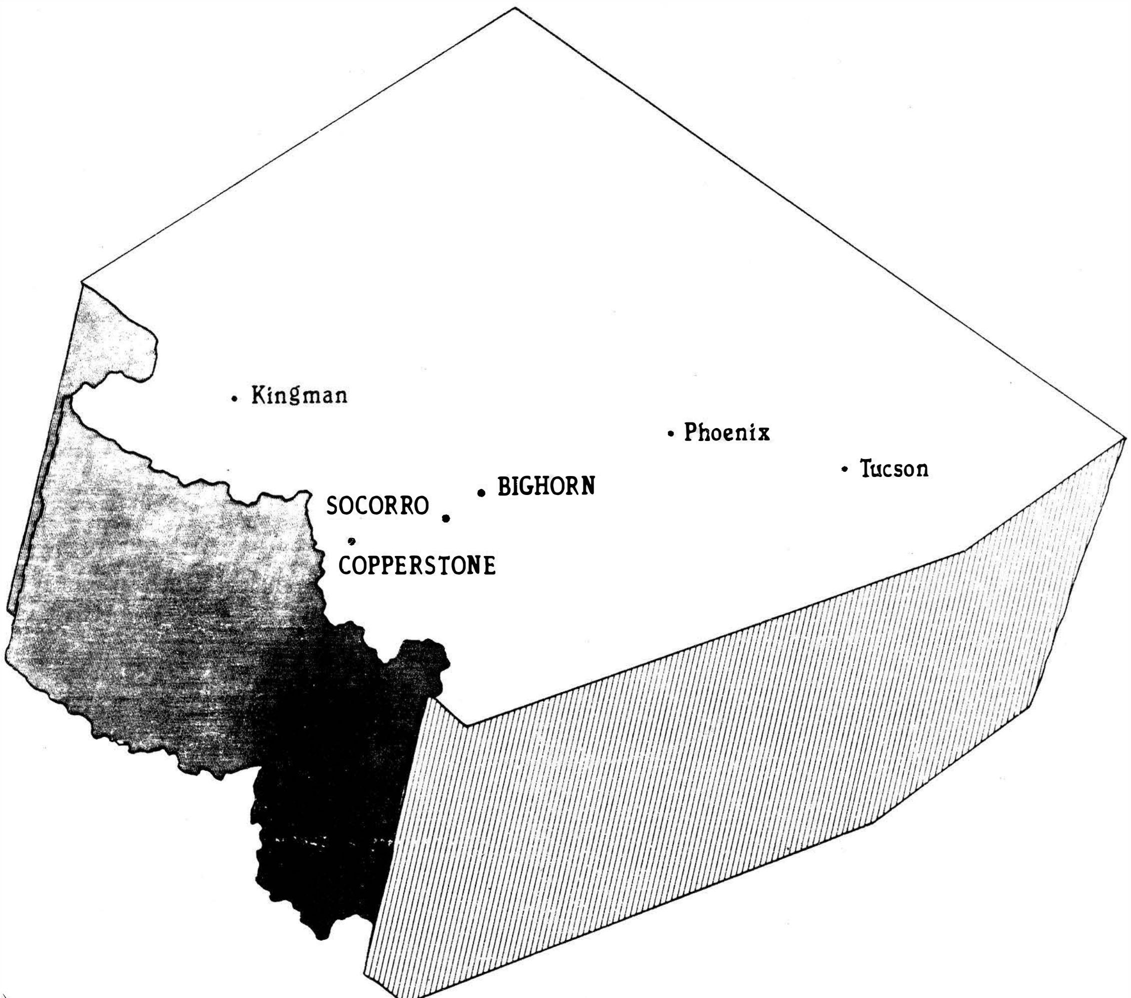

Field Trip to Bighorn Mine, Socorro Mine, and Copperstone Mine, Arizona

Led by, Hugo Dummett and Nora Colburn

ARIZONA
GEOLOGICAL
SOCIETY

ARIZONA GEOLOGICAL SOCIETY

1988 Spring Field Trip

VISIT TO THE BIGHORN, SOCORRO AND COPPERSTONE GOLD MINES, ARIZONA

April 16 and 17, 1988

Hugo Dummett and Nora Colburn, Trip Leaders.

COPPERSTONE GOLD MINE, LA PAZ COUNTY, ARIZONA.

View of the new open pit of Cyprus Copperstone Gold Corp.

The photo faces south towards the main ranges of the Dome Rock Mountains, which are on the skyline. The low foothills in the upper right hand part of the photo are called the Moon Mountains by some, but referred to as the Dome Rock Mountains at the mine. A large detachment fault that strikes NW-SE daylights in the these foothills and dips to the northeast (i.e. towards the lower left corner of the photo) under the orebody. The ore at the mine is in the Copperstone Fault which dips to the northeast at about 30°, and is exposed in the pit. The pit parallels the strike of this fault. The dark dump between the pit and the office-plant complex is ore. The access road to the property can be seen at the upper left edge of the photo.

CONTENTS

INTRODUCTION

On behalf of the Arizona Geological Society, we would like to welcome you to the 1988 Spring Field trip. As most of you know, the trip will include visits to two new gold mines at Bighorn and Copperstone, as well as a visit to the Socorro Mine, which is an important gold prospect.

The selection of Bighorn and Copperstone as two of the mine sites for this field trip has much to do with the fact that they are two of Arizona's newest gold mines - Bighorn will go into production this year, whereas Copperstone went into production late in 1987. They also represent a type of ore deposit and style of mineralization that appears, thus far, to be restricted to western Arizona, southeastern California and northwestern Sonora. In particular, the gold ± silver mineralization is hydrothermal, and is primarily associated with hypogene specularite ± hematite + silica in association with base metals (copper ±zinc ± lead).

The zones of mineralization are hosted by normal faults which may be listric in character, and which appear to be subordinate to larger, regional structures. In some instances the larger structures can be identified as detachments, whereas in some examples such a structural association is difficult to establish.

Two of the papers written for this guidebook by Dick Beane and Tony Kuehn review and discuss the geochemistry of the fluids that may be responsible for emplacing this type of gold mineralization. It is suggested, for example, that these particular fluids are moderately saline and that gold may be transported as a chloride complex. These two characteristics explain why iron is present as an oxide and why the associated minerals are base metals.

By way of contrast, it should be remembered that many of the volcanic-hosted and sediment-hosted gold deposits of Nevada and California are associated with iron sulfides and a suite of elements that commonly include antimony, arsenic and mercury. The fluids associated with these particular deposits are proposed to be dilute with respect to salinity and include gold complexed with sulfur.

These "Sonora-type" deposits then appear to be a distinctive class of gold deposit that exhibit a very strong structural control at their sites of emplacement and mineralization that has been accomplished by fluids that have a restricted and somewhat unique geochemistry.

We hope you all find the mines exciting and enjoy the opportunity to meet with other members of the AGS in a very informal setting.

ACKNOWLEDGEMENTS

As is the case with all functions of the Arizona Geological Society, a great many people have contributed their time and efforts to assist Nora Colburn and myself in our preparations for the field trip.

Firstly, we would like to thank the individuals, that represent the mines that we will be visiting, for making it possible for us to visit their properties;

- at Bighorn, Walter Cullum of Roddy Resources Inc. and Steven Harapiak of Belmoral Mines Ltd;
- at Socorro, Parry Willard of Tri-Con;
- at Copperstone, Bill Burton, Exploration Manager for Cyprus, as well as George Steffens, Mine Manager.

We would also like to thank:

George Allen of Alma American, for his comments and notes, and many discussions about the mineralization at the Bighorn Project, as well as in the Big Horn Mountains;

Stan Keith of Magmachem, for allowing us to use part of his very comprehensive data on, and description of, the mineralization at the Socorro Mine;

Graham Kelsey, Leon Hardy and Bill Burton of Cyprus for their description of the deposit, as well as Graham's willingness to be our tour guide for part of the trip;

Pat Palmer, Ron Palmer and Nora Dummett of Tucson, for arranging the catering of the BBQ at River Island State Park; and also to Pat for assistance with the typing of the drafts of the field trip logs;

Steve Reynolds and Jon Spencer of the Arizona Geological Survey, for maps and a wealth of data on the areas that we will be visiting as part of the trip;

Michael Rounds, with Cyprus' Corporate Communications Group, for making the magnificent color photograph of Copperstone available to the guidebook, and for paying for its duplication;

Jim Sammons of Tucson, for his super art work for the cover of the guidebook;

Don White of Prescott, for his comments and assistance with the description of the Vulture Mine.

ITINERARY

Field Trip Leaders: Hugo Dummett and Nora Colburn.

Saturday, April 16, 1988.

8:30 am	Depart from the Americinn Motel parking lot, Wickenburg.
9:00 am	Stop 1. Hills south of Vulture Mine.
10:30 am	Stop 2. Bighorn Project. Visit mine site.
11:45 am	Leave Bighorn Mine.
12:15 pm	Lunch stop (±45 minutes) - overview of Hassayampa Plain.
1:15 pm	Stop 3. Overview of Harquahala Mountains.
2:05 pm	Ambrosia Mill.
3:05 pm	Stop 4. Socorro Mine.
4:05 pm	Leave Socorro Mine.
5:30 pm	Arrive at Parker, Arizona. Field trip participants will stay at various hotels in Parker.
6:30 pm	BBQ for all field trippers at River Island State Park. The State Park is about 15 minutes drive north of Parker and a map is attached to the guidebook that will give you directions on how to get there.

Sunday, April 17, 1988.

8:00 am	Leave from parking lot of the Holiday Kasbah Motel and drive to Copperstone.
8:45 am	Arrive at Copperstone Mine and spend the morning visiting the mine. The tour of the mine will be led by the Cyprus Copperstone mine geologist, Graham Kelsey.
12:00 noon	Depart for home.

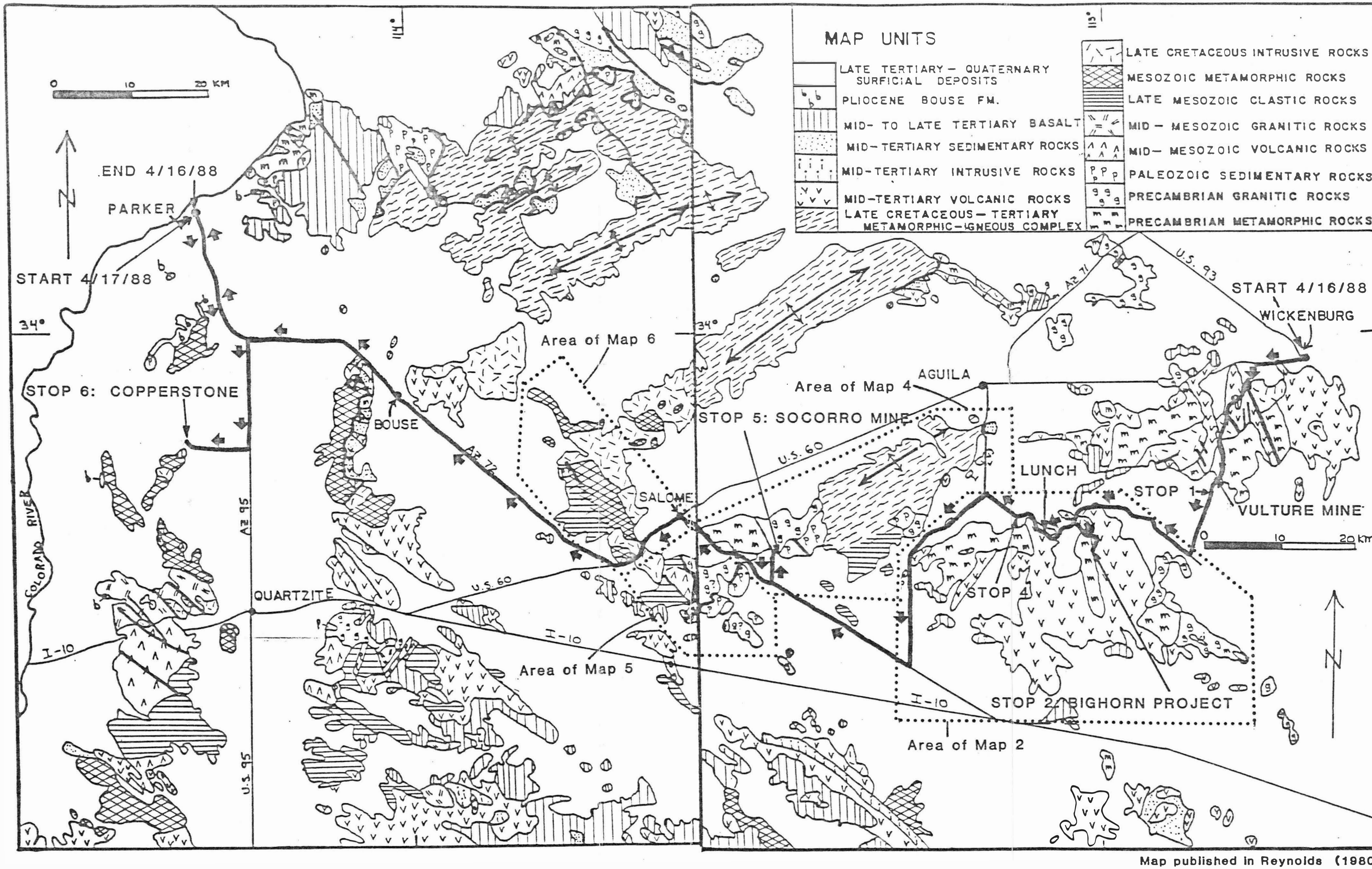

1988 AGS SPRING FIELD TRIP ROUTE AND MAP INDEX

DAY I
ROAD LOGS

GEOLOGIC OVERVIEW OF THE VULTURE MOUNTAINS

The Vulture Mountains consist of three principal time-lithologic units, Proterozoic metamorphics, Cretaceous (Laramide) intrusives and Tertiary volcanics and subordinate sediments. The Proterozoic and Cretaceous lithologies form the basement for the area and are unconformably overlain by the Tertiary rocks.

The oldest rocks are members of the Proterozoic Yavapai Supergroup (1.8-1.7 Ga), which consists of amphibolite, schist and gneiss, whose protoliths volcanic, sedimentary and plutonic rocks. Foliation attitudes commonly strike northeast to northwest and dip moderately to steeply to the north. The Late Cretaceous intrusives are equigranular to porphyritic granite and granodiorite of the Wickenburg Batholith, a northeast-trending body that is at least 15 miles long by 4 miles wide (see Fig.2 in this report)(Rehrig and others, 1980).

The Tertiary volcanics are early to middle Miocene in age and have an aggregate thickness of about 4500 feet (Rehrig and others, 1980, and Grubensky and others, 1987). The package is dominated by ultrapotassic rhyolite flows, that may be up to 1000 feet thick, and are separated by pyroclastic air-fall or base surge deposits. The more resistant of these flows form many of the prominent ridges in the Vulture Mountains, e.g. Vulture Peak. Intrusive rhyolites are common in the district as dikes and sills that are sometimes emplaced parallel to the Precambrian foliation.

The gross structural setting of the Vulture Mountains is dominated by mid-Tertiary crustal extension (18 to 15 Ma) that accompanied or post-dated volcanism. The oldest structures are low-to moderate-angle, planar and listric, normal faults that have strikes perpendicular to the northeast-southwest extension (Stimac and others, 1987). These are cut by north- to northwest-striking faults (dips of 10° to 50° to southwest) which tilt and rotate both the Tertiary and underlying basement rocks. Sense of rotation on these faults is down on the northeast side of each block, clockwise when facing northwest. Some blocks have been rotated to the extent that the units are now overturned.

Most of the important metal deposits in the Vulture Mountains are associated with gold and silver. The most important of these is the Vulture Mine, which will be discussed at the first of the stops. Precious metals at this mine occur mainly on the hanging-wall and footwall of a 85 Ma quartz monzonite sill hosted in Yavapai schists. Elsewhere in the Vultures, precious metal prospects, often with associated iron oxides and base metals (Cu, Zn and Pb), are localized along low- to moderate-angle faults that are intensely brecciated and healed by quartz and black calcite. This type of mineralization appears, in most examples, to post-date or even be contemporaneous with displacement along the host structures.

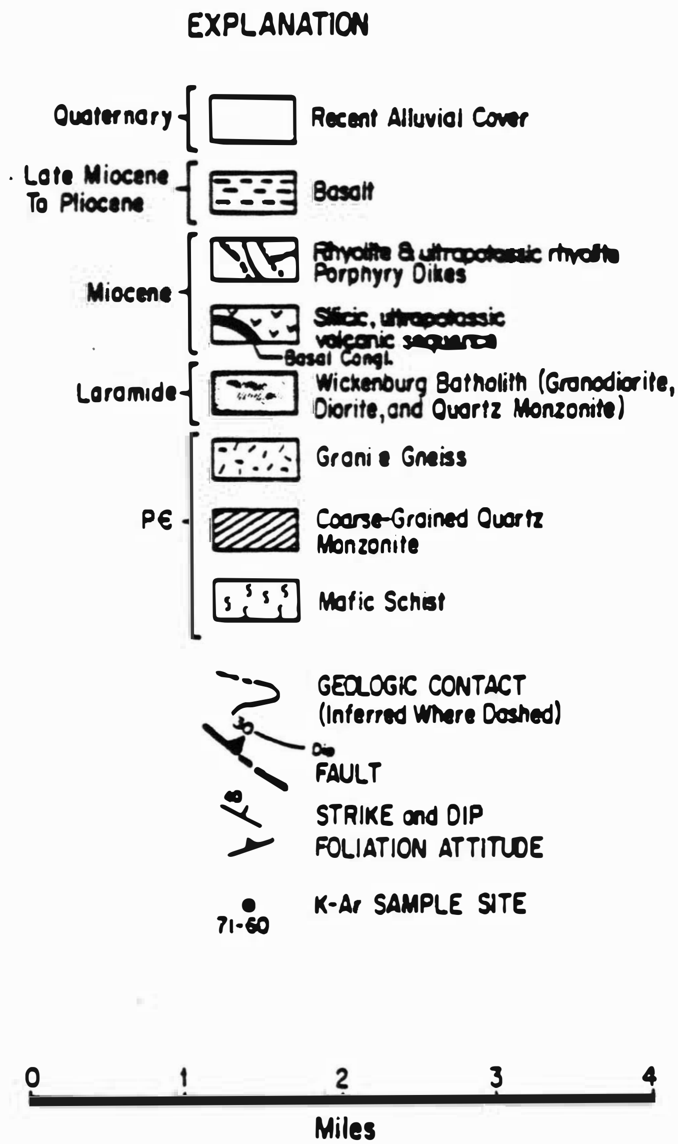

Explanation for Figure 2

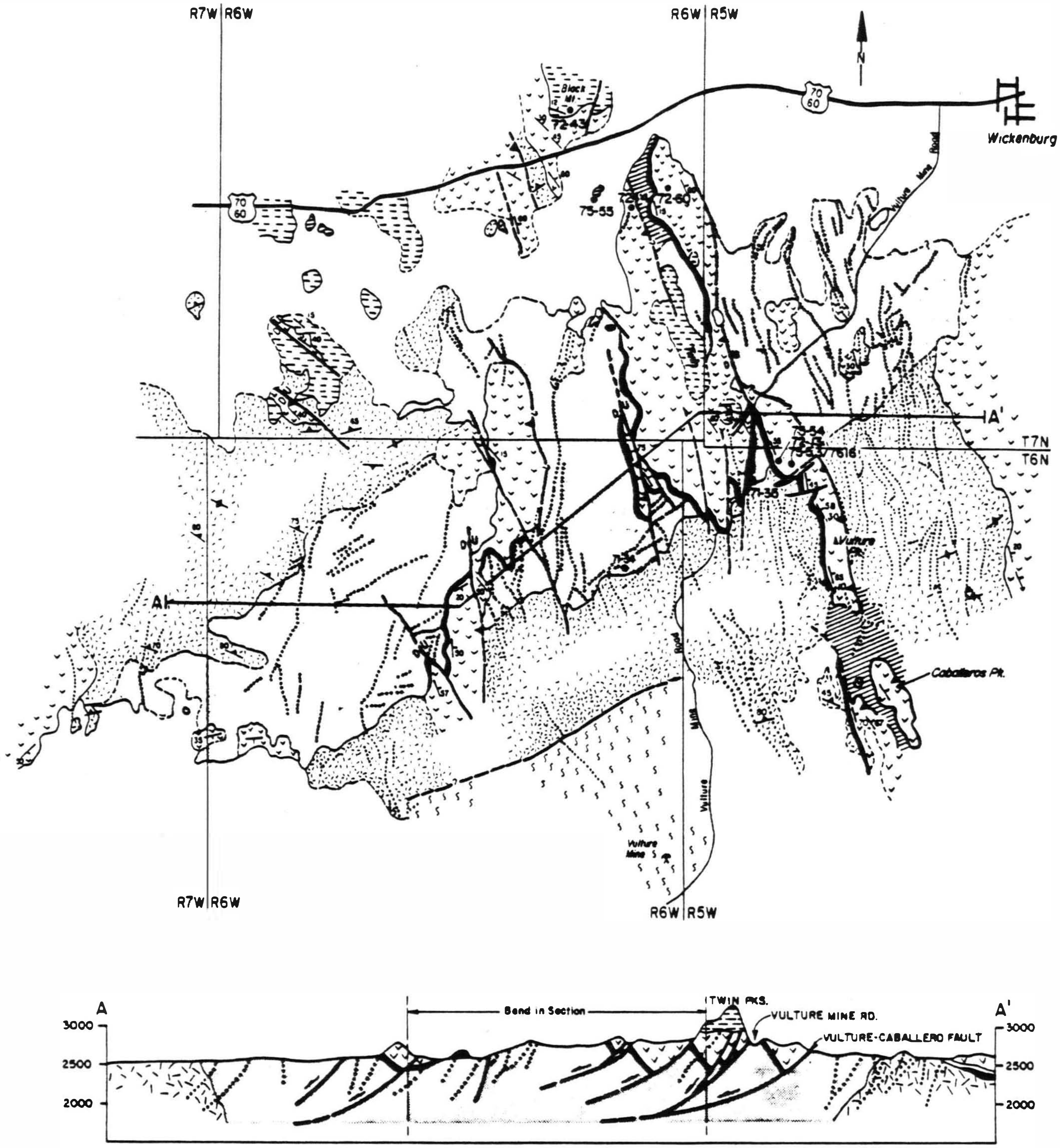

Fig. 2. Generalized geologic map and cross section of the Vulture Mountains. Note a crude northeast-oriented zonal pattern of Precambrian rocks. Mafic schists are common in the southern part. Silicic Tertiary rocks are intruded by a swarm of northerly trending dikes. Structural grain strikes north to northwest and is represented by dikes, normal faults, and tilted elongate fault wedges of silicic volcanic rocks.

ROAD LOG FROM WICKENBURG TO THE AMBROSIA MILL

Hugo Dummett, Nora Colburn and George Allen.

The field trip will assemble in the parking lot of the Americinn Motel, which is on U.S. Highway 60, 1.2 miles east of the bridge across the Hassayampa River at Wickenburg. All participants will leave from the hotel no later than 8.30 a.m. because we will have a fairly long day ahead of us. The cars will drive west through Wickenburg on U.S. 60, cross beneath the AT&SF tracks and proceed for another 2.5 miles to a shopping mall on the left that includes a Safeway store; at this point turn left onto the Vulture Mine Road and begin the road log.

CUM MIL	INCR MIL	
0.0	0.0	Vulture Mine Road. Historical marker commemorates discovery of the mine by Henry Wickenburg in 1863.
1.0	1.0	Road crosses alluvium covered granodiorite of the 68 Ma Wickenburg batholith. The Vulture Mountains are at 9:00 to 3:00 with Vulture Peak at 12:00. Porphyry copper mineralization(?) was drill evaluated on Wickenburg Mountain at 9:00. Oxidized copper minerals occur in irregular stockworks in granodiorite.
1.6	0.6	Trenches on right hand side of road are cut in Wickenburg granodiorite and expose copper carbonate mineralization with trace amounts of associated gold and silver. On the left of the road is the Rancho de los Caballeros golf course and housing estate.
3.0	1.4	Pavement ends.
4.4	1.4	Twin Peaks at 12:30 to 3:00. These hills are capped by 13-14 Ma olivine basalt flows that rest in marked angular discordance on 20-26 Ma silicic, felsic tuffs and flows.
4.6	0.2	Cross the unexposed trace of the Vulture Peak low-angle normal fault that underlies the tilted volcanic sections of Vulture and Caballeros Peaks.
5.0	0.4	Road crosses low pass. Reddish units adjacent to road are red beds (sandstone and conglomerate) that comprise the base of the Tertiary section. On the left of the road, these are overlain by prominent outcrops of gray-weathering rhyolite. Outcrops on right hand side of road are Cretaceous

granodiorites that are separated from the Tertiary units by a N-S striking fault that dips to the west at about 40°.

5.6	0.6	About here you have to look back to the west (right hand side of the road) to see very good exposures of northwest-dipping, light colored, Tertiary rhyolitic tuffs that are offset along a series of southwest-dipping, low-angle, normal faults at about 4:30. The dark unit that caps the ridge is a ±13.5 Ma, post-faulting, olivine basalt.
6.0	0.4	Mine workings at 9:00 are along a NE-striking brecciated quartz vein at the contact between Cretaceous granodiorite and Precambrian gneiss. Allen (1985) believes much of this style of gold mineralization (i.e. thick, iron-stained quartz veins) is Laramide in age.
6.1	0.1	Renegade and Lucky Day Mines turn-off on right side. These two mines are similar to the workings at 6.0 miles.
6.4	0.3	Road crosses zone between Cretaceous granodiorite and Proterozoic gneiss, which for next 2.5 miles is cut by a number of north-striking Tertiary rhyolite dikes. The gneiss is overlain, in part, by fault-bounded blocks of rotated Tertiary felsic flows and tuffs.
6.8	0.4	Vulture Peak at 9:00. Tertiary rhyolitic flows on the top of the peak dip to the northeast at about 60°. The rhyolites rest on a 10° to 30° west-dipping fault that separate the volcanics from underlying Proterozoic gneisses.
8.8	2.8	Cattle guard. Approximate position of Proterozoic gneiss-schist contact. The schists are part of the Proterozoic (1.8-1.7 Ga) Yavapai Supergroup whose protoliths include sediments, volcanics and foliated plutons. From here to the Vulture mine the road crosses Yavapai lithologies overlain, in places, by tilted fault blocks of the Tertiary volcanics.
9.0	0.2	Road on right hand side to Buckshot, Barons and Queen Lode; also the Stone Mine, operated by Phenix Mining Corp. These are a number of small workings that are principally irregular auriferous quartz vein zones(? age) in Yavapai schists.
9.5	0.5	Caballeros Peak at 9:00 and the White Tank Mountains on the skyline at about 10:00 to 11:00. The White Tanks are a metamorphic core complex.

10.7 1.2 Vulture Mine buildings at 2:00.

11.3 0.6 Main Gate to the Vulture Mine.

11.6 0.3 Vulture Mine tailings dumps at 2:00 to 3:00, headframe at 3:30.

12.0 0.4 Road junction. Field trip follows left fork which is the "Whispering Ranch" road. On the skyline at 10:00 to 1:00 are the Belmont Mountains.

12.7 0.7 STOP 1. Park along road edge and walk up hill on right. The hills at the viewpoint are strongly altered (clay ± silica) Tertiary volcanics. From this vantage point we will have an excellent view of both the Vulture Mine which is north of the viewpoint and the Belmont and Bighorn Mountains which form the skyline to the south and west.

The Vulture Mine is one of the most famous historic gold mines in Arizona. It was reportedly discovered in 1863 by Henry Wickenburg. Legend has it that Wickenburg threw a rock at a vulture that had come too close to inspect his obstinate and very tired pack burro. The rock missed the vulture but broke open when it hit the ground, revealing its golden interior, hence the discovery and the name of the mine (Williams, 1981).

Total recorded production from 1863 to 1942 is about 11,000 kg (290,000 ozs) of gold and 8,000 kg (210,000 ozs) of silver. Mined grades during the above period averaged ±0.35 opt gold and 0.25 opt silver (White, 1988).

Precious metal mineralization (gold and electrum) is Laramide in age and is intimately associated with a 1000 foot long and 60 foot thick, sill-like apophysis of porphyritic quartz monzonite, that dips to the north at about 35°, parallel to foliation in enclosing Proterozoic schists. Ore zones are localized in siliceous, pyritic zones that overlap the hanging-wall and footwall contacts of the sill.

The mine is currently under lease. For a much more comprehensive description of the mine refer to the 1988 paper by Don White that is included in the background materials for this guidebook.
The view to the south and west is of the Belmont and Big Horn Mountains. The Belmont Mountains are principally comprised of the mid-Tertiary, fluorite-bearing Belmont granite that has been tilted about 40° to the northeast and, in effect, is lying on its side (Reynolds and others, 1985).

West of the Belmont granite the range is largely Lower Proterozoic schist overlain by some small fault-bounded blocks of Tertiary volcanics, e.g. at Belmont Mountain.

At 1:30 to 3:00 (facing south) are the Bighorn Mountains. The ridges are Tertiary rhyolites and rhyodacites and the valleys are Tertiary basaltic andesites and Precambrian units. The Big Horns are similar to the Vulture Mountains inasmuch as they consist of the same three main time-lithologic units, i.e. Proterozoic metamorphics, Cretaceous (Laramide) intrusives and Tertiary volcanics.

The dominant rock unit within the range are the lower to middle Miocene (21 to 16 Ma) Big Horn volcanics, which comprise ten different members. From oldest to youngest these are the Morningstar, Old Camp, Hummingbird, Blue Hope, Sugarloaf, Mine Wash, unnamed basalt, Moon Anchor and Beer Bottle members. Basalts of the Dead Horse member are interbedded with the four lowermost units. The aggregate thickness of these volcanics is difficult to calculate because of faulting but is estimated to be between 1500 to 2000 feet (Capps and others, 1985).

The mid-Tertiary volcanism was accompanied by low-to high-angle normal faulting and rotation of the older volcanic units and subjacent crystalline basement. Most of the normal faults strike NW and have contemporaneous NE-striking faults that probably have a strike-slip component. The Big Horn Mountains comprise the upper plate of a southeast-dipping detachment fault that outcrops at the eastern edge of the Harquahala Mountains and may be an extension of the Bullard detachment (Rehrig and Reynolds, 1980, and Allen, 1985); the Harquahala Mountains are immediately west of the Big Horns.

There are three mid-Tertiary and one Laramide mineral districts in the Big Horns. Laramide gold mineralization occurs in the northwestern part of the range in the Big Horn distrhct associated with the northwestern margin of a large Cretaceous granodiorite. Tertiary districts, from west to east are the Tiger Wash barite-fluorite district, the Aguila manganese district and the Osborne base and precious metals district. The U.S. Mine is part of the Osborne district. Each of these districts is described in some detail in a copy of Allen's (1985) report that forms part of the background material for this guidebook.

12.8	0.1	At 12:00 are the Belmont Mountains, with the prominent mountain dead ahead being Belmont Mountain. The Tonopah-Belmont Mine is on the north and south sides of this mountain and is the second largest producer of precious metals in the Osborne district (the largest being the U.S. Mine). A galley proof of a paper on the mine authored by George Allen and William Hunt is attached as part of the background material for this guidebook. Mineralization at the mine is principally copper carbonates with minor gold and silver and which are hosted by east-northeast striking structures. These structures are filled with brecciated quartz veins that cut Miocene volcanics surrounded by Proterozoic phyllites except on the southeast where the volcanics are faulted against Belmont granite. Oxidation has produced a variety of good quality rare minerals of interest to the collector, e.g. rosasite and molybdofornacite. Recorded production from the mine totals approximately 1 million pounds of copper, 150,000 ozs of silver and 8500 ozs of gold. For the next 5.5 miles we will drive across the Hassayampa Plain which is a very large area of Tertiary basin fill.
13.8	1.0	Cattle guard. Bert Smith and Ber Mar Mines turn-off on right side. These mines are also operated by Phenix Mining Corp. They appear to be very small, placer operations on the pediment and are located about two miles to the west.
14.3	0.5	Nomad Energy Pilot Plant and Project Site turn-off on left side. Apparently this site is still under construction. Pieces of equipment include components of a large steel tank, a large cement mixer and an ore? bin with a screw-feed take-off.
14.5	0.2	Cross under the 345 KV Mead-Liberty power line.
18.1	2.6	Cross under the 161 KV Parker Dam-Phoenix power line.
18.2	0.1	Cattle guard and turn right onto the Buckeye-Tonopah Road. Prominent mountain at 12:00 is Black Butte with Eagle Eye Peak on the skyline at 11:00.
20.2	2.0	Cattle guard.
20.5	0.3	Belmont Ranch road turn-off on left side.
22.2	1.7	Cattle guard.

23.3	1.1	Cross Jackrabbit Wash.
24.1	0.8	Low rounded hill on right is composed of Lower Proterozoic amphibolite and granite(?). At least four small prospect pits are located on narrow, NW-striking, iron-stained quartz veins (also some Pb and Ag?). Epidote alteration locally present in the amphibolite.
24.4	0.3	Cross under powerline. Low hills at 3:00 are Tertiary Hummingbird rhyolite tuffs and flows.
25.3	0.9	Outcrops of massive and irregular white quartz veins in L. Proterozoic gneiss on left side of road. Low hills at 2:00 to 3:00 are more Hummingbird rhyolite flows and tuffs.
26.3	1.0	Foothills of the Bighorn Mountains at 9:00 to 12:00 are Tertiary Sugarloaf rhyolites.
28.3	1.0	On skyline at 10:00 to 12:00 are the Harquahala Mountains.
28.4	0.1	Cross Dead Horse Wash.
28.7	0.3	TURN OFF to U.S. Mine to the left. Please watch for the turn-off because it is not very obvious! Tertiary, Sugarloaf rhyolites form low, prominent ridges about a mile distant at 9:00 to 10:00.
29.5	0.8	Cross Dead Horse Wash again. Outcrops on right hand side are Tertiary, Dead Horse massive to vesicular iron-stained andesites.
29.9	0.4	Lead Dike Mine is just off the road on the left side at 9:00 to 10:00. This mine is the northernmost expression of the U.S. Mine mineralized zone. The main workings expose a 20 foot long breccia zone in Cretaceous (Laramide) granite, that is subvertical and filled with iron-stained, siliceous breccia. Limited exposures suggest a total strike length of at least 300 feet. Mineralization includes galena, cerussite, chrysocolla, barite, amethyst and hematite.
		For next 1.5 miles the road crosses Upper Cretaceous granite/granodiorite.
30.6	0.7	Turn left at fork for the U.S. Mine.
32.2	1.6	Contact Mine turn-off on right side of road. Prominent ridges at 2:00 to 3:00 are Tertiary Old Camp, quartz-rich, rhyolite flows.

The Contact Mine is on property controlled by the owners of the U.S. Mine. Gold mineralization occurs in a narrow (5'-10"), quartz-hematite filled structure that extends north from the U.S. Mine. At this site, the structure is hosted by L. Proterozoic gneisses. An amethyst stockwork is also exposed in road cuts at the mine.

32.7 0.5 Cross small wash. Outcrops in wash at 3:00 are Hummingbird rhyolites that include gray and blackish gray vitrophyre.

32.9 0.4 Prominent hill on left side of vehicle is capped by at least twenty feet of gray vitrophyre belonging to the Sugarloaf member. For next 1.3 miles the road cuts across north-striking, Old Camp rhyolitic flows and lithic tuffs that are interbedded with Dead Horse basalts.

34.2 1.3 Entrance to U.S. Mine.

The U.S. Mine is currently the "Big Horn Project" of the joint venture operated by Roddy Resources of Vancouver and Belmoral Resources of Toronto.
The earliest recorded production was by the Hauxhurst Copper Company between 1908 and 1920, although this production was reportedly very small. In 1943 about 4500 tons of ore was milled which contained 0.13 opt gold. In 1961, three shipments of ore, totalling 133 tons, sent to the Superior and Hayden smelters averaged 0.091 opt gold and 2.01% copper. The property was acquired by one of the present lessees in January, 1984.

Gold mineralization is associated with a large subvertical, NNW-striking, FeOx-stained, normal fault (listric?) that persists for at least three to four miles north and south of the mine and is the host for a number of other small gold prospects in the Osborne district. This structure transgresses the district fabric and in the mine area is close to a contact, that is subparallel to

the fault, between Tertiary volcanics on the east and a mixed package of Proterozoic metamorphic rocks on the west.

In the mine area the mineralized fault is enclosed by volcanics that are probably Dead Horse and Old Camp equivalents. At this site, as well, the "main" mineralized fault is also intersected by a younger, major, northeast-striking, northwest-dipping, normal fault that offsets the main fault to the west.

In detail, the mineralization occurs within an intense stockwork of quartz veins and veinlets, that are commonly banded and contain abundant drusy cavities. Black specular hematite and red, earthy hematite, up to 30 volume percent, occur as fine impregnations within the various episodes of silicification as well as the wallrocks. Intensely silicified and brecciated zones up to 16 feet wide are interior to the mineralized zones.

Gold in the mineralized structure is present in grades that vary between 0.01 and 1.0 opt in association with copper oxide, Announced open pittable, leachable, reserves for the mine are about 600,000 tons with an average grade of 0.09 opt gold. Production is anticipated at about 3000 tons per day.

Extended descriptions and additional information on the U.S. Mine can be found in George Allen's 1985 report (pages 101 through 109) and maps that are appended to this guidebook in the background information and map sections.

After the tour at the U.S. Mine we will return 3.2 miles to the fork that will take the us to the Aguila Microwave road for the continuation of the tour.

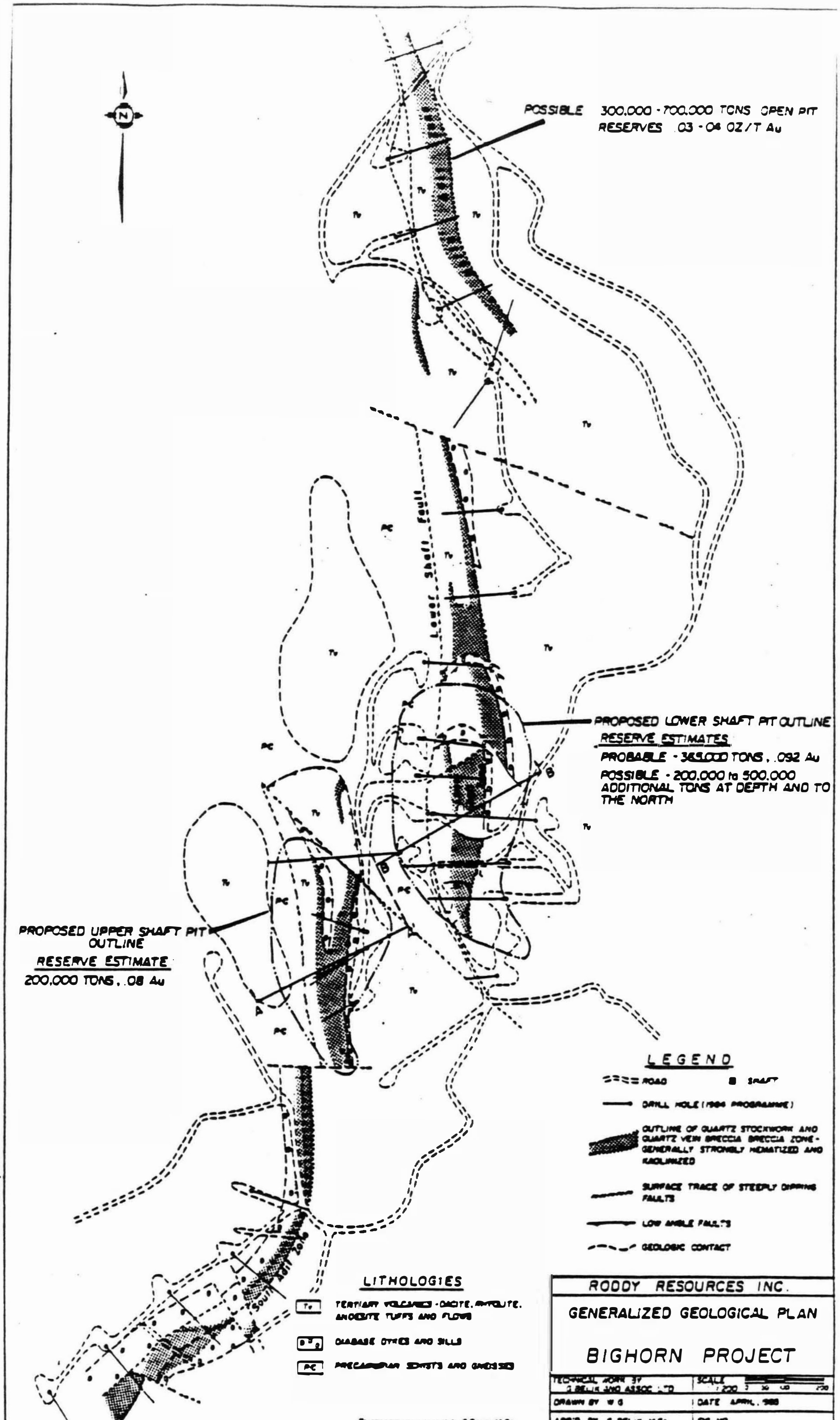

N
POSSIBLE 300,000 - 700,000 TONS OPEN PIT
RESERVES .03 - .04 OZ/T Au
Lower Shaft Fault
PROPOSED LOWER SHAFT PIT OUTLINE
RESERVE ESTIMATES
PROBABLE - 365,000 TONS, .092 Au
POSSIBLE - 200,000 to 500,000
ADDITIONAL TONS AT DEPTH AND TO THE NORTH
PROPOSED UPPER SHAFT PIT OUTLINE
RESERVE ESTIMATE
200,000 TONS, .08 Au
South Adit Zone
Tv
PC
A
B
LEGEND
ROAD
SHAFT
DRILL HOLE (1984 PROGRAMME)
OUTLINE OF QUARTZ STOCKWORK AND QUARTZ VEIN BRECCIA BRECCIA ZONE - GENERALLY STRONGLY HEMATIZED AND KAOLINIZED
SURFACE TRACE OF STEEPLY DIPPING FAULTS
LOW ANGLE FAULTS
GEOLOGIC CONTACT
LITHOLOGIES
Tv TERTIARY VOLCANICS - DACITE, RHYOLITE, ANDESITE TUFFS AND FLOWS
DIABASE DYKES AND SILLS
PC PRECAMBRIAN SCHISTS AND GNEISSES
To accompany a report by G Belik, M Sc
RODDY RESOURCES INC.
GENERALIZED GEOLOGICAL PLAN
BIGHORN PROJECT
SCALE 1:200
DRAWN BY W G
APP'D BY G BELIK, M Sc
FIG. 40

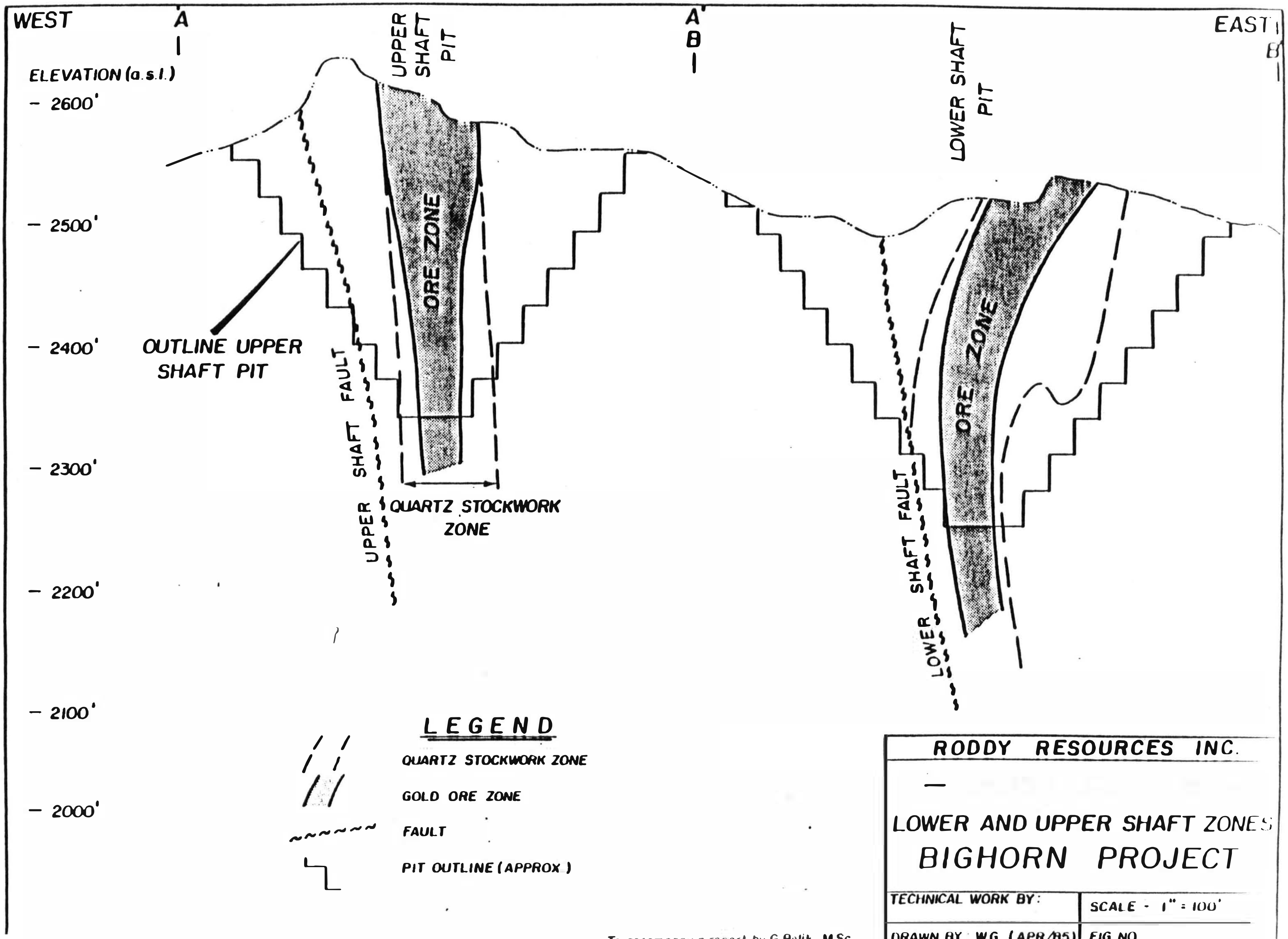
WEST
A
A'
B
EAST
B'
ELEVATION (a.s.l.)
2600'
2500'
2400'
2300'
2200'
2100'
2000'
UPPER SHAFT PIT
LOWER SHAFT PIT
ORE ZONE
ORE ZONE
OUTLINE UPPER SHAFT PIT
UPPER SHAFT FAULT
LOWER SHAFT FAULT
QUARTZ STOCKWORK ZONE
LEGEND
QUARTZ STOCKWORK ZONE
GOLD ORE ZONE
FAULT
PIT OUTLINE (APPROX.)
RODDY RESOURCES INC.
LOWER AND UPPER SHAFT ZONES
BIGHORN PROJECT
TECHNICAL WORK BY:
SCALE - 1" = 100'
DRAWN BY: W.G. (APR/85)
FIG. NO.

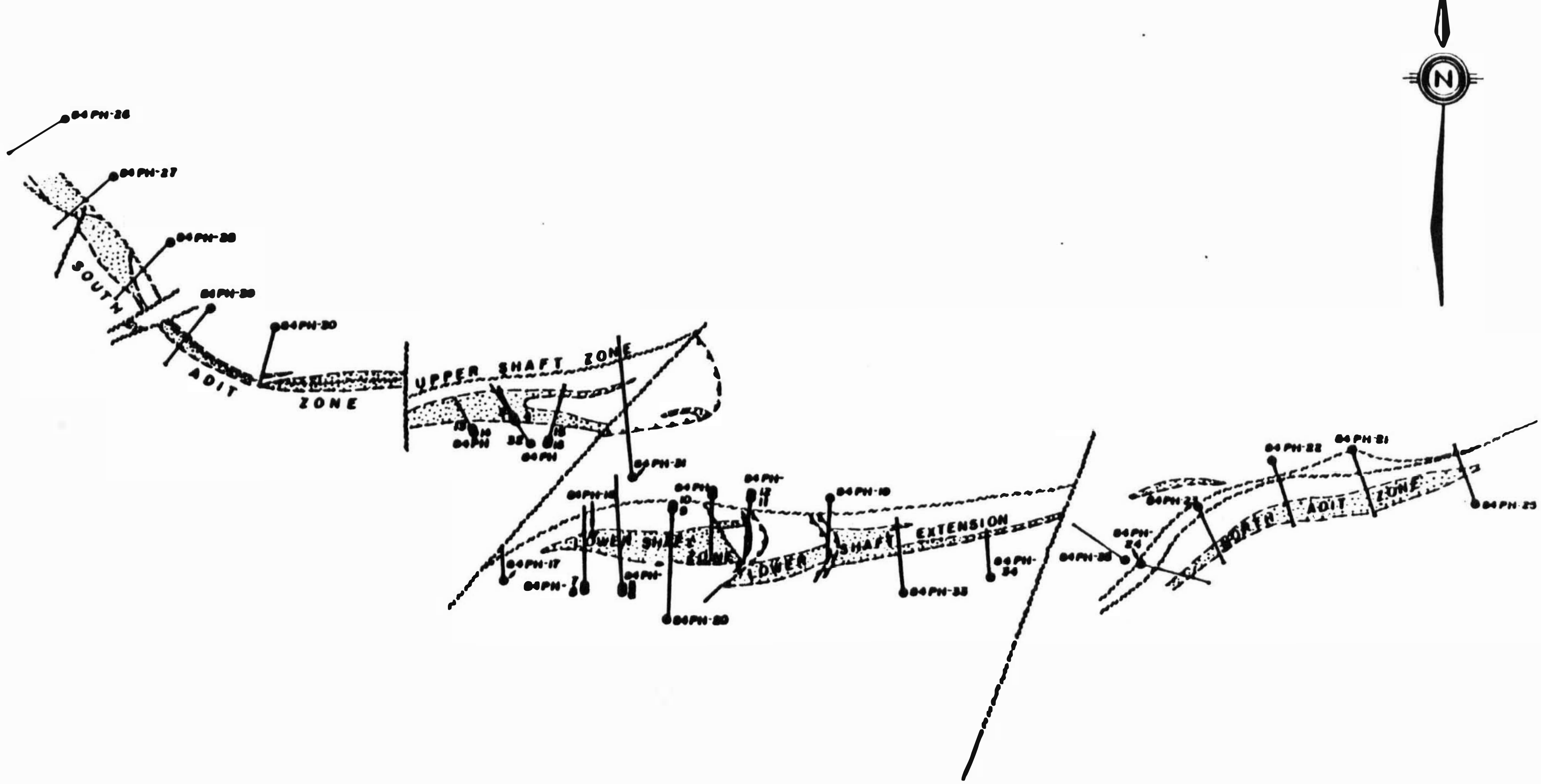

RODDY RESOURCES INC.

DRILL HOLE LOCATION PLAN

BIGHORN PROJECT

MARICOPA COUNTY, ARIZONA, U.S.A.

Steeply dipping faults

Low angle faults

SCALE 1" = 400'

0' 100' 200' 400' 800'

Outline of quartz stockwork and quartz vein breccia zone

Drill hole location with surface projection

RODDY RESOURCES INC.
1984 DRILL HOLE SUMMARY
BIGHORN PROJECT
MARICOPA COUNTY, ARIZONA

Hole #	Interval	Core Length	Oz/ton Gold (uncut)
84PH-1	70-120	50 Ft.	0.116 (incl. 20' 0.186)
2	140-185	45 Ft.	0.012
3	5-75	70 Ft.	.075 (incl. 5' .410)
4	0-120	120 Ft.	.092 (incl. 30' 0.179 & 15' 0.226)
5	70-90	20 Ft.	.031
	165-205	40 Ft.	.070
6	120-135	15 Ft.	.054
	230-245	15 Ft.	.044
7	130-150	20 Ft.	.030
8	Weakly Mineralized		
9	85-190	105 Ft.	.020
10	150-220	70 Ft.	.055 (incl. 15' 0.117)
	or 135-225	90 Ft.	.047
11	120-170	50 Ft.	.037
12	195-250	55 Ft.	.016
13	60-65	5 Ft.	.096
14	90-130	40 Ft.	.017
15	100-125	25 Ft.	.047
16	90-175	85 Ft.	.020 .019*
	175-225	50 Ft.	.177 .170* (incl. 15' .246 & 10' .[illegible]
	or 90-225	135 Ft.	.078
17	No Mineralization		
18	10-50	40 Ft.	.058
	50-110	60 Ft.	.022
	or 10-110	100 Ft.	.037
19	105-170	65 Ft.	.020 .019*
	170-220	50 Ft.	.092. (incl. 20' 0.171)
	220-310	90 Ft.	.027
	or 105-310	205 Ft.	.041
20	390-410	20 Ft.	.094
	410-425	15 Ft.	.032
	or 390-425	35 Ft.	.068
21	200-245	45 Ft.	.037 .041*
22	240-265	25 Ft.	.038
23	230-270	40 Ft.	.036
24	220-235	15 Ft.	.061
	or 190-245	55 Ft.	.028
25	85-115	30 Ft.	.021
	185-210	25 Ft.	.022
26-31	Missed zone, faulted off		
32	205-225	20 Ft.	.067
	or 160-230	70 Ft.	.033
33-35	Weakly mineralized over wide intervals		

* Check assays at a different laboratory.

Re-start mileage at fork connecting U.S. Mine road with Aguila Microwave road, i.e. at mileage "30.6" as above.

0.0	0.0	From turn-off for about one mile to crossing at Dead Horse Wash, road crosses Upper Cretaceous granite/granodiorite which is cut by small bodies of Lower to Middle Miocene mafic and intermediate intrusives, e.g. at 0.5 miles.
0.7	0.7	Dozer trench on left side of road exposes copper carbonates in irregular veinlets in the Cretaceous intrusive.
1.0	0.3	Cross small wash which is approximate position of trace of large, N-S striking normal fault, downthrow to the west. Fault juxtaposes Cretaceous granite/granodiorite on east against undifferentiated Tertiary (M. to U. Miocene) fanglomerate, sedimentary breccia and megabreccia on the west.
1.3	0.3	Cross Dead Horse Wash (±0.3 miles wide). Corrals and wells in and adjacent to the wash. After crossing the wash, the road is rough but passable for two-wheel drive vehicles. West of the wash road crosses the same Tertiary units that occur on east side of wash.
2.1	0.8	Outcrops on left and in the road are tertiary Sugarloaf rhyolites which include irregular patches of gray and black vitrophyre.
2.8	0.7	Join Aguila Microwave road and turn sharp right. Low outcrops on immediate left side of road are lithic tuffs of the Tertiary, Blue Hope rhyolite member.
3.0	0.2	Prominent small hill at 10:00 is Upper Cretaceous granite/granodiorite.
3.2	0.2	On right side of road is contact of Tertiary Dead Horse tuffs and sediments with U. Cretaceous intrusives. Outcrops on skyline at 9:00 to 12:00 are L. to M. Miocene rhyolites.
3.9	0.7	Trenches on right side expose copper carbonates in U. Cretaceous granite/granodiorite.
4.2	0.3	LUNCH STOP and overview. At 3:00 is Vulture Peak, at 2:00 is Black Butte. Ridge tops at 9:00 to 11:00 are sanidine-rich flows of the Tertiary, Hummingbird rhyolite. This unit is separated by a valley at 11:30 from hills at 12:00 and 1:00 that detached

brecciated blocks of Tertiary Dead Horse basaltic andesite that host a number of small manganese prospects.

The manganese oxides occur in highly irregular stockworks and interstices of the breccias as well as in some steeply-dipping faults. Up to 2.9 opt silver and 15% lead is reported from one of these prospects, the Valley View.

5.9 1.7 Cattle guard.

6.0 0.1 STOP. Overview of the Harquahalas.

6.3 0.3 Low ridges at 10:00 to 2:00 are L. Proterozoic schists, phyllites and gneisses.

6.9 0.6 Purple Pansey Mine (Pump Mine) and Fugatt Mine turn-off on left side.

The Purple Pansey mine has been recently evaluated as a heap-leach gold prospect. Gold mineralization occurs in an E-W striking quartz vein which is about 4500 feet long, varies in thickness from 6 inches to 6 feet and dips to the north at about 45°. The vein occupies a fault zone in Precambrian metamorphics that are strongly mylonitized near the vein.

The Fugatt Mine is a manganese mine that has reportedly produced at least 7500 tons of ore from a pit which is about 200 feet in diameter and 50 feet deep. The mineralization occurs as veinlets and irregular masses in Tertiary Dead Horse basalt.

From this turn-off to the Ambrosia Mill, the road traverses valley fill of U. Miocene to Holocene alluvium.

8.7 1.8 Black sand in small wash on left hand side is magnetite weathered from Precambrian metamorphics not manganese oxides.

10.0 1.3 Dumps at 3:00, part of the Ambrosia Mill.

10.3 0.3 Join Eagle Eye Road and turn left.

ROAD LOG AMBROSIA MILL TO SOCORRO MINE

Nora Colburn

CUM MIL	INCR MIL	
0.0	0.0	Ambrosia Mill road junction with Eagle Eye Peak road, heading southwest. Northward about 5.1 miles is the junction with the Tonopah-Aguila road, and 5.2 miles further on is the junction with US 60, in the town of Aquila. Looking north, Eagle Eye Mountain and Eagle Eye Peak should be visible. At the base of Eagle Eye Peak the contact between the mid-Tertiary volcanics and sediments (SW dipping) and the Precambrian mylonitic granitics is the chloritic/mylonite zone of the NE-dipping Bullard detachment surface.
1.4	1.4	Cross wide, shallow drainage, Pump Mine Wash. Black-manganese stained hills at 12:00, and low ridge of brown-weathering volcanics at 11.30 to 9:30. The high main mass of the Harquahala Mountains extends from 1:00 to 3:00 and has elevations above 5000 ft. The range front is dominated on this southeastern side by Mesozoic and Cenozoic intrusives (toward the NE end) and Proterozoic (1.7-1.8? Ga crystalline and metamorphic rocks in the central portion). From 3:30 to 5:30 the extreme northeastern peak (4525 ft. elev.) of the Harquahalas exposes mylonitic Brown's Canyon granite (U. Cretaceous(?)-L.Tertiary(?)) in contact with L. Proterozoic rocks. These rocks and a portion of the Bullard detachment surface are displaced by a NW-trending, west-down high-angle normal fault, isolating the unnamed peak from the rest of the mountain range. The varied crystalline and metamorphic sequences of the Harquahala block do not stop at the mountain base, but are found as scattered outcrops under a veneer of alluvial lag deposits. The erosion surface on top of these basement rocks is a true pediment, and may in certain areas also be the exposed thrust surface.
2.9	1.5	Black volcanic knob at 11:00. Just on the other side is the Black Nugget Mine area; manganese was actually recovered from here. Going south, the arbitrary line between the Bighorn Mountains on the east and the Harquahala Mountains is the Tiger Wash and the road.
3.0	0.1	"Metal Technology" on northwest side of road; on maps may be called "Rogers well" and was a Ba? prospect.

3.5	0.5	Road off to SE and a more travelled road, at C.3 miles south, lead to El Tigre Mine, about 2.9 miles towards Little Horn Peak. The El Tigre was mined for gold, and in the same area the Knabe Mine is also a Au prospect. See George Allen's M.S. thesis in background material for detailed descriptions.
		Other mines and prospects in this west portion of the Big Horn mountains form the Aguila manganese mineral-district, having an estimated total production (1950-1958) of >42 million pounds (Keith, and others, 1983). Mid-Tertiary in age, some of these Mn-occurrences are the Black Rock (Warrior),Apache (Dulcy) and Mollie Davenport (Pegram, Sisson).
3.8	0.3	Road on NW leads to several different prospects including marble/limestone and gold plus silver ± Cu, Be, Si in the Sunset Canyon area. One of the ubiquitous diorite dikes in the Harquahala-Harcuvar region has been sampled from this or the next canyon south and been dated by K-Ar on paired biotite: 22.10 ± 1.30 Ma and hornblende: 28.60 ± 1.90 Ma. The dike cuts metamorphics, mylonites and granitics (Reynolds, and others, 1986).
		The Paleozoic sequence in this portion of Arizona has sedimentological and provenance affinities to both northern and southern stratigraphies. The lower Paleozoic is similar to southeastern Arizona, so the terminology used is Bolsa and Martin for Cambrian and Devonian respectively. Both Escabrosa and Redwall have been used for the Mississippian limestone. The upper Paleozoic rocks are similar to the Supai, Coconino and Kaibab of the Grand Canyon sequence.
6.4	2.5	Windmill to southwest is Tiger Well.
6.6	0.2	The mine timbers at 9:00 mark a shaft at the Black Queen (Hatton) manganese mine.
6.8	0.2	Cross Tiger Wash. Road off to north at 4:00 goes to Arrastre Gulch area.
7.25	0.4	Mn-blackened, SW-dipping volcanics at 11:00 to 8:30. Road off to southeast leads to Lions Den mine (Mn) on other side of ridge.
7.45	0.2	Road to southeast goes to White Rock prospect-fluorite and Ba, Ca.
8.05	0.6	Cross small wash near a road that goes northwest to several prospects: Ag, Pb, Au at Leadville-Arizona and Cu, Au, Ag at Copper-, Gold- or Old Blue Belt. Harquahala Peak is visible; this portion of the range

is capped by the Harquahala thrust sheet, so that Lower Proterozoic granitic and metamorphic rocks now rest on the entire regional sequence. Exposed in erosional windows through this plate are completely inverted and amphibolite-grade metamorphosed Paleozoic sequences. The Arrastre Gulch - Sunset Canyon area is one of these windows. Stratigraphic relations as Bolsa quartzite on Precambrian rocks are preserved. Overturning occurred during recumbent folding (SE directed) sometime post-Jurassic(?) but prior to L. Cretaceous- E. Tertiary tectonic events. (Hardy, 1984).

8.55 0.5 Tiger Wash parallels road on southeast. Little Horn Peak is visible at 8.45.

8.65 0.1 Precambrian(?) schistose low hills from 10:00 to 1:30; Weldon Hill at 2:00; near road to Princess Ann fluorite - barite prospect located to the southeast.

9.45 0.8 Road on northwest side of road goes to Snowball prospect (F, Ca).

12.0 2.5 Road heading off to W/SW towards Weldon Hill (Cu, Al, Ca - F?) branches westward and northward to the Rainbow (Cu, Au, Ag) and Alaska (Au, Cu, Ag) mines, as well as the Snowball. Generally present are various intrusive rocks and/or olive-colored schists, somewhat altered and brecciated near quartz and/or fluorite-calcite veins.

12.7 0.7 Cross here, and for the next 0.4 miles, a series of channels draining a bajada surface sloping onto the Harquahala Plains and into Centennial Wash.

13.1 0.4 Low tan hills at 1:00 are outlier blocks of Mesozoic volcanic and clastic sedimentary rocks, Jurassic?-Cretaceous?.

15.7 2.6 Eagletail Mountains forming the ragged faulted skyline at 11:30 -2:00, are predominantly volcanics and related clastics. The Eagletail Volcanics consist of flows and at least one latitic to rhyodacitic ash-flow tuff lying directly upon basement, which dated 23.70 ± 0.60 Ma. (K-Ar, biotite, Reynolds and others, 1986). A massive welded zone is well-exposed in Courthouse Rock, where a younger quartz latite dike is dated at 19.98 ± 0.58 Ma. (K-Ar, biotite, Reynolds and others, 1986). Intruding some metasediments below the Tertiary units is a medium-grained diorite with an 52.80 ± 1.10 Ma. age-date (K-Ar, biotite, Reynolds, 1986). The mountains beyond, extending to 3:00, are the Little Horn Mountains. Cone-shaped Big Horn Peak and another southern peak in the Big Horn Mountains-Burnt Mountain- are at 10:30-11:00; even further to the southeast is Saddle Mountain and the Palo Verde Hills.

16.6 0.9 By looking back to north there is an erosional embayment into the upper plate rocks of the Harquahala thrust, composed of Lower Proterozoic metasediments and Middle Proterozoic granites. The whole range front here is essentially the dip slope of the thrust surface. The low red hills in the foreground are in part McCoy Mountains Formation (J?-K?) sediments.

James Hardy (1984), as part of his MS thesis, collected samples in and near the Harquahala thrust zone from the White Marble Mine area located on the northwest side of the range. These dates provide some constraints on the timing of the actual displacement motion. The minimum age is 49.50 ± 1.9 Ma (K-Ar on biotite) from a thrust-mylonitized Proterozoic porphyritic granite located 60 m below the thrust. There are a cluster of dates, which may reflect cooling ages (older dates positioned higher structurally than younger dates) rather than age of movement. These range from 56.10 ± 2.1 Ma (biotite schist /5 m above),58.4 ± 2.2 Ma (amphibolite gneiss /10 m above) to 62.5 ± 2.3 Ma (fluorite-bearing, muscovite schist /5 m above). So the Harquahala thrust was in motion during the Late Cretaceous-Eocene and the upper plate translated southward in response to a broad regional compresson.

17.1 0.5 Cross cattle guard.

*19.2 2.1 Pavements begins. Prepare to make STOP and sharp RIGHT TURN onto Salome-Buckeye road; heading northwest.

19.4 0.2 Big Horn Peak at 3.00; Granite Wash Mountains at 12:00; Harquahala Mountains at 1:00 to 2:30 - the peak at the northeasternmost end. The Little Harquahala Mountains at 10:30-11:30 consist of stacked thrust sheets - from base to top: Sore Fingers, Centennial and Hercules.

The ridge extending SW to 5:30 from the Little Harquahala Mountains is mainly the crystalline rocks (Proterozoic? and Jurassic?) forming the Hercules plate. The Sore Fingers granite has a partially reduced Jurassic age of 140.0 ± 4.0 Ma. (K-Ar, biotite, Reynolds and others, 1986). At the extreme SW end of this ridge is Lone Mountain consisting of Mesozoic sediments, including a conglomerate containing Permian Kaibab limestone clasts. Keith and others, 1980, have included these within the Golden Eagle thrust sheet.

21.1 1.7 Cross wash.

21.7 0.6 Leave Maricopa County - enter La Paz County.

22.0 0.3 Road to south is County 75-E (4 miles to I-10), Big Horn Peak at 5:00.

22.1 0.1 Cattle guard, 18 miles to Salome.

22.6 0.5 Reddish low hills, in foreground at 1:00 to 2:00 as road curves, are Mesozoic clastic rocks, including McCoy Mountains formation sediments Jurassic(?)-Cretaceous(?) and possibly older Jurassic(?) volcanics. As the road gradually approaches the pass between the Little Harquahalas and the western foothills of the Harquahalas the structurally jumbled nature of the repeatedly faulted thrust- and fold-sheets will become more obvious.

24.0 1.4 At 2:00 various workings and drillroads can be seen in metamorphosed Paleozoic rocks, predominantly limestone /marble) and quartzites. The Hidden Treasure (Magic) group is generally located to the west and the Why Not, Clipper and Gold groups are located to the east within the SE-dipping belt of N60E-trending Paleozoic meta-sediments. Other mine names may be in current usage however. Some of the larger cuts were probably from gypsum extracted from diagenetic evaporite lenses in the upper portion of the Permian Kaibab fomation. Past production or reported mineral occurences have included free to spotty gold with silver, associated with copper and minor lead-zinc. Consistently present are iron and/or manganese oxides related to alteration and silification near shears and/or diorite, sometimes felsic, dikes.

25.7 1.7 Harcuvar Mountains on distant skyline.

26.4 0.7 Granite Wash Mountains at 12:00 skyline.

27.1 0.7 Road to Pancho's on south side of road.

27.7 0.6 Price Ranch road to south.

27.9 0.2 Cross cattle guard as road curves. Mined-out gypsum cuts at 3.30.

30.0 3.0 Southern ridge of Harquahalas at 10:30. The Hercules and Centennial thrust plates are cut and offset by a high-angle fault. The great contrasts in lithology and metamorphic grade of adjacent plate assemblages are the result of a post-Permian tectonic history of multiple folding and faulting, including low-angle duplexing, all overprinted by the latest high-angle faulting of the Basin and Range type period.

30.6 0.6 Southward dipping layers and segments of thrust plates in peak at 2:30-3:00. Harquahala Mountain (5681 ft. elev.) and the main ridgeline are from about 2:15 to 4:00.

32.0 1.4 Fulmer Co. road to SW. As the road curves, 'S'Mountain comes into view, as well as the Socorro Mine area at 12:00 - low, near the apex of a major alluvial fan.

32.2 0.2 Light colored area at 1:30 is Socorro mine. Be prepared to make turn onto access road.

*32.4 0.2 TURN RIGHT onto road paralleling the high pressure gas line.

33.8 1.4 Road intersecting from west leads back to the Salome-Buckeye road about 1 mile away.

34.1 0.3 Trenched area. Low red hills at 11:00 in line with 'S' Mountain.

34.5 0.4 Good view of mid-Tertiary volcanic and sedimentary rocks southeast of road. North of the road from 9:00 to 10:30 southeastward tilting of units can be seen.

35.0 0.5 Road forks, take the north or left branch; they will rejoin in 0.1 mile .

*36.6 0.4 SOCORRO MINE GATE. Continue up road to the area near the old building and park where there is adequate space. For a very comprehensive discussion of the geology and history of the Socorro Mine, refer to Stan Keith's paper in the "Guidebook articles" section.

The Socorro Mine and other prospects located on the north and south slopes of this southwestward extension of the Harquahala Mountains, plus the various non-manganese mineral occurrences in the Arrastre Gulch-Sunset Canyon window and additional prospects along the curving front of the southeastern edge of the range are considered to form a single metallic mineral district. Overall, it is characterized as a gold district, with mid-Tertiary mineralization having variable to significant silver production and which may or may not have associated copper or lead ores.
Historical recorded production as summarized in Keith and others, 1983, for 1905 through 1981 is : copper-61,000 pounds; lead - 1,500 pounds; GOLD - 2,800 opt; SILVER - 7,300 opt. out of a total tonnage of 21,000.

It is an interesting comparison to make that the best-known and perhaps the better ore grades and larger production was from the what is now called the Little Harquahala mineral district. The initial gold discovery in the 'Salome' area was the "Glory Hole" pocket located in the southern Granite Wash Mountains. This led to further exploration after newspaper reports 'Back East' brought prospectors in on the train. However the Harquahala Mine also sometimes called a 'glory hole', and known as Bonanza, Golden Eagle or Yuma Warrior mine, was a major gold producer (although early records are inadequate) from 1888 to 1918, with additional recoveries from tailing and dumps in the mid-1960's and 1970's (?). Overall summary of production for the Little Harquahala district (Keith and others, 1983) for 1888 through 1964 is : copper- 50,000 pounds; lead - 156,000 pounds; GOLD - 143,000 opt; SILVER - 90,000 opt. out of a total tonnage of 159,000.

After visit to the Socorro Mine, return 4.2 miles to Salome-Buckeye road, make RIGHT TURN.

0.0 0.0 Turn onto Salome-Buckeye road and restart mileage log from this point.

2.1 2.1 Cross Centennial Dam and enter Harrisburg Valley. Centennial Wash is the single major drainage exiting McMullen Valley. The main McMullen Valley is ahead and is an unusual semi-isolated basin with a elongate NE-SW axis. Salome is at the southern end of the valley. The light-colored outcrop at the join between the Granite Wash Mountains and the southern Harcuvar Mountains is the 85 Ma Tank Pass Granite (a two-mica garnite). The age of the granite may be near the maximum age for thrust-fault motion between plates, in that only portions of this pluton are foliated or show the characteristic northeast lineation.

9.0 6.9 Road angling to SW to Salome Airpark, Indian Hills Estates also leads eventually to the Harquahala Mine.

9.2 0.2 Center of town of Salome at intersection with US 60 highway TURN LEFT. From a historical marker:

' SALOME WHERE SHE DANCED '

This desert town was made famous by the humour of Dick Wick Hall - Healthseeker and Operator of the Laughing Gas Station. Hall's publication, the SALOME SUN, was filled with extravagant tales of the Desert's adaptation of species. He told of his frog that was seven years old and never learned to swim.

10.7 1.6 (MP 55) Town of Harcuvar in 0.7 miles.

16.1 5.4 RIGHT TURN at intersection of U.S. 60 and AZ 72 to Bouse.

21.5	3.0	(MP 47) Rock shop on west.
24.4	2.9	Cross Central Arizona Canal.
27.3	0.2	(MP 44).
34.6	7.3	Utting siding.
42.7	8.1	Joshua road.
46.7	4.0	Saguaro Guards road.
53.5	6.8	(MP 17).
58.2	4.7	Junction with AZ 95, keep slightly to RIGHT to go to Parker.

DAY 2
ROAD LOG

ROAD LOG FROM PARKER TO COPPERSTONE MINE

Modified from the log of Stan Keith, Jan Wilt and Robert Scarborough (AGS Fall Field Trip, 1983).

The field trip will assemble in the parking lot of the Kasbah Motel, which is on State Route 62 on the northwest side of Parker just before the bridge across the Colorado River into California. The mileage for the log will commence at the intersection of State Route 72 and 95 with Mohave Road, which is on the southeast side of Parker just before the railroad crossing.

CUM MIL	INCR MIL	
0.0	0.0	Mohave Road. (Note turn-off to Parker hospital.) Stay on State Route 72 and 95 going south.
2.4	2.4	The northern extension of the Moon Mountains are at 12:00 to 1:00. The road for the next several miles traverses terraces in the alluvium related to the Colorado River drainage, which is off to the southwest.
4.1	1.7	The large butte at 9:00 is Black Peak ("P Mountain"). Black Peak is capped by a tilted middle Miocene (16 Ma) andesitic basalt sequence. These volcanics are overlain by flat-lying, younger basalt that are intercalated with clastic sedimentary rocks of about 8-15 Ma. Old Osborne Wash to the northeast.
4.4	0.3	Shallow road cut is in arrested dunes, which were developed by wind action although the source material was nearby, and are very well sorted, 100 feet thick or less, fluvial sands which originally rested on the Bouse Formation. The dunes contain eolian cross-bedding. Blow out pits in the dunes contain early Pleistocene remains of terrapins and/or terrestrial tortoises and other vertebrates indicative of near water, terrestrial conditions. The source bed sands of these dunes may be correlative with the Chemehuevi Formation farther north just south of the Lake Mead area.
7.4	3.0	The low terraced ridge at 2:00 to 3:00 is either Pliocene Bouse Formation or possibly older Osborne Wash Formation. An apparent unconformity can be seen at 2:30 between different phases of sedimentary material that underlie the terraced ridge. The large peak at 1:00 which is part of Mesquite Mountain is informally called Poston Peak (Keith and others, 1983) and is underlain by an undifferentiated gneiss

terrane. This assemblage of crystalline rocks at the southwest end of the Poston Peak area is apparently in contact with undifferentiated upper Paleozoic metasedimentary rocks. These rocks would presumably underlie the regional detachment faults in the Plomosa Mountains, which are southwest of here.

10.4 3.0 Turn right onto State Route 95, southbound for Quartzsite. Poston Peak at 3:00 after turning right.

10.8 0.4 Bridge over Bouse Wash.

17.5 6.7 To the east about eight miles away are the northern Plomosa Mountains. "The general geology of the northern Plomosa Mountains is best described as a sequence of low-angle faults that variously include older Cretaceous to early thrust faults and mid-Tertiary detachment faults at higher structural levels" (Keith and others, 1983). The Four Peaks area, which is at the northern end of the Plomosas consists of tilted, middle Tertiary, felsic to intermediate volcanics in the upper plate of the regional Plomosa detachment fault. This fault occurs mostly along the east side of the crest of the Northern Plomosa Mountains. Most of the crest line is Precambrian crystalline rocks of various kinds in the Bighorn Plate beneath the Plomosa detachment fault. This is the lowermost plate in the stacked, low-angle fault complex that pervades the northern Plomosa Mountains.

18.1 0.6 At 2:00 to 2:30 about five miles away are the Moon Mountains. The general geology of the Moon Mountains is depicted in enclosed Map 7, which also shows the location of Copperstone Mine. This area (excluding the mine lease) is currently being mapped as part of a doctoral program at M.I.T. by Jim Knapp. His mapping has identified three principal lithologies; Precambrian metasediments, gneisses and schists, Mesozoic sediments, and Cretaceous granitic intrusives. These lithologies form the lower plate assemblage of a low-angle detachment fault that outcrops at the northern end of the Moon Mountains. This fault (the Moon Mountain detachment fault) separates an area of pervasive detachment faulting northeast of the Moon Mountains from an area to the southwest, where these faults are absent (Jon Spencer, pers. comm., 1988).

The upper plate assemblage, which was transported to the northeast, is comprised of Mesozoic volcanics, which are very poorly exposed because most of these lithologies are covered by eolian sand. The detachment fault strikes NW-SE and dips to the northeast. Drilling on the Copperstone property indicates that this fault is undulatory and that it underlies the orebody at some depth. The Copperstone fault, that hosts the gold mineralization is in the upper plate of the Moon Mountain detachment fault. It is not known if the Copperstone fault is a splay off the underlying detachment fault. Where it has been drill intersected southwest of the mine, the Moon Mountain detachment fault does not contain gold mineralization.

20.9	2.8	Turn right onto the Cyprus Copperstone Mine road. This is a dirt road of 6.1 miles to the Office and Plant complex. After turning onto the mine road, dust should be a minimum, but please note the SPEED LIMIT on this road! As you drive west towards Copperstone there are two sets of dumps at 1:00. The dump to the left is the ore dump (>0.02 opt gold), which is on the color photo that is part of this guidebook, whereas the right dump is the "low grade waste" dump (0.010 to 0 019 opt gold).
27.0	6.1	Entrance to the Copperstone Mine. All vehicles will park outside gate and fence at the Office building, which is just inside the mine gate and to the left. As our group will be too large for a presentation in the office, we will given a geological presentation in the parking lot. This presentation will be by Graham Kelsey, the mine geologist, who co-authored the description of the mine especially for this guidebook.

After the talk by Graham Kelsey, we will visit the minesite and this will include a trip into the pit. So as to minimize the number of vehicles going into the pit, please try to have as many people per vehicle as is comfortable.

WHEN WE ARE IN THE PIT, WE WOULD ASK EVERYONE PLEASE TO EXERCISE AS MUCH CAUTION AS POSSIBLE AT THE PIT WALLS. THIS WILL MEAN NO CLIMBING UP OR DOWN THE WALLS, NO MATTER HOW TEMPTING THE SAMPLE!

GUIDEBOOK ARTICLES

A General Comment on FeOx-Gold Deposits and Gold Solubility

Supergene alteration, or weathering, of pre-existing pyrite generally results in common amorphous or very poorly crystalline Fe-oxides such as goethite and limonite. On the other hand, well-crystallized specular hematite is generally not associated with the supergene environment, however specularite is present at some gold deposits such as Copperstone, AZ, the Ross Mine and Kirkland Lake, Ontario as well as in gold deposits in the detachment fault environment. At moderately low temperatures ($\leq$250°C) gold is variably solubile under much of the same conditions in terms of oxidation state and pH where pyrite is stable. The common association of gold with pyrite in many types of precious metal deposits is explained by the fact that gold may be transported and deposited in equilibrium with pyrite. Gold deposits where native gold occurs with oxidized iron minerals therefore pose an interesting problem when viewed in light of the geochemistry of geothermal fluids and epithermal ore deposits (Berger and Bethke, 1985). If the specular hematite is hypogene and cogenetic with the Au, then certain constraints are put on the nature of the ore-bearing fluids as well as the possible modes of gold transport and deposition.

In the epithermal environment gold is generally transported as some sort of sulfide complex, where gold-bisulfide, or $Au(HS)_2^-$ is the dominant complex under neutral to slightly alkaline conditions (Figure 1). Maximum Au solubility occurs where the H_2S/HS^- boundary meets the SO_4^{2-} field. Because the stability field of hematite lies at higher aO_2 values, gold solubility will have decreased several orders of magnitude by the time the fluid is in equilibrium with hematite. This effectively precludes any gold-bisulfide transport giving rise to cogenetic gold-hematite associations.

FIGURE 1
Gold solubility as a function of Log aO_2 and pH at 100° and 250°C
Modified from D.M. Shenberger, 1985 M.S. Thesis Penn State University.

Diagrams are registered with respect to Log aO_2 axes.

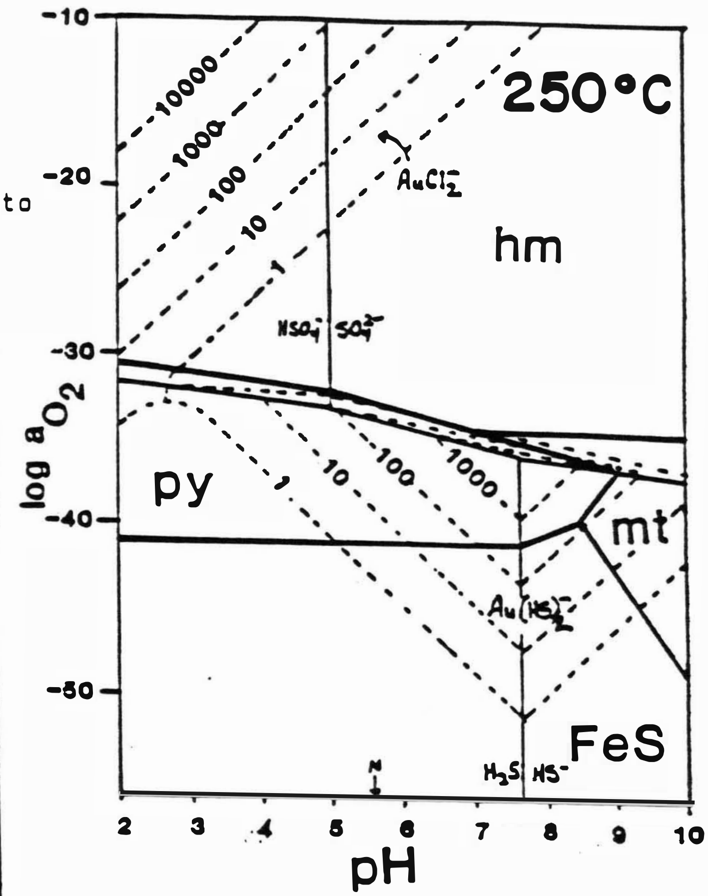

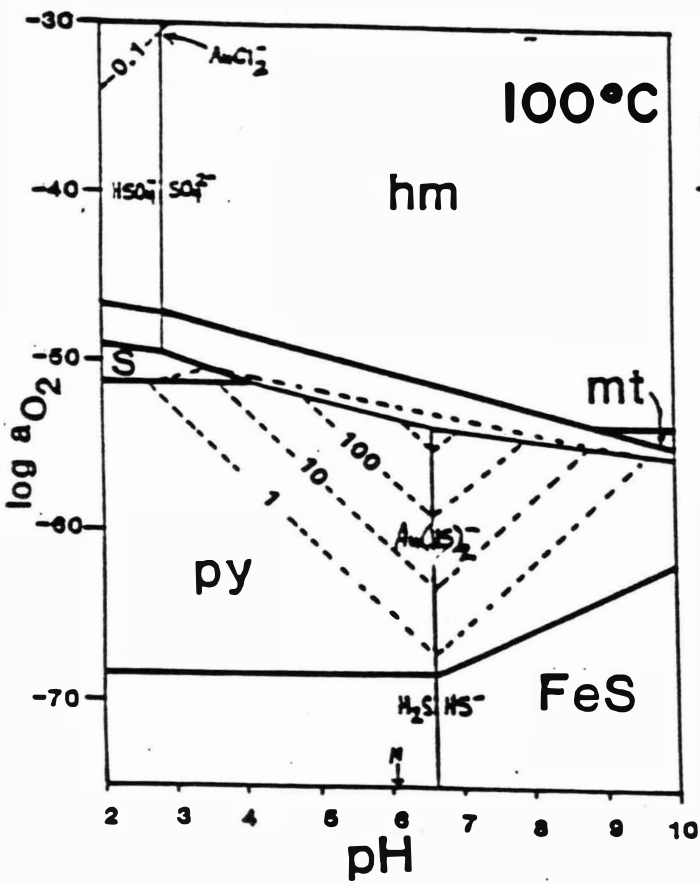

In both figures total chloride activity is equal to 1.0 and the total sulfide activity is equal to 0.01. The stability fields for the dominant iron minerals are shown by heavy lines and those for the sulfur species by light lines. The solubility contours for gold are shown by dashed lines and labeled in ppb.

Note how at higher temperatures the region of $AuCl_2^-$ solubility expands considerably and begins to coincide with the stability field of hematite over reasonable pH ranges. Both higher temperature and higher salinity promote Au-chloride solubility (Cathles, 1987). Gold deposition would be promoted by cooling, increasing pH, reduction through rock-water interaction or mixing and dilution with another fluid.

Figure 2 is similar to Figure 1 but calculated for an intermediate temperature of 200°C. Figure 2 also shows the topology for iron solubility countours as well as a reference point for Kaolinite/Muscovite stabilities. It is interesting to note how Fe solubility is also promoted by lower pH values, and that at the neutral to slightly alkaline pH conditions which optimize gold-bisulfide transport, the fluid effectively has minimal transport capacity for dissolved Fe. At more oxidizing conditions Fe-hydroxide complexes may significantly contribute to iron solubility.

Figure 2. Solubility of Au and Fe as a function of fO_2 and pH, along with speciation of dissolved S and Fe mineralogy at 200°C. Data from Seward (1973, Au-S complexes), Walshe and Solomon (1981, Fe solubility), EQ3 database of Wolery (1979, Revision of Nov. 1981) and Helgeson (1969, Au-Cl complexes, muscovite-kaolinite). Activity of $K^+=10^{-1}$, based on Na/K=10 and 1 M Na^+. Diagram by A.W. Rose, Penn State, 12/83

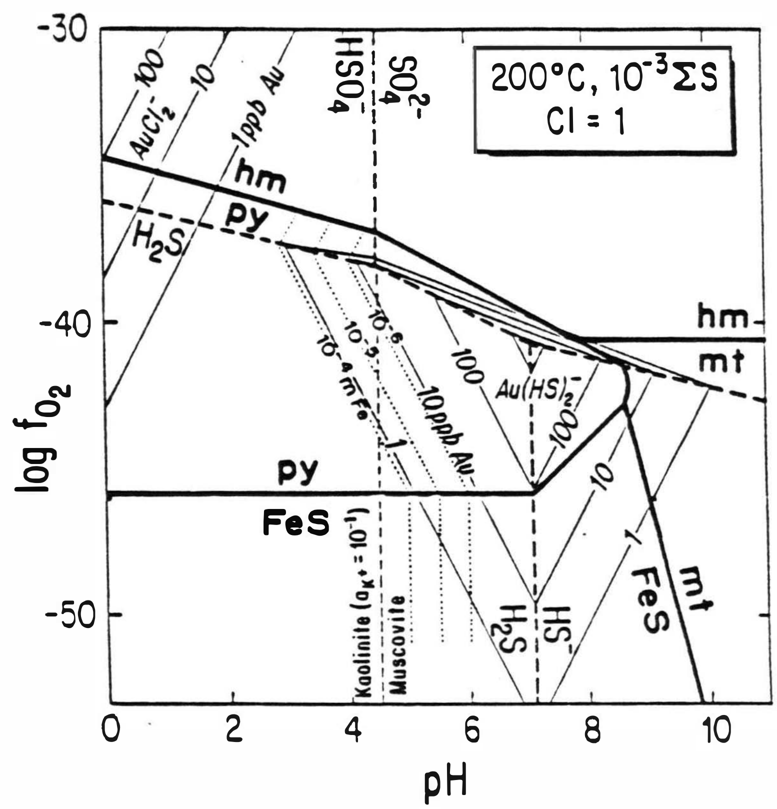

Fluids which can transport Au under oxidizing conditions are necessarily of low pH and high chloride content and therefore would also have ample transport capacity for silver and base metals. In gold deposits associated with cogenetic hypogene iron oxides this should be reflected by the absence of high Au/Ag ratios and anomalous Cu, Pb, and Zn as opposed to the more typical epithermal assemblage of As, Sb, Hg and Tl. Low-pH alteration assemblages such as carbonate removal and/or argillization of K±Al-bearing phases in igneous rocks would also be expected. Deposition of hypogene alunite would also be possible under very low pH and oxidizing conditions if ample sulfur were available.

REFERENCES ON GOLD SOLUBILITY

Berger, B.R. and Bethke, P.M., eds., 1985, Geology and Geochemistry of Epithermal Systems, Reviews in Economic Geology, V. 2. In particular chapters 1-2 by R.W. Henley and K.L. Brown, pp. 1-44.

Cathles, L.M., 1987, The geologic solubility of gold from 200-350°C, and its implications for gold-base metal ratios in vein and stratiform deposits: Can. Inst. Min. Met. Special Vol. 38, pp. 187-208.

Shenberger, D.M., 1985, Gold Solubility in Aqueous Sulfide Solutions: M.S. Thesis, The Pennsylvania State University, State College, PA, 102 p.

Seward, T.M., 1984, The transport and deposition of gold in hydrothermal systems: (in) Foster, R.P., ed., Gold '82: The Geology, Geochemistry and Genesis of Gold Deposits, Geol. Soc. of Zimbabwe Special Pub. No 1, pp. 165-181.

CONDITIONS OF GOLD MINERALIZATION IN THE DETACHMENT FAULT ENVIRONMENT

Richard Beane, Joe Wilkins, Jr.
Dallhold Resources, Inc., Tucson, AZ

Tom Heidrick
Chevron Oil Field Research Co., La Habra, CA

* *from a talk presented at the 1986 Arizona Geological Society meeting "Frontiers in Geology and Ore Deposits of Arizona and the Southwest", Tucson*

The material presented here is drawn from investigation of several gold prospects in detachment fault environments. The X's on Figure 1 show a number of locations in Arizona where gold mineralization occurs related to detachment faults. Predominant among these are the Picacho and the Copperstone deposits. The Planet District, located in the Buckskin Mountains and shown by the circled X on Figure 1, will be used as a prototype.

Figure 2 is a schematic cross-section which illustrates some of the geologic features of the detachment fault environment. A low-angle dislocation surface along which detachment faulting occurred is indicated by Line A-B. Lower plate crystalline rocks are crosscut by a low angle mylonitic fabric which is shown by the dashes (C). The mylonitic fabric increases in intensity moving upward, and merges into a chloritic breccia immediately below the detachment fault (D). Within the upper plate are sets of rotational listric-normal faults which flatten and merge into the detachment fault (Line E-F and parallel lines). High-angle tear faults in the upper plate strike parallel to movement of the detached block and perpendicular to the listric faults. Such a tear fault might make up the surface in the upper plate upon which the cross-section shown in Figure 2 is drawn.

Chlorite occurs at the detachment and in overlying listric faults (eg., G). Blocks of calcium carbonate of uncertain origin (H) appear above the detachment fault. Iron and copper mineralization of approximately the same age as detachment faulting has three modes of occurrence at or immediately above the detachment fault: 1) massive replacements in silicified and brecciated marble, 2) granulated, smeared-out bodies within and immediately above the detachment, and 3) open-space fillings in breccia zones related to listric faulting.

Two distinct mineral assemblages are recognized in the detachment fault environment. A *sulfide* assemblage consisting primarily of chlorite, specular hematite, chalcopyrite and pyrite occurs at the detachment fault or in related listric faults. An *oxide* assemblage composed of goethitic hematite, chrysocolla, muscovite, barite and calcite is most common in high-angle tear faults and adjacent listric faults. The oxide assemblage is usually later than the sulfide assemblage, with goethitic hematite replacing earlier-formed iron-magnesium chlorite or pyrite.

The sulfide assemblage is often seen to have undergone extensive supergene oxidation to chrysocolla and pulverulent limonite. The hypogene oxide assemblage is distinguished by dense chrysocolla which is not hygroscopic, and by dense goethite (often replacing chlorite) commonly with a lack of related boxworks which indicates the absence of pre-existing sulfide minerals.

A detailed study in the Planet area showed gold occurred only in association with the oxide assemblage. Gold contents of sulfide assemblage samples were very low, dominantly less than ten parts per billion gold. The only significant concentrations of gold with the sulfide assemblage occurred where this was cut by later fracture-fillings of the oxide assemblage. Figure 3 is a plot of coupled gold and copper contents of a group of dump samples. This diagram shows that whereas gold does not occur without copper, the reverse is not true. This is because gold accompanies chrysocolla from the oxide assemblage, but not chalcopyrite from the sulfide assemblage. Note that a significant portion of these dump samples have gold contents in excess of one part per million.

Approximately 300 fluid inclusions were analyzed from a prospect where the gold-bearing oxide assemblage replaces earlier chlorite and specularite (Figure 4). Sulfide minerals were not deposited with the chlorite and specularite at this location. Figure 5 is a histogram of fluid inclusion homogenization temperatures which have been resolved into two families. An early generation of quartz alone formed near 290°C. Homogenization temperatures for fluid inclusions with the intermediate stage of chlorite and specularite have a mean value of about 245°C. No quartz or other transparent minerals were related paragenetically to gold, so the formation temperature of mineralization could not be determined directly. Statistical analysis of the data related to quartz-chlorite-specularite (Figure 6) shows this population is composed of two subsets, one with a mean of 244 $^{+}$-12°C and the other with a mean of 244 $^{+}$-20°C. One of these is probably related to gold mineralization. No evidence of boiling was observed.

Figure 7 is a plot of fluid inclusion homogenization temperatures versus equivalent molal sodium chloride salinities for two locations. The crosses are data from the prospect described above. Salinities from 12 to 22 weight percent NaCl equivalent occur over a 60°C range in homogenization temperatures, and there is no systematic relation between the two parameters. The dots represent fluid inclusions from the Mineral Hill copper mine occurring in the detachment fault, and thus are representative of the sulfide mineral assemblage. The sulfide assemblage fluid inclusions have a mean salinity of slightly more than three molal NaCl equivalent (about 15 weight percent). As at the prospect, no evidence of boiling was seen in inclusions from the Mineral Hill Mine. Petroleum products were present in some of the fluid inclusions from the Mineral Hill Mine.

Figure 8 is a mineral stability diagram for the system Cu-Fe-S_2-O_2 at 300°C in terms of the chemical activities of sulfur and oxygen. The minerals shown (labeled) are pyrrhotite (po), pyrite (py), hematite (hm), and a minimum stability field for the iron component of chlorite (chl). The area enclosed by the dashed line is the region where chalcopyrite coexist with the various iron minerals. Bornite coexists with the iron minerals immediately outside the chalcopyrite stability field. The line between Points A and C indicates conditions under which hematite, pyrite, and chalcopyrite can coexist. Above Point A chalcopyrite is no longer stable. At Point C, chlorite joins the hematite, pyrite and chalcopyrite. The dotted line passing through Point B represents a minimum stability boundary for calcite relative to anhydrite and wollastonite in the presence of quartz. Increasing carbon dioxide pressure moves this dotted line toward the upper right on the diagram. Observed mineral assemblages in the Planet and other areas indicate that oxygen and sulfur activities attending formation of the sulfide assemblage lay somewhere along the line between Points B and C, possibly extending up to Point A.

Figure 9 shows mineral stability relations for the oxide assemblage at 225°C, again in terms of the activities of sulfur and oxygen. This temperature was chosen, based on fluid inclusion data and mineral stability considerations, as representative of oxide assemblage mineralization. The phases observed for this assemblage are hematite (hm), chrysocolla (xc), muscovite (mus), barite (bar), calcite (cal) and gold. The hematite plus chrysocolla stability region places a lower limit on oxygen activity (vertical Line A-B). The presence of muscovite rather than alunite places an upper limit on the oxide environment (diagonal Line C-D). Stability of calcite rather than wollastonite in the presence of quartz defines a minimum partial pressure of carbon dioxide. Use of this partial pressure in the barite-witherite reaction, shown by diagonal Line E-B, provides a lower limit on conditions of formation of the oxide assemblage which extends below Point B on this diagram. The area on the diagram corresponding to the oxide assemblage is shaded. The field extends to higher values of oxygen activity with corresponding decrease in sulfur activity.

The relative positions of the sulfide and oxide mineral assemblages in terms of the activities of sulfur and oxygen are shown on Figure 10. The oxide assemblage is formed at higher oxygen activities than the sulfide assemblage. The most distinctive difference between the two assemblages, however, is the drastically lower activities of sulfur for the oxide phases. Calculated total concentrations of dissolved sulfur for the two assemblages are comparable, although they exist in different forms: sulfide for the assemblage with the same name, and sulfate for the oxide assemblage.

At any position on a diagram such as Figure 10, oxygen and sulfur activities can be used to calculate gold solubilities as chloride and bisulfide complexes as a function of solution pH at appropriate temperatures using equilibrium constants for the following reactions:

$$Au + S_2 + 1.5\ H_2O = Au(HS)_2^- + 0.75\ O_2 + H^+$$

$$Au + 2\ Cl^- + 0.25\ O_2 + H^+ = AuCl_2^- + 0.5\ H_2O$$

The first equation defines dissolution as the gold bisulfide complex, and the lower equation shows dissolution of gold as the chloride complex. Temperature and chloride activity are determined from fluid inclusion analyses. Gold solubilities are calculated as a function of solution pH at oxygen and sulfur activities determined using mineral stability relations as described previously. Gold solubilities for the sulfide and oxide assemblages as a function of solution pH are shown on Figure 11. The dashed lines are 300°C solubilities for Points B and C on Figure 8. Gold dissolves as the chloride complex in acid solutions and as the bisulfide complex at pH values above about five. The solid line is the minimum gold solubility for the oxide assemblage at 225°C. This solubility is entirely as the gold chloride complex. As oxygen activities increase above that for the chrysocolla-cuprite (cr, Figure 9) equilibrium boundary, so too does the solubility of gold with the oxide assemblage as shown by the arrows.

At temperatures such as these, acid/base neutrality lies at a solution pH of about 5.5. Cation mass transfer and mineral stability relations for the sulfide and oxide assemblages indicate that solution pH values must have been at least moderately acidic. Below a pH of 4.5, which is only about one unit below neutrality at the temperatures being considered, gold solubilities for the oxide assemblage are at least two orders of magnitude higher than for the sulfide assemblage. This significant difference in gold solubilities between the two assemblages under moderately acidic conditions leads to two conclusions:

1) The high gold contents seen with the oxide assemblage compared to the sulfide are probably a direct result of the differences in gold transport capacity of the different fluids which formed these two assemblages.

2) The oxide assemblage fluids reached gold saturation at higher concentrations than those permitted for the sulfide assemblage. Therefore, the oxide assemblage fluids are not simply oxidized sulfide assemblage fluids, but have evolved independently.

Fluids responsible for both mineral assemblages in the detachment environment exhibit comparably high salinities. This suggests a common source for the two different fluids. The occurrence of the petroleum products in some detachment fluids, the high fluid salinities, and consideration of the geologic features of the detachment fault environment, lead us to suggest that the mineralizing fluids were originally saline basin brines.

We suggest that brines were initially heated in middle Tertiary graben-type basins (Figure 12) by the high geothermal gradient attending the extensional environment. The driving force for moving these brines into the detachment fault and overlying plate could have two origins. The first is simple basin expulsion resulting from overburden compaction as has been suggested for the Mississippi Valley-type deposits. We propose another possibility which is lateral compaction or compression at the leading edge of the detachment plate, moving as shown by the upper arrow.

The basin fluids would be chloride brines carrying significant concentrations of magnesium, iron, and copper with moderate amounts of sulfide sulfur. The temperature of these brines is estimated to have been on the order of 225°C, the necessary heat having been supplied by an abnormally high geothermal gradient related to the extensional tectonic environment. The basin fluids were driven along the detachment fault and then upward into listric and tear faults as shown by the solid arrows. The fluids moving in this manner retained their originally reducing character and precipitated chlorite and the other sulfide assemblage minerals. The temperature of the sulfide assemblage fluids was raised above that of the parent basin brine by heat provided by the crystalline lower plate rocks and from friction generated by plate movement.

Fluids moving at higher levels in the upper plate along tear faults, shown by the striped arrows, were more oxidizing in character. The oxidation is suggested to have been provided by mixing with <u>minimal</u> amounts of shallow ground water. Mixing of the parent basin brines with large fractions of shallow waters would increase the oxygen activity of the original fluids, but would also decrease the temperature and salinity of the brines. These factors would diminish the capacity of the fluids to dissolve gold as the chloride complex. Gold deposition resulted where the tear faults provided access of the oxidizing fluids to earlier-formed chlorite or pyrite which serve as reducing agents. Oxidation of chlorite resulted in generation of the goethitic hematite and muscovite observed as part of the oxide assemblage.

Calculated gold contents of the high-level fluids were significant, but they were lower in both the deeper fluids forming the sulfide assemblage and in the presumed parent basin brine. The single most important chemical characteristic leading to the gold transport capacity of the high-level fluids was their high oxygen activity which is defined by the hydrothermal chrysocolla. Our model requires acquisition of the dissolved gold <u>after</u> the brines were oxidized. This requires that gold carried by these fluids was derived from the rocks in the upper plate of the detachment fault through which the oxidizing fluids migrated.

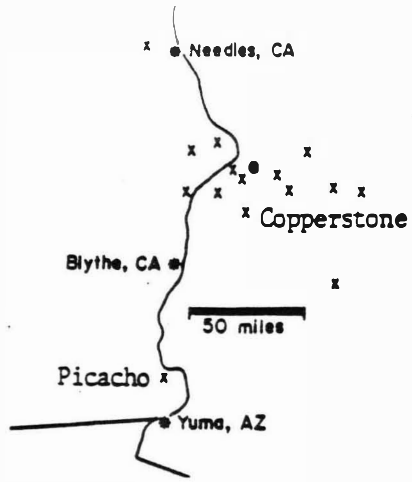

Figure 1. Detachment-related gold along the Colorado River.

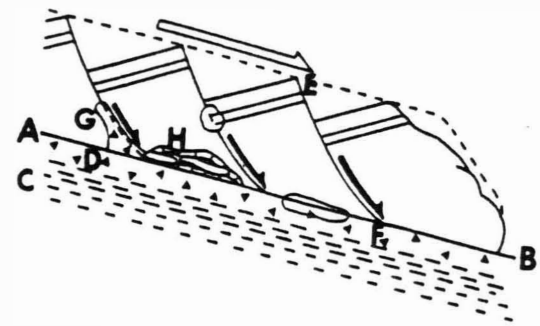

Figure 2. Geologic features of detachment-related mineralization.

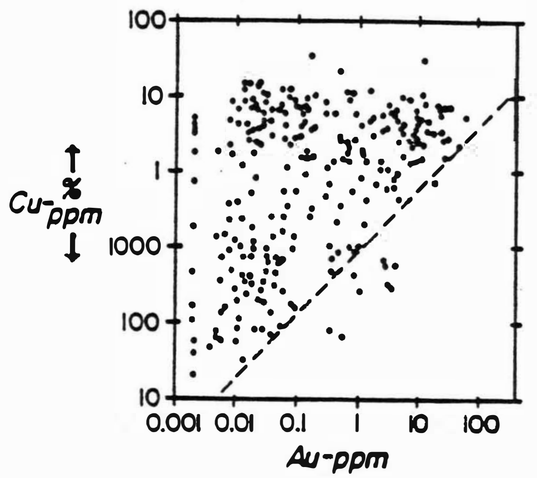

Figure 3. Gold and copper contents of dump samples.

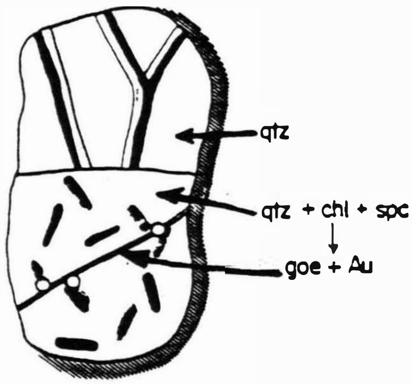

Figure 4. Paragenetic relations among hydrothermal minerals.

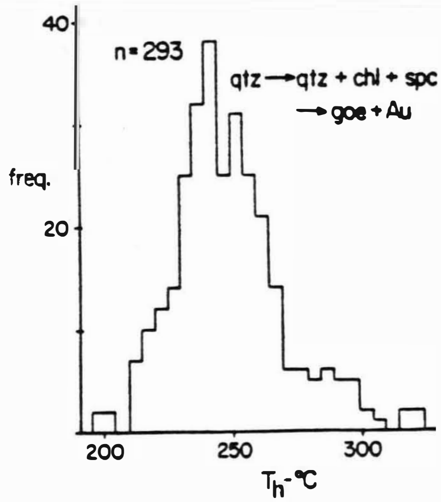

Figure 5. Fluid inclusion homogenization temperatures from combined assemblages.

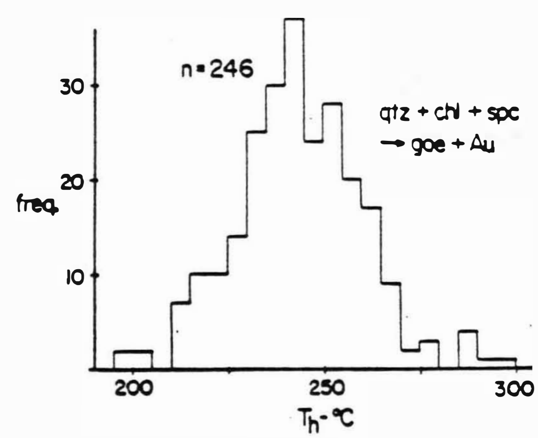

Figure 6. Fluid inclusion homogenization temperatures for mineralizing stages.

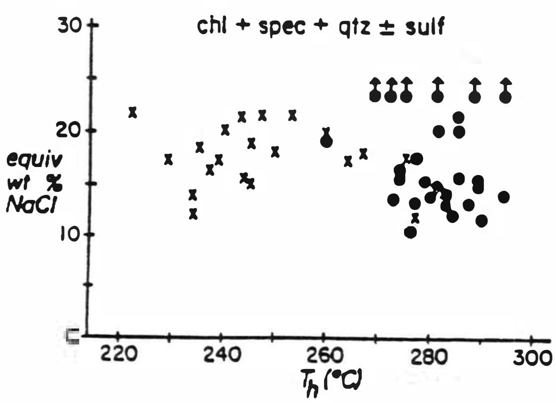

Figure 7. Fluid inclusion homogenization and melting temperatures.

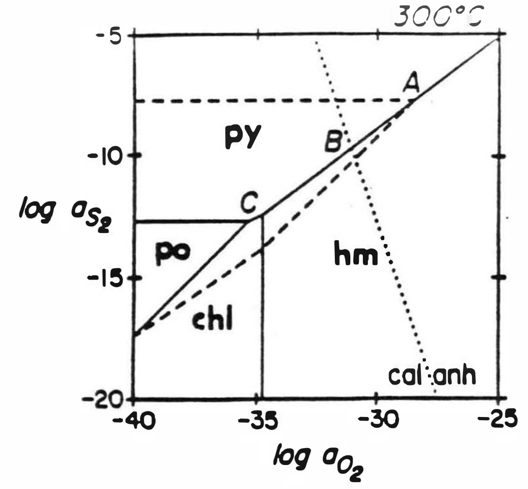

Figure 8. Stability relations of the sulfide assemblage minerals at 300°C

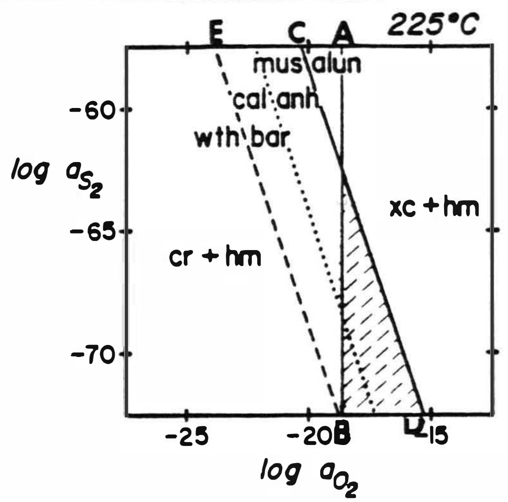

Figure 9. Stability relations of the oxide assemblage minerals at 225°C.

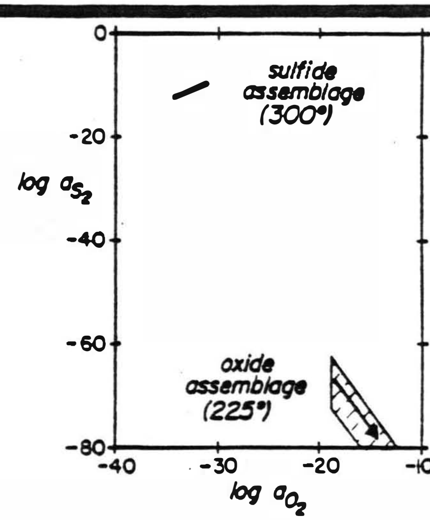

Figure 10. Comparison of mineral stabilities for the hydrothermal assemblages.

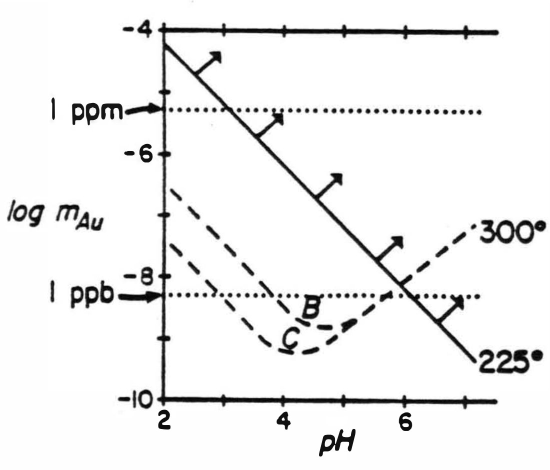

Figure 11. Gold solubility for the sulfide and oxide mineral assemblages.

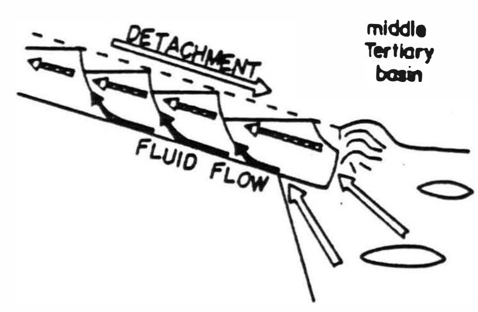

Figure 12. Suggested model for fluid flow and mineralization.

Data kindly furnished by:
Stanley B. Keith,
Magmachem Exploration Inc.
Ahwahtukee Professional Building
10827 South 51st Street, Suite 202
Phoenix, AZ 85044

PART II: DETAILED GEOLOGICAL AND
GEOCHEMICAL INVESTIGATIONS OF THE
SOCORRO REEF GOLD ANOMALY

Introduction

During geologic mapping and geochemical sampling on the Socorro Mining Corporation property in early April 1982 an intriguing alteration anomaly in the Bolsa Quartzite on the Palo Verde and Bluebird claims was encountered (See panorama in Figure 18A and 18B). The general geographic position of the Socorro Reef gold anomaly is shown on Plate 5. Eleven geochemical samples from the alteration anomaly all yielded weakly anomalous to strongly anomalous gold values (.016 to 6.0 ppm). Following my initial recommendation for further work on the gold anomaly (unpublished report dated May 3, 1982), at Socorro Mining Corporation's request I began negotiations with major mining companies in May, 1982 to obtain additional surface information on the gold anomaly which has been named the Socorro Reef gold anomaly. Subsequent visits to this ground by myself and numerous major mining companies have led to the acquisition of abundant surface data that strongly suggests the presence of a major, low-grade, large-tonnage, disseminated gold deposit with an indicated gold value of over 340 million dollars (at $450/oz) in over 35 million tons. Part I developed a regional disseminated gold model that was applied to the Salome region in general; this regional model was derived from data at the Socorro Reef gold anomaly and surrounding mineral deposits. Part II develops a detailed, site-specific, geochemical and geometric model for the disseminated gold deposit that is inferred to lie beneath the Socorro Reef gold anomaly.

Exploration and Development History

The history and development of the Socorro Peak area is strongly tied to the discovery of bonanza gold ores in 1888 at the Harquahala (Bonanza) Mine in the Little Harquahala Mountains 10 miles to the southwest (See Table 1 in Part I). By 1905 gold mineralization had been discovered and was being developed at the old Socorro Mine in the Socorro Peak area. The exploration and development of mineral deposits in the Socorro Peak area can be divided historically into four periods - before 1969, 1969-1979, 1979-April 1982, and April 1982-December 1982.

EARLY DEVELOPMENTS (BEFORE 1969)

The yearly reported production from mines in the Socorro Peak area is listed in Table 12. Three mines (the Socorro Mine, Mars and Mescal Mine, and Why Not Mine) operated discontinuously from 1905 to 1938. The exploration and development history for each of these mines is summarized below.

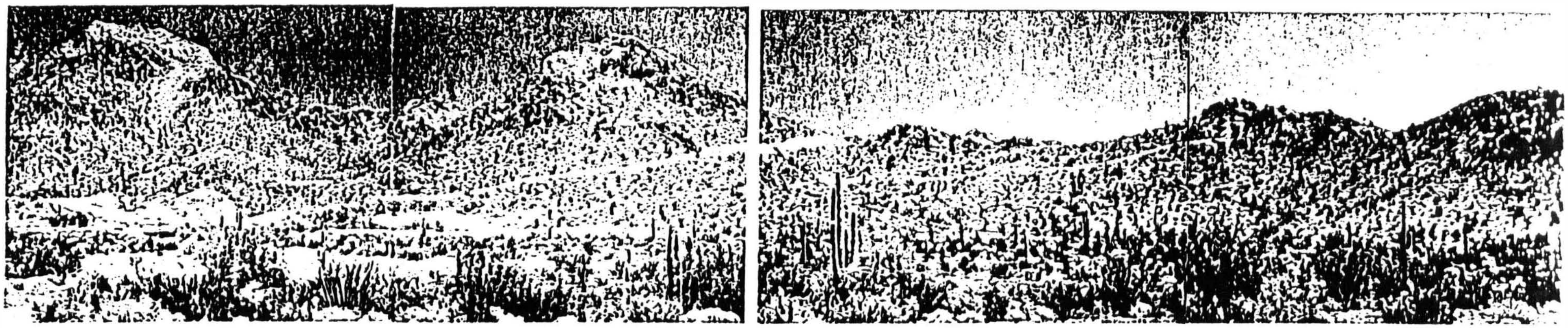

Figure 18A. Photographic panorama of Socorro Reef gold anomaly. The Socorro Mine and mill site at the northeast end of the anomaly is at the left of the panorama.

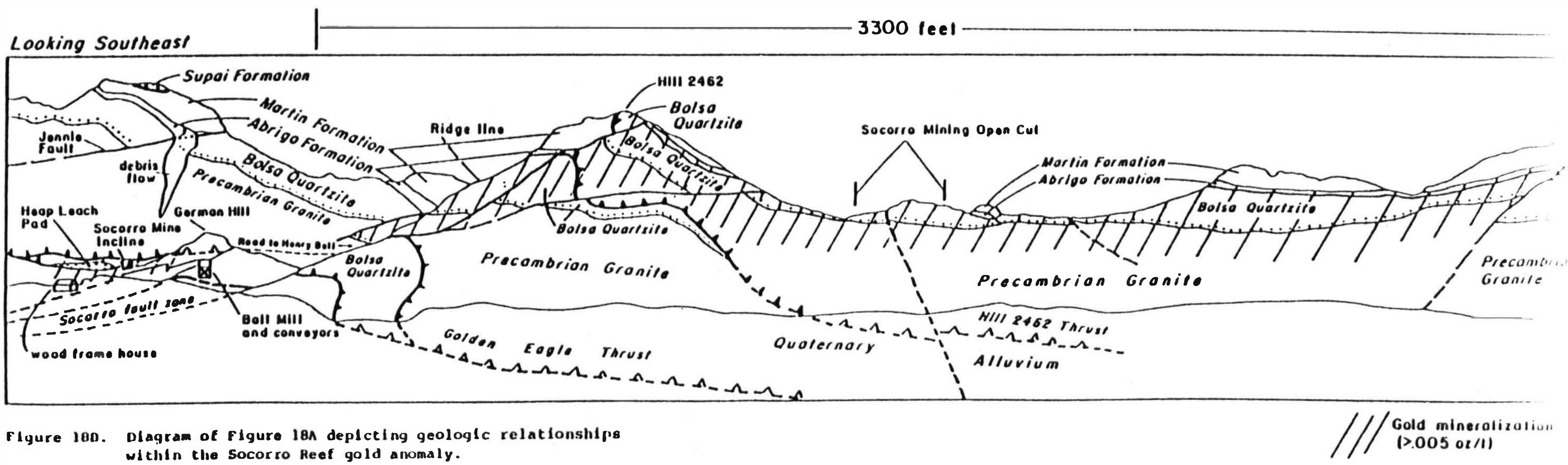

Figure 18B. Diagram of Figure 18A depicting geologic relationships within the Socorro Reef gold anomaly.

Table 12: Reported Production by year for mines within the Socorro Mining Corporation Property Position

Socorro

Operators: Death Valley, R.A. Salisbury, Gilbert and Schmidt, Socorro Gold Co., Socorro Mines, Inc.

Year	Ore Treated (Short Tons)	Gold	Silver	Lead	Au:Ag
1905	2200	230	145	-	1.59
1906	1461	207	122	-	1.69
1911	570	134	62	-	2.16
1913	59	59	37	-	1.59
1914	25	31	5	-	6.2
1934	60	18	12	-	1.5
1935	411	4	88	50	.045
Totals	4786	683	471	50	1.45

Iron Door 1 & 2 (Mars & Mescal)

Operators: Jerome Wenden Co., Nuevo Mundo

Year	Ore Treated (Short Tons)	Gold	Silver	Copper	Au:Ag
1916	56	15	18	15,234	.83
1917	21	1	8	6,746	.125
1918	32	0	30	1,876	-
Totals	109	16	56	28,856	.286

Iron Door 3 & 4 (Why Not)

Operators: Kuisto & Smith, A.E. Lang & Gilbert, A.E. Lang, T.F. Johnson

Year	Ore Treated (Short Tons)	Gold	Silver	Copper	Au:Ag
1932	41	37	40	0	.925
1933	142	112	134	960	.836
1934	65	16	75	0	.213
1935	30	25	90	338	.278
1936	8	2	1	0	2.0
1937	24	6	10	46	.60
1938	85	35	139	268	.252
Totals	395	233	689	1,612	.338

Socorro and Henry Bell Mines

The majority of the reported production in the Socorro Peak area was in 1905 and 1906 when the Socorro Mine produced 3461 tons of ore that yielded 437 ounces of gold and 267 ounces of silver. In 1901 the Socorro Gold Mining Company acquired the mine and within four years sank a 375-foot inclined shaft and developed 2300 feet of drifts away from the shaft. A 20-stamp mill equipped for amalgamation, concentration, and cyanidation was built in 1904. Intermittent operations from 1905 to 1914 yielded about $20,000 in gold bullion from at least 661 ounces of gold extracted from over 4000 tons of ore. In 1934 the Socorro Mine produced 60 tons of ore that yielded 18 ounces of gold.

The 1935 production listed under the Socorro Mine label may not actually have come from the Socorro Mine, but rather could have come from the Henry Bell property .3 mile southeast of the Socorro Mine site. The 1935 production listed from the Socorro Mine is predominantly silver production. The gold:silver ratio of the 1935 production is .045, which is very similar to geochemical results from recent drilling and sampling on the Henry Bell claim by Socorro Mining Corporation and Noranda in 1982 (Figure 12). The grades of the Socorro Mine production are plotted sequentially by year on Figure 9. All of the grades fall within the Socorro Reef gold anomaly field except the 1935 production, which plots in the Henry Bell field. In addition, George Campbell, Sr. has informed me that he worked as a miner at the Henry Bell property in 1934-1936 when the property was being developed by an adit. At that time the adit was connected by an aerial tramway to a millsite near the bottom of an unnamed canyon 500 feet southwest of what is now called the Henry Bell tunnel. Only the foundation for this mill remains today and no remains of the former tramway were noted during my mapping. According to George Campbell the mill did process some ore, which could well have been the 1935 production reported under the Socorro Mine label. The Henry Bell property was offered to ASARCO in 1936 and the results of their 1936 sampling are included with the ASARCO data in Appendix IX.

Why Not Mine

During my field work in 1982 claim notices were found in the NW 1/4 of Sec. 36, T.5N., R.12W. for the Jessie Allard claim located by W.J. Stoke on June 8, 1916. These claims were at least partially relocated under the Why Not Gold label on April 30, 1930 by Thomas F. Johnson and A.E. Linnell. It is probable that at least 16 Why Not Gold claims were located at this time. These claims are most likely related to the production in 1932-1938 from the Why Not Mine (Table 12). Most of this production probably came from numerous pits and adits in the NE 1/4 of Sec. 25 and the SE 1/4 of Sec. 24, T.5N., R12W. Geochemical values of samples from these locations closely approximate the recorded production (Figure 12).

Mars and Mescal Mine

During World War I the Mars and Mescal property produced 109 tons of copper ore from 1916 to 1918. The copper production most likely came from adits and inclined shafts in gold-bearing jasperoid lenses in the SE 1/4 of the NW 1/4 of Sec. 19, T.5N., R11W. Geochemical values of samples taken by Socorro Mine Corporation and by Noranda at this location closely approximate the reported production from the Mars and Mescal property (See Figure 12).

Other Activity

Reports for the Campbell family by Thomas C. King Engineering in 1973 indicate that during 1927 and 1928 a company named the El Tigre Mining Company of old Mexico evaluated much of the Socorro Peak area. King reportedly had information that the El Tigre Mining Company took possibly 5000 samples and assays during two separate channel campaigns. Various sample cuts were reportedly found by King on the Henry Bell and Tres Padres claims. In addition, King claims the El Tigre Mining Company concluded that there was an indicated 16,000,000 tons assaying .179 troy ounces of gold per ton in the Socorro Peak area between the Henry Bell claim and the Iron Door claim. No sample or assay results substantiating this gold grade have been conveyed to me. However, independent mapping and sampling by myself and Noranda fail to find anything even close to the reported El Tigre numbers.

Since 1935 there has been no reported production from mines in the Socorro Peak area and little is known of any verifiable exploration or production activity, except for claim staking in February of 1958, when George W., Sr., Henrietta, and John S. Campbell located the Henry Bell claim. There are reports that high grade pockets of gold ore were encountered in the Socorro Peak area (See King Engineering report of 11/24/72 in Appendix II), but none of these reports has been substantiated to date. Apparently the material that was taken out was processed by arrastre milling in Harrisburg, where the remains of numerous arrastres are reported to still exist.

DEVELOPMENT 1969 - 1979

On March 8, 1969, George Campbell, Jr., Robert K. Barritt, and Frank Sayre located the Tres Padres claim .3 miles northeast of the Socorro Reef gold anomaly. Thus began a new period of exploration and development in the Socorro Peak area. In June and July of 1969 George W. Campbell, Sr., located the Yellow Gold No. 1 claim, the Palo Verde No. 1 claim, and the Bluebird claims over what is now the center of the Socorro Reef gold anomaly. In May of 1973 Thomas C. King, George Campbell, Jr., and Hayden S. Brown located the Iron Door claims over what formerly had been the Mars and Mescal and the Why Not properties of earlier years. Also, Carl F. Ludwig located the Socorro claim on May 27, 1972, and the Socorro Annex claim in September of 1973. In June 1974 the Campbell family, in association with nine other parties (the Socorro Reef

Association) located the Reef Group of claims. (See Plate 1 for specific locations of all of the aforementioned claims). Between 1974 and 1978 the Socorro Reef Association leased the above mentioned claims to B and B Mining Co., now a member of the Noranda group. From conversations with George Campbell, Jr., B and B Mining sampled the Henry Bell claim, put in most of the open cuts, and stockpiled some of the mineralized material taken from the open cut. Following these operations they terminated their lease. I have not seen any assays or reports relating to the B and B Mining Co. work, although George Campbell, Jr., indicated that he has copies of material relating to this activity.

After the B and B Mining Company involvement and probably in early 1978, Campbell and associates leased the property to Jordan Industries Inc., a Utah-based company. Jordan Industries attempted to mine the block of ground beneath the old Henry Bell adit on the Henry Bell claim by open-cut techniques. They added an additional bench, installed a milling facility with a stated 1000 ton/day crushing capacity, and reportedly stockpiled at least several thousand tons of Henry Bell material on the old Socorro Mine dump. Mr. Joe Behunin was the principal representative for Jordan Industries during this time (early 1978 to early 1979). So far as is known no production was ever realized from these operations. Various reports and assay results for the 1969 to 1979 period are presented chronologically in Appendix II.

DEVELOPMENT 1979 - APRIL 1982

In 1978 and 1979 Jordan Industries experienced financial difficulties in raising capital to develop the Henry Bell claim and initiated bankruptcy proceedings. On April 23, 1979, the leases with Jordan Industries (i.e., Behunin and others) expired and the Campbell family locked the gate and had an injunction issued against Behunin to keep him off the property. My understanding is that in the spring of 1979 Mr. James M. Jacobson, Sr., and Simon Srybnik of Brooklyn, New York were shown the property by Mr. Behunin; they were favorably impressed and formed Socorro Reef Mining Company to infuse new capital into the Jordan Industries operation to get the property into production. After several reports (in chronological order in Appendix III) had been prepared by several different consultants who reached mostly favorable conclusions, Socorro Reef Mining Company entered into a joint venture with Jordan Industries to continue developing the property. However, sampling of the Henry Bell claim by Socorro Reef Mining Company personnel (Jake Jacobson, Jr., personal communication, May 1982) failed to substantiate the high gold values of the earlier reports. (See assay certificate dated October 17, 1980, Appendix III). Consequently, Jake Jacobson, Jr., sampled an area in the Bolsa Quartzite in a saddle where Behunin had formerly drilled several shallow percussion holes about 1/2 mile west of the Henry Bell adit. He obtained encouraging results that averaged .0153 ounces per ton of gold (See assay certificate dated November 20, 1980, Appendix III). These data are from the center of what would later become known as the Socorro Reef gold anomaly. On the basis of the assay results dated November 20, 1980, Socorro Reef Associates decided to develop a small open pit in the quartzite and to heap leach material taken from the pit. Socorro Reef Mining Company then commissioned Duane Grey to design and operate the heap leach pad. By late February 1981 precious metal-bearing solutions were being recovered from a leach pad from approximately 30,000 tons of material that had been placed above the Henry Bell material on the old Socorro Mine dump. Resampling of material from within the pit yielded discouraging results, but 37.7 troy ounces of metal (in six pieces that contained 66% gold) were recovered from leach solutions before recovery problems set in at the leach pad (Jake Jacobson, personal communication, May 1982). Much of the equipment currently on the property (see Appendix XII) relates to this period of activity.

On May 15, 1981, a new lease was signed between Socorro Reef Mining Company (Socorro Reef Associates) and the underlying property owners (the Campbell family and associates) to bring the property into full production within one year. After the lease was signed $10,000 of drilling totalling 600 feet was done from June 1, 1981 to June 4, 1981 by Arizona Drilling Services Company to explore for possible gold ore on the Palo Verde, Socorro, and Henry Bell claims. This drilling was done under the direction of Duane Grey, the heap leach operator, and Bob Rose, an accountant in Scottsdale, Arizona. The analytical results of this drilling are presented in Appendix X.

DEVELOPMENT APRIL 1982 - DECEMBER 1982

As part of the lease dated May 15, 1981, Socorro Reef Associates (now Socorro Mining Corporation) had to geologically assess gold deposits on the Iron Door and Tres Padres claims and, if geologic studies indicated the gold occurrences were economically feasible, Socorro Reef Associates was required to develop the area by roadwork and drilling. Initially Jake Jacobson of Socorro Reef Associates contacted Noranda Exploration Inc. in Tucson, Arizona, about examining this area. After an initial visit to the property in early 1982, Noranda conducted follow up sampling in mid-March 1982. However, it became apparent that Noranda would not be able to make a detailed geologic assessment of this ground available to Socorro Reef Associates by May 15, 1982, the expiration date of the 1981 lease. Hence, Socorro Reef Associates contacted me, at the suggestion of Noranda, about examining the Socorro Reef property position with special emphasis on the Iron Door and Tres Padres claims. My report dated May 3, 1982, identified an interesting gold anomaly on the Palo Verde and Bluebird claims and recommended further exploratory work. At the request of Socorro Reef Associates (now Socorro Mining Corporation) I initiated discussions with major mining companies to obtain additional surface geologic assessment of the Socorro Reef gold anomaly. What follows is a summary of my activity and that of various major mining companies between May 1982 and December 1982. The sequence of company summaries is arranged chronologically in the order of initial contact with these mining companies. Analytical data and correspondence relating to the various activities is contained in Appendices IV - X. A briefly summarized description of surface work commitment performed by the various major mining companies is presented in Table 13 along with its approximate dollar value.

Table 13: Dollar value of work commitments by major mining companies, 1982

Company	Type of Work	Approximate Dollar Amount
Noranda	Geochemical Sampling during March, June, and September	6,300
	Geochemical Induced Polarization Survey in June	4,500
Phillips	Geochemical Sampling in June	3,000
U.S. Borax	Analytical Geochemical Work on Socorro Mining and Phillips samples	7,000
St. Joe	Detailed surface geochemical sampling in August and September	4,800
Exxon	Confirmatory geochemical sampling	800
ASARCO	Confirmatory geochemical sampling	1,200
		27,600.00

Noranda Activity

Because Noranda Exploration, Inc. had already performed recent sampling, I contacted them first in mid May. During these initial discussions it became apparent that Noranda had independently identified the Socorro Reef gold anomaly and was interested in follow up studies. However, their budget was tight so that their timing for such work was indefinite. In late May I contacted Phillips about sampling the Socorro Reef gold anomaly. When Noranda learned about these contacts, they indicated they would conduct a detailed surface geochemical sampling and geophysical survey during mid-June. (See letter dated June 8, 1982 in Appendix V). Data relating to this work were transmitted to Socorro Mining Corporation on July 13, 1982. Noranda considered the results encouraging, but not encouraging enough to immediately acquire the ground. Subsequently, I initiated discussions with other major mining companies (see below) and kept Noranda informed of these activities. On September 29, 1982, I visited the property with Noranda personnel to further acquaint them with the property in view of what was currently known. At this time Noranda took additional samples from an adit. (See analytical report dated October 13, 1982). The next day Jeff Snow, President of Noranda Exploration in charge of U.S. exploration, visited the property, was favorably impressed, and authorized lease negotiations with Socorro Mining that evening in Phoenix, Arizona. The initial offer called for $30,000 of initial work commitment by Noranda over an initial period of three months in 1982. If results are favorable, Noranda proposes to escalate its work commitment to $100,000 a year for the next several years. Negotiations with Noranda are still ongoing.

Phillips Activity

After my initial contact with Phillips, I visited the Socorro Reef gold anomaly on June 1, 1982 with Robert D. Enz, Minerals Geology Supervisor for the Minerals Group of Phillips Petroleum Co. Enz was favorably impressed and indicated that Phillips would do follow up sampling in the Socorro Reef gold anomaly later in June. On June 21-23 Phillips collected 61 samples within the Socorro Reef gold anomaly. However, Phillips announced that week that they were terminating their Strategic Minerals Division as of September 1, 1982. Hence, Phillips was not able to obtain analyses for the samples, but did send me on July 15, 1982 sample descriptions, location data, and the samples they had collected.

U.S. Borax Activity

In late July I contacted Dick Ahern, a consultant for U.S. Borax about analyzing the Phillips samples. In return for monitor rights and receipt of existing Socorro Mining Corporation data regarding the Socorro Reef gold anomaly, U.S. Borax has analyzed the Phillips samples for copper, molybdenum, lead, zinc, gold, silver, arsenic, antimony, tungsten, mercury, and uranium. In addition, U.S. Borax has reanalyzed the Socorro Mining Corporation samples collected by myself in April 1982 for gold, silver, lead, zinc, and copper and has furnished additional analyses on the Socorro Mining Corporation samples for molybdenum, tungsten, uranium, antimony, arsenic, and mercury. These data have now been received in several lots from October 11, 1982 to the present. Numbers S-109 through S-143 remain outstanding and should be received shortly. U.S. Borax continues to monitor competitor activities at Socorro Reef, although it does not appear that they will compete with the Noranda offer.

Exxon Minerals Activity

In early August 1982 I contacted personnel in the Tucson office of Exxon Minerals Company about the Socorro Reef property. Following an initial examination of the property on August 31, 1982, Richard Chuchla of Exxon Minerals was favorably impressed and recommended follow up sampling. Exxon spent two addditional days performing confirmatory sampling at Socorro Reef in September of 1982 and the results of that sampling were transmitted to me by phone on October 8, 1982 (Appendix VII). The Tucson office has recommended that Exxon obtain Socorro Reef for drilling evaluation, but have yet to make a formal offer to Socorro Mining Corporation. Whether they will compete with the Noranda offer at this point in time is somewhat doubtful.

St. Joe American Activity

In late July of 1982 I contacted geologists for St. Joe American Corporation about the Socorro Reef property and on August 3, 1982 I presented the property to Tom Chapin of St. Joe in the field. He was favorably impressed and recommended a detailed sampling program which St. Joe conducted September 9-13, 1982. The results of this program were encouraging and St. Joe geologists have recommended to their district manager that St. Joe acquire the ground for drilling evaluation. On December 2, 1982 Joe Rankin, the southwestern U.S, exploration manager for St. Joe out of Tucson, visited the property with Noel Cousins, the St. Joe supervisor for St. Joe's exploration at the Socorro Reef property to date. Rankin was favorably impressed with the surface geology, but when he observed several air-track drill holes on the ridge west of Socorro Mining Corporation's open cut, he became more skeptical. His impression was the the ground may already have been evaluated by these air-track holes (probably former Jordan Industry work by Behunin). Cousins indicated to me by phone on December 3, 1982 that St. Joe would proceed no further until Socorro Mining determines the status of information relating to these holes and conveys it to St. Joe.

ASARCO Activity

During my initial mapping and sampling activities in April 1982 a representative of ASARCO, Inc. also visited the Socorro Reef property. Following that evaluation ASARCO remained inactive until I contacted them on September 9, 1982 and showed them the Noranda and Socorro Reef data. After examining this data ASARCO reevaluated its position and contacted me with a verbal work commitment offer for $20,000 of air-hammer drilling and supportive assay work. They made this offer contingent upon favorable results from additional surface sampling by their acting regional manager, Bill Kurtz. This work was conducted on September 23, 1982 and the results of that work, together with analytical data for the April 1982 sampling and for 1936 sampling of the Henry Bell adit workings, are presented in Appendix IX. ASARCO has been informed of the Noranda offer and, while they were favorably impressed with the ground, I do not believe they will compete with the Noranda offer.

Newmont Activity

On September 9, 1982 I made an office presentation to geologists for Newmont Mining Corporation using the Noranda and Socorro Mining data. Their geologists were favorably impressed and indicated that they would contact me about visiting the Socorro Reef property in the field. They have yet to make this contact. My feeling is that Newmont prefers to "let the traffic clear" before initiating any work.

Hecla Activity

On September 13, 1982 I received a call from Dick Nielsen, a consultant for Hecla Mining Corp., who had heard about the Socorro Reef property "on the grapevine". After further contact with Hecla I visited the Socorro Reef property on September 24, 1982 with Lou Knight, the regional exploration manager from the Denver office of Hecla. He was favorably impressed with the ground, but has since indicated to me that Hecla is not interested in any "bidding wars". They also believe that the available data indicate the Socorro Reef deposit is slightly too low grade to warrant a major entry by Hecla into Socorro Reef at this time. However, if Socorro Mining has not entered into an exploration lease with a major mining company by the first of 1983, Dr. Knight has instructed me to make additional contact with him regarding the Socorro Reef property because he expects that his 1983 budget will be much more flexible in terms of acquiring new drilling projects.

Utah International Activity

On October 18, 1982 I received a phone call from Alex Ascencios, district manager of Utah International exploration office in Tucson. Mr. Ascencios had heard about Socorro Reef "on the grapevine" and was interested in looking at the Socorro Reef data. That day I made an office presentation to Utah International and they indicated they were interested and would contact me later about a subsequent field examination of the property. At the time I talked with them I informed them that several other companies were interested and that Noranda had made a formal offer.

When St. Joe geologists were visiting the Socorro Reef property on December 2, 1982, they encountered one geologist (Miles Shaw) and an assistant who were collecting numerous geochemical samples. In a telephone conversation with Alex Ascencios on December 3, 1982 he related that he and Shaw had visited Socorro Reef in mid-November and had decided to follow up their first visit with a detailed sampling program for 3 days in early December. They were scheduled to complete this sampling by December 3, 1982. Ascencios indicated that Utah International was taking 50 to 75 samples which would be analyzed for gold, silver, mercury, arsenic, lead, zinc, thallium, and at my suggestion, tungsten. From our conversation it appeared that Utah was interested in sampling the granite to increase the potential minable tonnages. They indicated interest in all of the data Socorro Mining Corporation has accumulated since my contact with Utah in October and that perhaps they would be ready to "swap" data by mid December. I informed them that Socorro Mining was very close to cutting a deal with Noranda and Ascencios indicated Utah would proceed accordingly.

Gulf Minerals Activity

In early November of 1982 Monte Swan, a consultant with Gulf Mineral Resources Company, a division of Gulf Oil, contacted me about the Socorro Reef package. I showed him the data on November 8, 1982 and later that week he recommended the property to Tom Heidrick, the regional manager for western U.S. exploration in Denver. On November 16, 1982 I transmitted Socorro Reef data to geologists in the Tucson office of Gulf Mineral Resources Co. for inclusion in their 1983 budget meetings in Denver on the 17th and 18th of November. Tom Heidrick has since informed me by phone on November 22, 1982 that he is seriously considering putting Socorro Reef into his 1983 budget if the financial terms are right. I indicated that I believed a minimum of $50,000 in drilling would be needed to fairly test the Socorro Reef gold anomaly. (See my letter dated May 20, 1982 in Appendix X). Heidrick indicated that they could spend at least $50,000 in an initial work commitment. Thus, I strongly believe that Gulf Mineral Resources Co. will seriously complete with the Noranda offer. I am scheduled to give an office presentation to Gulf Mineral Resources Co. geologists including Tom Hedrick on December 7, 1982. Following this presentation I expect that Gulf geologists will visit the Socorro Reef property later in the week.

Keith Activity

In addition to all of my activities with the major mining companies between May and December, of 1982, I have conducted detailed geologic mapping in the area of the Socorro Reef gold anomaly, acquired additional protection ground immediately south of the Socorro Reef gold anomaly, obtained and evaluated the June 1981 Socorro Reef drill hole information for inclusion in the Socorro Reef data base, and conducted discussions and negotiations with the Campbell family who own part of underlying property.

After receipt of the Noranda data in July 1982 it became apparent that some of the gold mineralization might extend south of the Socorro Reef property position as of July 1982. Also, it was apparent that any open pit mining would include a small part of the ground in the NW 1/4 of Sec. 36, T.5N., R.12W. in which the mineral rights were owned by the State of Arizona. After approval from Socorro Mining Corporation 16 Reef Annex claims were located on August 16 and 25, 1982. After September 1, 1982 the Reef Annex group was repapered on October 13, 1982 and recorded at the Yuma County Courthouse on October 19, 1982. The repapering was done so that Socorro Mining would have an additional assessment year to evaluate the ground. The repapering in effect saves Socorro Mining Corporation $1600 of 1983 assessment and ties the ground up until September 1, 1984. The location and recording notices for the Reef Annex group are contained in Appendix XI along with ownership information for the Reef, Iron Door, Palo Verde, Bluebird, and Tres Padres claims.

During my various trips to the Socorro Reef property in August and September of 1982, I conducted about 2 days of detailed geologic mapping at a scale of 1 inch = 500 feet to obtain more precise geologic information about the occurrence of gold within the Socorro Reef gold anomaly and also to obtain tighter sample control for all of the various major mining company geochemical sampling. During discussions with Noranda geologists in Tucson it was learned that Arizona Drilling Services had done drilling at the Socorro Reef property in mid 1981. I was previously unaware of this information. After phone calls with James L. Witt of Arizona Drilling Services and Bob Rose, Socorro Mining Corporations accountant in Scottsdale, Arizona, I obtained over the telephone the drill hole names and locations and the analytical results for gold and silver in 120 five-foot composite samples collected during the reverse-circulation drilling. Notes bearing these data are contained in Appendix X.

On September 29, 1982, I visited with the Campbell family in Salome, Arizona. At this time I discussed my new geologic interpretations and the economic implications of those interpretations with the Campbells. I also transmitted to the Campbells a copy of my May 10, 1982 report. The main intent of these discussions was to convince the Campbells of the poor commercial potential for deposits on the Iron Door claims and to stress the high commercial potential of the Socorro Reef gold anomaly. This was done to allow the Campbells to more realistically reassess ore deposits on their claims and to convince them that the Socorro Reef property is not yet a mine and that much exploration remains to be done before a mine could be brought into production. My overall purpose in this regard was to explain to the Campbells that terms in the May 15, 1981 lease agreement pertaining to mine production and royalty payments were unrealistic considering the incompleteness of geologic data regarding the Socorro Reef property as of May 1981. My recommendation to the Campbell's was to replace the mine production requirements with new requirements pertaining to efficient exploration of the Socorro Reef property.

Geology

The regional geology of the Socorro Reef gold anomaly is shown on Plate 2. During August and September of 1982 two days were spent revising the geologic map of the Socorro Reef gold anomaly and vicinity at a scale of one inch equals 500 feet (Plate 19). Three cross sections were drawn through the Socorro Reef gold anomaly and are presented in Figure 19.

ROCKS

The regional stratigraphy in the Socorro Peak area was summarized in Part I. Rock units specifically present in or near the Socorro Reef gold anomaly include the Precambrian (probably 1.4 b.y. old) porphyritic biotite granite, the depositionally overlying Middle to Upper Cambrian Bolsa Quartzite and Abrigo Formation, the Upper Devonian Martin Formation, the Mississippian Redwall Formation, and the Pennsylvanian-Permian Supai Formation. For lithologic descriptions of these units see Figure 4 in Part I. The highly anomalous to moderately anomalous portion of the Socorro Reef gold anomaly is contained entirely within the Bolsa Quartzite and Abrigo Formations. In addition, weak to moderate gold values are present in the Precambrian porphyritic granite beneath the Bolsa Quartzite.

Significantly, gold values drop to background in the Paleozoic carbonate section immediately south and southeast of the Bolsa-Abrigo contact. Thus, the contact between the Bolsa-Abrigo formations and the Martin Formation represents a firm assay wall and abrupt geologic boundary for the southern boundary of the Socorro Reef gold anomaly. Thus the southern boundary of the Socorro Reef gold anomaly is strongly controlled stratigraphically by the basal Martin contact. Conversely, on the basis of present geochemical data, no firm assay wall exists in the Precambrian porphyritic granite beneath the Bolsa Quartzite.

Paleozoic carbonate strata also exert a strong stratigraphic control on peripheral mineralization south of the Socorro Reef gold anomaly. Erratic gold-bearing jasperoid lenses exclusively occur in the upper cherty carbonate member of the Mississippian Redwall Limestone (for example at several prospects south of the Socorro Reef gold anomaly in the NE 1/4 of the NE 1/4 of Sec. 35, T.5N., R.12W.).

A sequence of northwest-trending, calc-alkalic, microdiorite dikes is present along the Socorro fault zone at and south of the Socorro Mine for about 1/2 mile along the fault. Three such dikes were mapped; a fourth microdiorite dike was mapped 500 feet southwest of the Socorro fault zone about 1000 feet south of the Socorro Mine. The microdiorite dike swarm along the Socorro fault mostly occurs within the northeast end of the Socorro Reef gold anomaly and is chloritically altered, especially where the dikes traverse the gold anomaly.

STRUCTURE

Structural geology in the region around the Socorro Mine has already been outlined in Part I. The main elements of the structural geology locally present at Socorro Reef are shown in cross sections A-A', B-B', and C-C' on Figure 19. The locations for these section lines are on Plate 19.

Low-angle Thrust Faults

The main structure at the Socorro Mine and vicinity is the Golden Eagle thrust, one of the middle thrusts in the regional thrust fault sandwich that is present throughout the Salome region. As can be seen in the cross sections, the Golden Eagle thrust divides the area into two major plates. The lowermost plate is composed mostly of Precambrian porphyritic granite with minor metasedimentary inclusions. Several exotic lenses of Paleozoic rocks occur along the thrust fault (See Plate 19 for the map position of these lenses). The largest of these lenses is composed of Bolsa Quartzite. The northeast end of this lense, which actually is composed of several lenses, begins about 500 feet northeast of the Socorro Mine within the Golden Eagle thrust zone. The lense reaches its maximum thickness about 200 feet southwest of the Socorro Mine where the quartzite is about 150 feet thick. The quartzite lense progressively attenuates to the southwest and is no longer present about 1000 feet southwest of the Socorro Mine. Other tectonic lenses of Paleozoic strata within the Golden Eagle thrust zone include a small, one-hundred-foot long lense of Martin Formation about 1000 feet northwest of the Socorro Mine and a 500-foot long sliver of Supai Formation beginning about 200 feet southwest of the collar of the Socorro Mine incline.

The upper plate of the Golden Eagle thrust is composed of Precambrian, coarse-grained, porphyritic biotite granite, which is depositionally overlain by a steeply south- to southeast-dipping Paleozoic section that contains a normal Paleozoic stratigraphic sequence from basal, Middle Cambrian Bolsa Quartzite to Permian Kaibab Limestone. Porphyritic granite rests tectonically on the Paleozoic tectonic lenses in the Golden Eagle thrust zone. This older over younger juxtaposition of rock units demonstrates the fundamental thrust nature of the Golden Eagle thrust. The steep south and southeastward dip of the Paleozoic section and westward attenuation was probably imposed during regional, F_1 southeast-directed folding in mid-Cretaceous time. The Socorro Mine area and the Socorro Reef gold anomaly are within the lower, right-side-up limb of a major F_1 fold. The hinge of this fold is exposed one mile east of the mine area (Figure 7). A few F_1 minor folds are present in the Pennsylvanian-Permian Supai section southeast of the Socorro Mine. Fold hinges for these folds are shown in Plate 19.

The Golden Eagle thrust throughout the Socorro Mine area consistently dips either south or southeast. The south or southeast dip is post-thrust in age and is probably related to F_3 folding (Event No. 11, Geologic History Section, Part I). Hence, the Socorro Mine area is inferred to be in the south limb of a broad northeast-trending anticline whose axis is about one mile north of the Socorro Mine (See Plate 2).

High-angle Faults

The thrust plates in the Socorro Mine area are broken by numerous members of the high-angle, northwest- to west-northwest-striking fault set. The principal fault of this set in the Socorro Mine area is the Socorro fault. The Socorro fault dips about 60 degrees to the northeast and displaces the Paleozoic slivers in the Golden Eagle thrust zone northeast of the Socorro fault up and to the southeast. Hence, there is about 250 feet of right separation and about 200 feet of reverse separation through the Socorro fault zone. Southwest of the Socorro fault numerous high-angle, north-northwest-striking to west-northwest-striking faults offset the Paleozoic section between the Socorro fault and the Bluebird fault (See Plate 19). Separation on the northwest- to west-northwest-trending faults is sinistral, whereas separation of the more northerly trending faults is generally dextral. Sinistral or left separation on the west-northwest-striking faults is only about one-third that of the dextral separation on more northerly faults. However, the Bolsa-granite contact west of Hill 2462 has been offset repeatedly (6 inches to 3 feet) in a sinistral way by numerous northwest- to west-northwest-striking faults that were too small to map.

The geology about 1000 feet south of the Socorro incline has been complicated by the presence of an additional thrust (now tilted) that trends directly through Hill 2462 (See Figure 18B). As shown on cross section B-B' (Figure 19) Bolsa Quartzite is repeated three times on now-tilted thrust faults. The Hill 2462 thrust probably formed just before the F_1 folding event and was tilted during the F_1 folding event.

Inspection of Plate 19 reveals that the generally northeast-striking, southeast-dipping Paleozoic section which occurs northeast of the Socorro fault bends into an east-west, steeply south-dipping orientation southwest of the Socorro fault near the edge of outcrop (especially in the NE 1/4, Sec. 35, T.5N., R.12W.). This bending may be due to drag along a major west-northwest-striking fault concealed just beneath the alluvium in the NE 1/4, Sec. 35. This fault could be an extension of or a sliver of the high-angle, northwest- to west-northwest-striking Centennial Wash fault zone, which trends up Centennial Wash west of the Socorro Peak area (See Figure 3). Movement on this fault and the associated right drag of the Paleozoic section in the Socorro Mine area might reflect regional right shear along the northwest-trending fracture system about 12.5 to 5 m.y. ago (Event No. 11, Geologic History Section, Part I). If this interpretation is correct, east-west bending of the Paleozoic section would be post-mineral in age.

ALTERATION AND MINERALIZATION

The geographic position of the Socorro Reef gold anomaly (Plate 5, Part I) essentially coincides with the alteration and mineralization. Alteration and mineralization is expressed in several different ways within the Socorro Reef gold anomaly: 1) supergene hematite-clay alteration and hypogene quartz-sericite-pyrite phyllic alteration in the Bolsa Quartzite; 2) quartz-veining and moderate phyllic alteration and chloritization of the Precambrian porphyritic granite; and 3) epidote-chlorite alteration in the calc-alkalic microdiorite dikes.

Within the Bolsa Quartzite gold mineralization is specifically related to areas of pervasive phyllic alteration. Supergene expressions of this alteration feature a hematite-goethite-jarosite-clay alteration assemblage, which is commonly associated with replacements of euhedral pyrite by goethite. Hematite occurs as the earthy red variety and the highest gold values are associated with rock that contains red, pulverulent hematite and limonite and/or goethitic replacements of euhedral pyrite cubes. Locally, weak, copper oxide staining (malachite and/or chrysocolla) occurs in areas of strong hematite-goethite coatings and/or goethite replacements of pyrite cubes. Areas where a visual copper association was noted also commonly carried highly anomalous gold values.

Hypogene expressions of phyllic alteration in the Bolsa-Arigo section are manifested by sericitic replacements of detrital feldspar within the more arkosic lithologies and by pyritic cubes disseminated throughout the rock near closely spaced, quartz-filled microfractures and quartz-filled stockworks and microfracture networks. Locally the pyrite cubes are numerous enough so that the alteration may be termed pyritic. These areas consistently yield strongly anomalous (>.9 ppm gold) gold values. Figure 20A and 20B are photographs of some of the better pyritic alteration. Within the Socorro Reef gold anomaly phyllic alteration within the Bolsa Quartzite-Abrigo section is developed between a north-northwest-trending, unnamed fault about 600 feet northeast of the Socorro fault and an unnamed north-northwest-trending fault east of the Bluebird fault (See Plate 19). This area of altered Cambrian clastic rocks is about 3300 feet long and about 200 feet wide. In the structurally complicated area on Hill 2462 the southernmost band of Bolsa Quartzite is the best mineralized section. Phyllic alteration within the Bolsa Quartzite-Abrigo Formation section is terminated abruptly to the south at the contact with the Devonian Martin Formation.

Phyllic alteration does extend, however, into the Precambrian porphyritic granite north of the Bolsa Quartzite. Here the phyllic alteration is more specifically limited to macroscopic fractures which are lined with quartz-sericite-pyrite or its supergene equivalents, quartz-clay-hematite-goethite. Ferromagnesian minerals in the porphyritic biotite granite between phyllically altered fractures are generally chloritized. Precambrian granite further north of the Bolsa Quartzite-granite depositional contact is less phyllically altered but it does contain moderate propylitic alteration in the form of chloritization and minor epidotization of the biotite and plagioclase feldspars within the granite. Areas of propylitically altered granite north of the Bolsa Quartzite generally contain weakly anomalous gold values, whereas more phyllically altered granite closer to the Quartzite generally contains weakly to moderately anomalous gold values. The precise geographic extent of the altered granite north of the Bolsa Quartzite is yet to be quantitatively determined. On a preliminary basis phyllic or porphyritic alteration in the granite probably extends from 100 to 400 feet north of the phyllically altered Bolsa Quartzite-Abrigo Formation block.

As was previously mentioned several microdiorite dikes occur along the Socorro fault zone southeast of the Socorro Mine. Where these dikes cross the Socorro Reef gold anomaly they commonly exhibit moderate to strong chloritization and epidotization of the ferromagnesian minerals. Also the dikes contain moderate to strong hematite and goethite along fractures and locally contain small goethitic replacements of former pyrite cubes.

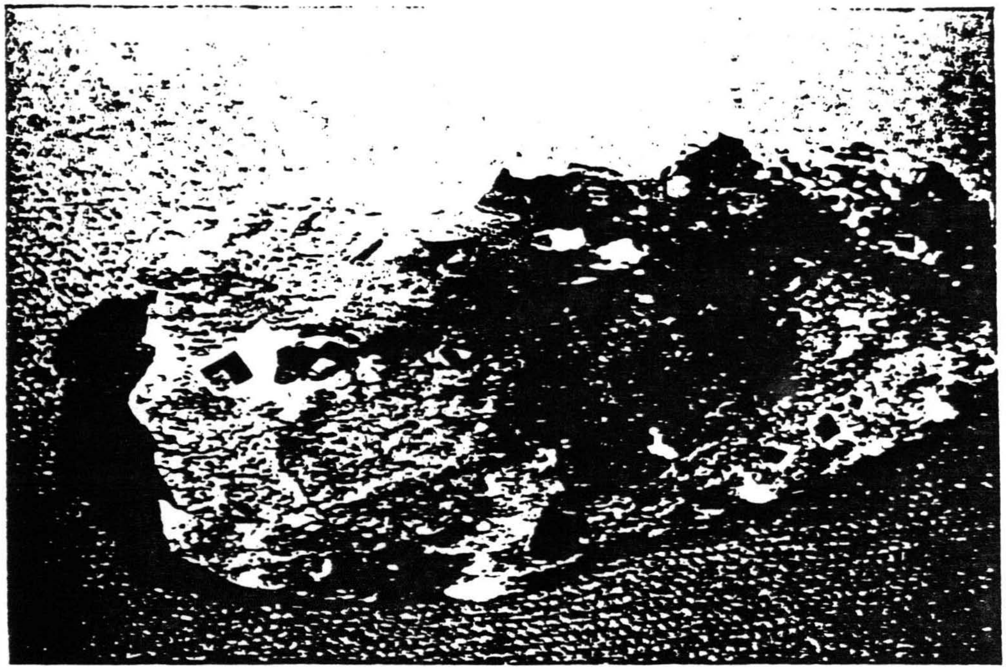

Figure 20A. Photograph of Bolsa Quartzite specimen from Socorro Reef Gold Anomaly exhibiting pyritic alteration. Euhedral pyrite cubes in this specimen have been replaced by goethite.

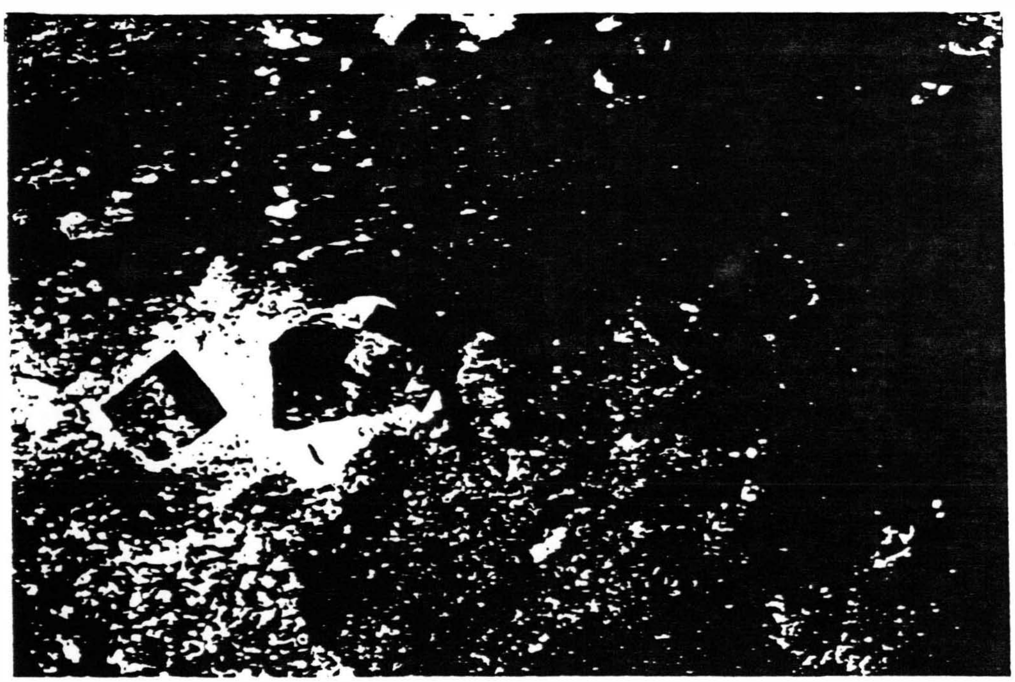

Figure 20B. Close-up photograph of goethite replaced pyrite cubes.

Peripheral alteration outside of the Socorro Reef gold anomaly is less common, less pervasive where it occurs, and is limited to discrete fractures or stratigraphy. North of the Socorro Reef gold anomaly alteration is expressed as quartz veins with minor sericitic envelopes within fractures in the Precambrian granite below the Golden Eagle thrust. East of the Socorro Reef gold anomaly similar quartz veins occur in the Precambrian granite; irregular, flat-lying quartz lenses occur in the Redwall Limestone on the Tres Padres claims; and minor silicification with moderate goethite occurs along northeast-trending fractures in the Bolsa Quartzite. Southeast of the Socorro Reef gold anomaly moderate silicification is locally accompanied by barite, manganese oxides and iron oxides and occurs along fractures and stockworks in the Martin-Redwall section on the Henry Bell claim northeast of the Socorro fault. South of the Socorro Reef gold anomaly siliceous, gold-bearing jasperoid lenses occur in the upper cherty carbonate member of the Redwall Limestone and black calcite with local goethite occurs along faults and locally along small-scale fractures in the Martin Formation.

PHYSICAL CONTROLS OF GOLD MINERALIZATION

The cross sections in Figure 19 show the physical distribution of gold mineralization with respect to the structural geology outlined previously. Gold mineralization at the Socorro Mine occurred within the lower part of the Golden Eagle thrust zone below the Bolsa Quartzite sliver (See cross section C-C', Figure 19). Gold mineralization at the Socorro Mine is inferred to extend down the dip of the Golden Eagle thrust and in cross sections A-A' and B-B' gold mineralization is shown penetrating into the plate above the Golden Eagle thrust where it mineralized highly fractured, Cambrian Bolsa-Abrigo strata. The cross sections also show how the mineralization is abruptly truncated at the contact with the overlying Paleozoic carbonate strata. This structural interpretation is strongly reinforced by geophysical data that will be discussed in a subsequent section.

At the Socorro Mine and in prospects 500 feet south of the Socorro Mine gold mineralization is controlled by the high-angle, northwest-striking fracture system. In these fractures gold-bearing quartz pods are common. Also, several high-grade (greater than 1 ppm) samples came from northwest- to west-northwest-striking fractures in the Bolsa Quartzite-Abrigo section about 300 feet west-northwest of the common corner of Sec. 26, 25, 35, and 36, T.5N., R.12W. The Bolsa Quartzite in this general area also contains moderately common, northeast-trending, gold-bearing quartz lenses along high-angle fractures. Indeed, bedding planes within the Cambrian clastic strata and northeast-trending fractures within the underlying Precambrian granite have exerted a subtle secondary fracture control on gold mineralization within the Socorro Reef gold anomaly. Offsets on fractures of this orientation have not been mapped and no significant faults of this orientation exist within the gold anomaly.

Geochemistry

The Socorro Reef gold anomaly is now one of the best documented, though yet undrilled, surface gold anomalies that I am aware of anywhere in the southwestern U.S. Since March 1982, 745 samples yielding 4806 analyses for various metals have been collected and analyzed by seven mining companies. About 360 of these samples were collected from within the Socorro Reef gold anomaly. The geochemical sampling programs of the various companies are summarized in Table 14 and sample locations for this work are shown in Plates 20 and 21. As a result of this work the geographic position of the gold anomaly is now firmly known and has been rigorously confirmed. Geological implications of the geochemical data are discussed below. Economic implications of the geochemical data are discussed in the section entitled Economic Evaluation.

RESULTS

Gold

Gold contents and locations of all samples collected by Socorro Mining Corporation, Noranda, and Phillips in the Socorro Mine area are presented in Plate 22. Gold contents and locations of all samples collected by St. Joe, ASARCO, and Exxon in the Socorro Mine area are shown on Plate 23. A composite gold anomaly map for all samples collected is presented as Plate 24.

The main components of the Socorro Reef gold anomaly are the moderately intense gold zones (0.09 to 0.9 ppm gold) that coincides with highly fractured, phyllically altered, and locally pyritized Bolsa Quartzite. The strongest and most continuous of these moderately intense gold zones begins at the Socorro fault where it intersects the southerly Bolsa Quartzite unit southwest of the fault (See Plate 19); it extends for about 2500 feet to the southwest along the Bolsa Quartzite outcrops to its termination by a north-northwest-trending fault that is 300 feet east of the Bluebird fault. This anomaly is about 250 feet wide. A second area of moderately intense gold values occurs in the Bolsa Quartzite northeast of the Socorro fault and extends indefinitely into the underlying Precambrian granite. A third area enclosed by the moderately intense gold contour is at the old Socorro Mine site where high-grade quartz lenses in the Golden Eagle thrust zone were mined in the early 1900's.

Several "hot spots" of strongly anomalous gold values occur within the moderately intense contour. The strongest and most continuous of these strongly anomalous areas is a zone about 600 feet long that begins in the Bolsa Quartzite about 400 feet west of the NE corner of Sec. 35, T.5N., R.12W. This zone is about 100 feet wide and has been extensively prospected by means of several adits and shafts. A second "hot spot"

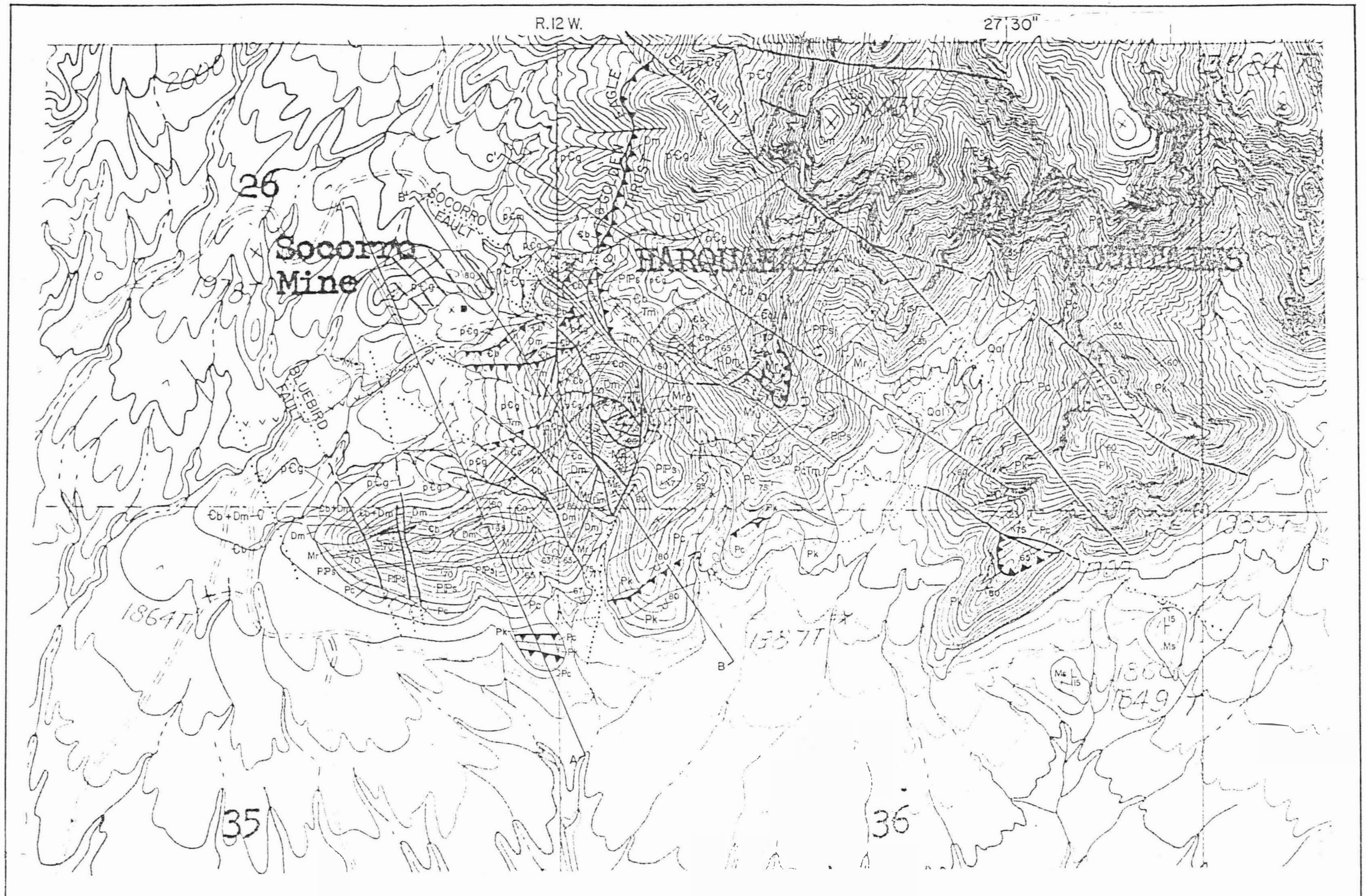

EXPLANATION

ROCKS

Hd	Mine dump
Qal | Ql	Qal-surface alluviums; Ql-landslide and/or debris flow materials
Tm	microdiorite dikes
Ms	undifferentiated clastic sedimentary rocks
Pk	Kaibab Formation
Pc	Coconino Formation
PIPs	Supai Formation
PIPs$_l$	Supai Formation-lower red shale member
Mr | Mr$_u$	Mr-Redwall Formation; Mr$_u$-upper cherty carbonate member of Redwall Formation
Dm	Martin Formation
Ꞓa	Abrigo Formation
Ꞓb	Bolsa Quartzite-small circles show basal conglomerate
pꞒg	porphyritic biotite granite (probably 1.4 b.y. old); locally contains K-feldspar megacrysts
pCm	alaskitic muscovite granite (probably 1.4 b.y. old)

STRUCTURE

60 — lithological contact; dashed where approximated, dotted where concealed, dip shown where measured

55 — faults dashed where approximated, dotted where concealed, dip shown where measured

15 — thrust fault (barbs on upper); dashed where approximated, dotted where concealed, dip shown where measured

trace of anticline showing plunge where observed

trace of shallowly inclined or recumbent fold showing plunge where observed

60 strike and dip of bedding

50 strike and dip of overturned bedding

N

GEOLOGIC MAP OF THE SOCORRO REEF GOLD ANOMALY, WESTERN HARQUAHALA MOUNTAINS YUMA COUNTY, ARIZONA

500 0 500 1000 Feet

Scale 1" = 500'

CONTOUR INTERVAL - 20 feet

Portion of Preliminary 7.5' Lone Mtn Quad

NOVEMBER 1982

by STANLEY B. KEITH

Table 14: Summary of Geochemical Sampling Programs by Various Companies in the Socorro Peak Area June, 1981 to October, 1982

Company	Date(s) Collected	Lab	Au	Ag	Pb	Zn	Cu	Mo	W	U	As	Sb	Hg	# of samples analyzed	x	# of elements per sample	=	Number of Analyses
			Elements analyzed for															
Socorro Mining Corp Rotary Drill-hole Samples	early June 1981	Arizona Testing Labs - Phoenix	x	x	-	-	-	-	-	-	-	-	-	120	x	2	=	240
Socorro Mining Corp.	March 30- April 4, 1982	Skyline - Tucson	x	x	x	x	x	-	-	-	-	-	-	162	x	5	=	810
Reanalysis of Socorro samples by U.S. Borax	August - October 1982	Borax - Anaheim	x	x	x	x	x	x	x	x	x	x	x	162	x	11	=	1,782
Noranda	March, 1982	Skyline - Tucson	x	x	-	-	-	-	-	-	x	-	-	88	x	3	=	264
Noranda	June, 1982	Skyline - Tucson	x	x	-	-	-	-	-	-	x	-	-	64	x	3	=	192
Noranda '108' Adit Samples	September 1982	Skyline - Tucson	x	x	-	-	-	-	-	-	x	-	-	12	x	3	=	36
Phillips	June, 1982	Borax - Anaheim	x	x	x	x	x	x	x	x	x	x	x	59	x	11	=	649
Exxon	August 1982	Exxon - Tucson	x	-	-	-	-	-	-	-	-	-	-	23	x	1	=	23
St. Joe	August 1982	Skyline - Tucson	x	x	x	-	x	-	-	-	x	-	-	14	x	5	=	70
St. Joe	September 1982	Skyline - Tucson	x	x	x	-	x	-	-	-	-	-	-	167	x	4	=	668
ASARCO	April, 1982	Skyline - Tucson	x	x	-	-	-	-	-	-	-	-	-	25	x	2	=	50
ASARCO	September 1982	Skyline - Tucson	x	x	-	-	-	-	-	-	-	-	-	11	x	2	=	22
Totals														745				4,806

exists in the Bolsa Quartzite and Precambrian granite about 200 feet west of Hill 2462. A third "hot spot" of high-grade gold was mined at the old Socorro Mine.

The moderately anomalous zones of gold occur within a larger, more diffuse, weakly anomalous field that constitutes the overall area of the Socorro Reef gold anomaly. The southern contact of the weakly anomalous contour is essentially the contact between the Abrigo Formation and Martin Formation. North of the Bolsa Quartzite, however, a large area of Precambrian granite is apparently weakly anomalous and the northwestern boundary of the Socorro Reef gold anomaly is indefinite in several areas (See Plate 24).

The Socorro Reef gold anomaly is flanked outward by several, smaller discontinuous anomalies. These discontinuous anomalies are associated with tungsten-bearing quartz veins in the Precambrian granite north of the Socorro Reef gold anomaly, with siliceous, northeast-trending fracture zones in the Bolsa Quartzite, and with irregular quartz lenses in the Redwall Limestone northeast of the Socorro Reef gold anomaly. Scattered, moderately anomalous gold values are associated with silicified fractures in the Martin Formation at the Henry Bell property southeast and south of the Socorro Reef gold anomaly on the Henry Bell and Palo Verde claims; the moderately anomalous values are also associated with jasperoid lenses in the upper cherty member of the Redwall Limestone south of the Socorro Reef gold anomaly on the Reef No. 50 claim.

Silver

Silver contents of samples collected by Socorro Mining Corporation, Phillips, and Noranda are shown on Plate 25 and silver contents of samples collected by Exxon, ASARCO, and St. Joe are shown on Plate 26. A composite silver anomaly map for all the samples collected is presented as Plate 27. As shown on Plate 27, anomalous silver values in the Socorro Mine area occur much less frequently and are much more erratically distributed than anomalous values of gold. The moderate to strongly anomalous values of silver that do occur are in the outlying prospects mentioned in the gold section north and east of the Socorro Reef gold anomaly. Also, anomalous silver values occur in the Paleozoic carbonate section that is immediately south of the Socorro Reef gold anomaly and also occur within the Socorro Reef gold anomaly at its westernmost end. Hence, high silver values appear to be arranged concentrically around the Socorro Reef gold anomaly.

Gold:Silver Ratios

Gold:silver ratios of samples collected by Socorro Mining Corporation, Phillips, and Noranda are depicted on Plate 28 and gold:silver ratios of rock chip and rock channel samples collected by Exxon, ASARCO, and St. Joe are shown on Plate 29. A synoptic gold:silver ratio map for the entire Socorro Mine area is presented as Plate 30. This map strongly emphasizes the theme developed in previous sections, namely that gold-dominant areas within the Bolsa Quartzite are flanked outward by peripheral prospects with gold-silver and silver-dominant ratios. Virtually all of the gold-dominant ratios are restricted to the Bolsa Quartzite-Abrigo sections that are northeast of and southwest of the Socorro fault; a smaller gold-dominant area occurs in the Golden Eagle thrust zone at the old Socorro Mine. Interestingly, the part of the Socorro fault zone that occurs between the Socorro Mine and the Bolsa Quartzite outcrops to the southeast appears to have a silver-dominant character. The gold:silver ratio map (Plate 30) strongly highlights the gold-dominant character of the Bolsa Quartzite that crops out in an arcuate area southwest of the Socorro fault. Here, an arcuate-shaped outcrop area exists that contains numerous samples with gold:silver ratios that are gold-dominant. This zone is about 2500 feet long and 250 feet wide. It is, by far, the most interesting disseminated gold target within the Socorro Reef gold anomaly.

Other Metals

The distribution of other metals in the Socorro Reef gold system has already been discussed in Part I and is only summarized here. As developed in Part I, gold-dominant portions of the Socorro Reef gold anomaly carry high concentrations of tungsten, which are positively correlated with gold content. Lead and minor copper base metal anomalies occur locally within the gold-dominant area. The gold-dominant area is also characterized by a distinct lack of silver, zinc, molybdenum, arsenic, antimony, and mercury. Conversely, zinc, silver, molybdenum, arsenic, antimony, and mercury are frequently anomalous in outlying prospects. Tungsten is locally strongly anomalous in outlying prospects, especially in a tungsten-bearing silver vein in Precambrian granite 500 feet northwest of the wood frame house that is west of the Socorro Mine (George Campbell, Jr., personal communication, summer 1982). Mercury is consistently anomalous in Paleozoic rocks east of the Socorro Reef gold anomaly.

Metal Zoning at Socorro Reef

Plate 31 shows the inferred zonal relationships of the Socorro Reef gold system. In this plate the Socorro Reef gold anomaly represents the gold-tungsten-lead-copper-rich central zone of a disseminated gold system. The gold-tungsten-dominated central zone is flanked outward by a surrounding, gold-silver-polymetallic zone and by a silver-dominant peripheral area at the Henry Bell Mine. More complete descriptions and implications of this metal zoning for other calc-alkalic gold districts of mid-Tertiary age in the Salome region were discussed in Part I.

Geophysics

In order to obtain preliminary information about three-dimensional aspects of the Socorro Reef gold anomaly, Mining Geophysical Surveys Inc. conducted a time-domain, induced polarization and resistivity survey (IP) for Noranda Exploration Inc. in June of 1982. Two north-south IP lines (Lines 1 & 3) were run through the Socorro Reef gold anomaly and one north-south IP line (Line 2) was run through non-mineralized Bolsa Quartzite 500 feet west of the Socorro Reef gold anomaly. The locations for these lines are shown in Figure 21 and the time-domain, induced polarization and resistivity profiles are reproduced in Figures 22 (Line 1), Figure 23 (Line 2), and Figure 24 (Line 3).

The IP survey yielded intriguing results; namely, the presence of a weak to moderate, southward-inclined, apparent polarization response in the Bolsa Quartzite that terminates approximately 300 to 400 feet below the surface. The bottom of this anomaly could be structural and could reflect the presence of the Golden Eagle thrust beneath the southward-dipping Paleozoic sedimentary section. By analogy with surface exposures to the northeast in Sec. 17, T.5N., R.11W. (See Plate 2), the Golden Eagle thrust probably truncates the southward-inclined Paleozoic section; it would, therefore, represent the geologic bottom of the gold mineralization in the Bolsa Quartzite. The termination of the southward-inclined IP anomaly is consistent with this interpretation. The consistency of the moderate intensity IP anomaly suggests that the Bolsa Quartzite and underlying granite are well enough fractured and contain enough pyrite (probably about 2/3 wt. %) and intervening intergranular fluids to continously conduct current. Consequently, the shape of the IP anomaly effectively outlines the downdip projection of surface alteration and gold mineralization in the Bolsa Quartzite and underlying Precambrian granite.

The southward-inclined, moderate intensity IP anomaly, which is well developed in Lines 1 and 3, is absent from Line 2. In Line 2, however, there is a noticeable polarization contrast between the granite and the Paleozoic section to the south where the contact is crossed between stations C-5 and C-6 on Line 2. The granite north of the contact is more conductive with apparent polarization values ranging between 10 and 15 millivolt-seconds/volt whereas the Paleozoic section south of the contact is clearly more resistant with apparent polarization values ranging between 1 and 6 millivolt-seconds/volt. The polarization contrast in Line 2 appears to have a near vertical dip to about 400 feet. This dip is consistent with the vertical dip of the contact at the surface.

Implications of the time-domain, induced polarization data for the gold mineralization at Socorro Reef were taken into consideration during the construction of the geologic cross sections (Figure 19). In cross sections A-A' and B-B' gold mineralization is shown within the Bolsa Quartzite and Precambrian granite as a tabular mineralized body that parallels the strike and dip of the Bolsa Quartzite. The mineralization is shown to extend into the granite and terminate somewhere in the granite because of the IP data in Lines 1 and 3. Mineralization is then shown to dip southward into the Golden Eagle thrust where it is terminated by the thrust. Mineralization is also shown within the Golden Eagle thrust zone beneath the Paleozoic section. Although the IP data did not verify this idea, it is reasonable based on an analogy with the gold mineralization that was mined at the old Socorro Mine.

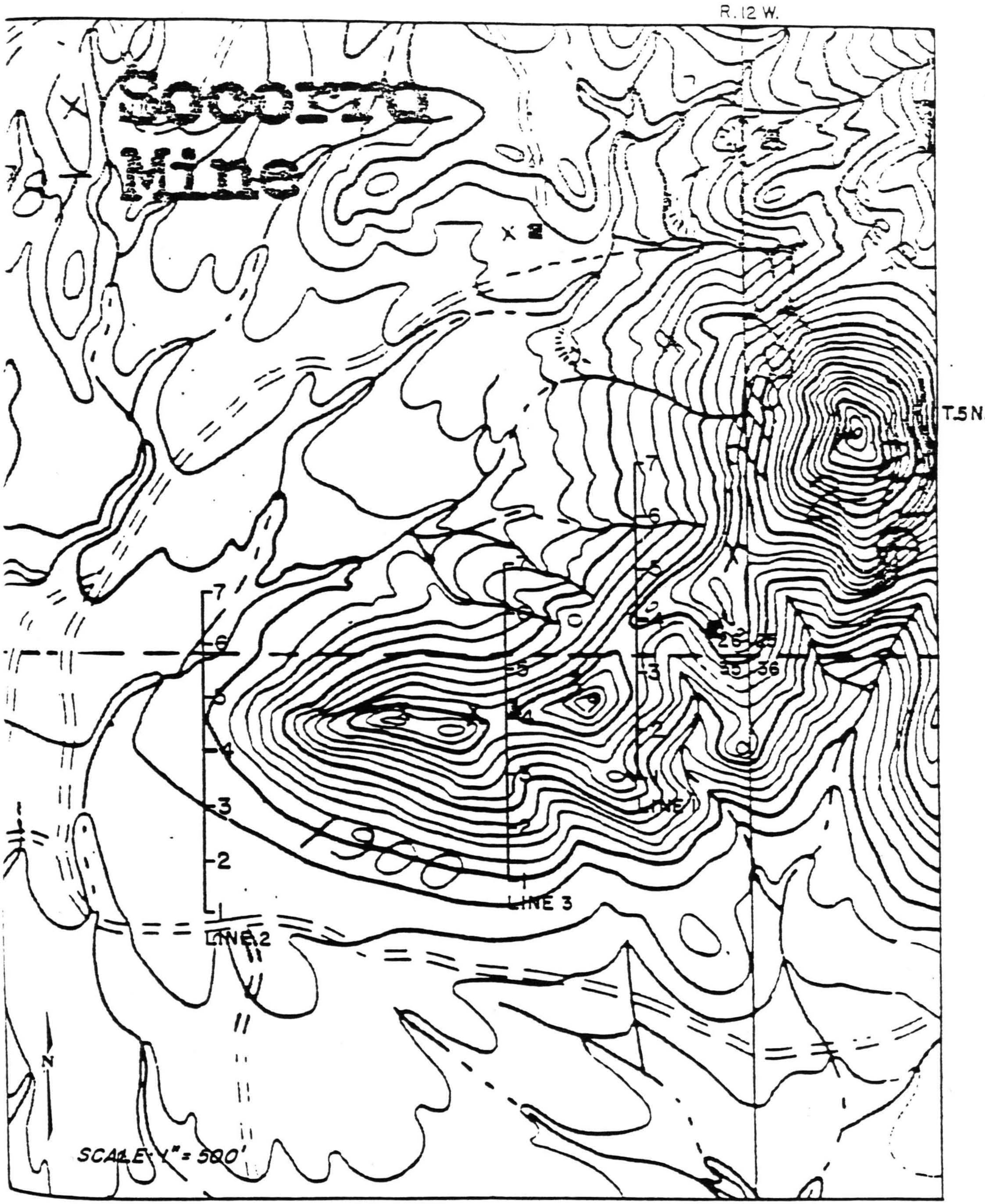

Figure 21. Location map for induced polarization lines from geophysical survey for Noranda Exploration, Inc.

TIME DOMAIN INDUCED POLARIZATION AND RESISTIVITY SURVEY

SOCORRO REEF PROJECT – YUMA COUNTY, ARIZONA

for

Noranda Exploration, Inc.

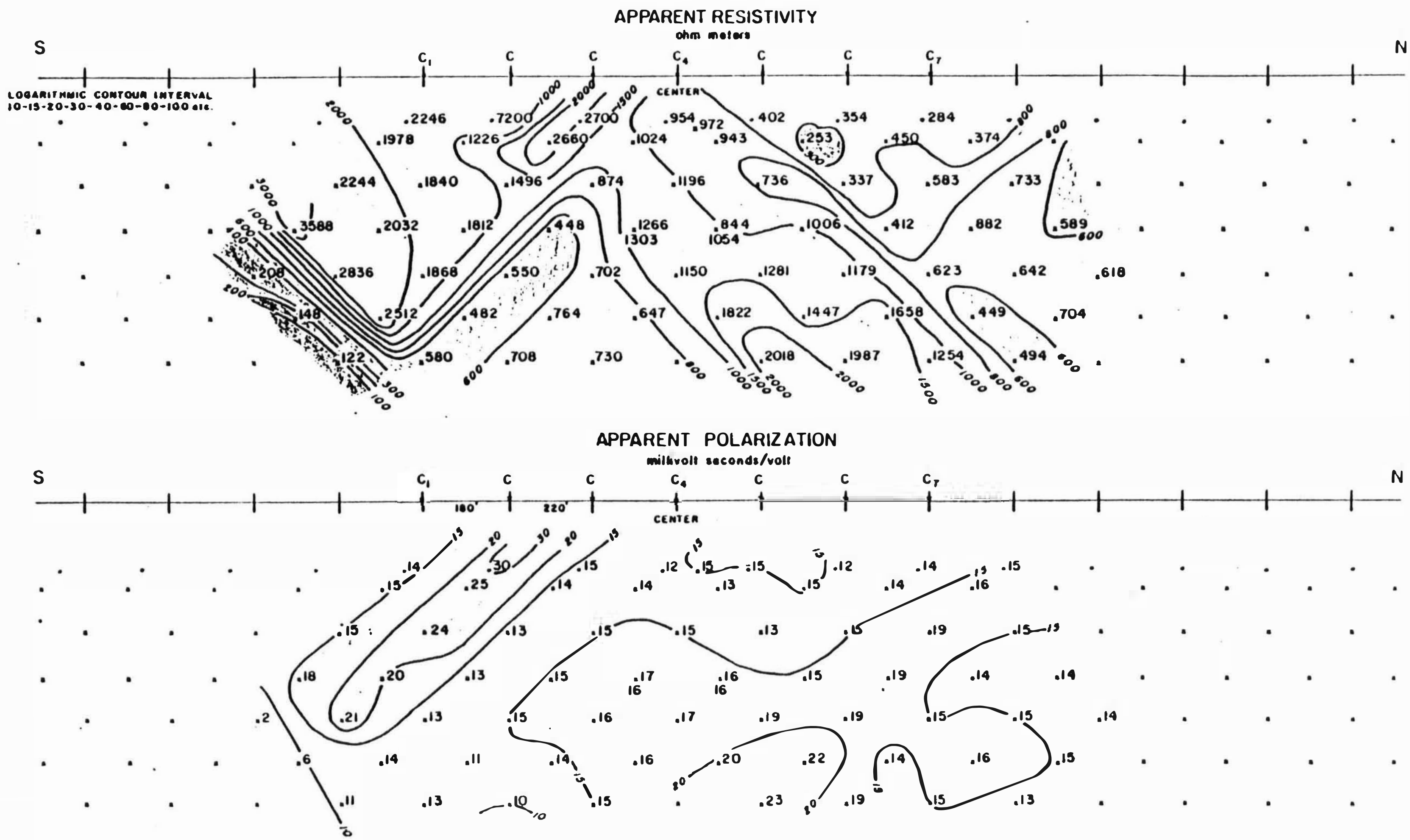

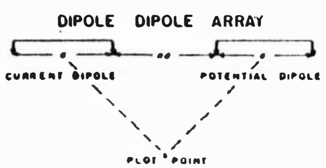

LINE 1

LOOKING WEST

DIPOLE LENGTH 200'

DATE 6/15/82

LEGEND

FENCE ....

PIPELINE........

POWERLINE......

ROAD, R.R.

FIGURE 22

TIME DOMAIN INDUCED POLARIZATION AND RESISTIVITY SURVEY

SOCORRO REEF PROJECT – YUMA COUNTY, ARIZONA

for

Noranda Exploration, Inc.

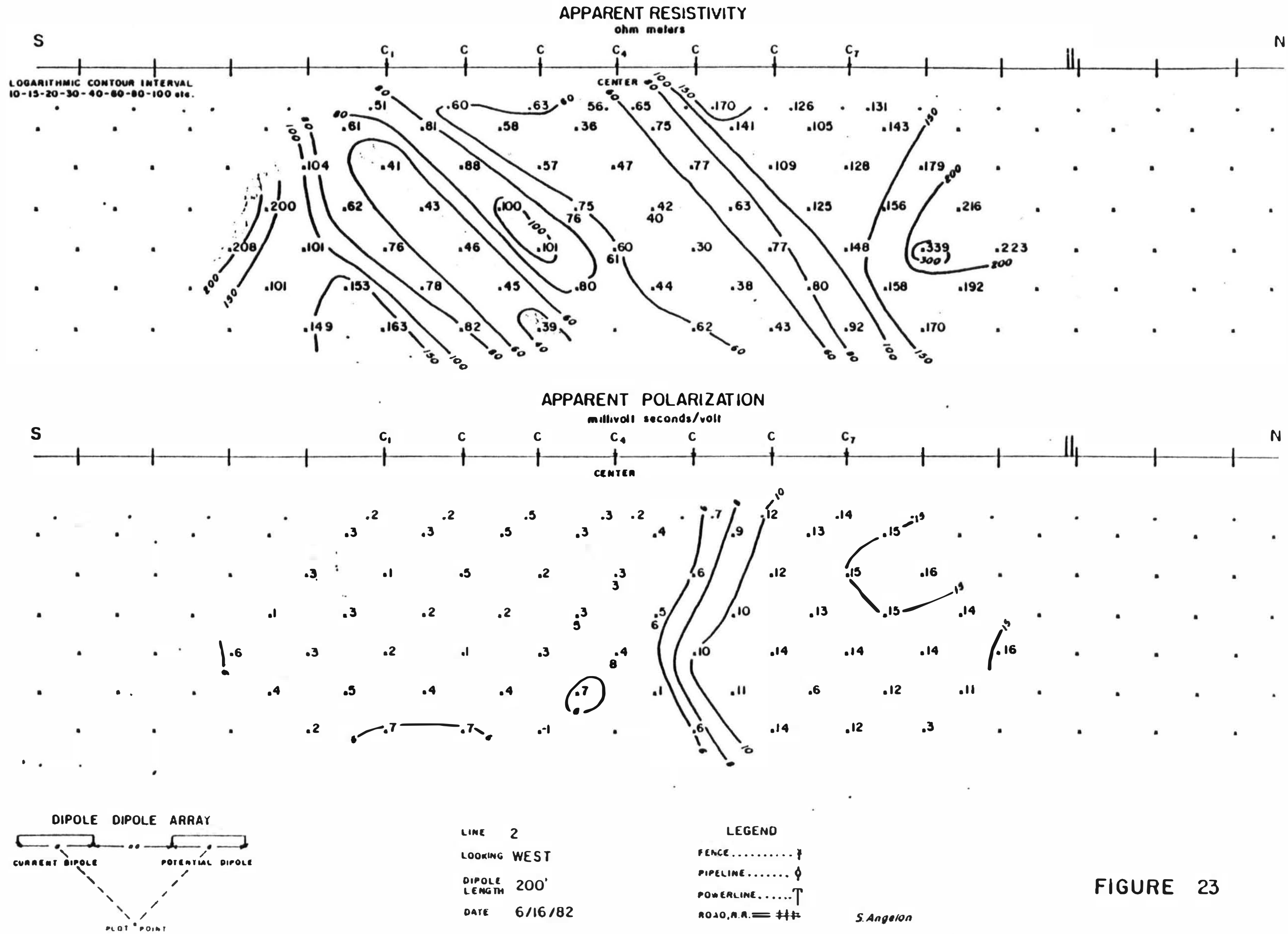

FIGURE 23

TIME DOMAIN INDUCED POLARIZATION AND RESISTIVITY SURVEY

SOCORRO REEF PROJECT – YUMA COUNTY, ARIZONA

for

Noranda Exploration, Inc.

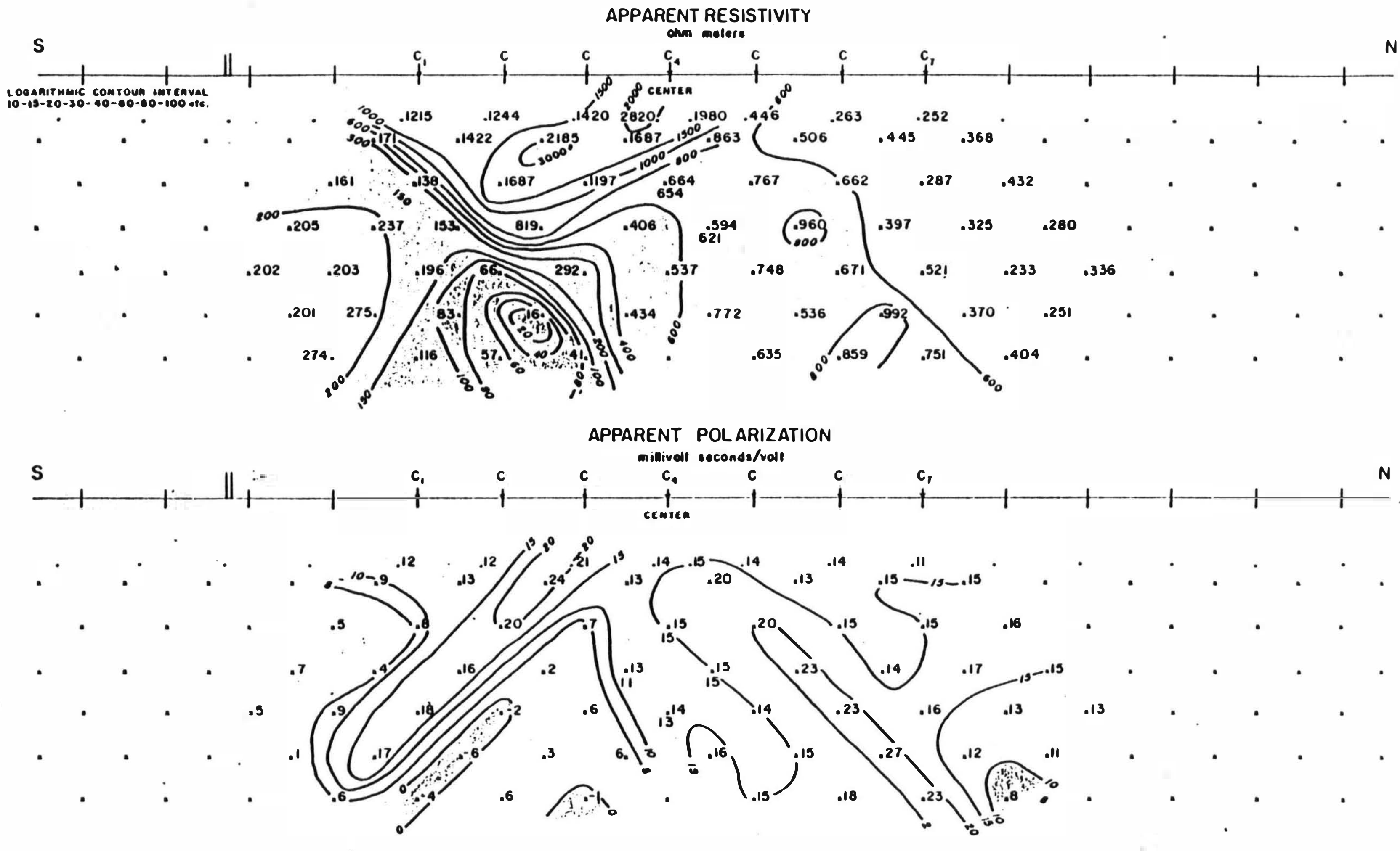

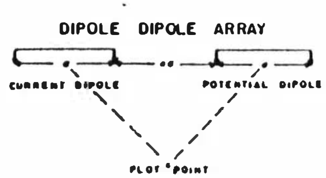

S Angelon

LINE 3

LOOKING WEST

DIPOLE LENGTH 200'

DATE 6/18/82

LEGEND

FENCE..........

PIPELINE.......

POWERLINE......

ROAD, R.R.

FIGURE 24

Geologic Model for Socorro Reef Disseminated Gold Deposit

Figure 25 is a geometric model for gold mineralization beneath the Socorro Reef gold anomaly and is based on data discussed in previous sections. In this model gold mineralization ascended the Socorro fault zone following the emplacement of microdiorite dikes about 25 m.y. ago. When the gold-bearing hydrothermal fluids encountered the pre-mineral Golden Eagle thrust zone, the increased premeability induced deposition of the gold-tungsten-lead-copper assemblage in the central zone. This mineralization was deposited along the thrust and in the upper plate of the Golden Eagle thrust in permeable Precambrian granite and the overlying, south- and southeast-dipping, Bolsa Quartzite-Abrigo section. Lateral migration of fluids along the thrusts to the north and to the south of its intersection with Bolsa Quartzite led to deposition of the peripheral gold-silver-polymetallic assemblage. Also, cooling hydrothermal fluids laterally and vertically migrated into the upper plate Paleozoic section where deposition of the gold-silver-polymetallic assemblage and the silver-base metal-mercury-manganesse assemblage occurred peripheral to the gold-tungsten-lead-copper-rich central assemblage in the Bolsa Quartzite. Consequently, one should not expect the gold-dominant assemblage to occur directly beneath silver-dominant deposits, such as those on the Henry Bell ground, because of their predicted lateral position away from the gold-dominated central core. That is, the gold-dominated central core is inferred to have near-vertical walls with perhaps minor lateral extensions near the Golden Eagle thrust (See Figure 25). The entire Socorro Reef gold system has subsequently been tilted south and southeastward by post-mineral tilting around northeast-trending fold axes. For a more general discussion of the disseminated gold deposit model as it applies to gold districts in the Salome region and the geologic history of the Salome region, the reader is referred to Part I.

Economic Evaluation of the Socorro Reef Gold Anomaly

CONFIRMATION AND DOCUMENTATION

Following the initial identification of the Socorro Reef gold anomaly by Socorro Mining Corporation and Noranda in March and April 1982, follow up field studies were conducted by Noranda, Phillips, Exxon, St. Joe, and ASARCO from June through September 1982. Most recently, follow up studies have just been completed on December 3 by Utah International. The results of these studies have confirmed and documented the existence of the Socorro Reef gold anomaly in an impressive way. From what is presently known, the moderate-intensity portion of the Socorro Reef gold anomaly in the Bolsa Quartzite is over 3300 feet long and averages about 250 feet wide (See Figure 26) and is inferred to be about 350 feet deep. This constitutes about 35.5 million tons of gold-rich material.

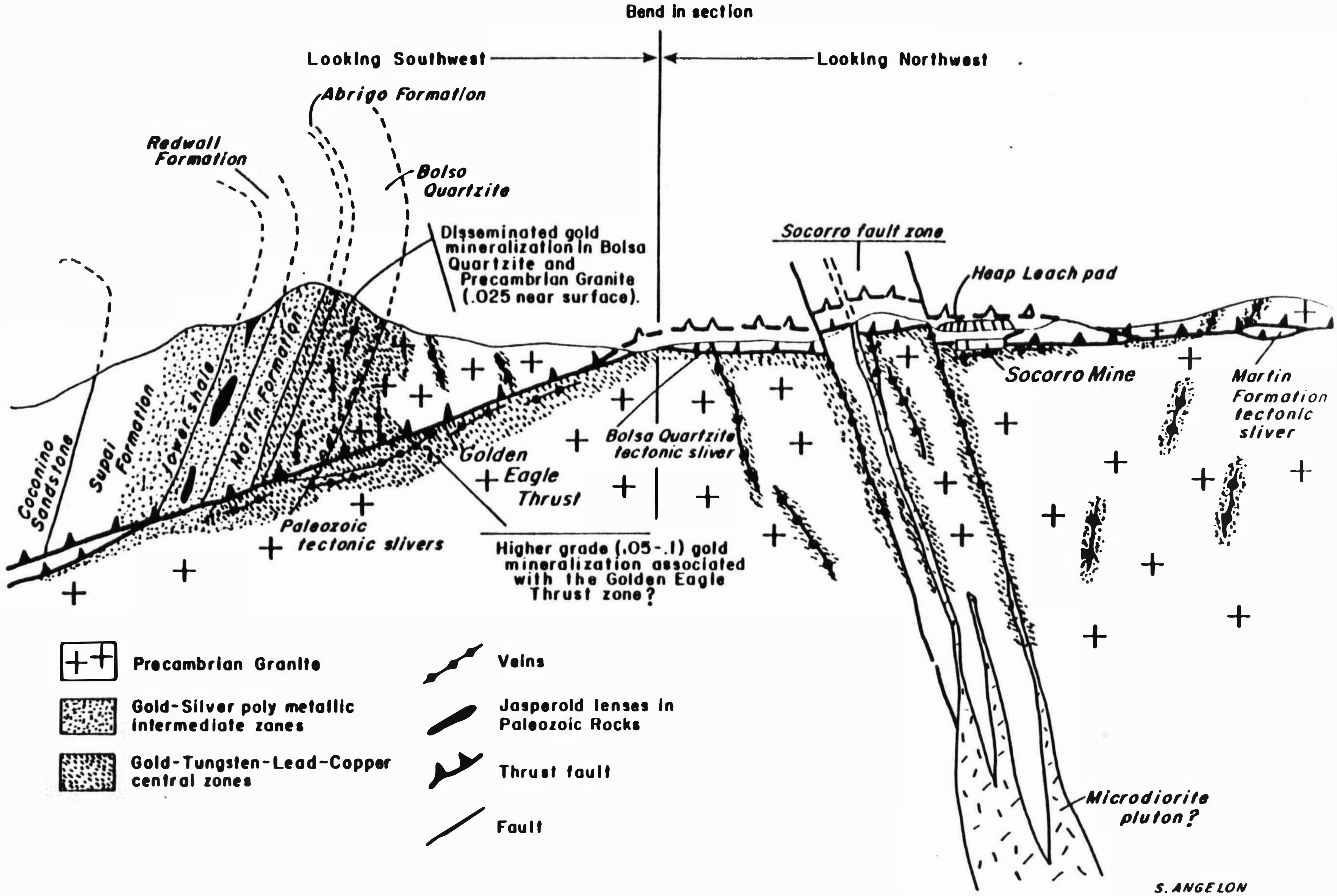

Figure 25. Cross section illustrating exploration model for inferred disseminated gold deposit beneath the Socorro Reef gold anomaly.

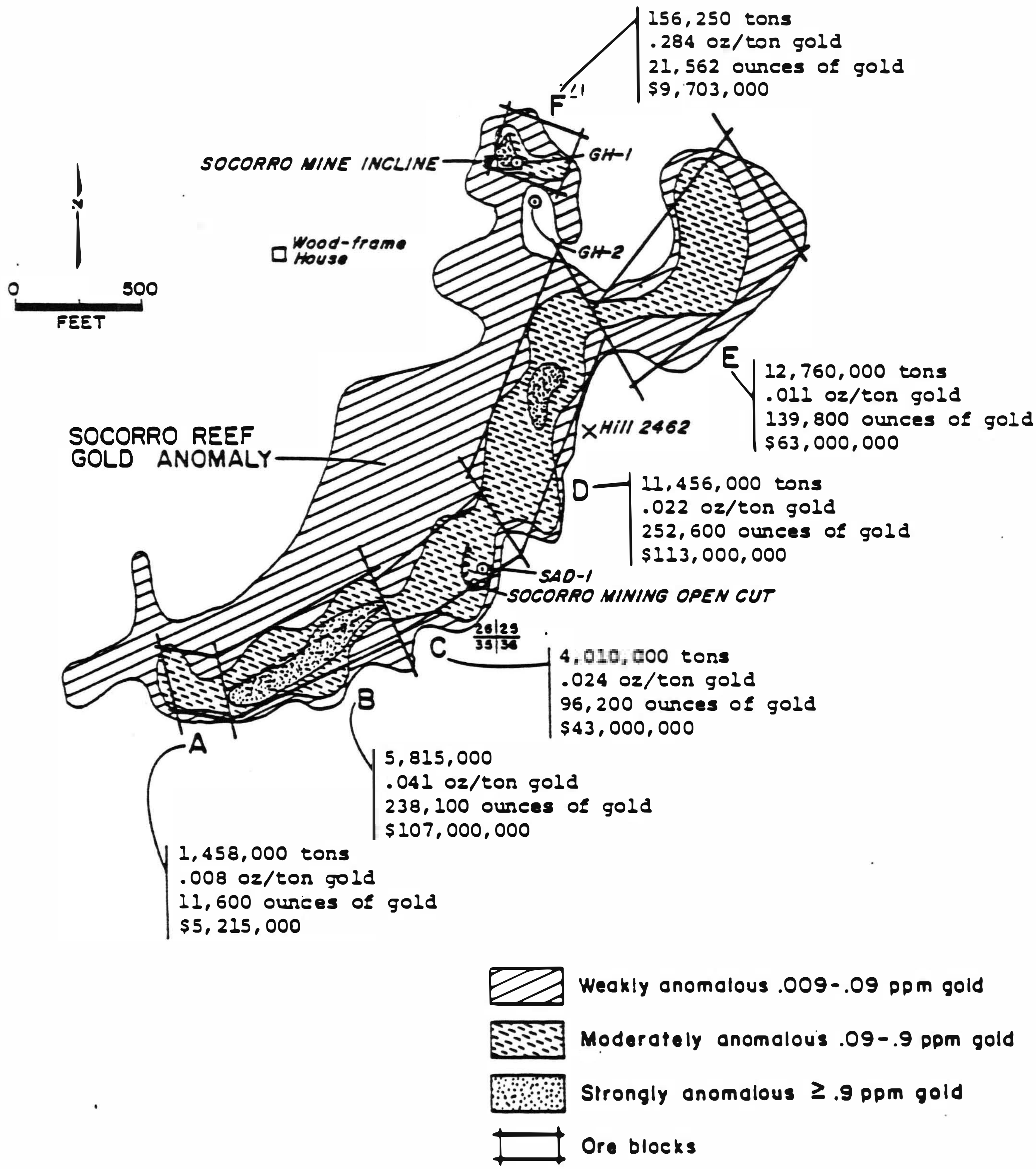

Figure 26. Map of Socorro Reef gold anomaly showing drill hole locations and grade-tonnage blocks discussed in text.

The Phillips sampling in June 1982 was designed to confirm the existence of the auriferous quartzite block to the west of the open cut in the saddle southwest of Hill 2462 and to sample the granite north of the quartzite in order to add additional tonnage. Noranda work during the same period was designed to confirm the known block of anomalous quartzite and to determine how far northeast and west of the Socorro Mining Corporation open cut the anomalous quartzite persisted. Noranda also obtained geophysical information to estimate the depth extent of the surface anomaly. Results of these studies defined the west limit of the anomaly about 500 feet west of the Bluebird fault (See Plate 19) and extended the anomaly for at least 900 feet to the northeast of the Socorro Mining open cut.

In August and September of 1982 Exxon Minerals and ASARCO took 48 samples to confirm the existence of the anomalous quartzite as established by the Noranda and Socorro Mining work. Exxon took more samples in the Paleozoic carbonate section south of the quartzite section to confirm that the carbonate section did not carry anomalous gold. The objectives of the Exxon and ASARCO work were met. The work by Exxon firmly established that the carbonate section south of the Socorro Reef gold anomaly contains very little gold.

In August and September of 1982 St. Joe conducted extensive sampling of the Socorro Reef gold anomaly to confirm the preexisting geochemical data and to determine how much gold was contained in Bolsa Quartzite exposures northeast of the known auriferous quartzite and how far gold mineralization extended to the northeast of the Socorro Mine along the Golden Eagle thrust zone. Also, the method of sampling by St. Joe within the known anomalous quartzite was by continous rock channel sampling rather than by point rock chip sampling, as the previous sampling programs had been. Again, St. Joe rock channel sampling within the known quartzite gold anomaly confirmed the existence of the gold anomaly and suggested that this anomaly was very continuous because of the sampling method employed. Also, St. Joe established that the quartzite block northeast of the Socorro fault was weakly to moderately auriferous for about another 875 feet. St. Joe sampling northeast of the Socorro Mine failed to uncover any continuous gold mineralization within or below the Golden Eagle thrust zone. St. Joe sampling also established that granite and quartzite exposures between Hill 2462 and the Socorro Mine were weakly anomalous. Hence, as of the St. Joe sampling, the Socorro Mine, which had constituted a separate anomaly on previous maps, is now known to be physically continuous with the moderate to strong intensity gold anomaly in the quartzite to the south.

In October and November of 1982 Borax analyses of the June Phillips sampling became available. These analyses again reaffirmed the existence of moderately to strongly anomalous quartzite west of the Socorro Mining open cut. The Borax analyses of granite samples, which were taken at the Bolsa-granite contact and for about 100 feet north into the granite, showed that the granite also was weakly to moderately anomalous. These results added another 50 to 75 feet of width to the moderate intensity portion of the Socorro Reef gold anomaly west of the Socorro Mining open cut in the saddle southwest of Hill 2462.

Accumulated data from all studies to date allows the inference that much of the Precambrian granite north of the quartzite-granite, moderate intensity anomaly is at least weakly anomalous with spotty gold values of moderate intensity. More sampling would be needed to discover any large areas of moderately intense gold values, but the granite block does represent a potential addition of large tonnages to existing tonnages (perhaps as much as 40,000,000 Tons). However, alteration patterns in this granite do not look promising enough to directly allow inference of these tonnages at the surface and much of this area would have to be evaluated by drilling for a blind, thrust-related target. Such drilling at this time is considered a wildcat venture, especially in light of the more essential drilling that would confirm mineable ground beneath the moderately intense gold anomaly in the Bolsa Quartzite and immediately underlying granite.

GOLD AND SILVER GRADES

Gold Grades

Average Gold Grades. Figure 27 is a frequency histogram for all 368 samples analyzed for gold within the Socorro Reef gold anomaly. Average yearly gold values for seven years of reported production data from the Socorro Mine are also shown for comparison (also refer to Table 12). Samples within the moderately intense gold anomaly exhibit a bimodal frequency distribution with one mode between 0.11 and 0.4 ppm and another mode at 1.15 ppm. Samples from the weakly to moderately anomalous Precambrian granite (which is north of the moderately intense portion of the Socorro Reef gold anomaly) are weakly anomalous (mode at 0.065) to moderately anomalous (mode at 0.015).

Excluding the 1904-1934 production data, gold values for all 368 samples collected by surface sampling and drilling within the Socorro Reef gold anomaly average 1.02 ppm (0.03 oz/T). Excluding high grade samples (greater than 9 ppm) and low-grade samples (less than 0.02 ppm), 334 samples averaged 0.5172 ppm (0.0152 oz/T). Of these, 100 samples fell within the weakly anomalous interval (0.11 to 0.09 ppm) and averaged 0.053 ppm gold; 193 occurred in the moderately anomalous interval (0.09 to 0.9 ppm) and averaged 0.319 ppm; and 48 samples occurred in the strongly anomalous category (0.9 to 9 ppm) and averaged 2.59 ppm.

Gold Content by Rock Type. During the sampling it became apparent that both the Bolsa Quartzite section and the Precambrian granite north of the Bolsa Quartzite contained gold mineralization. To evaluate the distribution of gold values within these two rock types, a frequency histogram was prepared for samples collected within the quartzite and another for those from the granite. Inspection of Figure 28 reveals that the Bolsa Quartzite carries systematically higher values of gold. 158 samples known to have been collected from the Bolsa Quartzite-Abrigo section contained an average of 0.485 ppm gold, whereas 49 samples known to have been taken from the Precambrian porphyritic granite contained an

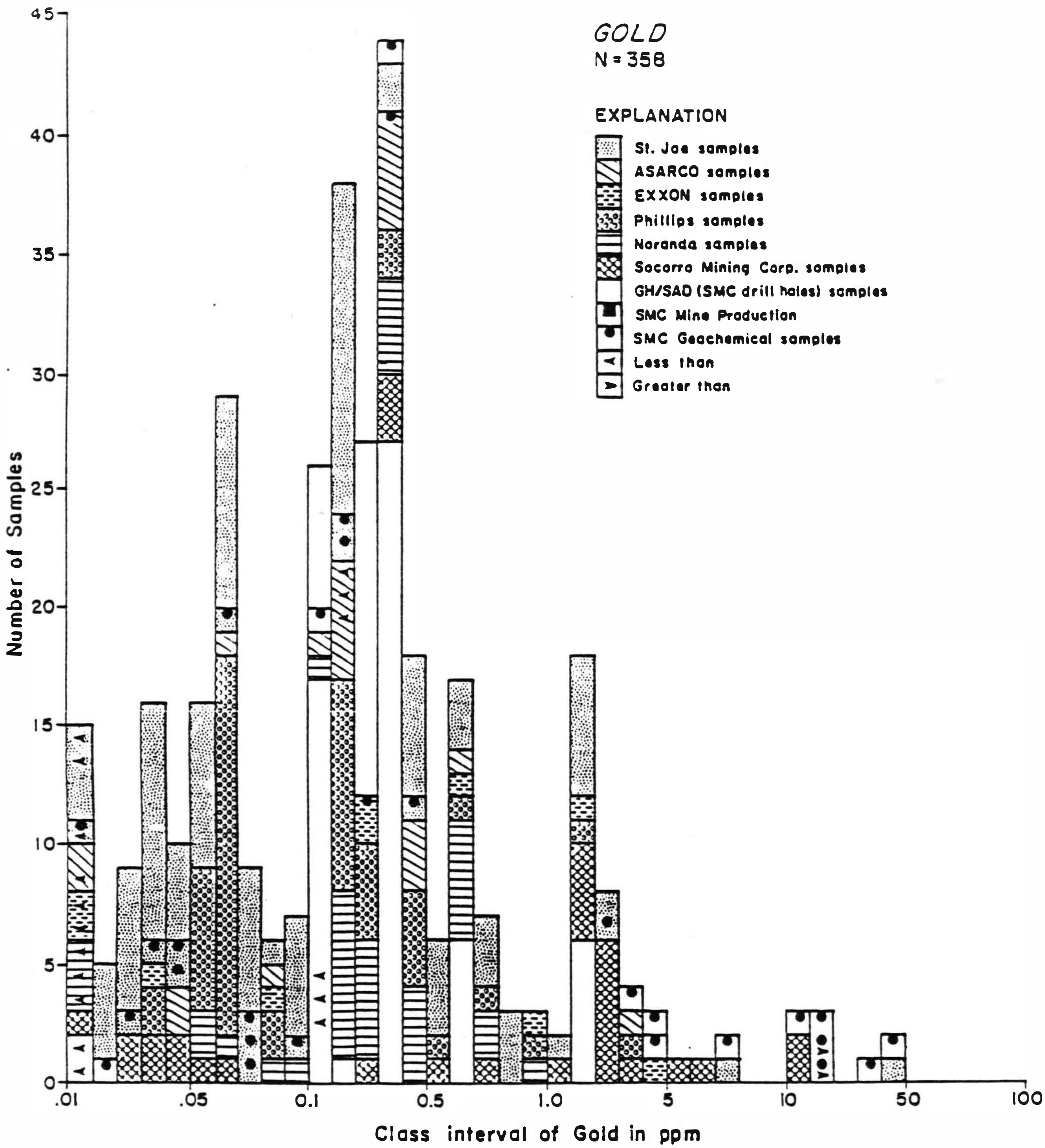

Figure 27. Frequency histogram for Gold values in samples from the Socorro Reef Gold anomaly.

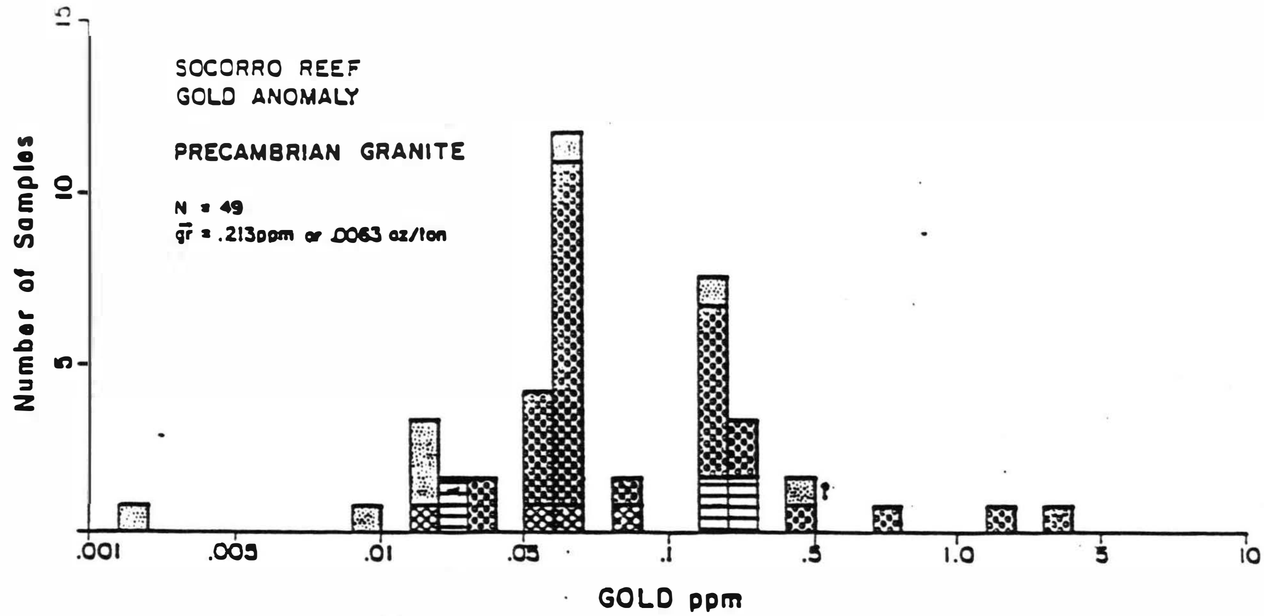

Figure 28A. Frequency histogram of gold contents in samples from Precambrian granite within the Socorro Reef anomaly.

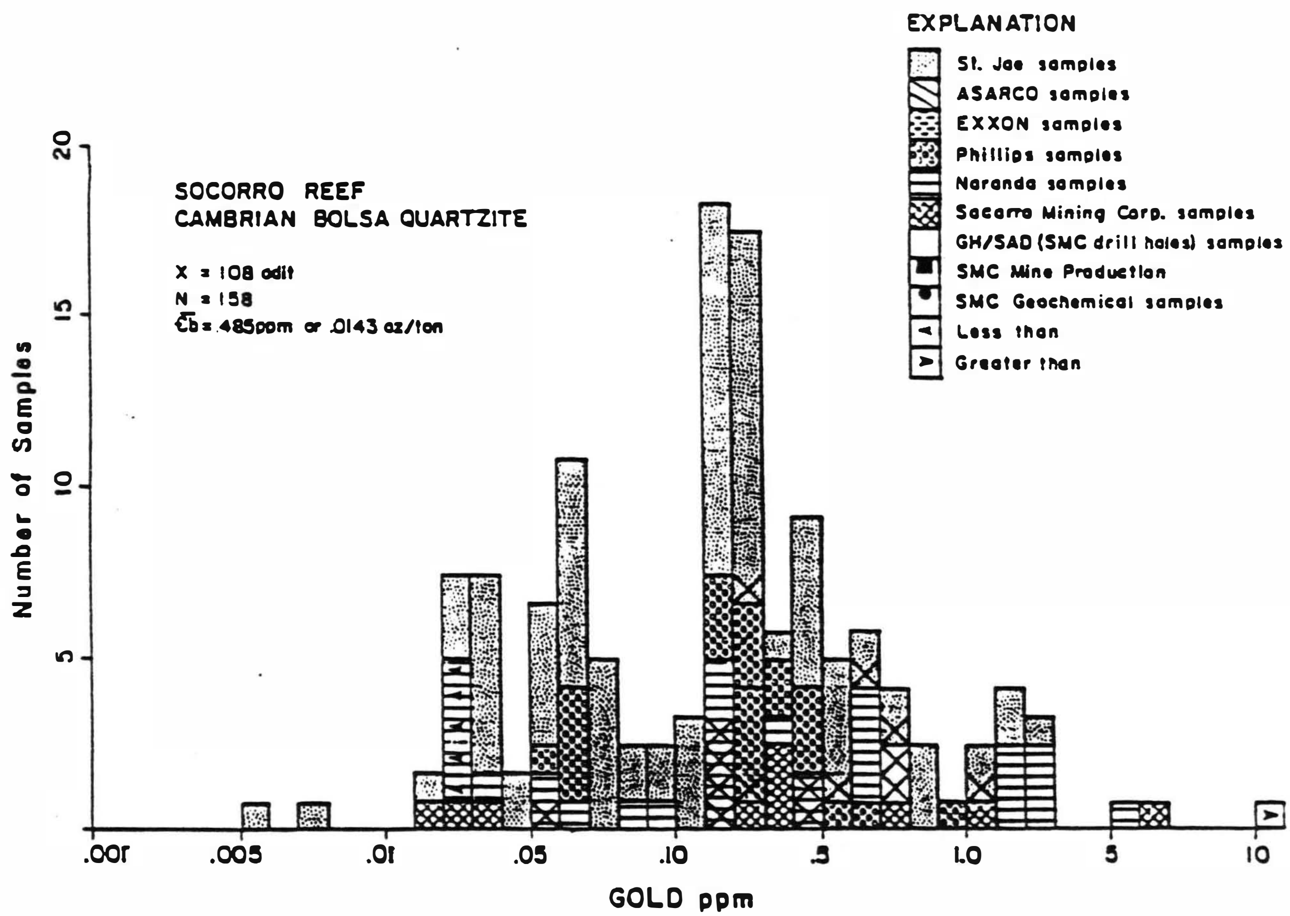

Figure 28B. Frequency histogram of gold contents in samples from Bolsa Quartzite within the Socorro Reef anomaly.

average of 0.213 ppm gold. Both groups of samples are bimodal and in both groups the principal modes are at 0.065 ppm gold and 0.15 ppm gold. However, the principal mode for the Precambrian granite is 0.065 ppm gold, whereas the principal mode for the Cambrian Bolsa Quartzite-Abrigo section is 0.15 ppm gold. In summary, Figure 28 clearly shows the preference of higher grade gold values for the Bolsa Quartzite-Abrigo section. Thus, rock type exerts a considerable control on the distribution of gold grades. Nevertheless, samples of the Precambrian granite, especially where it occurs directly below the Bolsa Quartzite, are anomalous and do add to the overall tonnage amounts at Socorro Reef.

<u>Presence of Coarse Gold</u>. The bimodal character of samples enclosed by the contour around the moderately intense anomaly within the Socorro Reef gold anomaly suggests that coarse gold might be present. That is, there could be two or more populations of sizes of gold particles within the auriferous quartzite. The coarse gold fraction would produce fewer particles per given volume of rock. This would introduce a sampling problem in that sampling would mainly sample the fine gold fraction and would irregularly sample or miss the coarse gold fraction.

To evaluate to what extent there might be coarse gold present, Exxon analyzed two sample splits from the same samples in the anomalous Bolsa Quartzite-Abrigo section by the same analytical technique (atomic absorption). They found significantly increased gold contents in one out of seven samples that contained anomalous gold. These data suggest that some coarse gold is present within the moderate intensity portions of the Socorro Reef gold anomaly; they also support the idea that the bimodal aspects of the Socorro Reef gold anomaly are, at least in part, possibly due to size differences between fine gold and coarse gold. Thus, when a particle of coarse gold enters into an analytical split, it will significantly increase the gold contents to one ppm or more from a background, fine-gold population that would range between 0.3 and 0.5 ppm. Enough samples have been collected so that the average figures quoted in the preceding paragraphs on gold grades probably represent realistic average values for gold at the ground surface within the Socorro Reef gold anomaly and would include a representative sample of the coarse gold fraction.

Silver Grades

Figure 29 is a frequency histogram for 267 samples that were analyzed for silver within the Socorro Reef gold anomaly. As can be seen from Figure 29 silver is not an important ingredient in the Socorro Reef gold system. Average silver values for the 267 samples was much, much less than 1.23 ppm because most of the samples within the Socorro Reef gold anomaly contained less than detectable silver at the 0.2 ppm level. The probable silver content can be estimated by assuming that the gold:silver ratio for the 1904-1934 Socorro Mine production applies to the Socorro Reef gold anomaly in general. Thus, if one divides 0.5172 ppm (the average gold content of the Socorro Reef gold anomaly without the high and low grade samples) by 1.77 (the gold:silver ratio

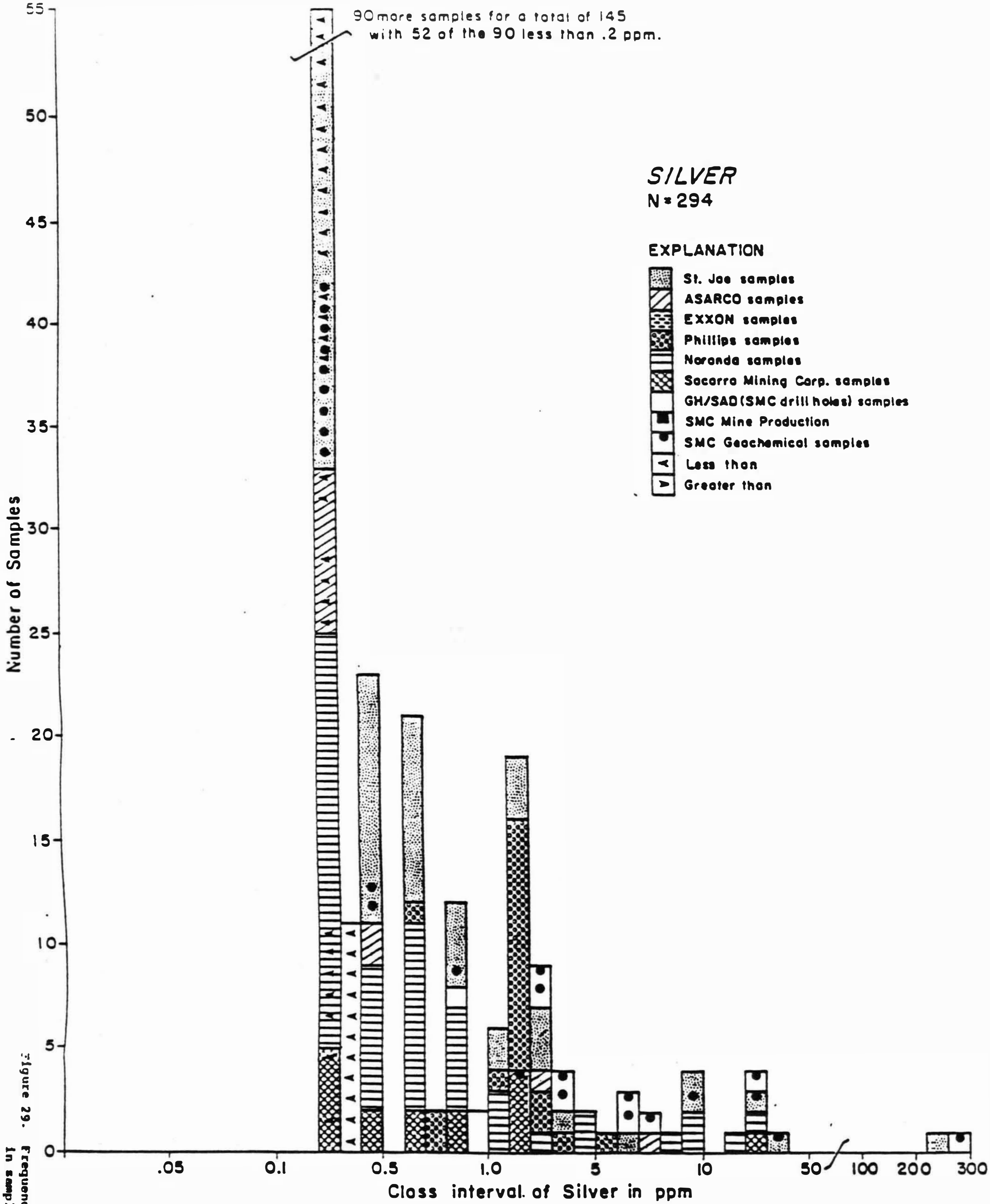

Figure 29. Frequency histogram for silver value in samples from the Socorro Reef gold anomaly.

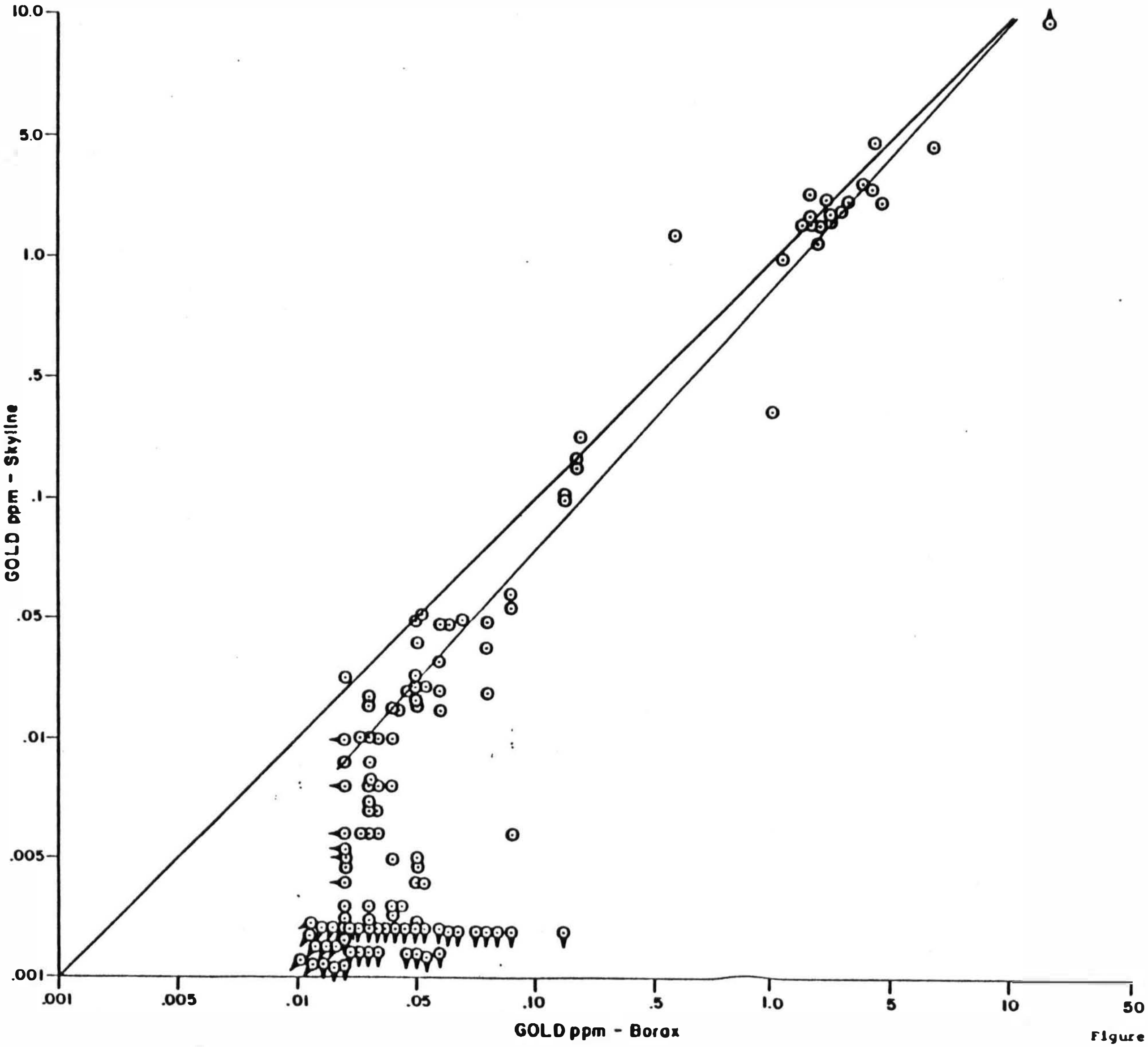

Figure 31. Comparison of U.S. Borax analyses and Skyline analyses for gold in Socorro Mining Corporation rock chip geochemical samples.

for the 1904-1934 Socorro Mine production), a value of 0.29 ppm silver is obtained. This number is probably a realistic number for silver values within the Socorro Reef gold system.

Possible Variations in Gold Content with Depth

Figure 30 is a gold-silver variation diagram for all samples analyzed for gold and silver within the Socorro Reef gold anomaly. As is Figure 9 in Part I, gold exhibits a good positive correlation with silver values over the domain of the Socorro Reef gold anomaly. A minor exception to this correlation is silver data analyzed by Borax on Phillips samples, which yielded systematically higher values of silver for samples below the 2 ppm level. This discrepancy is probably a function of the different analytical techniques for silver used by the two laboratories.

Figure 30 also shows the production data for the Socorro Mine from 1904 to 1934. The significant point about the Socorro Mine production and geochemical sampling within the Socorro Mine portion of the Socorro Reef gold anomaly is that this mineralization was deposited at a lower structural level; that is, the gold mineralization at the Socorro Mine was deposited along the Golden Eagle thrust rather than structurally higher in the upper plate quartzite. If it is assumed that the Golden Eagle thrust directly beneath the anomalous Bolsa Quartzite is mineralized with gold grades similar to those encountered in the Socorro Mine, then there is a good possibility that gold contents obtained from surface samples of Bolsa Quartzite might systematically increase downward towards the Golden Eagle thrust. Sampling to date within the Socorro Mine portion of the Socorro Reef gold anomaly (Block F on Figure 26) averages 0.138 oz/Ton based on 23 samples. This grade is slightly less than the 0.155 oz/Ton average grade for the 1904-1934 Socorro Mine production. This grade is about three and a half times higher than average values for gold on the surface within the quartzite portion of the Socorro Reef gold anomaly.

Some information is available about what happens to gold values in the quartzite portion of the Socorro Reef gold anomaly with depth. In June of 1981 Arizona Drilling Services drilled one 200-foot, reverse-circulation, rotary hole in the floor of the Socorro Mining open cut southwest of Hill 2462. The location for this hole, named SAD-1, is shown on Figure 26. Cuttings were collected and composited for every 5-foot interval in the drill hole. The first 50-foot interval averaged 0.0105 oz/Ton, the interval from 50-100 feet averaged 0.0135 oz/Ton, the interval from 100-150 feet averaged 0.016 oz/Ton, and the interval from 150-200 feet averaged 0.015 oz/Ton. Thus, in the SAD-1 drill hole, there is a slight increase in grade with depth, although the grade level is not as high as one would like. Appendix X contains analytical data for the SAD-1 drill hole, for two holes (designated GH-1 and GH-2) drilled in and near the Socorro Mine portion of the Socorro Reef gold anomaly, and for two holes designated CAM-1 and CAM-2 drilled on the Henry Bell claim. Locations for these holes are shown on Figure 26.

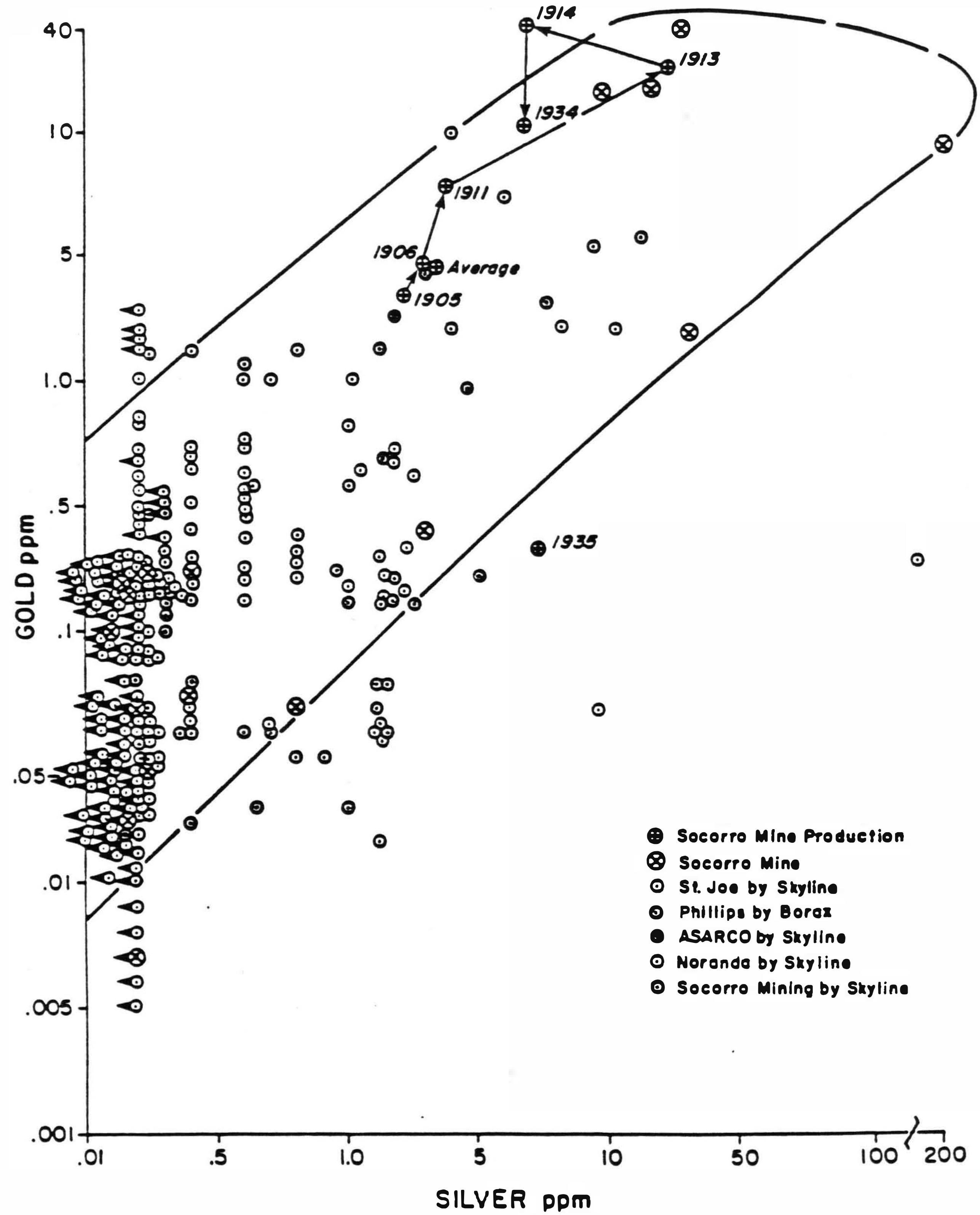

Figure 30. Gold:Silver variation diagram for samples within the Socorro Reef Gold anomaly.

Based on all the data currently at hand it is reasonable to suggest that grades near the surface in the quartzite portion of the Socorro Reef gold anomaly might double with depth towards the Golden Eagle thrust. One could, of course, assume that grades might be as much as 3.5 times higher from the foregoing discussion, but a factor of 2 is more reasonable given the possible tonnages involved. The influence of depth on dollar values for gold within the Socorro Reef gold anomaly will be discussed in a subsequent section.

Verification of Gold Grades

Gold grades in the preceding section are almost entirely based on atomic absorption analyses performed by Skyline Laboratory in Tucson, Arizona. Although atomic absorption techniques are reliable for establishing the presence of anomalous gold, they lack resolution in identifying quantitatively the exact concentration of gold in anomalous samples. Typically, atomic absorption underestimates the amount of gold in an anomalous samples where gold is greater than 0.1 ppm. Hence, the Socorro Mining Corporation samples were resubmitted to U.S. Borax for reanalysis by a fire assay data with an atomic absorption finish technique. St. Joe also obtained fire assay data for many of their samples where gold exceeded 1.2 ppm.

Figure 31 compares gold values determined by Skyline Laboratory by atomic absorption with gold values determined by Borax-Anaheim Laboratory by fire assay methods with atomic absorption finish for the same samples. The diagonal line through the diagram represents a line of perfect correlation between laboratories. Samples that appear above and to the left of this line indicate that Skyline analysis is high relative to the Borax analysis of the same sample. The opposite is the case for samples that plot below and to the right of the line; these samples indicate the Borax analysis is high relative to Skyline analysis of the same sample. It can be seen on the diagram that Borax analyses are systematically higher than Skyline analyses for the same sample. It is also apparent from Figure 31 that above 0.1 ppm Borax samples exhibit a good correlation with Skyline samples. The slope for this correlation falls below the line of perfect correlation indicating a bias towards higher gold values for the Borax samples. Below 0.1 ppm and especially below 0.05 ppm a significant number of Borax analyses have no correlation at all with Skyline analyses. Thus, in samples with less than 0.1 ppm gold, it is impossible to tell whether or not gold contents based on Borax analytical data alone are weakly anomalous. However, one can evaluate whether or not Borax data is weakly anomalous for gold by comparing Borax data with Skyline data for the same sample. From the diagram it is apparent that weakly anomalous Skyline samples above 0.009 ppm gold correlate positively with Borax data. A line fit through this data corresponds closely with a line fit through Borax and Skyline data in samples above 0.1 ppm gold. Thus, the Borax analyses that do correlate positively with Skyline data in the weakly anomalous gold category are probably real. It is also apparent that the line which fits all weakly through strongly anomalous Borax and Skyline analytical pairs is systematically steeper than the line of perfect correlation. Thus, Borax samples with low gold values (below 0.1 ppm gold) are systematically much higher than Skyline analyses. At higher gold values Borax numbers are systematically higher than Skyline analyses but to a much less extent.

The degree to which Borax analyses were systematically higher than Skyline analyses for the same sample is shown on Figure 32 and was determined in the following manner. First, all samples where the Skyline analysis contained less than 0.009 ppm gold were ignored, because of the complete lack of correlation with Borax analyses. Secondly, the Borax analysis of a given sample was divided by the Skyline analysis for that sample. In 44 out of 53 cases the Borax analysis was higher than the Skyline analysis. In the 9 cases where the Skyline analysis was greater than the Borax analysis, the Skyline analysis was divided by the Borax analysis. The results of these calculations are presented in Figure 32. On the diagram the factor by which a Skyline or Borax analysis is greater than the other is plotted with reference to gold contents in the Skyline samples. The variation diagram shows that, for samples above 0.09 ppm gold, Borax analyses, on the average, are about 1.3 times greater than the Skyline samples. For samples below 0.09 ppm gold, Borax data are much higher than Skyline analyses by a factor of 1.3 to 3.5 times. Consequently, based on this exercise, average gold values for a given portion of the Socorro Reef gold anomaly may be increased by a factor of about 1.3 where stated gold contents exceed 0.09 ppm gold. For example, the average gold content determined for the entire Socorro Reef gold anomaly on the basis of atomic absorption data was stated in the gold grade section to be about 0.0152 oz/Ton. If this number is multiplied by 1.3, a value of 0.0198 oz/Ton is obtained. This amounts to an increase of about 0.01 oz/Ton gold for gold grades between about 0.02 and 0.04 ppm. As will be seen in the next section, this factor will significantly increase the gold yields in both ounces and dollars.

DETERMINATION OF POTENTIAL ORE RESERVES AND DOLLAR VALUE

Data in the foregoing sections now allows the construstion of economic models of the Socorro Reef gold deposit. Based on geology and average gold contents, the moderately intense portions of the Socorro Reef gold anomaly were divided into six blocks denoted A - E on Figure 26. Average gold grades within each block were calculated by averaging the gold contents for all samples within each block, including subsurface data where available. Tonnages (in short tons) were calculated by determining the volume of each block in cubic feet and dividing that volume by a tonnage factor of 12, which is the number of cubic feet of granite and/or quartzite per ton. The map dimensions of each block were obtained from the 1 inch = 500 foot scale map of the Socorro Reef gold anomaly (Plate 24). These blocks are also outlined on Figure 26. The vertical dimension or depth of Blocks A, B, C, and E was estimated to be about 350 feet based on geophysical data and structural modeling discussed in previous sections.

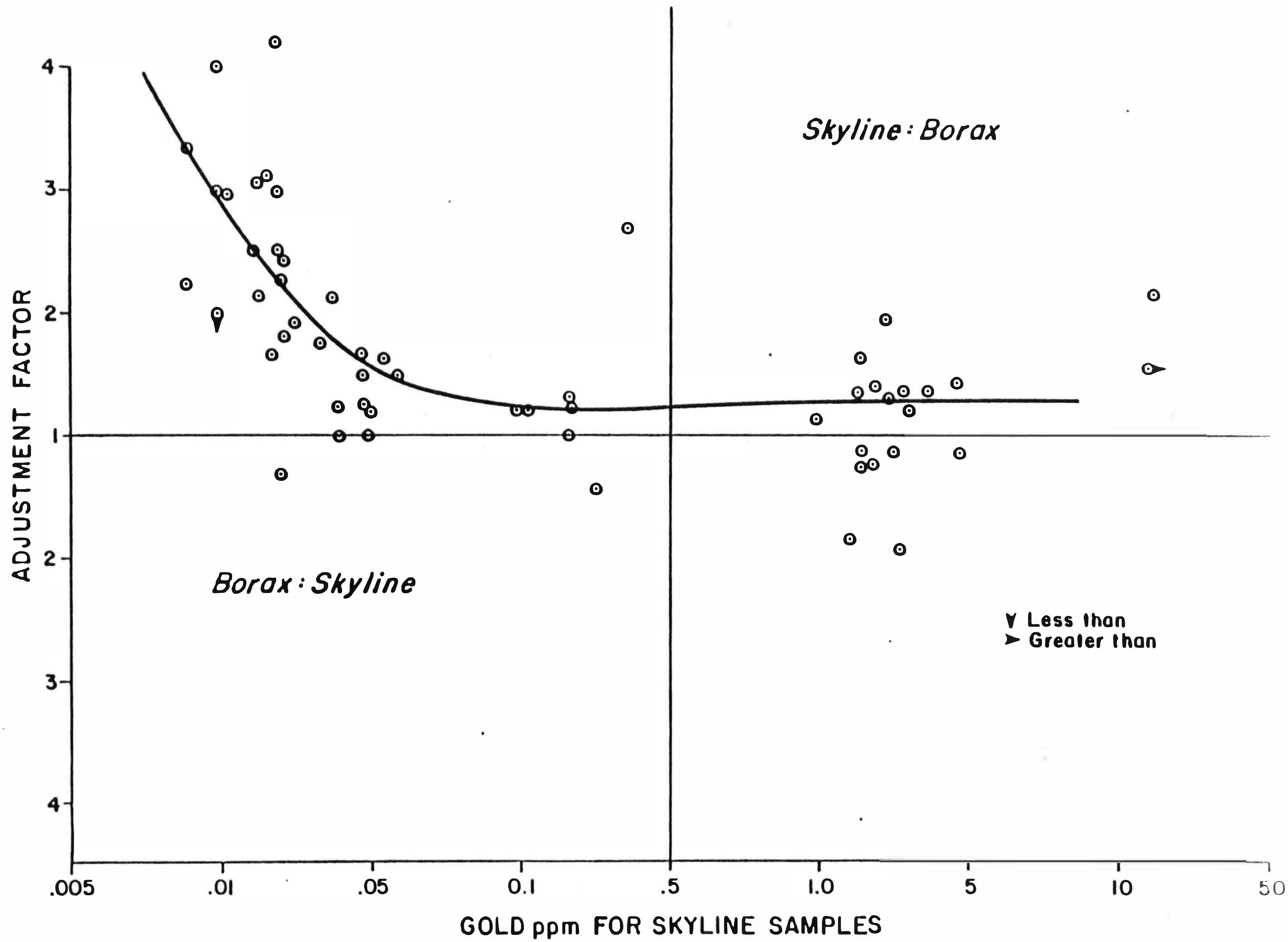

Figure 32. Variation diagram showing factors to adjust Skyline Laboratory atomic absorption data to U.S. Borax Laboratory fire assay data.

The depth of Block D, which contains Hill 2462, was taken as 450 feet with the additional 100 feet added because of higher elevations in the hill. Plan dimensions of Block F were taken from the maps and the vertical dimension of 20 feet was taken from intercepts in the GH-1 drill hole and from estimated heights of stopes within the old Socorro Mine workings. All of the above information is summarized in Table 15.

Total gold content, gold grade, and dollar value of gold within each block was calculated according to three models (Table 15). The first calculation (Model 1) assumed a conservative model where average gold values derived from Skyline Laboratory's analytical data were assumed to represent true surface values and do not increase with depth. The second model (Model 2) assumed that the Skyline Laboratory analytical data is systematically low by a factor of 1.3 (See section on Verification of Gold Grade), and that there was no increase in grade with depth. The third and most optimistic model (Model 3) assumed the average gold values from Skyline Laboratory were low by a factor of 1.3 and therefore had to be adjusted upward as in Model 2 and also assumed the gold grades increased with depth by a factor of 2 (See section on Possible Variations of Gold Content with Depth).

Dollar values for all models in Table 15 were calculated at a gold price of $450/oz. Gold contents and dollar values at various gold prices for various combinations of blocks and economic models are shown in Table 16. From present data the silver content within the Socorro Reef gold anomaly is too low to be of economic interest (Table 17). The total indicated silver value for all blocks within the Socorro Reef gold anomaly is only $2,300,000; this is 79 times less than the dollar value of gold. The above numbers for silver assumed a gold:silver ratio of 1.77 over the Socorro Reef gold anomaly and a gold:silver price ratio of 45:1.

Model 1 is clearly the most conservative of the three models and probably is too conservative because of the analytical technique used to obtain the gold values. Model 2 is perhaps the most realistic of the three models given what is <u>currently</u> known about the Socorro Reef gold anomaly. If it is assumed (and this is a sizeable assumption) that the SAD-1 drill hole represents a fair test of gold grades with depth, then a significant increase in depth from surface values is not predicted. The SAD-1 drill hole data is reinforced with the induced polarization (IP) data, which suggests the sulfide-bearing material is fairly evenly distributed throughout the quartzite portion of the Socorro Reef gold anomaly and does not increase with depth.

However, there are substantial reasons to question the Model 2 assumptions. First, one drill hole is probably not representative. Second, as outlined in the previous section on Variations in Gold Content with Depth, gold grades within the SAD-1 drill hole do increase slightly with depth. The lower 100 feet of the hole averaged 0.0155 oz gold/Ton based on 40 5-foot composite samples of drill cuttings, whereas surface samples within Block C average 0.0123 oz gold/Ton based on 44 samples. This latter number is very close to the average grade (0.012 oz gold/Ton) for 40 composite samples from the upper 100 feet of the SAD-1 drill hole.

Table 15: Gold Grade and tonnage information for various gold-bearing blocks within the Socorro Reef gold anomaly

ECONOMIC PARAMETERS	BLOCK A	B	B high grade	C	D	E	F
Map Dimensions (feet)	250 x 200	725 x 275	725 x 130	550 x 250	940 x 325	875 x 500	250 x 375
Depth extension (feet)	350	350	350	350	450	350	20
Number of surface samples	14	64 (.023)	37 (.035)	44 (.0123)	41	23	9 (.0144)
Number of subsurface samples	-	16 (.012) (from adit)	16 (.012) (from adit)	40 (.0138) (from SAD-1)	-	-	11 (.23)
Number of surface and subsurface samples	14	80	53	84	41	23	23
Average gold grade from subsurface and surface data (oz/ton)	.0041	.021	.028	.013	.0113	.0056	.138
Standard deviation (oz/ton)	.006	.0415	.0491	.0166	.0156	.0114	.284
Tonnage (short tons)	1,458,000	5,815,000	2,749,000	4,010,000	11,456,250	12,760,000	156,250
Total gold content (oz)	5,978	122,115	76,972	52,130	129,453	71.456	21,562
Dollar value (@ $450/oz)	2,690,000	54,952,000	34,637,000	23,458,000	58,354,000	32,155,000	9,703,000
	* (1.84)	(9.45)	(12.60)	(5.85)	(5.09)	(2.52)	(62.20)
RECALCULATION OF ABOVE ASSUMING GOLD GRADE ADJUSTMENT FROM BORAX DATA (Model 2)							
Average gold grade of all data (oz/ton)	.0053	.0273	.0363	.016	.0147	.0073	.179
Total gold content (oz)	7,727	158,750	99,789	64,160	168,403	73,148	27,969
Dollar value (@ $450/oz)	3,477,150	71,437,000	44,905,000	28,872,000	75,781,000	41,917,000	12,586,000
	* (2.38)	(12.28)	(16.34)	(7.20)	(6.61)	(3.28)	(80.68)
RECALCULATION OF ABOVE ASSUMING INCREASE IN GOLD GRADE WITH DEPTH (Model 3)							
Average gold grade of lower 1/2 of block (oz/ton)	.0106	.0546	.0726	.032	.0294	.0146	
Tonnage of lower 1/2 of block	729,000	2,907,500	1,374,500	2,005,000	5,728,125	6,380,000	
Gold content of lower 1/2 of block	7,700	150,700	99,800	64,200	168,400	93,200	
Average gold grade of upper 1/2 of block (oz/ton)	.0041	.021	.028	.013	.0113	.0056	
Tonnage of upper 1/2 of block	729,000	2,907,000	1,374,500	2,005,000	5,728,125	6,380,000	
Average gold grade of entire block (oz/ton)	.008	.0409	.0543	.024	.022	.011	
Gold content of upper 1/2 of block (ounces)	3,900	79,400	49,500	32,100	84,200	46,600	
Total gold content of block (ounces)	11,600	238,100	149,300	96,200	252,600	139,800	
Dollar Value (@ $450/oz)	5,215,000	107,000,000	67,000,000	43,000,000	113,000,000	63,000,000	
	* (3.57)	(18.40)	(24.37)	(10.72)	(9.86)	(4.94)	

* Number in parenthesis is gold value in dollars per ton.

Table 16: Gold content and Dollar value combinations of various blocks

ECONOMIC PARAMETERS	B + C Model 1	B + C Model 2	B + C Model 3	B + C + D Model 1	B + C + D Model 2	B + C + D Model 3
Tonnage (millions of short tons)	9.825	9.825	9.825	21.281	21.281	21.281
Gold Grade (oz/ton)	.018	.023	.034	.0143	.0184	.0276
Gold Content (oz)	174,245	222,910	334,300	303,698	391,313	586,900
Dollar Value						
@ 400/oz	70,000,000 * (7.12)	89,000,000 (9.06)	134,000,000 (13.64)	121,000,000 (5.71)	157,000,000 (7.40)	235,000,000 (11.08)
@ 450/oz	78,000,000 * (7.94)	100,000,000 (10.18)	150,000,000 (15.27)	137,000,000 (6.46)	176,000,000 (8.30)	264,000,000 (12.45)
@ 500/oz	87,000,000 * (8.85)	111,000,000 (11.30)	167,000,000 (16.99)	152,000,000 (7.17)	195,000,000 (9.20)	293,000,000 (13.82)
@ 600/oz	105,000,000 * (10.69)	134,000,000 (13.64)	201,000,000 (20.46)	182,000,000 (8.58)	235,000,000 (11.08)	352,000,000 (16.60)

ECONOMIC PARAMETERS	B+C+D+F Model 1	B+C+D+F Model 2	B+C+D+F Model 3	A+B+C+D+E+F Model 1	A+B+C+D+E+F Model 2	A+B+C+D+E+F Model 3
Tonnage (millions of short tons)	21.437	21.437	21.437	35.655	35.655	35.655
Gold Grade (oz/ton)	.0152	.0192	.0284	.0113	.0144	.0213
Gold content (oz)	325,260	412,875	608,462	402,694	513,750	759,862
Dollar Value						
@ 400/oz	130,000,000 * (6.06)	165,000,000 (7.69)	243,000,000 (11.33)	161,000,000 (4.51)	205,500,000 (5.76)	304,000,000 (8.61)
@ 450/oz	146,000,000 * (6.81)	185,000,000 (8.63)	273,000,000 (12.73)	181,000,000 (5.08)	231,000,000 (6.48)	342,000,000 (9.59)
@ 500/oz	162,000,000 * (7.56)	206,000,000 (9.61)	304,000,000 (14.18)	201,000,000 (5.64)	257,000,000 (7.21)	380,000,000 (10.66)
@ 600/oz	195,000,000 * (9.10)	247,000,000 (11.52)	365,000,000 (17.03)	242,000,000 (6.79)	308,000,000 (8.64)	456,000,000 (12.79)

* Number in parenthesis is gold value in dollars per ton.

Table 17: Economic data for silver within the Socorro Reef Gold Anomaly

ECONOMIC PARAMETERS	Block						
	A	B	B high grade	C	D	E	F
Gold grade (oz/Ton)	.0041	.021	.028	.013	.0113	.0056	.138
Silver grade (oz/Ton)*	.0023	.012	.016	.0073	.0064	.0032	.078
Tonnage (short ton)	1,458,000	5,815,000	2,749,000	4,010,000	11,456,000	12,760,000	156,250
Total Silver (oz)	3,353	69,780	43,984	29,273	73,139	40,370	12,182
Dollar Value (@ 10./oz)	33,534	697,800	439,840	292,730	731,390	403,700	121,820

Total Silver in dollars
$2,291,000

* Calculated assuming a gold:silver ratio of 1.77 (based on 1904-1934 Socorro Mine production)

Third, the induced polarization (IP) data discussed in the geophysics section is not resolved enough to identify small tonnage zones (about 200,000 tons or less) that contain higher sulfide-bearing zones which are presumably more gold rich, even though the method does generally identify a zone of moderately intense, apparent polarization within the quartzite-granite blocks. Fourth, Model 2 assumes that no high-grade, bonanza pockets are present within Blocks A-E. Even one bonanza pocket, like the one encountered in the 'Castle Garden' stope within the Bolsa Quartzite at the Harquahala Mine in the Little Harquahala Mountains, would substantially increase the overall gold content of the Socorro Reef gold deposit. As outlined in the previous section on Variation in Gold Content with Depth, there are substantial geologic reasons (by analogy with the high-grade material within the Golden Eagle thrust at the old Socorro Mine) to expect an increase in gold content with depth towards the Golden Eagle thrust. The presence of high-grade bonanza pockets, the presence of intermediate-tonnage, moderate-grade gold zones (0.08 to 0.12 oz/ton), and the overall increase in grade with depth are all taken into consideration in Model 3. Because the removal of the large tonnages that are involved would considerably dilute the effect of bonanza pockets and moderate-tonnage, higher grade zones, the overall factor by which the grade can be reasonably expected to increase above surface grades is taken to be a factor of two or double the known surface grades. This increase is projected for the lower one half or the lower 175 feet of Blocks A-E. Economic aspects of Models 1, 2, and 3 are shown in Tables 15 and 16.

The summation of all data for Blocks A-F (Table 16) reveals that in the moderately anomalous portion of the Socorro Reef gold anomaly there is an indicated tonnage of 35.6 million tons with an average grade (using Model 3 assumptions) of 0.0213 oz gold/Ton. At $450/oz, and using Model 3 assumptions, this amounts to a total of $342,000,000 of gold with a gold value of $9.59/Ton. It is clear from Tables 15 and 16, however, that the average gold grade quoted above is not evenly distributed over all blocks; within the moderately anomalous granite and quartzite blocks, Blocks B, C, D, and F have substantially higher grades and constitute an attractive gold target with an indicated 21.4 million tons of potential gold ore. Of these, Blocks B and C are the most economically attractive.

From the existing data the Blocks with the most potential for mining are Blocks B, C, and F and a 'high-grade' subblock within Block B containing an indicated 2.75 million tons comprises the most attractive possibility. With Model 2 assumptions, the indicated surface grade for this subblock is 0.036 oz gold/Ton, which is comparable to gold grades of cyanide heap leach properties in Nevada that were operating in 1979 (See Table 18). With Model 3 assumptions for this higher grade subblock of Block B, the average indicated gold grade for this ground increases to 0.054 oz gold/ton, which is very close to the grade of most of the properties listed in Table 18. Obviously, Block B should be given the highest priority for confirmation drilling. Several larger tonnage targets within the Socorro Reef gold anomaly are also attractive, particularly a 9.8 million ton block that comprises Blocks B and C. This block of ground contains $100,000,000 of gold (using Model 2 assumptions) or $150,000,000 of gold (using Model 3 assumptions) (See Table 16). The 0.034 oz/Ton grade of this block (using Model 3 assumptions) is similar to the grades of producing properties at Windfall, Cortez, and Gold Acres

Table 18: Comparison of Socorro Reef with other disseminated, low-grade gold deposits in the western United States

Deposit	Tons (short)	Gold Grade (oz/ton)	Gold Content Dollars/ton (@ $450./oz)	Mining Costs Dollars/ton (pre-tax)	Recovery Method	Reference
Ortiz, New Mexico	6,841,000	.053	23.85	9.84 (mid-1981 total mining, processing and administrative cost)	Cyanide Heap-Leach	Hickson (1981)
Carlin, Nevada	9,370,000 (1965-77 Production)	.32	144.07	37.20 (Nov. 1981)	Milling	Mining Record (Nov. 1981)
Bootstrap, Nevada		.063 #1 heap .028 #2 heap		1.67 direct (1979) costs	Cyanide Heap-Leach	McQuiston & Shoemaker (1980)
Cortez, Nevada	422,000 tons/year	.036	16.20	1.22 (1979)	Cyanide Heap-Leach	McQuiston & Shoemaker (1980)
Gold Acres, Nevada	907,000 tons/year	.036	16.20	1.22 (1979)	Cyanide Heap-Leach	McQuiston & Shoemaker (1980)
Round Mtn, Nevada		.06	27.00	5.32 (1979 direct and administrative)	Cyanide Heap-Leach	McQuiston & Shoemaker (1980)
Windfall, Nevada	220,000 tons/year	.028	12.60	3.93 (1980 mining and processing costs)	Cyanide Heap-Leach	McQuiston & Shoemaker (1980)
Socorro Reef, AZ						
B+C+D+F Model 3	21,437,000	.0284	12.73			
B+C+D+F Model 2	21,437,000	.0192	8.63			
B+C Model 3	9,825,000	.034	15.27			
B+C Model 2	9,825,000	.023	10.18			

in Nevada (Table 18). Grade continuity and a slight increase in grade

with depth for Blocks B and C have already been tested to some degree by the SAD-1 drill hole in Block C. If Block D is added to the Block B and C package, the indicated tonnage increases to over 21 million tons and (using Model 3 assumptions) contains $264,000,000 of gold at $450/oz. However, mining costs within Block D would be substantially higher because of the additional waste material that would have to be removed from Hill 2462 to gain access to the mineralized quartzite block. Thus, drilling confirmation should be acquired first for Blocks B and C. The high-grade ground within Block F is too low in tonnage to justify an open cut mine by itself. However, high grade portions of this ground could be blended with lower grade rock in Blocks B and C to obtain higher and more evenly distributed gold grades for recovery purposes. Blocks A and E, while containing about 14 million tons of gold-bearing material, do not contain high enough grades to justify drilling confirmation at this time.

From Table 18 it can be seen that pre-tax operating costs per ton for various, recently operating, open-cut gold mines in the southwestern U.S. are substantially lower than the overall dollar value of gold content per ton of ore mined by at least a factor of 3. As can be inferred from the table this factor can be considerably influenced by the price of gold, so that one would like the difference between actual gold content and cost of mining to be as high as possible. It should be noted that the Windfall Mine, which has the lowest grade of the operating properties in Table 18, closed in 1981 when the price of gold fell below $350/oz, but is expected to open soon as the price of gold has now been consistently above $400/oz. Therefore, the difference between gold content and pre-tax operating costs at Socorro Reef gold deposit should consistently be greater than 2.5 to 1 before the Socorro Reef gold deposit could be brought into profitable production. At a gold price of $450/oz a 2.5 to 1 ratio of gold value to cost of production seems viable for Blocks B, C, D, and F using Model 3 assumptions, for Blocks B and C using Model 3 assumptions, for Block B using either Model 2 or Model 3 assumptions, and for the 'high-grade' subblock within Block B using Model 1, 2, or 3 assumptions. Thus, based on present data, Block B at the surface is comparable to producing, open-cut, heap-leach, gold operations elsewhere and could be brought into production if drilling confirmed the surface grades to depth. Blocks B and C could be brought into production if drilling substantiates Model 3 assumptions or if the price of gold increases to and remains above $550/oz. Thus, about 10 million tons of ground within the Socorro Reef gold deposit is commercial pending drilling confirmation of Model 3 assumption, and is commercial as it stands if the price of gold increases to and remains over $550/oz and mining costs do not escalate.

Conclusions and Recommendations

Geologic, geochemical, and geophysical data presented in Part II strongly suggest the inference that the Socorro Reef gold anomaly is the surface expression of a large-tonnage, low-grade, disseminated gold deposit. Economic evaluation of all available surface data using optimistic, but reasonable, geologic assumptions (Model 3) suggest that about 760,000 ounces of gold (0.0213 oz of gold/Ton) are contained within 35.6 million tons of gold-bearing material in six blocks (Figure 26). At a gold price of $450/oz the above material contains $342,000,000 of gold. Under present economic conditions about 10 million tons of gold-bearing rock in Blocks B and C are commercial pending drilling confirmation of gold grades with depth. The estimated value of gold in the 10 million ton block using Model 3 assumptions is about $150,000,000. If economic conditions improve slightly, that is, if the price of gold increases to and remains over $500/oz, then another 11 million tons of gold-bearing rock can be added to the 10 million tons described above and the net worth of the Socorro Reef gold deposit would increase to about $293,000,000.

It is recommended that drilling priority be given to Blocks B and C with the objective of confirming and hopefully increasing gold grades in ground beneath surface exposures of these blocks. A fair test of these blocks would consist of five shallow drill holes (fully cored) of 500 feet each to obtain subsurface information on gold grades beneath Blocks B and C. At a cost of $20/foot this amounts to about $50,000 of drilling. Supportive geochemical work should consist of gold, silver, and tungsten assays for every 10-foot interval of core; this amounts to approximately $2750.00 of analytical work. Some of the holes should be angled across the width of the exposed gold anomaly in order to obtain information about gold grades in representative cross sections. At this time, no new surface information is required because abundant data has already been obtained from previous surface sampling programs conducted by the various major mining companies. The recommended drilling work can be done by Socorro Mining Corporation under my supervision or by one of the major mining companies currently interested in the property. This work could easily be done within six to nine months of the lease date. It is recommended that the confirmatory drilling be done as soon as possible by either Socorro Mining Corporation or a mining company lease-partner, because the economic climate is becoming increasingly favorable for development of low-grade, disseminated gold deposits. With many major mining companies now directing their exploration programs toward such targets, the Socorro Reef gold deposit is now a prime exploration target.

Acknowledgments

The entire report presented herein was prepared within three and one-half weeks, a considerable achievement. Completion of this report would have been impossible without the cooperation and support of several people who spent many overtime hours doing word processing, editing, drafting, collating, layout, typing, etc. These people deserve special mention. Susan Angelon, in particular, organized and supervised most of the graphic design, layout, and drafting for the text with its many plates, figures, and gatefolds. She was ably assisted by Chris Smith and Susanne Baker who drafted many of the figures and plates and by Thelma J. MacArthur (Mac) who spent many overtime hours providing superb hand coloring for all of the figures and plates. Jan Wilt, one of my colleagues helped with the word processing and provided invaluable editorial assistance and last minute assembly help. Pat Pileggi did an admirable job of word processing, which also included many hours of overtime. Supplemental typing help was also provided by Christine Dodson. Finally, Socorro Mining Corporation is gratefully acknowledged for its support during the entire Socorro Reef gold project. With a little more perseverence, Socorro Reef could well become a profitable gold mine.

List of References

Hickson, R. J., 1981, Heap leaching practices at Ortiz Gold Mine, Santa Fe County, New Mexico: Soc. Min. Eng. of AIME, Preprint No. 81-347, 14p.

Keith, S. B., and Reynolds, S. J., 1980, Geochemistry of Cordilleran metamorphic core complexes; Chapter 4, in Coney, P. J., and Reynolds, S. J., eds., Uranium favorability of Cordilleran metamorphic core complexes: Dept. of Energy (DOE) report GJBX-80-

Keith, Stanley B., Reynolds, Stephen J., and Richard, Stephen M., 1981, Laramide thrust-fault sandwich in the Salome region, west-central Arizona, in Keith, S. B., and others, eds., Low-angle tectonic phenomena between Tucson and Salome, Arizona: Arizona Bureau of Geology and Mineral Technology, Open-file Report 81-2, 114 p.

Keith, Stanton B., 1978, Index of mining properties of Yuma County, Arizona: Ariz. Bureau of Geology and Mineral Technology, Bull. 192, 185 p.

Laskey, S. G., and Webber, B. N., 1949, Manganese resources of the Artillery Mountains region, Mohave County, Arizona: U. S. Geol. Survey Bull. 961, 86 p.

McQuiston, J. R., and Shoemaker, R. S., 1980, Gold and silver cyanidation plant practice, v. 2: AIME, 263 p.

Rehrig, W. A., and Reynolds, S. J., 1980, Geologic and geochronologic reconnaissance of a northwest-trending zone of metamorphic core complexes in southern and western Arizona: Geological Soc. of America Memoir 153, p. 131-157.

Reynolds, S. J., 1980, Geologic framework of west-central Arizona: Arizona Geological Soc. Digest, v. 12, p. 1-16.

Reynolds, Stephen J., 1982, Multiple deformation in the Harcuvar and Harquahala Mountains, west-central Arizona, in Frost, E. G., and Martin, D. L., eds., Mesozoic-Cenozoic tectonic evolution of the Colorado River region, California, Arizona, and Nevada: Cordilleran Publishers, San Diego, CA, p. 137-142.

Reynolds, Stephen J., Keith, Stanley B., and Coney, Peter J., 1980, Stacked overthrusts of Precambrian crystalline basement and inverted Paleozoic sections emplaced over Mesoaoic strata, west-central Arizona: Arizona Geological Society Digest, v. 12, p. 45-51.

Richard, Stephen M., 1982, Preliminary report on the structure and stratigraphy of the southern Little Harquahala Mountains, Yuma County, Arizona, in Frost, E. G., and Martin, D. L., eds., Mesozoic-Cenozoic tectonic evolution of the Colorado River region, California, Arizona, and Nevada: Cordilleran Publishers, San Diego, CA, p. 235-244.

Shackelford, T. J., 1980, Tertiary tectonic denudation of a Mesozoic-early Tertiary(?) gneiss complex, Rawhide Mountains, western Arizona: Geology, v. 8, p. 190-194.

Shafiqullah, M., and others, 1980, K-Ar geochronology and geologic history of southwestern Arizona and adjacent areas: Arizona Geological Society Digest, v. 12, p. 201-260.

Varga, R. J., 1976, Stratigraphy and superposed deformation of a Paleozoic and Mesozoic sequence in the Harquahala Mountains, Arizona: unpub. M.S. thesis, Tucson, Univ. of Arizona, 61 p.

Varga, Robert J., 1977, Geology of the Socorro Peak area, western Harquahala Mountains: Arizona Bureau of Geology and Mineral Technology, Circular 20, 20 p.

Wilson, E. D., 1960, Geologic map of Yuma County, Arizona: Tucson, Arizona Bureau of Mines, scale 1:375,000.

AGS field trip
April 17, 1988

Geology of the Copperstone Gold Deposit, Arizona

Graham L. Kelsey and K. Leon Hardy
Cyprus Copperstone Gold Corp.
P.O. Box A.I.
Parker, Arizona 85344

W.D. Burton
Cyprus Minerals Co.
P.O. Box 3299
Englewood, Co. 80155

INTRODUCTION

The Copperstone mine is an epithermal vein - breccia gold deposit situated in La Paz County, Arizona about 16 miles north of Quartzsite (Figure 1). There is good access by way of U.S. Highway 92 for 12 miles north from Quartzsite, then northwest on graded road for 6 miles to the mine. The deposit is owned by Cyprus Minerals Company and is located on 290 contiguous claims.

HISTORY

The Copperstone claim block has no early mining history preceeding the 1960's.

During 1968 to 1980 the area now covered by the Copperstone claims was held by Charles Ellis of the Southwest Silver Company. The property was then known as the Continental Silver claim group. Six rotary holes were drilled at widely scattered locations, but data for only one of these holes was available. This 710 - foot drill hole was completed, cuttings were panned, and a preliminary log prepared. Chrysocolla-amethyst-quartz-barite-specularite mineralization was noted intermittently to the bottom of the hole. The Southwest Silver Company let the claims lapse in 1980 for lack of assessment work. The area was then restaked by local prospector Dan Patch of Quartzsite, Arizona.

Cyprus/Amoco acquired the 64 Copperstone claims from Mr. Patch in 1980 and initiated a drilling program shortly after land acquisition. These initial rotary holes encountered gold intercepts from 10 feet to 150 feet wide, ranging from 0.05 to 0.10 ounce gold per ton. From 1980 to present, 359 rotary and reverse circulation holes and 73 diamond core holes have been drilled to outline the gold mineralization.

GEOLOGIC SETTING

The Copperstone claim block contains a Precambrian basement complex of gneiss, schist, quartzite, and augen gneiss with several generations of intrusive rocks. A thin section of Paleozoic limestone and clastic strata overlays this basement. Thick sequences of middle Mesozoic clastic rocks and quartz latite extrusive rocks cap the Paleozoic strata. Low angle normal faults separate the Mesozoic and Paleozoic strata from the underlying Precambrian basement. These low angle faults may represent detachment surfaces resulting from isostatic uplift of metamorphic/crystalline core complex rocks. As the upper plate Mesozoic and Paleozoic strata migrated away from the uplift, a series of subsidiary listric faults formed during the sliding event. The low angle and listric faults are in turn cross-cut by high-angle NNW and NNE faults. The Copperstone gold deposit is localized in listic faults where mineralizing solutions have deposited a complex mineral assemblage.

MINE GEOLOGY

Host

The Copperstone mine is hosted by three lithologic units (Figure 2). The stratigraphically lowest unit is a middle Mesozoic porphyritic quartz latite. This quartz latite is a weakly metamorphosed, welded tuff composed of 1 mm to 4 mm quartz, k-feldspar, and plagioclase phenocrysts set in a fine to medium grained quartz-feldspar-sericite-chlorite matrix.

A chaotic breccia overlying the quartz latite tuff forms the second lithologic host. The breccia contains angular to subrounded cobbles and blocks of quartz latite in a non-metamorphosed, hematite-sericite-clay matrix. Its chaotic, unsorted nature and clayey unmetamorphosed matrix suggests the breccia may represent a mudslide event post-dating deposition and metamorphism of the quartz latite tuff. However, several other genetic models have been postulated for the breccia's origin which include: (1) a hydrothermal breccia; (2) collapse breccia; and (3) fault breccia.

The third and primarily minor host is a vesiculated Tertiary (?) basalt. The basalt is cross-cut by gold bearing amethyst-quartz-specularite veins and saturated by a clay-hematite alteration.

Structure

Copperstone gold mineralization is localized along the moderately dipping portion of a listric fault (Figure 3). The fault separates mineralized footwall quartz latite tuff from gold-bearing hanging wall chaotic breccia. This downward curving structure referred to as the Copperstone Fault strikes N25W and dips 25 to 40 degrees northeast. A series of high-angle NNW and NNE faults cross-cut the Copperstone Fault. These high-angle faults appear to have been active during the Copperstone mineralizing event. The entire fault system provides excellent ground preparation and represents the pathway through which gold-bearing solutions were deposited.

Mineralization

Surface and subsurface observations at the Copperstone mine suggest multiple phases of fluid introduction to form a complex vein system associated with intersecting structures. The minerology is composed of numerous, intersecting quartz-amethyst, specularite, goethite (magnetite), barite-fluorite, carbonate and chrysocolla veins with locally associated earthy, red hematite saturation. Texturally the veins are coarsely banded and vuggy with comb and cockade quartz-amethyst. A hydrothermal breccia, fractures and brecciates the veins, surrounding the fragments with fine-grained silica and carbonate. Finely laminated, chalcedonic quartz as well as colloform, framboidal (rasberry texture) and liesegang textures are also present.

Gold mineralization is not related to pyrite but to specular hematite, which appears to be introduced into the host by hydrothermal mechanisms. Secondary effects have altered the specular hematite to earthy, red hematite with associated MnO_2.

MINERALIZATION -Cont.

The alteration minerology associated with the veining consists of sericite-kaolinite(?) and chlorite.

Mine Production and Reserves

Surface mine production is expected to last 6 years and recover 447,000 ounces. The life of mine strip ratio is 7.0 to 1., which equates to 41,389,720 tons of waste material and 5,880,017 tons of ore grading .082 ounces per ton.

The mine operates 2 shifts per day, 40 hours per week. The ore is stockpiled for blending to the mill which operates 7 days per week, 24 hours a day. The actual mining is contracted to Morrison-Knudsen Corporation, which operates 15 yard front end loaders and 120 ton electric drive haultrucks. The mining contractor has 55 employees on site and Cyprus has 41 employees associated with mining and milling.

CONCLUSION

The Copperstone deposit is localized along the moderately dipping portion of a downward curving fault that separates Mesozoic quartz latite tuff from a chaotic breccia. This postulated listric normal fault should converge at depth with a low angle dislocation surface (detachment) which separates the brittle, well fractured upper plate from the mylonitized, metamorphic to plutonic basement terrane. High angle faults and associated veining respectively, refractured and permeated the previously established structures. The intersecting fault system appears to represent the pathway through which multi-stage, hydrothermal fluids deposited gold in an episodic manner.

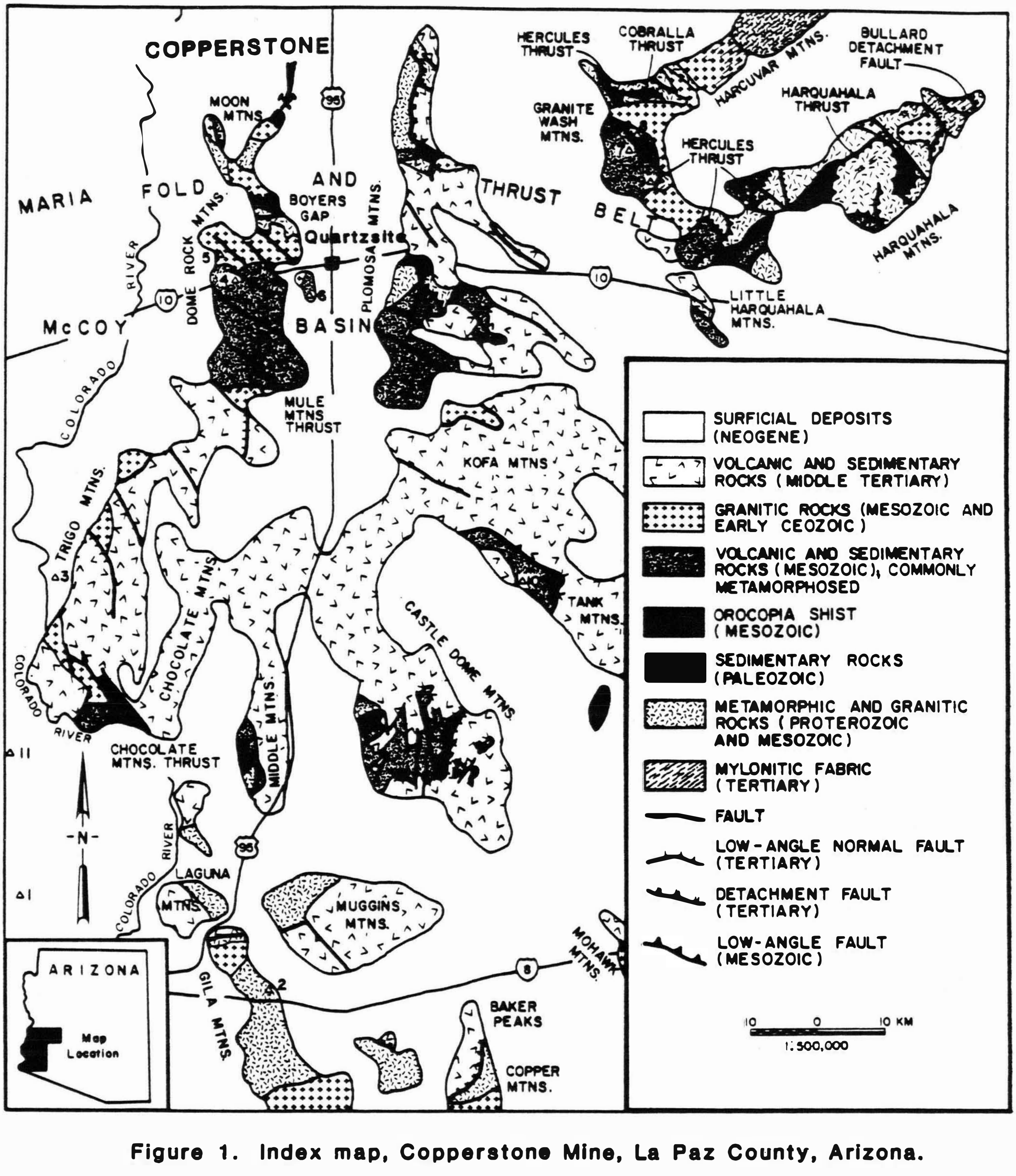

Figure 1. Index map, Copperstone Mine, La Paz County, Arizona.

BACKGROUND MATERIALS

CONTROL OF MINERALIZATION BY MESOZOIC AND CENOZOIC LOW-ANGLE STRUCTURES IN WEST-CENTRAL ARIZONA

Jon E. Spencer, Stephen J. Reynolds, and John W. Welty

Arizona Geological Survey
845 N. Park Ave.
Tucson, Arizona 85719

ABSTRACT

Mesozoic and Tertiary mineral deposits in west-central Arizona are commonly associated with Mesozoic thrust faults and Tertiary detachment faults, respectively. Quartz-kyanite rocks and pyritic quartz-sericite schists with local anomalous gold are the product of probable Jurassic argillic alteration of Jurassic volcanic, sedimentary, and plutonic rocks followed by Cretaceous thrust burial and associated metamorphism. Slivers and sheets of Paleozoic carbonates along Mesozoic thrust faults were locally sites of syn- and post-thrust mineralization. Widespread brecciation along Tertiary detachment faults resulted in increased permeability along fault zones. Elevated thermal gradients also resulted from detachment faulting and apparently caused convective aqueous-fluid circulation along detachment faults and associated Fe+Cu$\pm$Au mineralization.

INTRODUCTION

Quartz-kyanite-pyrophyllite mineral assemblages with locally occurring pyrite and anomalous gold have recently been recognized within Mesozoic metasedimentary and metavolcanic rocks of west-central Arizona and southeasternmost California. These deposits are most common in the wall rocks of Jurassic plutons and below thrust sheets of crystalline rocks (Reynolds et al., in press). Thrust faulting and tectonic burial are not considered to be responsible for the genesis of the deposits, but are thought to be responsible for their preservation and, in part, their metamorphism. Major gold deposits are associated with similar aluminous mineral deposits in the southern Appalachian Mountains, raising the possibility that significant gold deposits of similar origin are present in the Southwest as well.

Detachment-fault-related mineral deposits of mid-Tertiary age are numerous in west-central Arizona and southeastern California. Virtually all of these deposits have the same mineral assemblage: massive or fracture-filling specular hematite with younger, fracture-filling chrysocolla and malachite or brochantite. Some deposits contain early-formed copper and iron sulfides that are now largely oxidized. The larger deposits form replacements in upper-plate rocks directly above the detachment fault. Numerous smaller replacement and fracture-filling deposits are present along detachment faults or are within a few tens to perhaps a hundred meters above or below the faults. Consistent mineralogy, structural style, and association with Tertiary detachment faults indicate that these deposits are genetically related to faults (Reynolds, 1980; Wilkins and Heidrick, 1982; Spencer and Welty, 1986). Copper has been the primary commodity produced from these deposits, with additional production of minor gold, silver, lead, and zinc.

MESOZOIC ALUMINOUS METASOMATIC DEPOSITS

Mesozoic metavolcanic, metasedimentary, and plutonic rocks in west-central Arizona and southeasternmost California host aluminous metasomatic rocks that are locally associated with anomalous gold. The most striking of the aluminous metasomatic rocks are those composed almost entirely of quartz and kyanite; other common combinations are quartz-muscovite and quartz-pyrophyllite. Minor associated minerals are andalusite, sillimanite, pyrite, tourmaline, rutile, ilmenite, biotite, lazulite (hydrous Mg-Fe aluminophosphate), apatite, dumortierite, staurolite, K-feldspar, and magnetite. The most common assemblage comprises quartz, an aluminosilicate, a Ti-bearing mineral, and a P-bearing mineral (Reynolds et al., in press).

Aluminous metasomatic rocks are most common in schistose metavolcanic and metasedimentary rocks, especially near Mesozoic thrust faults (Granite Wash Mountains) or near the intrusive margins of Jurassic plutons (Dome Rock Mountains). They have also been recognized as pods within granitic rocks (Fig. 1). Schistose fabrics and evidence of greenschist-grade metamorphism are common in host rocks, especially near thrust faults and plutons. Virtually all of the Mesozoic supracrustal rocks in west-central Arizona and southeasternmost California underwent Cretaceous thrust burial and associated prograde metamorphism and fabric development. The coarse aluminous minerals in the aluminous meta-

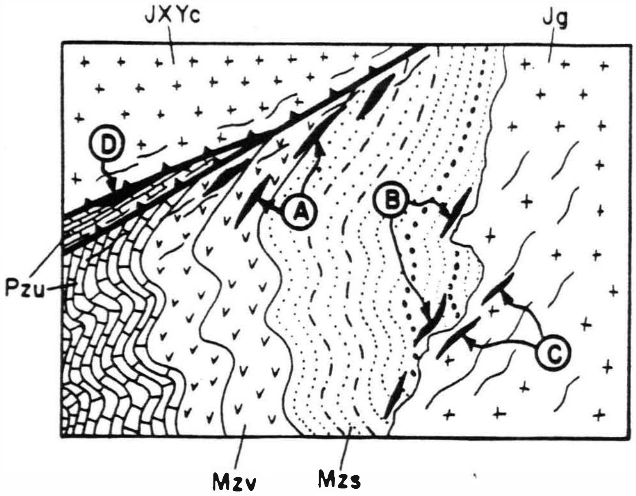

Figure 1. Schematic diagram showing sites of mineralization in Mesozoic mineral deposits commonly found in association with thrust faults. (A) Aluminous metasomatic deposits below thrust faults. (B) Aluminous metasomatic deposits in the wall-rocks of Jurassic plutons. (C) Aluminous metasomatic deposits forming pods in Jurassic granite. (D) Cu-Au deposits within Paleozoic carbonate slivers along thrust zones. Wavy line segments indicate shearing and foliation. Symbols are as follows: JXYc=Jurassic to Proterozoic crystalline rocks, Pzu=Paleozoic metasedimentary rocks, Mzv=Mesozoic metavolcanic rocks, Mzs=Mesozoic metasedimentary rocks, Jg=Jurassic granitoid.

somatic rocks almost certainly formed during this period of deformation and metamorphism (Reynolds et al., in press).

Pyrite and anomalous gold occur in metavolcanic rocks adjacent to massive aluminous metasomatic rocks in the central Granite Wash Mountains. Disseminated, low-grade gold deposits are present within and adjacent to areas of aluminous metasomatism in the Dome Rock Mountains.

Aluminous metasomatic rocks in west-central Arizona and southeasternmost California are possibly the product of hydrogen-ion metasomatism of quartzo-feldspathic rocks during circulation of Cl-rich, acidic fluids at high water-to-rock ratios (Wise, 1975; Dillon, 1976). During metasomatism the rocks were leached of relatively mobile elements and left enriched in the relatively immobile elements Al, Ti, and P. The aluminous metasomatic rocks in the Granite Wash Mountains are interpreted as metamorphosed products of a shallow-level hydrothermal system; synvolcanic near-surface argillic alteration produced clay-rich rocks and hydrothermal sinter that were subsequently converted to quartz-kyanite rocks during thrust-related tectonic burial and metamorphism. In the Dome Rock Mountains, it is inferred that wall rocks underwent argillic alteration during emplacement of granitic magmas and were later metamorphosed to quartz-kyanite-pyrophyllite rocks. Sulfides and gold were probably introduced during the earlier, argillic alteration event associated with magmatism. Metamorphism and preservation of such deposits was largely the result of Cretaceous thrust burial during a time of elevated geothermal gradients associated with Late Cretaceous plutonism (Reynolds and others, in press).

Metamorphic rocks in the Blue Ridge and Piedmont provinces of the eastern Appalachian Mountains of the southeastern United States contain numerous quartz-kyanite, quartz-sillimanite, and quartz-pyrophyllite deposits commonly associated with upper Proterozoic to lower Paleozoic metavolcanic rocks (Espenshade and Potter, 1960). These deposits contain virtually identical mineral assemblages as the Arizona-California deposits. Pyritiferous gold deposits in the southern Appalachian Mountains with associated aluminous metamorphic minerals have been interpreted as metamorphosed volcanogenic epithermal-exhalative deposits (Kiff and Spence, 1987).

OTHER MESOZOIC THRUST-RELATED DEPOSITS

Slivers and sheets of metamorphosed Paleozoic and Mesozoic metasedimentary rocks along thrust faults in west-central Arizona and southeastern California are locally sites of copper and gold mineralization. Such deposits, such as the Yuma Mine deposit in the Granite Wash Mountains, possibly formed by movement of aqueous fluids along thrust zones and into contact with reactive carbonate host rocks.

TERTIARY DETACHMENT-FAULT-RELATED DEPOSITS

Detachment faults are large-displacement, low-angle normal faults that are thought to have formed at low angles. Much of the crustal extension that affected the Basin and Range Province in Tertiary time was accommodated by movement on detachment faults. Upper-plate rocks are generally cut and distended by numerous listric and planar normal faults that merge downward with, or are cut by, the underlying detachment fault. Mylonitic fabrics present in rocks exposed beneath many detachment faults are inferred to have formed by ductile shearing along the downdip projection of detachment faults early in their movement history (Wernicke, 1981; Davis, 1983; Reynolds, 1985; Davis et al., 1986).

A major detachment fault exposed in the Buckskin, Rawhide, Harcuvar, and Harquahala Mountains of west-central Arizona and in the Whipple Mountains of southeastern California juxtaposes a wide variety of Proterozoic and Phanerozoic rock types over variably mylonitic crystalline rocks. Middle Tertiary mineral deposits associated with this fault are more numerous than in any other known area of detachment faulting. Detachment-fault-related deposits are also present in the northern Plomosa Mountains, Moon Mountains, and Bighorn Mountains.

Specular hematite (specularite) is by far the most volumetrically significant mineral in detachment-fault-related mineral deposits of west-central Arizona and southeastern California. Where massive, it is typically fractured and contains fracture-filling chrysocolla and less common malachite, brochantite, quartz, calcite, barite, fluorite, and manganese oxides. In some lower-plate deposits, such as those on the flanks of Planet Peak in the Buckskin Mountains, quartz and chlorite are intimately intergrown with 1- to 10-mm-diameter crystals of unusually hard specularite. Upper-plate deposits hosted by noncarbonate rocks, such as the Mesozoic calc-silicate, metasandstone, and phyllite in the area of the Mineral Hill and Planet mines in the Buckskin Mountains, contain much fine-grained (1mm or less) specularite and earthy hematite. In these deposits, abundant earthy hematite and fracture-filling specularite are common at the margins of the zone of massive specularite mineralization.

Copper and iron sulfides formed early in the genesis of many of these deposits, although their significance is difficult to assess because of extensive oxidation and overprinting by younger specularite-chrysocolla mineralization. Pyrite is rare to nonexistent in most deposits, but relict, limonite-stained cubes or cubic pits are locally common. Chalcopyrite veins and disseminations within massive specular hematite were the target of underground mining at the Swansea Mine in the central Buckskin Mountains, and are locally present at many other deposits.

Common sites and styles of mineralization are as follows (Fig. 2): (1) replacement deposits in slivers of Paleozoic(?) carbonate rock within lower-plate crystalline rocks, (2) fracture-filling and replacement(?) deposits within high-angle, lower-plate shear zones, (3) fracture-filling deposits within crushed and fractured rocks within or directly adjacent to the detachment fault, (4) massive replacement deposits within Paleozoic carbonate rocks and Mesozoic calc-silicate rocks directly above the detachment fault, (5) fracture-filling deposits along high-angle shear zones in upper-plate rocks, and (6) stratabound sedimentary manganese deposits within Miocene clastic sedimentary rocks (Wilkins and Heidrick, 1982; Spencer and Reynolds, in press).

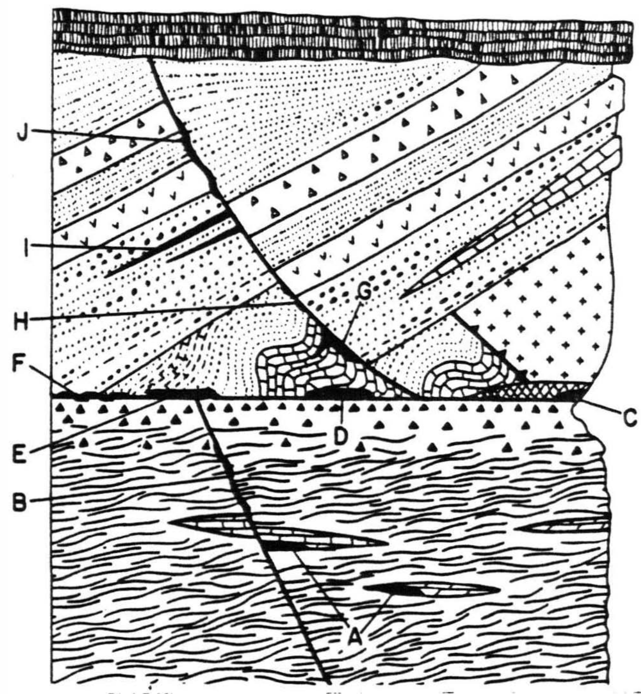

Figure 2. Schematic diagram showing sites of mineralization in Tertiary mineral deposits associated with detachment faults. Sites and styles of mineralization are as follows: (A) Replacement deposits in carbonate slivers within lower-plate crystalline rocks, (B) Fracture-filling and replacement(?) deposits along lower-plate high-angle shear zones, (C, D, E) replacement deposits within a variety of calcareous, upper-plate host rock types, (F) fracture-filling mineral deposits within and along the fault zone, (G) replacement deposits adjacent to upper-plate normal faults, (H, J) fracture-filling deposits adjacent to upper-plate normal faults, (I) stratabound sedimentary manganese deposits.

Fluid-inclusion studies indicate that mineralizing aqueous fluids ranged from approximately 175 to 300 degrees C minimum temperature with salinities ranging from 12 to 22 % NaCl equivalent (Wilkins et al., 1986). Replacement mineralization in calcareous host rocks was the primary style of mineralization in the larger deposits, whereas many of the smaller deposits are fracture filling. High geothermal gradients that caused convective fluid circulation are interpreted as the result of rapid tectonic uplift of hot footwall rocks, possibly locally augmented by magmatic heat input.

Gold production from the approximately one dozen detachment-fault-related mineral districts in west-central Arizona and adjacent southeastern California (not including deposits near Yuma) ranges from less than 100 oz to as much as 12,000 oz (Keith et al., 1983; Spencer and Welty, 1986). Copper has been the primary metal produced from detachment-fault-related mineral districts. The recently discovered Copperstone gold deposit in the northern Moon Mountains rekindled interest in mineralization related to detachment faults, although it is uncertain what the relationship is between the Copperstone deposit and the adjacent detachment fault.

CONCLUSION

Low-angle tectonic features were important in the formation and preservation of many mineral deposits in west-central Arizona and southeastern California. Mesozoic thrust faulting was responsible for thrust burial and, in part, for metamorphism of argillically altered and locally gold-mineralized Mesozoic sedimentary and igneous rocks. Fault slivers along thrust faults were locally the sites of syn- to post-thrusting mineralization, presumably because of aqueous-fluid circulation in the thrust zone. Tertiary mineral deposits related to detachment faults were the product of circulating, largely ascending brines that moved along the highly fractured rocks within and adjacent to the detachment fault. Fluid circulation was probably caused by elevated geothermal gradients associated with uplift of hot mylonitic footwall rocks. Many mineral deposits related to detachment faults have yielded gold, although they are primarily base-metal deposits.

REFERENCES CITED

Davis, G. A., Lister, G. S., and Reynolds, S. J., 1986, Structural evolution of the Whipple and South Mountains shear zones, southwestern United States: Geology, v. 14, p. 7-10.

Davis, G. H., 1983, Shear-zone model for the origin of metamorphic core complexes: Geology, v. 11, p. 342-327.

Dillon, J. T., 1976, Geology of the Chocolate and Cargo Muchacho Mountains, southeasternmost California: Santa Barbara, University of California, Ph.D. Dissertation, 405 p.

Espenshade, G. H., and Potter, D. B., 1960, Kyanite, sillimanite, and andalusite deposits of the southeastern United States: U.S. Geological Survey Professional Paper 336, 121 p.

Keith, S. B., Gest, D. E., DeWitt, Ed, Woode-Toll, Netta, and Everson, B. A., 1983, Metallic mineral districts and production in Arizona: Arizona Bureau of Geology and Mineral Technology Bulletin 194, 58 p.

Kiff, I. T., and Spence, W. H., 1987, Volcanogenic epithermal-exhalative gold deposits of the Haile-type in the Carolina slate belt: Geological Society of America Abstracts with Programs, v. 19, p. 394.

Reynolds, S. J., 1980, A conceptual basis for the occurrence of uranium in Cordilleran metamorphic core complexes, in Coney, P. J., and Reynolds, S. J., eds., Cordilleran metamorphic core complexes and their uranium favorability: U.S. Department of Energy Open-File Report GJBX-258(80), p. 187-245.

Reynolds, S. J., 1985, Geology of the South Mountains, central Arizona: Arizona Bureau of Geology and Mineral Technology Bulletin 195, 61 p.

Reynolds, S. J., Richard, S. M., Haxel, G. M., Tosdal, R. M., and Laubach, S. E., in press, Geologic setting of Mesozoic and Cenozoic metamorphism in Arizona, in Ernst, W. G., ed., Metamorphism and crustal evolution of the conterminous western United States: Englewood Cliffs, New Jersey, Prentice-Hall.

Spencer, J. E., and Welty, J. W., 1986, Possible controls of base- and precious-metal mineralization associated with Tertiary detachment faults in the lower Colorado River trough, Arizona and California: Geology, v. 14, p. 195-198.

Wernicke, Brian, 1981, Low-angle faults in the Basin and Range Province--nappe tectonics in an extending orogen: Nature, v. 291, p. 645-648.

Wilkins, Joe Jr., and Heidrick, T. L., 1982, Base and precious metal mineralization related to low-angle tectonic features in the Whipple Mountains, California and Buckskin Mountains, Arizona, in Frost, E. G., and Martin, D. L. eds., Mesozoic-Cenozoic tectonic evolution of the Colorado river region, California, Arizona and Nevada: San Diego, Cordilleran Publishers, p. 182-203.

Wilkins, Joe Jr., Beane, R. E., and Heidrick, T. L., 1986, Mineralization related to detachment faults: a model, in Beatty, Barbara, and Wilkinson, P. A. K., eds., Frontiers in geology and ore deposits of Arizona and the Southwest: Arizona Geological Society Digest, v. 16, p. 108-117.

Wise, W. S., 1975, The origin of the assemblage: quartz+Al-silicate+rutile+Al-phosphate: Fortschutte Mineralogie, v. 52, p. 151-159.

The crustal heritage of silver and gold ratios in Arizona ores

S. R. TITLEY *Department of Geosciences, University of Arizona, Tucson, Arizona 85721*

ABSTRACT

The ratios of produced grades of silver and gold in ore deposits of Arizona, representing nearly a century of mining, correlate with their geologic setting. The deposits occur south and west of the Colorado Plateaus where two geological domains are recognizable on the basis of type and age of rocks and geological history. The eastern or "Naco" domain has a basement of Proterozoic Pinal Schist, formed from a protolith of mostly clastic sedimentary rocks, and widely scattered younger Proterozoic granites, overlain by Paleozoic platform strata and Mesozoic volcanic and clastic rocks. The "Western Deserts" domain is characterized by an older Proterozoic section of largely submarine volcanic and volcaniclastic strata, together with Proterozoic granites; it is largely devoid of Paleozoic strata, but Mesozoic clastic and volcanic strata are widely exposed. In both domains, middle and late Tertiary volcanic rocks are extensive.

Ore deposits of many genetic types, of Proterozoic, Nevadan, Laramide, and younger Tertiary ages, are present; deposits of Laramide and younger Tertiary ages occur in both domains, but deposits of Proterozoic age are confined mostly to the Western Deserts, and those of Nevadan age are restricted to the Naco domain. The ore deposits evolved at different times under different conditions of tectonic stress.

The produced grades of silver and gold, and the silver to gold ratios, reveal a bimodal distribution. Most deposits of all epochs and genetic type in the Naco domain show Ag enrichment relative to the ratio of the Ag:Au crustal abundance (clarke ratio) (17.5:1). Except for two Laramide porphyry copper deposits and the Proterozoic massive Cu-Pb-Zn ores, whose ratios are close to the clarke ratio, most other districts of the Western Deserts domain are enriched in gold with respect to the ratio.

The regional zoning transgresses ore-deposit type, time, tectonic style, and reported igneous rock types and metal associations. It does not appear to be related to the hypothetical results of subduction processes wherein metals and magmas are directly derived from partial melting of a descending slab of oceanic rocks. Rather, the precious-metal characteristics may represent inheritance from specific kinds of crust.

INTRODUCTION

Metallogenesis in Arizona resulted in formation of precious and base metal ores of many genetic types during the complex evolutionary history of the region. Base-metal mining since the early 18th century in Arizona has had a varied history influenced by advances in the technology of mining and metallurgy as well as broad-scale economic changes. On the other hand, mining of precious metals (silver and gold) has been more or less continuous, relatively less affected by technology and vagaries of economics.

This study presents an analysis of the distribution of silver and gold from a hundred years of production by Arizona mines. The produced grades of these metals in mining districts have been compared on the basis of their production from two different geologic settings in the southern half of the State. The results reveal broad characteristics of the precious-metal ratios in mining districts that relate to the geological domains in which the districts occur. None of the many variables that may influence the compositions of ores, such as epoch, ore deposit type, tectonic history, or igneous rock associations appears to have had the subtle, but real, effect that appears to have been brought about by the crustal setting of mining districts in this region. These characteristics of occurrence establish a substantial basis for the notion that metals of these ores are inherited from the crust.

GEOLOGICAL DOMAINS

An essential and integral basis of this study has been the fact that Arizona may be separated into three distinctive geological domains (Fig. 1) based upon different basement and other geological characteristics. Each domain manifests a distinctive evolutionary history that commenced in the Proterozoic and continued through the Phanerozoic in episodic pulses that affected parts of the State in different ways. The domains of Figure 1 have been generalized from a more detailed analysis (Titley, 1981; Titley and Anthony, 1987), and two are termed here the "Naco domain" of the southeastern part of the State and the "Western Deserts domain" of the central and southwestern part; the third domain is the Colorado Plateaus of the northeastern third of the State. Two of the domains are characterized by the nature of bedrock geology and tectonic history rather than on the traditional basis of geomorphic features. The Colorado Plateaus province (domain III) remains as established in the traditional geomorphic sense, but both southern domains comprise rocks of both the Central Mountain region and Basin and Range province.

Domain I of Figure 1 is underlain by a complex and variable basement dominated by Pinal Schist (ca. 1.68–1.70 Ga) intruded by granite of at least two ages (ca. 1.65 and 1.4 Ga) (Silver, 1978). Pinal Schist comprises a varied section dominated by metamorphosed clastic strata, now quartz-sericite schist, quartzite, argillite, and slate. Locally thick sections of amphibolite are present, as are thin rhyolite flows and breccias, as well as intrusive rhyodacite (Cooper and Silver, 1964; Condie and others, 1985). The base of the column is not exposed, but the Pinal section in the Little Dragoon Mountains of domain I may be at least 6 km thick (Silver, 1978).

Additional material for this article (an appendix) may be secured free of charge by requesting Supplementary Data 8735 from the GSA Documents Secretary.

Geological Society of America Bulletin, v. 99, p. 814–826, 10 figs., 4 tables, December 1987.

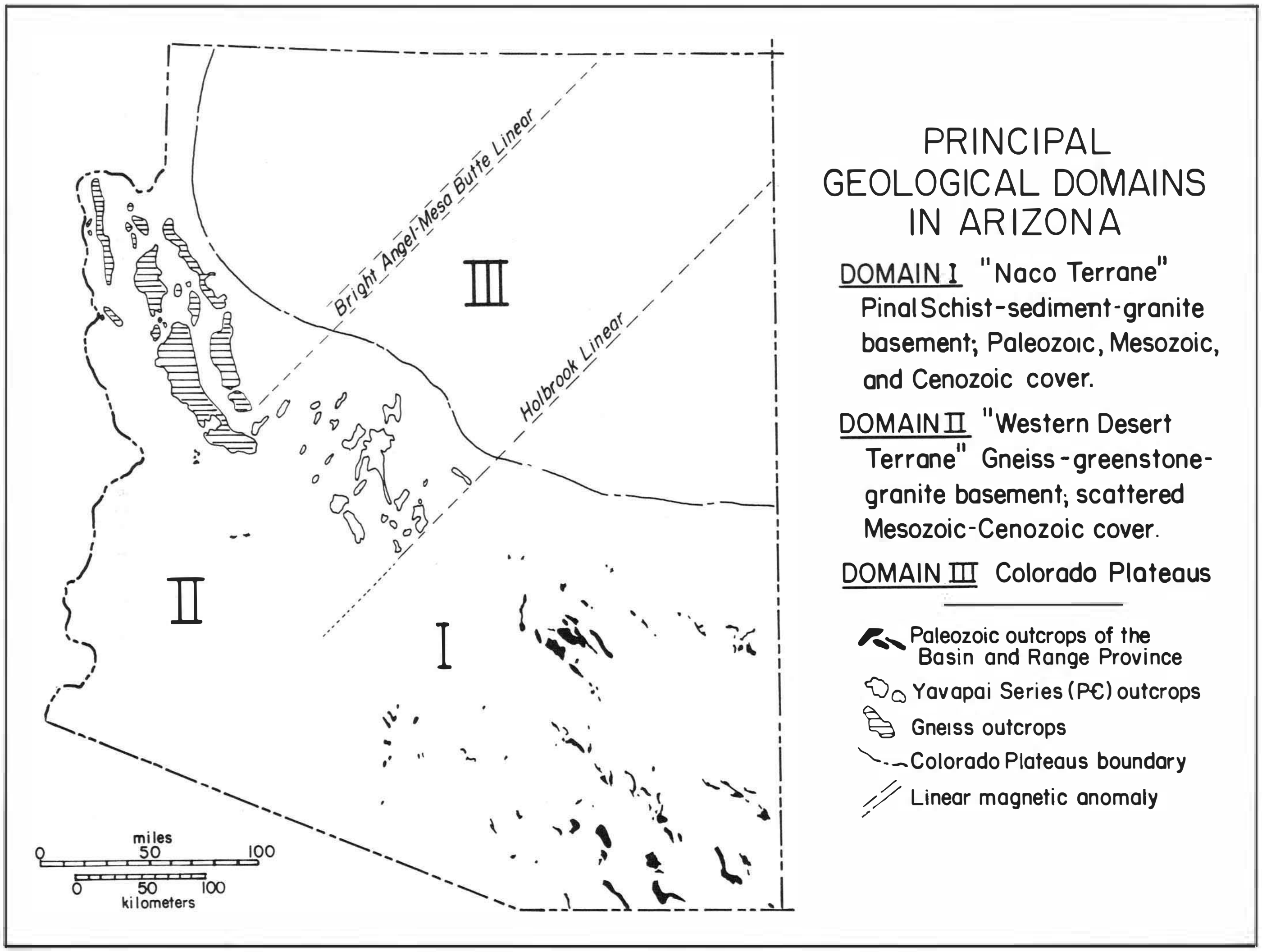

Figure 1. Map of geological and metallogenic domains in Arizona as established for this analysis. Features of geology shown are principal distinguishing features for domains, separated by linear magnetic anomalies and their projections.

Pinal strata are flanked on their northwestern edge by rocks of the Mazatzal Quartzite, believed to be basin margin facies of the Pinal (Silver and others, 1986). A succession of still younger Proterozoic rocks (Apache Group) and diabase sills and dikes locally compose the uppermost Precambrian rocks of the domain.

The Paleozoic of domain I comprises carbonate-dominated sections whose original thickness was in excess of 2 km. The Mesozoic consists of remnants of clastic and volcanic rock successions whose original thickness may have been as great as 4 to 6 km. The Cenozoic is represented by widespread volcanic rocks representing many local centers of origin, and by sediments and sedimentary rocks of clastic and mixed clastic-volcanic lithologies.

Precambrian rocks of the Naco domain have undergone syntectonic metamorphism of varying but low grade between 1.625 and 1.680 Ga (Silver, 1978). The domain was a site of Triassic volcanism as well as Jurassic volcanism, intrusion, and deformation. In Laramide times, basement cored uplift (Davis, 1979), the result of regional compression, was accompanied by widespread volcanism and intrusion; the middle to late Tertiary was a time of widespread volcanism and, ultimately, evolution of extensional tectonism and formation of present-day landforms. Ore deposits formed in the Naco domain during the Proterozoic, Jurassic, Laramide, and the middle to late Tertiary.

Domain II of Figure 1 also is characterized by a Proterozoic basement but a basement more variable in lithology from that of the Naco domain. Over the extent of the Western Deserts, the basement consists of two distinct, northeasterly trending belts of metamorphic rocks. Age and metamorphic grade of the basement increase northwestward. Metamorphic strata of the Yavapai Series (Anderson and others, 1971), about 1.78 Ga, flank Proterozoic strata of domain I and are flanked to the northwest by gneisses derived from volcanic protoliths (Thomas, 1949). Yavapai Series strata consist of mixed volcanic and sedimentary rocks of a thickness on the order of 12–15 km (Anderson and Creasey, 1958). Detailed studies by Anderson (1968, 1972), Anderson and co-workers (1955), Anderson and Blacet (1972), and Anderson and Nash (1972) reveal sections where several-kilometre thicknesses of basalt and andesite are present together with relatively thinner strata of tuff and sediment, as well as

TABLE 1. REPRESENTATIVE OREBODY TYPES, AGES, DOMAINS, RELATED IGNEOUS ROCKS, AND METALS IN SOUTHERN ARIZONA

Age	Genetic type	Domain	Associated rock types	Metals	Ag/Au	Example	References
Proterozoic X (ca. 1.75 Ga)	Volcanigenic massive sulfide	II II	Andesite, rhyolite Andesite, volcanogenic sediments, etc.	Cu-Zn(Au-Ag) Pb-Zn(Ag)(Au)	36 200-36	United Verde Bruce, Iron King	Anderson and Nash (1972) Gilmour and Still (1968), Larson (1984)
	Intrusion-centered, vein or contact ore	II	Granite/sedimentary rocks	W	n.a.	Money Maker (Peck)	Dale (1961)
Proterozoic Y (ca. 1.4 Ga)	Vein or contact ore	I	Granite	W	n.a.	Wagner	Keith and others (1983a, 1983b)
Nevadan (ca. 180 Ma)	Intrusion-centered and carbonate replacement ore	I	Granite, qtz monzon. Granite, qtz monzon.	Cu-Pb-Zn-Ag-Au Cu-Pb-Ag(Au)	28 49	Bisbee Courtland-Gleeson	Hogue and Wilson (1950) Wilson (1927)
Laramide (ca. 70–50 Ma)	Intrusion-related vein and replacement	I II	Peraluminous granite Peraluminous granite	Cu-Pb-Ag(Au) Cu-Au(Ag)	215 0.11	Cochise Fortuna	Cooper (1957) Wilson (1933a), Smith and Graubard (1987)
	Porphyry copper	I II	Calc-alkaline granite and granodiorite ser.	Cu-Mo(Ag-Au) Cu-Mo(Ag-Au)	19 57	San Manuel Bagdad	Thomas (1966) Anderson and others (1955)
	Vein-replacement ores	I II	Sediment and metasedimentary rocks, felsic intrusions	Cu-Ag(Au)	57 0.40	Superior LaPosa(?)	Hammer and Petersen (1968) Keith and others (1983a, 1983b)
	Pyrometasomatic ores	I	Granite, Granodiorite, Paleozoic sed. rocks	Cu-Pb-Zn(Ag-Au)	326	Washington Camp	Lehman (1978)
Middle to late Tertiary (ca. 28–12 Ma)	Veins	I II	Rhyolite, andesite, latite, trachyte	Ag(Au) Au(Ag)	98 0.58	Pearce Oatman	Howell (1977) Durning and Buchanan (1984)
	Veins and replacement	I II	Granite/granodiorite, carbonate/clastic sed.	Cu-Pb-Ag(Cu)	255 0.44	Middle Pass La Paz	Keith (1973) Wilson and Others (1934)
	Detachment faults	I II	Metamorphic granites, volcanics, and seds. mid-Tert. volcs.	U Au-(Ag)(Cu)	n.a. 5.66	Blue Rock Sheep Tanks	Warner (1982) Wilson and others (1934)
Quaternary	Placers	I, II		Au-Ag	0.10		Wilson (1933b)

pyritic or other iron-bearing sedimentary rocks. Intrusions of Proterozoic granite of ~1.4 and ~1.6 Ga age are widespread, apparently more abundant than in domain I.

Remnants of Paleozoic strata are uncommon in the Western Deserts domain, although they are inferred to have been widely deposited as platformal sediments (McKee, 1951; Peirce and others, 1970). The Phanerozoic cover of domain II is dominated by Mesozoic clastic and volcanic strata, locally strongly metamorphosed, and widespread Tertiary volcanic cover.

Only a few Laramide ore deposits occur in the Western Deserts, although Laramide intrusions are common; ores of Proterozoic and Tertiary ages are present. In a way comparable to that of the Naco domain, the crust of the Western Deserts has been subjected to the extensional tectonism of the middle and late Tertiary and the compressional tectonics of the Laramide.

Domain III, the Colorado Plateaus province, is not considered further here because of the absence of significant base- and precious-metal production up to this time, although the province has been a region of major production of uranium ores.

Domains I and II are separated on the basis of contrasting basement ages and compositions, as well as sharply contrasting Mesozoic and Cenozoic geologic histories. The boundary between them, however, is difficult to establish in a rigorous sense in the Basin and Range province. Figure 1 shows the trace of a linear magnetic anomaly beneath the Colorado Plateaus, which, if extended, approximates the domain boundaries premised on geological bases. This discontinuity, informally termed the "Holbrook linear" (Titley, 1981), separates Proterozoic Mazatzal-Pinal strata from Yavapai Series units in the Central Mountains of Arizona; projection of the line southwestward separates terrane comprising widespread outcrops of Paleozoic strata of the Naco domain from the Western Deserts where only sparse remnants of Paleozoic strata remain. The projection of the line is also a northwestern limit to Laramide porphyry-ore systems in the Basin and Range province of southeastern Arizona (Titley, 1981). Another geophysical linear anomaly in Figure 1 marks a well-defined geological boundary between metamorphic terranes in the Central Mountains. This feature, the Bright Angel–Mesa Butte linear (Shoemaker and others, 1978), separates the gneissic terrane of northwestern Arizona from the greenschist-amphibolite terrane of the Yavapai Series in central Arizona.

CHARACTERISTICS OF ORE GENESIS IN ARIZONA

Ores have been formed in Arizona, in both geological domains, in a wide variety of deposit types and at different times (Table 1). The predominating production has been from both the bodies of complex ores and the porphyry-related ore systems. Silver- or gold-dominant ores have been mined from some orebodies, but such ores have been subsidiary to silver and gold extracted from complex orebodies. Table 2 lists production of principal metals as related to epoch. Proterozoic production is dominated by sedimentary/volcanic exhalative ores with lesser production from vein systems; the Nevadan is almost solely represented by production from Bisbee, an intrusion and breccia-cored replacement, vein, and porphyry system; Laramide production is dominated by porphyry-related ores where copper, molybdenum, silver, and gold have been significant, and to a lesser degree by complex base-precious–metal vein and replacement ores. Middle to late Tertiary ores have been taken from vein-dominant systems. Epigenetic ores of every epoch are hosted by a variety of rock types, but in the Laramide deposits, Paleozoic and Mesozoic sedimentary sections predominate, whereas the hosts of younger Tertiary ores appear dominated by metamorphic, volcanic, or clastic rock successions. In central Arizona, a variety of Precambrian rocks are hosts to ores of all ages.

Metals produced from deposits of Nevadan, Laramide, and the middle and late Tertiary ages have been closely associated with centers of intrusion. The Nevadan and Laramide deposits are associated with stocks or small plutons of calc-alkaline or alkali-calcic series (Peacock, 1931; Titley and Beane, 1981). Igneous rocks associated with middle Tertiary and younger ores represent various differentiation series that include alkalic, alkali-calcic, high K–calc-alkalic, and others (Keith, 1978; Westra and Keith, 1981). Some of these rock types are inferred to be associated with, or related to, different kinds of ores (Spencer and Welty, 1987). Ores of the different epochs are interpreted as having formed under tectonic regimes influenced by normally converging plates resulting in crustal compression during the Proterozoic (Anderson, 1986), the Nevadan (Coney, 1978), and the Laramide (Heidrick and Titley, 1976, 1982). Oblique plate convergence in the middle Tertiary is inferred to have resulted in, or to have been coincident with, extensional tectonics in the Basin and Range province.

In Arizona, the many combinations of genetic ore type, associated igneous rock type, epoch of formation, tectonic setting, and metal assemblages compose an unusual sampling of process, time, and geological associations.

TABLE 2. ARIZONA METAL PRODUCTION AND PRODUCTION BY METALLOGENIC EPOCH

	Cu (K tons)	Pb (K tons)	Zn (K tons)	Ag (10^6 oz)	Au (10^6 oz)	Mo (K tons)
Total state production of metal (ca. 1880–1980)	33,306	682	1,132	474.3	13.8	244
Percentage of State production by metallogenic epoch	Cu%	Pb%	Zn%	Ag%	Au%	Mo%
Proterozoic	6	18	45	19	26	..
Nevadan	11	23	15	16	5	..
Laramide	81	41	31	47	33	83
Middle to late Tertiary	2	18	9	18	36	17
Percent totals	100	100	100	100	100	100

Note: approximate figures based upon data in Keith and others (1983a, 1983b), Keith (1973, 1974, 1975, 1978), Elsing and Heinemann (1936), and miscellaneous sources. Production by epoch based upon weight percentages of total State production. Base metals in thousands of short tons; precious metals in Troy ounces.

SILVER AND GOLD PRODUCTION

Production figures published by Keith and others (1983a, 1983b), as well as data from Elsing and Heineman (1936), Wilson and others (1934), Keith (1973, 1974, 1975, 1978), and Welty and others (1985) have been used to determine produced grades of silver and gold from 233 mining districts representing about 5,500 mines in Arizona (Appendix 1).[1] In every case, the production values have been determined from values of total production of ore and total production of metal for each district. The number includes both porphyry and nonporphyry production from 12 Laramide districts as examples of differences of grade and precious-metal ratio between contrasting types of ore occurrence in the same district.

The use of data from districts, rather than from mines, and use of production figures must be further explained. Many Arizona districts are "complex" in the sense that several genetic types of ore occurrences may be present. The use of grades based upon district production in this study are believed to yield values that integrate metal compositions and include the different kinds of ore that are present in most Arizona districts. District values would also appear to accommodate effects of lateral zoning of grade across ore deposits of the same genetic type as well as differences in precious metals of different base-metal mineral assemblages.

Production figures of precious metals may be a measure of concentration of base metals in complex mining districts, even though in many instances, particularly before the turn of the century, base metals were not recovered unless of exceptionally high grade or minimally amenable to existing metallurgical treatment. Attempts to discover meaningful relationships between base metal production and the precious metals in this study, however, have been only partially successful. Nonetheless, it is held that, in the 100-yr period of recorded production from the state, and the fact that mining was occurring simultaneously in many districts throughout the state, miners and metallurgists were seeking to optimize their profits, and extraction of gold and silver was carried out with more or less the same efficiency on the same kinds of ores, regardless of where they occurred. There is no reason to suspect that either metallurgy or economic goals differed with geography at any particular time.

Production grades of silver and gold are expressed in g/tonne (parts per million). They are plotted on a series of diagrams, of the same logarithmic scale and format, showing produced grade of gold versus produced grade of silver. A reference line on each plot represents a constant ratio of crustal abundances (or the ratio of the clarkes) (Ahrens, 1965) of silver (.07 ppm) to gold (.004 ppm). Grades are illustrated and discussed in three formats; the first is by known or inferred age of metallogenesis, the second is related solely to geological domain, and the third is a sampling of mineralization of all ages within or hosted by Precambrian rocks in central Arizona.

Production Grades of Silver and Gold by Epoch

Figures 2A and 2B show, respectively, a map of areas of Precambrian mineralization and a plot of produced precious-metal grades. The districts shown are distinguished (as in succeeding plots) according to geological domain. As shown in Figure 2A, most deposits of Precambrian age correspond to the distribution of exposed Proterozoic rocks in domain II (see Fig. 1). Two districts of domain I shown in Figure 2B occur in sedimentary rocks adjacent to the inferred domain boundary. Although Proterozoic rocks of the Pinal-Mazatzal strata, Apache Group strata, and granite bodies are widespread in ranges of domain I, other Precambrian precious-metal–bearing deposits are unknown in this terrane.

Figures 3A and 3B show, respectively, a map of Laramide districts, and a plot of their produced precious-metal grades. Figure 4A shows the location of porphyry copper districts, and Figure 4B plots precious-metal grades of both porphyry and nonporphyry ores in porphyry copper districts. The data in Figure 4B are incorporated with values shown in Figure 3B.

Data from the Laramide districts show pronounced differences in silver and gold values with respect to domain. Districts of the Western Deserts show enrichment in gold with respect to the ratio of the clarkes, contrasting with enrichment in silver with respect to the ratio, of districts in the Naco domain. Although the sample population for Laramide deposits of domain II is small, the values nonetheless reflect the relatively higher gold values from both vein and intrusion-centered ore districts of this region.

The location of middle and late Tertiary districts is shown in Figure 5A, and a plot of precious-metal grades is shown in Figure 5B. The map of districts reveals the fact that southeastern Arizona, where Laramide porphyry-centered districts have been so economically dominant, is also a region of widespread post-Laramide districts. Middle Tertiary ores have also formed in central Arizona, where Precambrian wall rocks are dominant. In Figure 5B, produced grades of precious metals reveal the same general and gross separation of silver to gold ratios with respect to domains that are shown in values for Laramide production.

[1]Appendix 1 consists of tabulated production grades for Arizona deposits separated by metallogenic epoch and sorted on the values of the Ag:Au ratios. It may be secured free of charge by requesting Supplementary Data 8735 from the GSA Documents Secretary.

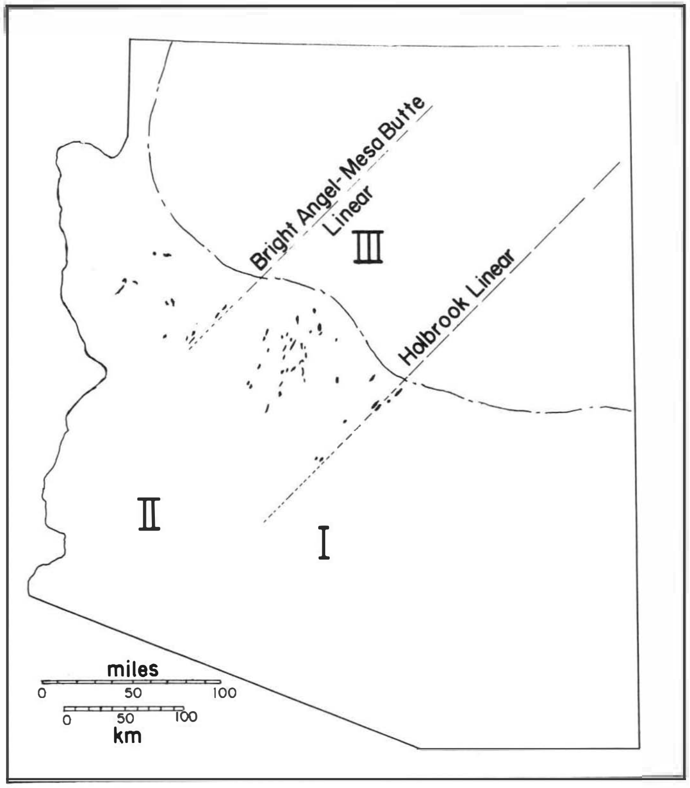

Figure 2A. Map of areas of Proterozoic mineralization in Arizona, adapted from Keith and others (1983a, 1983b). This figure and the following maps of Figures 3A and 5A are of mineralized *areas* rather than of *districts* as historically and traditionally considered. Designation of *areas* is the convention adopted on maps and in tables of the principal source materials (Keith and others, 1983a, 1983b) and is followed here. In these reports, many traditional districts of Arizona have been redefined on the basis of coherence of geological features and other metallogenic criteria and in many instances renamed. Thus a "district" in the sense of Keith and others, and consequently in the sense used in this paper, may compose a group of separated outcrops, hills, or small ranges and are shown as such in the maps of this report; conversely, more than one "district" may be located in a single area shown on the map. The reader is referred to the citations for detailed information.

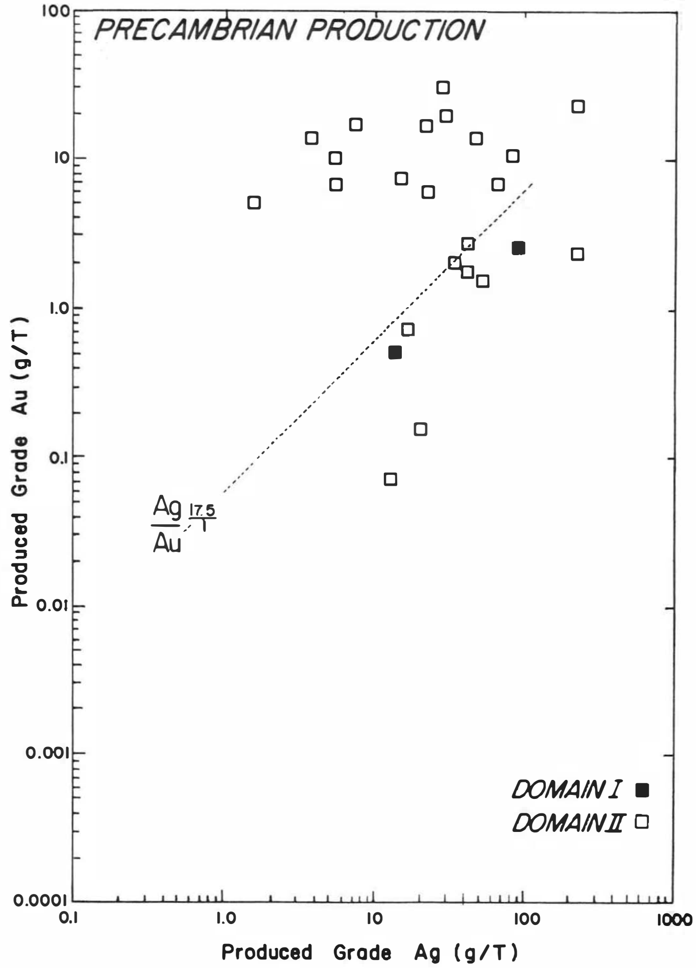

Figure 2B. Logarithmic plot of produced grades of silver and gold in districts of Proterozoic ores in Arizona. In this figure and in Figures 3B, 4B, 5B, 6, and 7, a reference line representing a constant ratio of crustal abundances of silver and gold (17.5) is reproduced for comparative purposes. See text for further discussion.

Production Grades of Silver and Gold by Domain

Production values of districts of all ages are plotted according to domain (Figs. 6 and 7). Although the separation of composition, along the line of the constant ratio of clarkes, is not exact, there is an overall difference in the silver to gold ratios that is clearly related to different terranes. At high produced grades of silver and gold, compositions overlap, and the distinction between domains is not discernible. Figure 8 is a plot of production grades from deposits of Precambrian, Laramide, and younger Tertiary ages that occur in Precambrian wall rocks in domain II where Yavapai Series strata and Precambrian granites occur. It is noteworthy that precious-metal ores of domain II reveal grades in the same compositional ranges as those of all deposits in Precambrian rocks shown in Figure 8.

Summary of Production Data

The data presented here establish more rigorously than has been done heretofore the generally gold-rich character of districts of western Arizona and the relatively silver-rich character of the districts of eastern and southeastern Arizona. This is not a revelation, as these differences have been part of conventional knowledge for many decades. The *significant* aspect of the data is the fact that this difference in metallogenic character transgresses time, deposit style, variations in igneous-rock compositions, and episodes of different tectonic evolutionary styles.

Data for districts in adjoining states are scattered and mixed, treating reserves as well as partial or total production (Wilkins, 1984). Nevertheless, those data reveal the existence of relatively gold-rich ores of many ages and types in southeastern California and Nevada, and relatively silver-rich ores in southwestern New Mexico. Further consideration of these adjoining states in this study is not possible, however, because of the lack of published and comparable data.

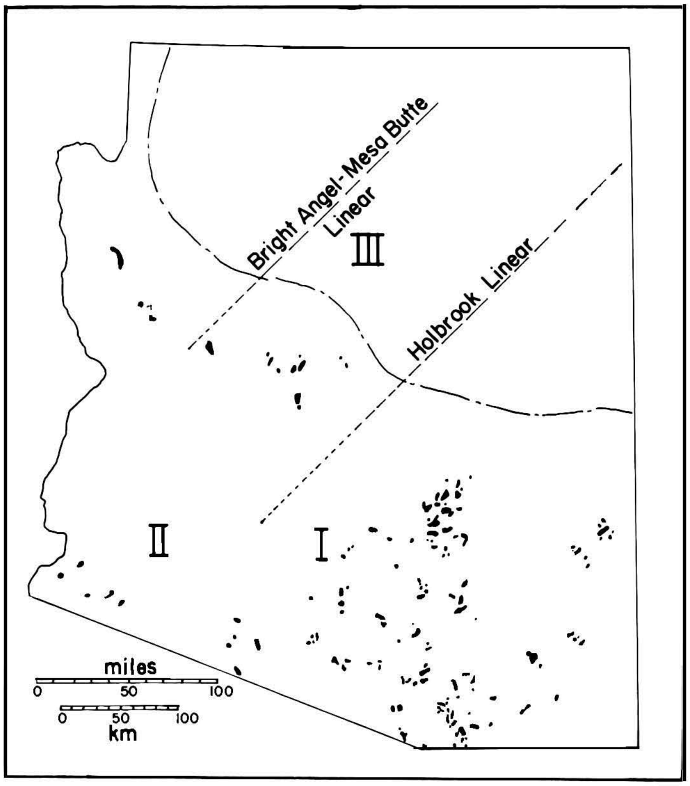

Figure 3A. Map of areas of Laramide mineralization in Arizona.

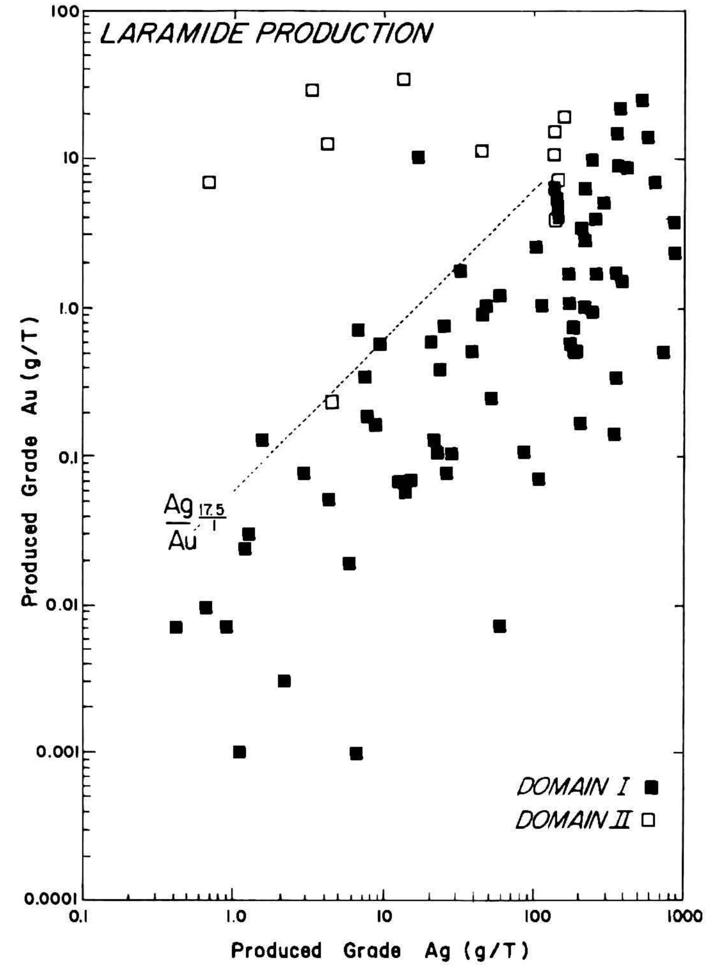

Figure 3B. Logarithmic plot of produced grades of silver and gold in districts of Laramide ores in Arizona. See text for further discussion.

A small number of districts show strikingly different compositions, with respect to the ratio of clarkes and domains. Relatively gold-rich deposits in domain I are known in the Mammoth district where middle Tertiary ores are also anomalously rich in molybdenum and vanadium; other relatively gold-rich ores of domain I occur in the Rincon, Apache Pass, Teviston, and Mammon districts. Relatively silver-rich ores occur in domain II in the Peck, Shea, Tiptop, McCracken, Silver, and New Water districts. Why such districts differ so much from others in their respective domains is not known; their number, however, is less than 5% of the total considered in this analysis.

Within the Proterozoic districts, there are four districts with synvolcanic or synsedimentary mineralization (Old Dick, Hualapai, Big Bug, and Verde), where ores are best characterized as Pb-Zn-Ag(Au) or Cu-Zn-Ag(Au). In the plots of production, Big Bug and Verde districts lie in the area of overlapping compositions of the two domains. Old Dick and Hualapai show anomalous ratios for their domain. Precambrian deposits of this nature, however, are sometimes distal parts of larger metallized systems where gold is sometimes concentrated with copper close to a thermal center.

If the distribution of precious-metal grades with respect to domain may be tentatively accepted as a manifestation of some regional metallogenetic control, the districts cited above merit further study to assess causes for their apparently anomalous characteristics. Such difference may result from contrasts in metal sources, local contrasts in crustal compositions, erosion across vertically zoned mineralization, unknown aspects of ore-solution chemistry, or possibly even the existence of undiscovered parts of broader and as yet unrecognized zoned districts.

SILVER AND GOLD METALLOGENESIS

In many districts of both domains, silver and gold are associated with a diverse base-metal mineral assemblage. Silver and gold occur as trace elements in sulfide minerals; as discrete complex minerals, such as sulfides or sulfosalts; as electrum; and more rarely as native silver. As members of the hypogene assemblage, the precious-metal minerals can seldom be set apart in time or space from the mainline of mineral paragenesis, although insufficient rigorous mineralogical studies exist to be certain that this is always the case. Importantly, however, the tenor of precious metals in base-metal deposits may vary directly with the tenor of base metals—in vein and replacement deposits with lead, zinc, or copper (individually or in combinations), and in the porphyry ores with copper or molybdenum. In zoned districts, silver and gold may occur with all mineral assemblages, as well as occurring in discrete spatial locations where they are the sole members of mineral assemblages (Fig. 9).

The characteristics of hypogene mineralization suggest that gold and silver are contained within hydrothermal solutions that were carrying other metals as well as sulfur. Whereas it may be that both base and

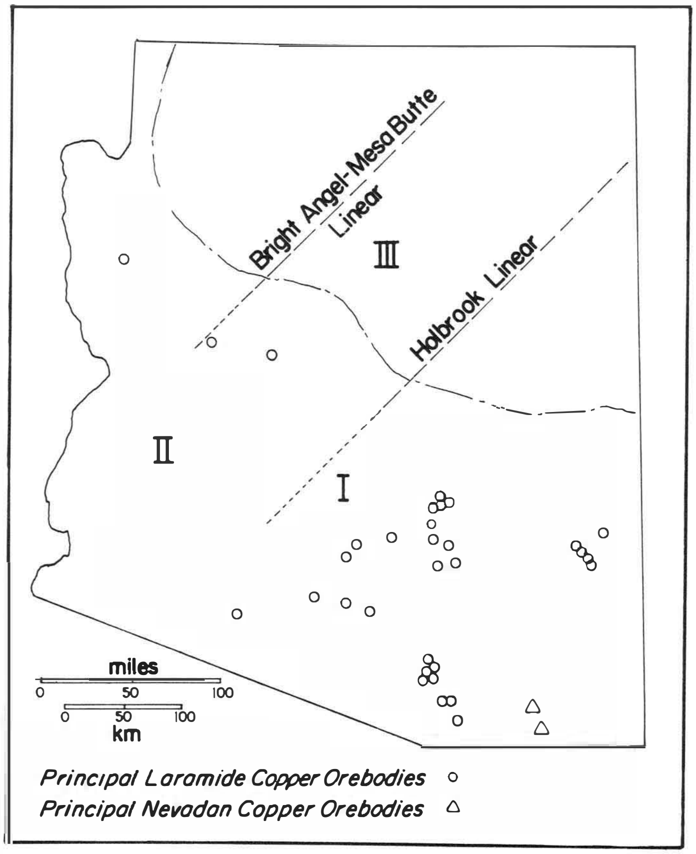

Figure 4A. Location map of Laramide and Nevadan porphyry copper deposits, Laramide porphyry copper districts (where porphyry ores are known or inferred but not developed), and Nevadan districts.

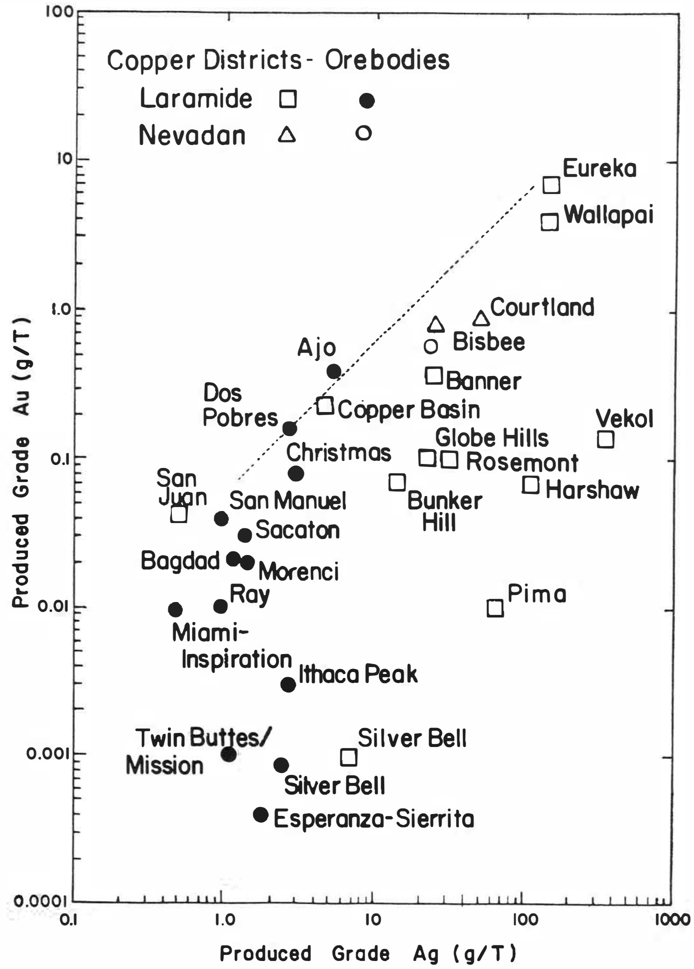

Figure 4B. Logarithmic plot of produced grades of silver and gold for Laramide and Nevadan porphyry deposits and nonporphyry ores from related districts in Arizona. Values shown for the Bisbee, Wallapai, and Eureka *districts* exclude values of porphyry copper production. Values for Dos Pobres have been interpolated from maps of Langton and Williams (1982). Values shown for copper orebodies include, for the most part, a cumulative value that includes production away from copper centers. Data available for these districts are inadequate to make a separation of grades by genetic type or other mines.

precious metals have a common source, such a characteristic cannot be determined to any greater degree of certainty than can the provenance of solutions which carried them. In the context of modern ideas of Cordilleran ore genesis, reasonable and substantiated hypotheses involve solutions of different provenance and metalliferous characteristics interacting at sites of metal concentration. Results of this study point to a strong correspondence of precious-metal ratios with specific geological domains from which may be inferred a fundamental relationship of both metal and solution to some characteristic of geographic position; although the base metals of precious-metal–containing deposits may have a similar association, this cannot yet be convincingly demonstrated.

An unknown but probably significant proportion of the silver and gold produced in this region has been from oxidized ores. Both metals tend to be enriched either chemically or residually in this process. Because of its relatively greater solubility, silver would be expected to be depleted with respect to gold. Oxidized, silver-rich ores, however, were mined in domain I; whereas oxidized, gold-rich ores, together with the predominance of gold placer production in the State, were characteristic of domain II. There is no evidence to suggest that weathering histories of the late Tertiary and Quaternary were different in the two domains. Although the ratios of metals determined from production of oxidized ores may not be precise representations of their original proportions in hypogene ores, the data suggest nonetheless that the gold- versus silver-rich character of oxidized ores in the two domains represents their fundamental proportions in primary ores.

From this overview of general metallogenic characteristics of Arizona ores, further aspects of silver and gold mineralization in Arizona may be outlined, and constraints on metallogenetic theories may be proposed.

1. The silver-to-gold ratios are unrelated to metallogenic epoch. Except at high produced grades, most ores of all ages appear to contain gold concentrated in excess of the Ag:Au clarke ratio in western Arizona, and silver in excess of the ratio in southeastern Arizona.

2. The silver-to-gold ratios have not been affected by variations in deformational style. Comparison of districts related to Laramide compression and Tertiary extension in both eastern and western Arizona suggests

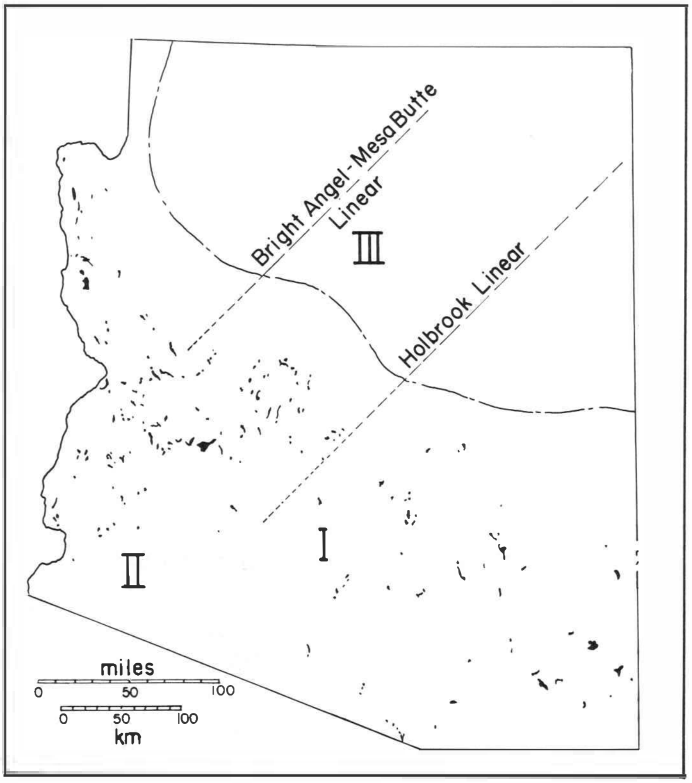

Figure 5A. Map of areas of middle to late Tertiary mineralization in Arizona.

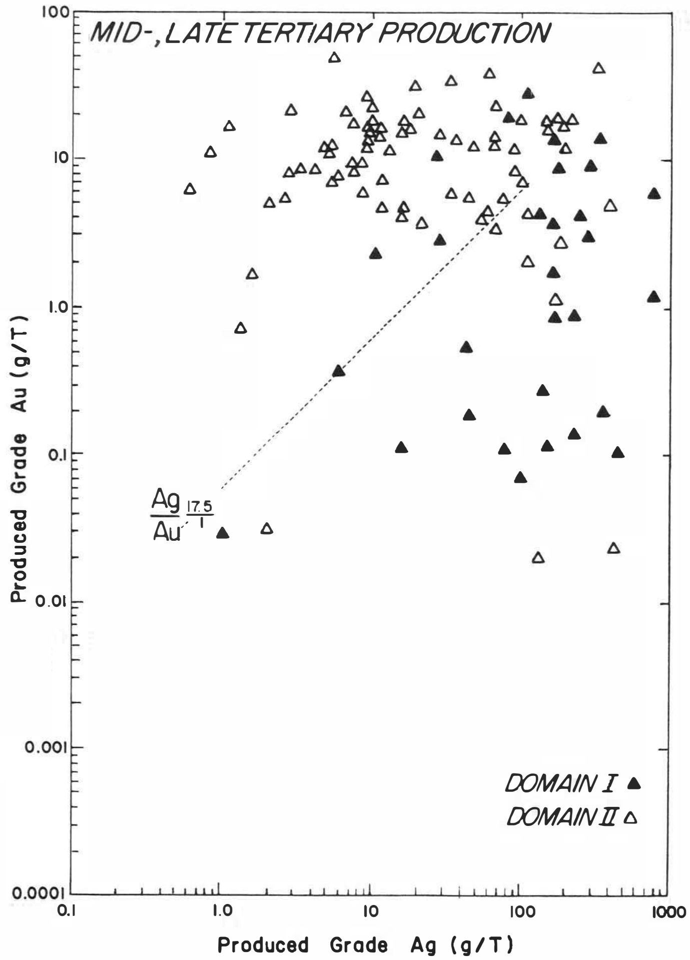

Figure 5B. Logarithmic plot of produced grades of silver and gold in districts of middle and late Tertiary mineralization in Arizona. See text for further discussion.

only that styles of structural control of ores change, not the broad characteristics of silver-to-gold ratios.

3. The diversity of igneous rocks and the ranges of compositions within different differentiation series that have evolved since the Precambrian in this region appear to have had little effect upon distribution of precious-metal ratios. This interpretation may be best assessed by comparing metal compositions of the two domains during Laramide and younger Tertiary metallization. In southern Arizona, the Laramide was a time of emplacement of a variety of calc-alkalic and alkali-calcic rocks as well as two-mica granites during its close; the middle and late Tertiary were times of emplacement of numerous granite bodies, as well as volcanic rocks in western Arizona (Westra and Keith, 1982) and some volcanic rocks of alkalic-subsilicic composition. The differences between metal ratios at district scale in the domains, however, appear to have been largely unaffected.

4. The precious-metal ratios, where composited at the scale of districts, appear to have been little affected by the diverse styles of ore occurrence. Although there are gold mines, silver mines, and copper mines in individual districts, compositing their production at district scale leads to the conclusion that, where district-scale anomalies are considered, there appear to be fundamental properties of metal content that transcend characteristics of ore occurrence at mine scale.

5. Whereas silver and gold are sometimes vertically zoned with respect to each other in ore deposits, there is no evidence for contrasts in weathering styles or weathering histories across southern Arizona that would preferentially expose one metal or the other in the different domains.

GENETIC CONSIDERATIONS

The points elaborated above lead to the conclusion that the ratios of silver to gold in Arizona deposits define two metallogenic provinces. There remain the questions of metal source and of reasons for the time-enduring metallogenic contrast. The identification of geographically related distinctions in the ores of Arizona provides a new basis upon which concerns about general problems of ore genesis and metal source may be further addressed.

The Interrelationship of Metal Source and Process

Notwithstanding many theories concerning the source of metals in hydrothermal ore deposits, such sources remain enigmatic in a truly definitive sense. Furthermore, the credibility of any theory of source is heavily dependent upon the validity of theories of process. The two are inextricably linked in establishing the origins of hydrothermal ore deposits and, importantly, in consideration of the nature of metallogenic provinces.

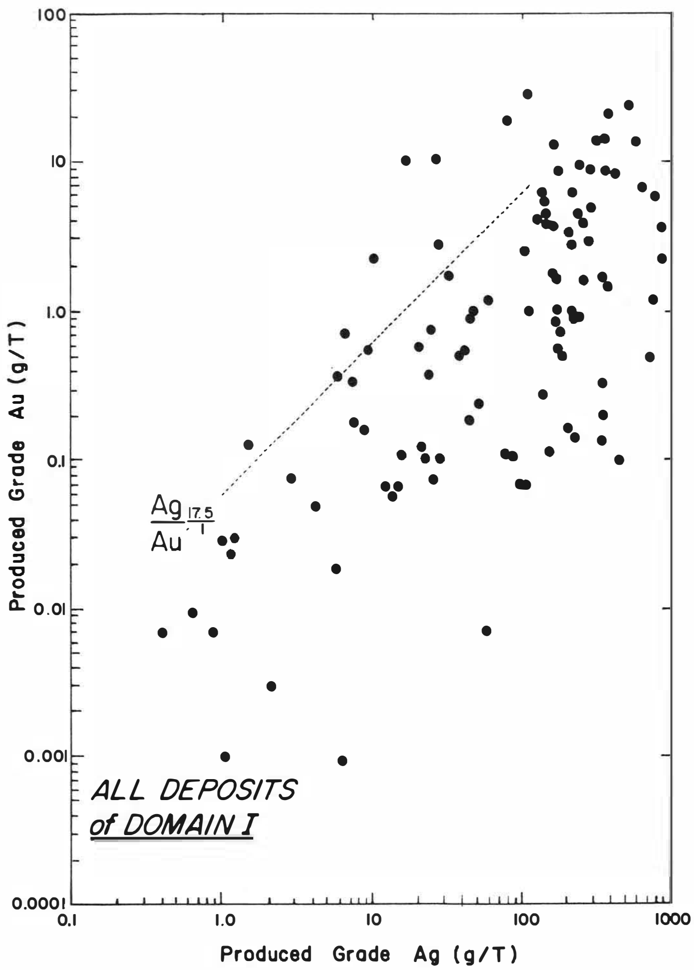

Figure 6. Logarithmic plot of produced grades of silver and gold for districts of all ages in domain I.

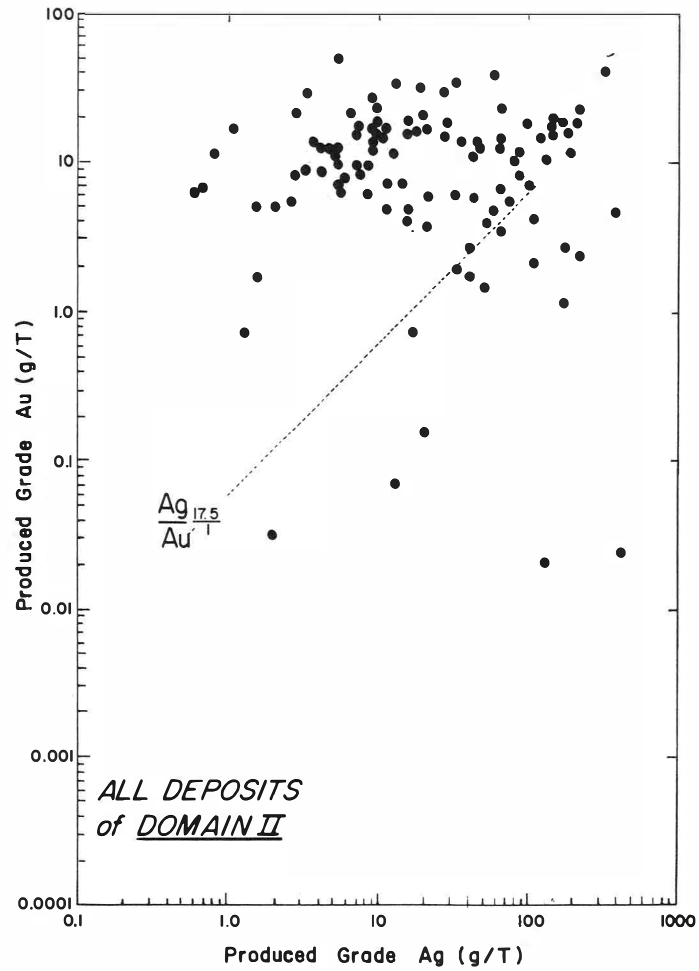

Figure 7. Logarithmic plot of produced grades of silver and gold for districts of all ages in domain II.

The numerous kinds of ore deposits of this region except, perhaps, some of the Proterozoic deposits that formed at contemporary surfaces (Derry, 1973), resulted from hydrothermal flow through and deposition of metal in rocks. The argument may be made that the mere heating of solutions and driving them through rocks results in the productive or barren metallogenic properties seen and, furthermore, that such a process acting anywhere would result in deposits of identical metallogenic character. It is not clear that unequivocal examples of such solely *process-dependent* hydrothermal metallogenesis exist. Alternatively, it may be argued that the metallogenic character of ores is *source dependent.* As considered here, and at the scale of districts, identical processes in the two domains formed virtually identical ore deposits with different precious-metal content. At this scale, however, it is also obvious that precious-metal content of the preponderance of Arizona *districts* bears a strong correspondence with the different geology of domains, and thus a source-rock dependence is hypothesized.

Processes

Results of many detailed studies of ores during the past two decades from a wide variety of hydrothermal ore deposits in Arizona reveal that, for the most part, those exposed of Nevadan and Laramide age formed under conditions of the mesothermal environment, whereas those of the younger parts of the Cenozoic formed mostly in the epithermal environments. In regionally zoned mineralization of many Laramide districts, however, the distinction is difficult to establish, district scale mineralization transgressing the "boundaries" of the hydrothermal classification. Stable-isotope studies in deposits of this region have shown that in the porphyry copper systems the hydrothermal fluids contained a large component of meteoric water at various stages of alteration and mineralization (Sheppard and others, 1971); similarly, epithermal deposits have been found in most instances to have formed from solutions dominated by meteoric waters (Field and Fifarik, 1985).

Debate concerning the role of igneous rocks in formation of intrusion-related ore systems continues. Beyond the problems of implied or argued metal sources, the intrusions in large systems are surrounded by areas, more than an order of magnitude greater than the intrusions, of densely fractured rock through which solutions flowed, depositing and forming a wide spectrum of ore and alteration minerals (Titley and others, 1986). Field evidence of these phenomena in this region is widespread and abundant. It may be concluded that at the very minimum the process of ore formation was influenced by the energetics of pluton emplacement and

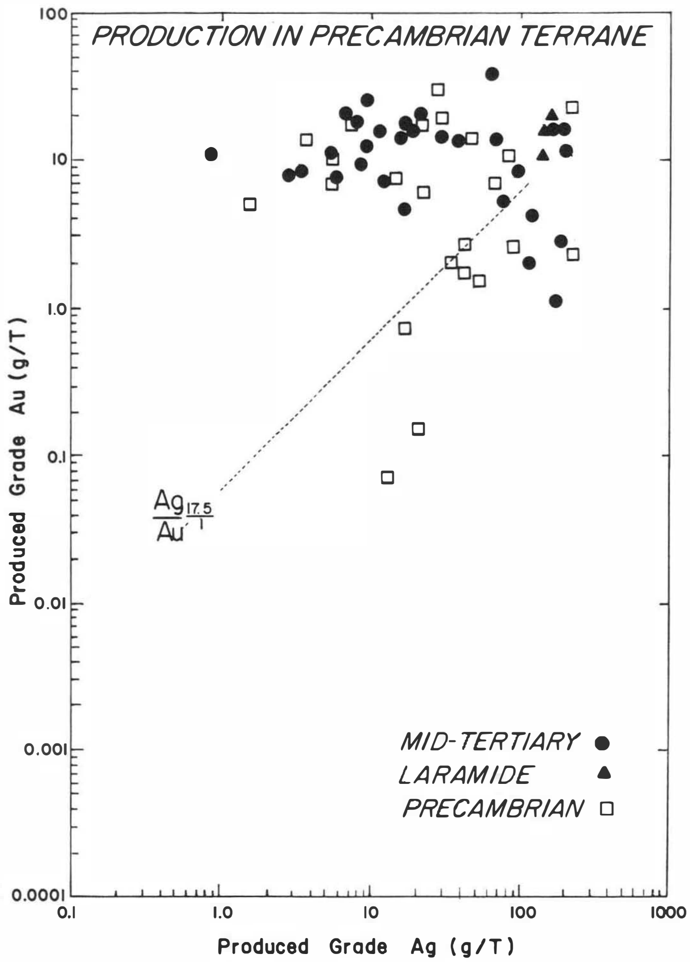

Figure 8. Logarithmic plot of produced grades of silver and gold for districts of middle and late Tertiary, Laramide, and Precambrian ages in Proterozoic host rocks of domain II in central Arizona. The preponderance of compositions are closely clustered in the same ranges of composition as Proterozoic ores shown in Figure 2B.

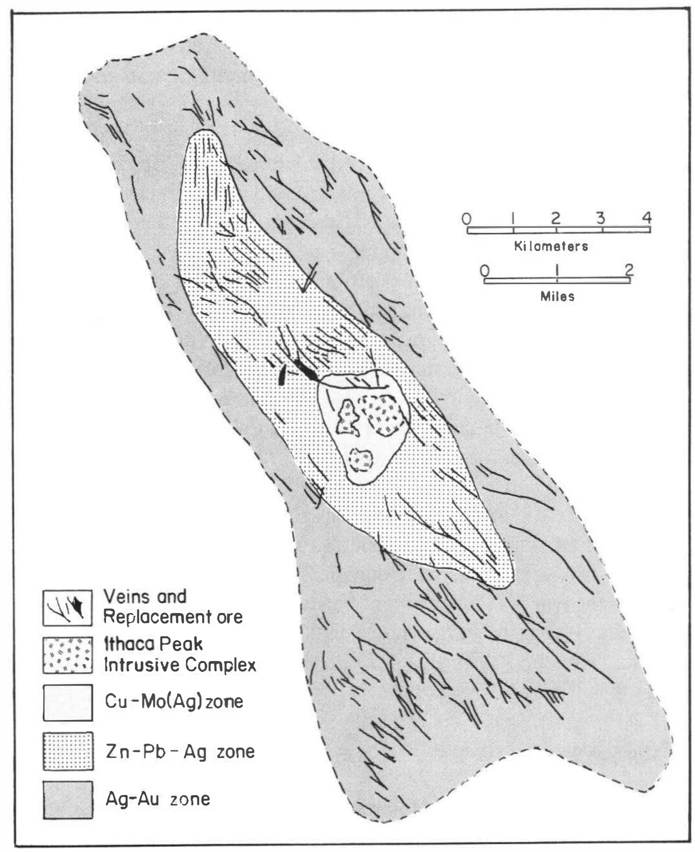

Figure 9. Metal zoning map of the Eureka (Chloride, Cerbat, Mineral Park) district of northwestern Arizona. Zoning shown is a well-studied example of the style of zoning in many Laramide districts and represents deposition of metals from a hydrothermal system at an original level about 2 km beneath the surface. Geology adapted from Eidel and others (1968) with data from Wilkinson and others (1982).

cooling, the results of which were to form large fracture-controlled flow networks in substantial volumes of wall rock, through which large volumes of fluid were driven by pluton-derived heat. At district or large-orebody scale, the evidence for involvement of crustal rocks and their contained water is compelling.

Metal Sources

The source of metals in hydrothermal ores has been an object of many studies and comment but with few convincing arguments to substantiate any particular point of view. The nature of the problem has been outlined by Krauskopf (1967, 1971) and Skinner (1979); Meyer (1981, 1985) has reviewed time-dependent aspects of the origin of ores. A mantle source of metals in ores of the Cordillera has been proposed by Noble (1970); Spurr (1922) was explicit in his contention that metals originated beneath the crust. Lowell (1974) suggested that Laramide copper ores of this region were derived from the crust or upper mantle, but those ideas were opposed by Sillitoe (1975), who favored a metal source in a subducted oceanic slab. Clearly, there is no consensus on the solution to the problem in the American Southwest.

The evidence of widespread igneous activity coincident with many hydrothermal ore districts in this part of North America is conspicuously and unequivocally clear. Most districts were formed in proximity to igneous rocks and/or at times and under regimes of locally elevated crustal temperatures. Recent studies of Laramide and younger intrusions in the Southwest have identified a source of magma within the crust at Bingham, Utah (Farmer and DePaolo, 1983), and at several localities in southern Arizona (Farmer and DePaolo, 1984). Results of a study of a suite of Laramide igneous rocks at Sierrita, Arizona, indicate a contribution of mantle material in earliest volcanic rocks but with progressively greater contributions of crust to ensuing metal-related intrusions (Anthony and others, 1985; Anthony and Titley, 1987). If the tenet of a direct relationship between metals and igneous rocks of ore deposits is to be held, this growing body of evidence suggests that metal sources of some ore deposits must still be constrained to crustal sources. A resulting theory of ore genesis would invoke crustal anatexis with metals of ores inherited from resulting magmas.

Complementary processes that extract metals from wall rock may also be important. The presence of district-wide, fracture-related, wall-rock permeability in numerous pluton-centered districts of Arizona (see Fig. 9) requires consideration of a hypothesis that metals may be extracted from crust by solely hydrothermal processes and that wall rocks to the systems are the metal sources.

Crustal sources may be further considered. Figure 10 is a histogram of the log of ratios for domains plotted at intervals of 0.25 against numbers of occurrences. Tables 3 and 4 present compilations of means of the log of ratios related to domains (Table 3) and as related in domains to epoch (Table 4). Shown, as well, in Table 4 are means of the logs of silver:gold ratios for separate groups of rocks from Boyle (1979), representing important lithologies of Proterozoic basement rocks in the two domains. The ratios shown in Figure 10 are bimodal in each domain, and each domain shows a peak very close to the ratio of the clarkes. Although it is unwise to press the interpretations of this sort of information too far, it is noteworthy that districts close to the clarke ratio are related to rhyolites in which the ratio of silver to gold is close to that of the ratio of clarkes—13.5 (Boyle, 1979).

In Table 4, it may be seen that irrespective of age, silver-to-gold ratios of deposits within domains are similar to each other, but the ratios differ by an order of magnitude between domains. The compositions of Proterozoic rocks of the two domains are approximated by the lithologies shown in the table, and it may be further noted that the silver-to-gold ratios of these rocks as presented by Boyle (1979) are closely similar to the averages of districts in the respective terranes.

Metallogenic Inheritance

Many points in evidence prompt a consideration of a hypothesis of metallogenic inheritance for the precious metals of Arizona ores; that is, the evolution of ores by processes that have acted on pre-existing rocks to extract and transport metals and to concentrate them in younger rocks. In 1957, Knight proposed the "source bed concept," a genetic hypothesis that proposed that metals of ores in sedimentary rocks were derived from their hosts by processes of later heating. Tweto (1960) described scheelite occurrences in Colorado in which inheritance may be strongly inferred. Schuiling (1967) suggested a crustal source of some tin ores; those ideas were tested by Lehmann (1982), who modified the idea by suggesting that certain tin-bearing granites were of crustal origin. In broadly based considerations of these problems, Routhier (1969) and co-workers (Laboratoire de Geologie Appliquée, 1973) have discussed the concepts of consanguinity, heritage, and province—interrelated aspects of metal occurrence, process, and time.

Production data for Arizona have been presented here, and the ultimate interpretation is left to the reader. Inheritance may take place by many stages of concentration, and it is not possible to rule out, for certain, potentially important roles of mantle evolution, subduction, and crustal evolution. The coherence of evidence of what is presently understood about processes and the many sources of water, of the provenance of magmas in this region, and, most importantly, the fact that ores of two regions mimic basement compositions in a striking way must lead to a consideration of inheritance of precious metals, in these deposits, from the crust. It is not at all clear what different kinds of processes resulted in the compositions of ores observed. Anatexis of crustal rocks and preservation of metals in their original ratios in ore fluids, or irreversible solution of metals by ore fluids moving through crustal rocks are each likely, acting independently or in concert.

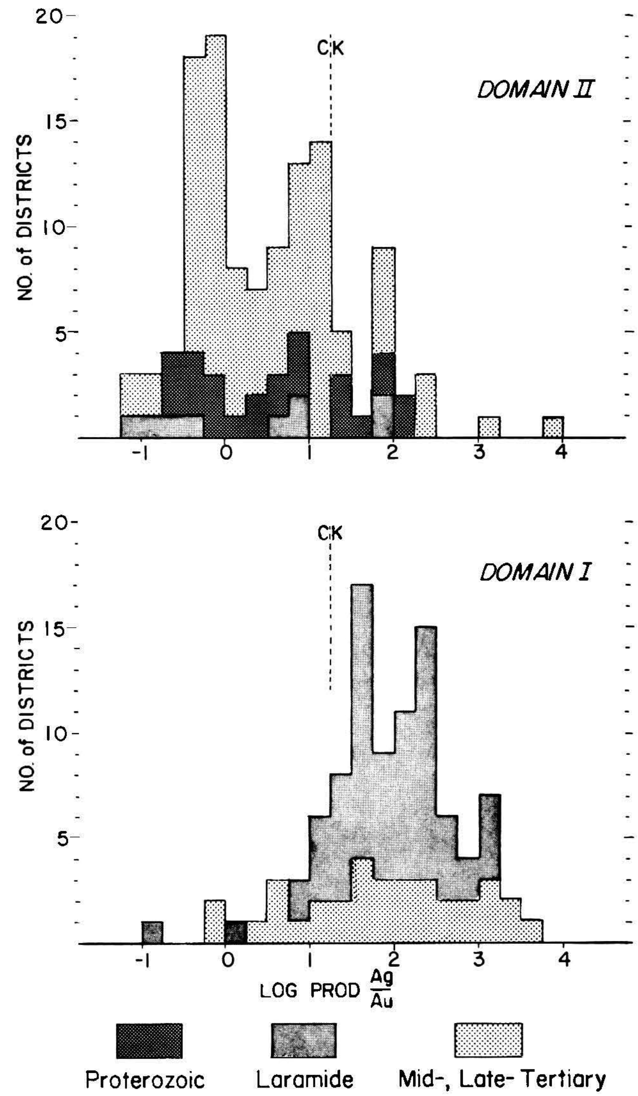

Figure 10. Histogram of logs of ratios of silver to gold in domains I and II, plotted at 0.25 log intervals. Dotted line is at a value of 1.24, the log of the ratio of the crustal abundance (ratio of clarkes) of silver to gold.

TABLE 3. SUMMARY OF SILVER TO GOLD RATIOS IN PRODUCED ORES OF ARIZONA BY DOMAIN

	Ag/Au*	mean log Ag/Au*
Southern Arizona districts (234)	18.5	1.268
Domain I districts (116)	88.9	1.949
Domain II districts (120)	4.5	0.660

*Ag and Au in weight units.

The Role of Subduction

Whereas it is obvious from the distribution of Mesozoic and younger ores in the circum-Pacific terranes that there is both spatial and temporal coincidence of their formation with subduction of oceanic plates, the effects of the process (Sillitoe, 1972a, 1972b; Keith, 1978; Mitchell and Garson, 1981; Sawkins, 1984) must be constrained in interpretations of

TABLE 4. SUMMARY OF SILVER TO GOLD RATIOS BY DOMAIN AND AGE AND COMPARISON WITH DATA OF VARIOUS LITHOLOGIES FROM BOYLE (1979)

	Ag/Au*	mean log Ag/Au*
Domain I (all)	88.9	1.949
3 Nevadan districts	23.4	1.370
79 Laramide districts	105.4	2.023
23 Middle to late Tertiary districts	65.2	1.814
Common rocks of the Proterozoic of Domain I (from data of lithologies by Boyle, 1979)		
Slates	90.8	1.958
Amphibolites	35.5	1.550
Shale, mudstone, argillite	24.5	1.390
Domain II (all)	4.5	0.660
27 Proterozoic districts	7.7	0.887
9 Laramide districts	2.0	0.307
82 Middle to late Tertiary districts	3.4	0.528
Common rocks of the Proterozoic of Domain II (from data of lithologies by Boyle, 1979)		
Sulfidic shale, pyritic graywacke	4.5	0.650
Granite, aplite	4.4	0.642
Andesite, trachyte, dacite, etc.	6.4	0.792

*Ag and Au in weight units.

hydrothermal ore genesis in the American Southwest. From a different perspective, Guild (1978) has also expressed similar reservations. Through the times of subduction-related tectonic compression and extension, through times of evolution of different igneous rock suites, and across a spectrum of kinds of ore-deposit types, the precious-metal ratios in Arizona ores have maintained a consistency that can be identified for certain only with a geographic location that corresponds to distinctively different successions of rocks. There is no evidence that this regional zoning can be related to selective evolution of metals from a subducted slab; further, the evidence of crustal sources of many ore-related magmas would appear to preclude their direct parentage from subducted slab or sandwiched mantle. The production of subduction-derived heat, however, may be very important in generating magmas at higher levels. An additional important effect of the process is that of structural preparation of the crust, which develops deeply penetrating channelways for transfer of heat by magma or solutions.

CONCLUSIONS AND IMPLICATIONS

The distinctions of gold and silver character of ores, as they relate to geological domain, are not inferred to stop at the political boundaries of the State. The ramifications of this study have a more far-reaching impact. That this analysis has been carried out in this region is a result of the existence of an excellent data base for a region with a complex history of ore genesis. Importantly, it must be noted again that comparable data for contiguous regions are not available for public use to extend the analysis further.

Regardless of how the precious metals and their distinctive ratios originated in the Arizona terranes, the fact remains that the ratios are broadly different when viewed from the perspective of domain of occurrence. This suggests that certain characteristics of ores may be used in the analysis of metallized regions as a basic aid to prospecting, in assessment of metal potential or endowment, and to geological interpretation—or as an adjunct to tectonic analysis. As examples of such analysis, Campa and Coney (1983) have noted general differences in kinds of ore deposits in different accreted terranes of Mexico. Albers (1981, 1983) has shown a correspondence of ores and ore types with crustal geology of California, as well as regional correspondence in the varied geological settings of the Great Basin.

Beyond the potential applications to study of regional geology and ore search, this study reveals important characteristics relevant to continuing study of source and process in ore formation. The time-enduring character of precious-metal metallogenesis present in the Arizona domains appears to be a manifestation of properties of specific kinds of crust and defines, in a fundamental way, the nature of metallogenic provinces. Further, it is believed that identification of probable metal sources of hydrothermal ores, as is suggested to have been done here, constrains an important variable in continuing studies of processes of formation of hydrothermal ores.

ACKNOWLEDGMENTS

This paper has benefited from reviews by P. M. Bethke, C. J. Estoe, D. Menzies, and A. W. Rose. Discussions of many ideas here with D. L. Norton and Charles Meyer resulted in a sharpened view of many of the problems discussed. None of the above, however, necessarily agrees with all of the interpretations set forth. S. J. Reynolds and J. W. Welty kindly provided some nonrestricted material that resulted in more meaningful interpretations of production data. This study is part of a broader analysis of Laramide metallogenesis supported in part by the National Science Foundation under Grant EAR 8218775.

REFERENCES CITED

Ahrens, L. H., 1965, Distribution of the elements in our planet: New York, McGraw-Hill, 110 p.

Albers, J. P., 1981, A lithologic-tectonic framework for the metallogenic provinces of California: Economic Geology, v. 76, p. 765–790.

——1983, Distribution of mineral deposits in accreted terranes and cratonal rocks of western United States: Canadian Journal of Earth Sciences, v. 20, p. 1019–1029.

Anderson, C. A., 1968, Metamorphosed Precambrian silicic volcanic rocks in central Arizona, *in* Coats, R. R., Hay, R. L., and Anderson, C. A., eds., Studies in volcanology: Geological Society of America Memoir 116, p. 9–44.

——1972, Precambrian rocks in the Cordes area, Yavapai County, Arizona: U.S. Geological Survey Bulletin 1345, 36 p.

Anderson, C. A., and Blacet, P. M., 1972, Precambrian geology of the northern Bradshaw Mountains, Yavapai County, Arizona: U.S. Geological Survey Bulletin 1336, 82 p.

Anderson, C. A., and Creasey, S. C., 1958, Geology and ore deposits of the Jerome area, Yavapai County, Arizona: U.S. Geological Survey Professional Paper 308, 185 p.

Anderson, C. A., and Nash, J. T., 1972, Geology of the massive sulfide deposits at Jerome, Arizona: Economic Geology, v. 67, p. 845–863.

Anderson, C. A., Scholz, E. A., and Strobel, J. D., Jr., 1955, Geology and ore deposits of the Bagdad area, Yavapai County, Arizona: U.S. Geological Survey Professional Paper 278, 103 p.

Anderson, C. A., Blacet, P. M., Silver, L. T., and Stern, T. W., 1971, Revision of Precambrian stratigraphy in the Prescott-Jerome area, Yavapai County, Arizona: U.S. Geological Survey Bulletin 1324-C, 14 p.

Anderson, Phillip, 1986, 1900–1600 Ma Arizona Proterozoic plate tectonic evolution: Geological Society of America Abstracts with Programs, v. 18, p. 338.

Anthony, E. Y., and Titley, S. R., in press, Magmatic processes in porphyry copper deposits: International Association on the Genesis of Ore Deposits, Lulea Meeting, 1986, Proceedings.

Anthony, E. Y., Titley, S. R., Patchett, P. J., and Hess, J. J., 1985, Isotopic evidence for crustal melting in the evolution of a porphyry copper-related igneous suite in southeastern Arizona: EOS (American Geophysical Union) 1985 Fall Meeting Abstracts, v. 66, no. 46, p. 1142.

Boyle, R. W., 1979, The geochemistry of gold and its deposits: Canada Geological Survey Bulletin 280, 584 p.

Campa, M. F., and Coney, P. J., 1983, Tectono-stratigraphic terranes and mineral resource distributions in Mexico: Canadian Journal of Earth Sciences, v. 20, p. 1040–1051.

Condie, K. C., Bowling, G. P., and Vance, R. K., 1985, Geochemistry and origin of early Proterozoic supracrustal rocks, Dos Cabezas Mountains, southeastern Arizona: Geological Society of America Bulletin, v. 96, p. 655–662.

Coney, P. J., 1978, Mesozoic-Cenozoic Cordilleran plate tectonics, *in* Smith, R. B., and Eaton, G. P., eds., Cenozoic tectonics and regional geophysics of the western Cordillera: Geological Society of American Memoir 152, p. 33–50.

Cooper, J. R., 1957, Metamorphism and volume losses in carbonate rocks near Johnson Camp, Cochise County, Arizona: Geological Society of America Bulletin, v. 68, p. 577–610.

Cooper, J. R., and Silver, L. T., 1964, Geology and ore deposits of the Dragoon quadrangle, Cochise and Pima Counties, Arizona: U.S. Geological Survey Professional Paper 416, 196 p.

Dale, V. B., 1961, Tungsten deposits of Gila, Yavapai, and Mohave Counties, Arizona: U.S. Bureau of Mines Information Circular 8078, 104 p.

Davis, G. H., 1979, Laramide folding and faulting in southeastern Arizona: American Journal of Science, v. 279, p. 543–569.

Derry, D. R., 1973, Ore deposition and contemporary surfaces: Economic Geology, v. 68, p. 1364–1380.

Durning, W. P., and Buchanan, L. J., 1984, The geology and ore deposits of Oatman, Arizona, *in* Wilkins, Joe, ed., Gold and silver deposits of the Basin and Range province, western U.S.A.: Arizona Geological Society Digest, v. 15, p. 141–158.

Eidel, J. J., Frost, J. E., and Clippinger, D. M., 1968, Copper-molybdenum mineralization at Mineral Park, Mohave County, Arizona, *in* Ridge, J. D., ed., Ore deposits of the United States, 1933–1967: New York, American Institute of Mining, Metallurgical, and Petroleum Engineers, p. 1258–1281.

Elsing, M. J., and Heineman, R.E.S., 1936, Arizona metal production: Arizona Bureau of Mines Bulletin 140, 112 p.

Farmer, G. L., and DePaolo, D. J., 1983, Origin of Mesozoic and Tertiary granite in the western United States and implications for pre-Mesozoic crustal structure 1. Nd and Sr isotopic studies in the geocline of the northern Great Basin: Journal of Geophysical Research, v. 88, p. 3379–3401.

——1984, Origin of Mesozoic and Tertiary granite in the western United States and implications for pre-Mesozoic crustal structure 2. Nd and Sr isotopic studies of unmineralized and Cu- and Mo-mineralized granite in the Precambrian craton: Journal of Geophysical Research, v. 89, p. 10141–10160.

Field, C. W., and Fifarek, R. H., 1985, Light stable isotope systematics in the epithermal environment, *in* Berger, B. R., and Bethke, P. M., eds., Geology and geochemistry of epithermal systems: Society of Economic Geologists, Reviews in Economic Geology, v. 2, p. 99–128.
Gilmour, Paul, and Still, A. R., 1968, The geology of the Iron King mine, *in* Ridge, J. D., ed., Ore deposits in the United States, 1933–1967: New York, American Institute of Mining, Metallurgical, and Petroleum Engineers, p. 1238–1257.
Guild, P. W., 1978, Metallogenesis in the western United States: Journal of the Geological Society, London, v. 135, part 4, p. 355–376.
Hammer, D. F., and Peterson, D. W., 1968, Geology of the Magma mine area, Arizona, *in* Ridge, J. D., ed., Ore deposits in the United States, 1933–1967: New York, American Institute of Mining, Metallurgical, and Petroleum Engineers, p. 1282–1310.
Heidrick, T. L., and Titley, S. R., 1976, Structural evolution of southwestern North American Laramide porphyry copper deposits and its relationship to the history of plate interactions: International Geological Congress, 25th, Sydney, Australia, Abstracts, v. 3, p. 740.
——— 1982, Fracture and dike patterns in Laramide plutons and their structural and tectonic implications, *in* Titley, S. R., ed., Advances in geology of the porphyry copper deposits, southwestern North America: Tucson, Arizona, University of Arizona Press, p. 73–91.
Hogue, W. G., and Wilson, E. D., 1950, Bisbee or Warren district, *in* Arizona zinc and lead deposits: Arizona Bureau of Mines Bulletin 156, p. 17–29.
Howell, K. K., 1977, Geology and alteration of the Commonwealth mine, Cochise County, Arizona [M.S. thesis]: Tucson, Arizona, University of Arizona, 225 p.
Keith, Stanley B., 1978, Paleosubduction geometries inferred from Cretaceous and Tertiary magmatic patterns in southwestern North America: Geology, v. 6, p. 516–521.
Keith, Stanley B., Lehman, N. E., Sell, J. D., and Wilt, J. C., 1978, Supplemental road log no. 1; Tucson to Benson via Nogales, Patagonia, Sonoita, and Whetstone Junction, *in* Callender, J. F., Wilt, J. C., and Clemons, R. E., eds., Land of Cochise, southeastern Arizona: New Mexico Geological Society 29th Field Conference Guidebook, p. 157–163.
Keith, Stanley B., Gest, D. E., DeWitt, Ed, Toll, N. W., and Everson, B. A., 1983a, Metallic mineral districts and production in Arizona: Arizona Bureau of Geology and Mineral Technology Bulletin 194, 58 p.
Keith, Stanley B., Schnabel, Lorraine, DeWitt, Ed, Gest, D. E., and Wilt, J. C., 1983b, Map description and bibliography of the mineralized areas of the Basin and Range province in Arizona: U.S. Geological Survey Open-File Report 84-0086, 129 p.
Keith, Stanton B., 1973, Index of mining properties in Cochise County, Arizona: Arizona Bureau of Mines Bulletin 187, 98 p.
——— 1974, Index of mining properties in Pima County, Arizona: Arizona Bureau of Mines Bulletin 189, 156 p.
——— 1975, Index of mining properties in Santa Cruz County, Arizona: Arizona Bureau of Mines Bulletin 191, 94 p.
——— 1978, Index of mining properties in Yuma County, Arizona: Arizona Bureau of Mines Bulletin 192, 185 p.
Knight, C. L., 1957, Ore genesis—The source bed concept: Economic Geology, v. 52, p. 808–817.
Krauskopf, K. B., 1967, Source rocks for metal-bearing fluids, *in* Barnes, H. L., ed., Geochemistry of hydrothermal ore deposits: New York, Holt, Rinehart and Winston, p. 1–33.
——— 1971, The source of ore metals: Geochimica et Cosmochimica Acta, v. 35, p. 643–650.
Laboratoire de Geologie Appliquée, 1973, Some major concepts of metallogeny: Mineralium Deposita (Berlin), v. 8, p. 237–258.
Larson, P. B., 1984, Geochemistry of the alteration pipe at the Bruce Cu-Zn volcanogenic massive sulfide deposit, Arizona: Economic Geology, v. 79, p. 1880–1896.
Langton, J. M., and Williams, S. A., 1982, Structural, petrological, and mineralogical controls for the Dos Pobres orebody, Lonestar mining district, Graham County, Arizona, *in* Titley, S. R., ed., Advances in geology of the porphyry copper deposits, southwestern North America: Tucson, Arizona, University of Arizona Press, p. 335–352.
Lehman, N. E., 1978, Pyrometasomatic deposits of the Washington Camp–Duquesne district, Santa Cruz County, Arizona: Mining Engineering (American Institute of Mining, Metallurgical, and Petroleum Engineers), v. 93, p. 181–188.
Lehmann, Bernd, 1982, Metallogeny of tin: Magmatic differentiation versus geochemical heritage: Economic Geology, v. 77, p. 50–59.
Lowell, J. D., 1974, Regional characteristics of porphyry copper deposits of the southwest: Economic Geology, v. 69, p. 601–617.
McKee, E. D., 1951, Sedimentary basins of Arizona and adjoining areas: Geological Society of America Bulletin, v. 62, p. 481–506.
Meyer, Charles, 1981, Ore-forming processes in geologic history: Economic Geology, Seventy-Fifth Anniversary Volume, p. 6–41.
——— 1985, Ore metals through geologic history: Science, v. 227, p. 1421–1428.
Mitchell, A.H.G., and Garson, M. S., 1981, Mineral deposits and global tectonic settings: London, England, Academic Press, 405 p.
Noble, J. A., 1970, Metal provinces of the western United States: Geological Society of America Bulletin, v. 81, p. 1607–1624.
Peacock, M. A., 1931, Classification of igneous rock series: Journal of Geology, v. 39, p. 54–67.
Peirce, H. W., Keith, S. B., and Wilt, J. C., 1970, Coal, oil, natural gas, helium, and uranium in Arizona: Arizona Bureau of Mines Bulletin 182, 289 p.
Routhier, P., 1969, Sur trois principes generaux de la Metallogenie et de la recherche minerale: Mineralium Deposita (Berlin), v. 4, p. 213–218.
Sawkins, F. J., 1984, Metal deposits in relation to plate tectonics: Berlin, Springer-Verlag, 325 p.
Schuiling, R. D., 1967, Tin belts on the continents around the Atlantic Ocean: Economic Geology, v. 62, p. 540–550.
Sheppard, S.M.F., Nielsen, R. L. and Taylor, H. P., Jr., 1971, Hydrogen and oxygen isotope ratios in minerals from porphyry copper deposits: Economic Geology, v. 66, p. 515–542.
Shoemaker, E. M., Squires, R. L., and Abrams, M. J., 1978, Bright Angel and Mesa Butte fault systems of northern Arizona, *in* Smith, R. B., and Eaton, G. P., eds., Cenozoic tectonics and regional geophysics of the western Cordillera: Geological Society of America Memoir 152, p. 341–368.
Sillitoe, R. H., 1972a, A plate tectonic model for the origin of porphyry copper deposits: Economic Geology, v. 67, p. 184–197.
——— 1972b, Relation of metal provinces in western America to subduction of oceanic lithosphere: Geological Society of America Bulletin, v. 83, p. 813–817.
——— 1975, Subduction and porphyry copper deposits in southwestern North America—A reply to recent objections: Economic Geology, v. 70, p. 1474–1477.
Silver, L. T., 1978, Precambrian formations and Precambrian history in Cochise County, southeastern Arizona, *in* Callender, J. F., Wilt, J. C., and Clemons, R. E., eds., Land of Cochise, southeastern Arizona: New Mexico Geological Society 29th Field Conference Guidebook, p. 157–163.
Silver, L. T., Conway, C. M., and Ludwig, K. R., 1986, Implications of a precise chronology for early Proterozoic crustal evolution and caldera formation in the Tonto basin–Mazatzal Mountains region, Arizona: Geological Society of America Abstracts with Programs, v. 18, p. 413.
Skinner, B. J., 1979, The many origins of hydrothermal mineral deposits, *in* Barnes, H. L., ed., Geochemistry of hydrothermal ore deposits (2nd edition): New York, John Wiley & Sons, p. 1–21.
Smith, G. M., III, and Graubard, C. M., 1987, Geology and mineralization of the Fortuna mine; a peraluminous gold deposit, southern Yuma County, Arizona: American Institute of Mining, Metallurgical, and Petroleum Engineers, 116th Annual Meeting, Denver, February 1987, Program with Abstracts, p. 30.
Spencer, J. E., and Welty, J. W., 1987, Mid-Tertiary ore deposits in Arizona, *in* Jenny, J. P., and Reynolds, S. J., eds., Geological evolution of Arizona: Arizona Geological Society Digest 17 (in press).
Spurr, J. E., 1923, The ore magmas, Volume 2: New York, McGraw Hill, p. 431–915.
Thomas, B. E., 1949, Ore deposits of the Wallapai district, Arizona: Economic Geology, v. 44, p. 663–705.
——— 1953, Geology of the Chloride quadrangle, Arizona: Geological Society of America Bulletin, v. 64, p. 391–420.
Thomas, L. A., 1966, Geology of the San Manuel orebody, *in* Titley, S. R., and Hicks, C. L., eds., Geology of the porphyry copper deposits, southwestern North America: Tucson, Arizona, University of Arizona Press, p. 133–142.
Titley, S. R., 1981, Geologic and geotectonic setting of porphyry copper deposits in the southern Cordillera, *in* Dickinson, W. R., and Payne, W. D., eds., Relations of tectonics to ore deposits in the southern Cordillera: Arizona Geological Society Digest, v. 14, p. 79–97.
——— 1982, Some features of tectonic history and ore genesis in the Pima mining district, Pima County, Arizona, *in* Titley, S. R., ed., Advances in geology of the porphyry copper deposits, southwestern North America: Tucson, Arizona, University of Arizona Press, p. 387–406.
Titley, S. R., and Anthony, E. Y., 1986a, Metallogenesis of Proterozoic-floored terranes in southern and southwestern Arizona: Geological Society of America Abstracts with Programs, v. 18, p. 419.
——— 1987b, Laramide mineral deposits in Arizona, *in* Jenny, J. P., and Reynolds, S. J., eds., Geological evolution of Arizona: Arizona Geological Society Digest, v. 17 (in press).
Titley, S. R., and Beane, R. E., 1981, Porphyry copper deposits; Part I. Geologic settings, petrology, and tectogenesis: Economic Geology, Seventy-Fifth Anniversary Volume, p. 214–235.
Titley, S. R., and Heidrick, T. L., 1978, Intrusion and fracture styles of some mineralized porphyry systems of the southwestern Pacific and their relationship to plate interactions: Economic Geology, v. 73, p. 891–903.
Titley, S. R., Thompson, R. C., Haynes, F. M., Manske, S. L., Robison, L. C., and White, J. L., 1986, Evolution of fractures and alteration in the Sierrita-Esperanza hydrothermal system, Pima County, Arizona: Economic Geology, v. 81, p. 343–370.
Tweto, Ogden, 1960, Scheelite in the Precambrian gneisses of Colorado: Economic Geology, v. 55, p. 1406–1428.
Warner, J. D., 1982, Geology and mineralization of the Blue Rock mine, northeastern Rincon Mountains, Pima County, Arizona [M.S. thesis]: Tucson, Arizona, University of Arizona, 132 p.
Welty, J. W., Spencer, J. E., Allen, G. B., Reynolds, S. J., and Trapp, R. A., 1985, Geology and production of middle Tertiary mineral districts in Arizona: Arizona Bureau of Geology and Mineral Technology Open-File Report 85-1, 88 p.
West, R. J., and Aiken, D. M., Geology of the Sierrita-Esperanza deposit, Pima mining district, Pima County, Arizona, *in* Titley, S. R., ed., Advances in geology of the porphyry copper deposits, southwestern North America: Tucson, Arizona University of Arizona Press, p. 433–465.
Westra, Gerhard, and Kieth, S. R., 1981, Classification and genesis of stockwork molybdenum deposits: Economic Geology, v. 76, p. 844–873.
Wilkins, Joe, Jr., 1984, The distribution of gold- and silver-bearing deposits in the Basin and Range province, western United States, *in* Wilkins, Joe, Jr., ed., Gold and silver deposits of the Basin and Range province, western U.S.A.: Arizona Geological Society Digest, v. 15, p. 1–27.
Wilkinson, W. H., Jr., Vega, L. A., and Titley, S. R., 1982, Geology and ore deposits at Mineral Park, Mohave County, Arizona, *in* Titley, S. R., ed., Advances in geology of the porphyry copper deposits, southwestern North America: Tucson, Arizona, University of Arizona Press, p. 523–541.
Wilson, E. D., 1927, Geology and ore deposits of the Courtland-Gleeson region, Arizona: Arizona Bureau of Mines Bulletin 123, 79 p.
——— 1933a, Geology and mineral deposits of southern Yuma County, Arizona: Arizona Bureau of Mines Bulletin 134, 234 p.
——— 1933b, Arizona gold placers and placering: Arizona Bureau of Mines Bulletin 135, 148 p.
Wilson, E. D., Cunningham, J. B., and Butler, G. M., 1934, Arizona lode gold mines and gold mining: Arizona Bureau of Mines Bulletin 137, 261 p.

MANUSCRIPT RECEIVED BY THE SOCIETY JULY 11, 1986
REVISED MANUSCRIPT RECEIVED MAY 4, 1987
MANUSCRIPT ACCEPTED MAY 12, 1987

SOCIETY OF MINING ENGINEERS

P.O. BOX 625002, LITTLETON, COLORADO 80162-5002

PREPRINT NUMBER

88-44

GEOLOGY OF THE VULTURE MINE, ARIZONA

D. C. White

Prescott, Arizona

For presentation at the SME Annual Meeting
Phoenix, Arizona - January 25-28, 1988

Abstract. The Vulture Mine near Wickenburg, Arizona was a major gold producer from 1863 to 1942, having yielded about 11,000 kg Au and 8,000 kg Ag. Gold occurs as coarse native metal and electrum in quartz veins and also finely disseminated within a quartz monzonite sill and its silicified wall rock. The sill is semi-conformable within a Proterozoic volcaniclastic-dominated sequence, all dipping north about 35°. Early mining focused on the vein-hosted gold, particularly in the immediate hanging wall and footwall of the sill. Later efforts included some open-pitting of the outcropping sill and adjacent altered and mineralized rock. Two sets of post-mineral faults have complicated the orebody geometry.

The sill is a 350m long apophyeis from a quartz monzonite stock to the west of the mine area. The stock has been dated at 85 my and contains abundant lesser gold occurrences in its core and about its margins. The Proterozoic rocks are notably lean in precious metals except where altered in proximity to the Cretaceous stock and sill. Circumstances dictate an interpretation of epigenetic mineralization related to the Laramide intrusion.

Introduction

The Vulture Mine is 17 km southwest of Wickenburg in Maricopa County, Arizona and accessible by the Vulture Mine Road south from State Highway 60 (Figure 1). Despite its preeminence as a gold producer, it has not been well understood because very little geology was recorded during its major period of production in the late nineteenth century, and because it has long been patented and guarded, effectively preventing modern-day study. Only exploration in the 1930's and 1980's accumulated much information of substance on the nature of the gold occurrence and much of that has been proprietary. This paper is an effort to consolidate and share what is known for the benefit of the entire geologic community.

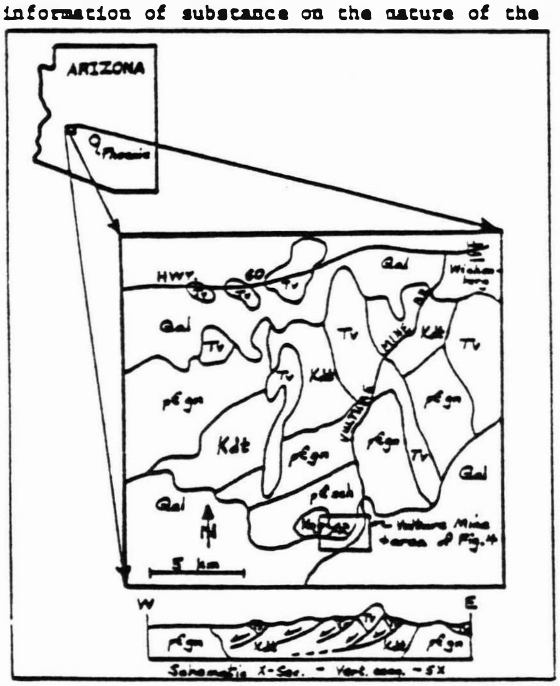

Figure 1: Location Map, and regional geology of the Vulture Mtns after Rehrig, et. al., 1980.

History and Production

Henry Wickenburg is credited with discovery of native gold in outcrop in 1863. For the next 80 years, the camp experienced the classic booms and busts of western mining including problems of Apache raids, no water, diminishing grade, and discontinuities caused by faults. Milling was by arrastras on the Hassayampa River, a 21 km haul by burro or wagon train, until water was piped to the mine in 1880 and an 80-stamp mill installed. Early amalgamation was eventually replaced by cyanidation. Stopes caved to the surface and openings so formed were enlarged into open pits to include low grade material during the 1930's. Tailings reprocessing and pillar robbing completed production to 1942 from which time it has remained closed. Scenic residences, offices, shops, and mill structures remain as does a vintage headframe (Figure 2).

Production figures are approximate because accounts were either not kept or were lost. Overall value of production by various operators from 1863 through 1942 is estimated at 900 metric tons (1 million s.t.) containing about 11,000 kg (350,000 ounces) of gold and 8,000 kg (250,000 ounces) of silver. Grade hence averaged 12 grams Au and 9 grams Ag, .35 and .25 oz. respectively. There was minor copper and lead production. These figures do not include the undocumented but likely small placer gold production.

Geology

Regional Setting

The Vulture Mine is in the Vulture Mountains where the edge of the pediment merges with the low desert alluvium of the Hassayampa Plain. The middle to low elevations are underlain by foliated thin flows of basalt, pyroclastic and volcaniclastic rocks and clastic sedimentary rocks of Proterozoic age which are greenschist to lower amphibolite facies of regional metamorphism. These rocks are intruded by a stock of quartz monzonite which is 85± 3 my old by Rb/Sr age determination (Krueger, 1987) and which has a sill-like apophysis containing the Vulture Mine. This stock outcrops over an area of 1.3 km^2 but is known from geophysical surveys to extend over an area of 6.5 km^2 (2.5 mi^2). The sill-like apophysis extends 350 m (1150 ft) from the east edge of the stock through the mine area. (Figures 3 and 4)

The Wickenburg batholith, a granitoid body 68 my old by K/Ar age determination (Rahrig, et. al., 1980) outcrops within the Vulture Mountains 5 km north of the mine site. The peaks of the mountains are basalt flows and potassic rhyolite pyroclastic rocks of mid-Tertiary age (Rehrig, et. al., 1980). All of these rocks, and the gold occurrence of the Vulture Mine, are broken by low angle faults of probable early Cenozoic age and steep faults of mid-Cenozoic age.

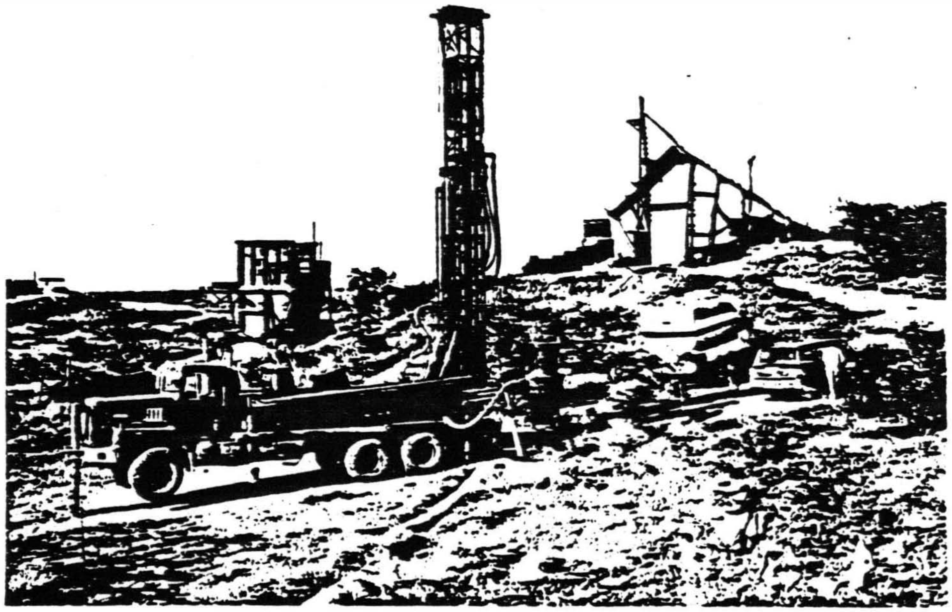

Figure 2: 1987 exploration for low grade, open-pitable reserves adjacent to circa 1890 headframe on the west incline, site of 19th century high-grade underground mining.

The Gold Occurrence

Gold at the Vulture Mine is native metal and electrum with euhedral pyrite, argentiferous galena, and minor chalcopyrite and sphalerite in quartz veins within and subparallel to the porphyritic quartz monzonite sill, as dispersed grains within the sill, and in veins, veinlets, and areas of silicification within the Proterozoic rocks immediately adjacent to the sill (Figures 3 and 5).

Within the sill, gold grade is typically 1 to 2 g/t (.03 to .06 oz/s.t.). Near the sill's margins and within the immediate wall rock, grade is more fickle but generally higher. Old stopes typically follow the hanging wall and footwall of the sill. Hanging wall stopes are more continuous and were generally of better grade. Precious metal content appears to diminish with depth as base metal content increases.

Many geologists suspect a Precambrian, syngenetic origin for the Vulture gold. However, this seems unlikely given the notable absence of gold within the Precambrian rocks of the area and the presence of only a few thin, barren, horizons of oxide-facies iron formation. Only within and about the Vulture stock does gold occur. Quartz veins within the stock are generally auriferous. Such veins are very small and have been prospected thoroughly for more than a century but rarely have more than 3 g/t which occurs locally as visible gold.

The spatial and temporal relationship of gold distribution to the apophysis of the quartz monzonite stock suggests that gold concentration was related to emplacement of that stock and, at most, the significance of the Proterozoic basement is one of structural permissiveness and perhaps some geochemical inheritance. Disruption of the gold occurrence by low angle and steep Tertiary faults confine age of mineralization to pre-middle Tertiary (Figures 4 and 5).

Placer gold is also known. It is juvenile coarse and fine gold. Nuggets containing quartz, galena, and dendritic gold have been found in the basal Quarternary gravels within hundreds of meters from the mine.

Alteration

Amphibolite-bearing schists in the footwall, generally dark green to black, and foliated, are pale green, hard, less distinctly foliated, and contain more quartz, sericite, and epidote within 20 m of the porphyritic quartz monzonite sill. The hanging wall is very sericitic, quartzose, and light colored. Quartz veins within the sill commonly have indistinct margins or merge with patches of fine grained quartz which occur erratically throughout the sill and into wall rock, particularly the hanging wall. Quartz is almost always accompanied by pyrite and abundance of both minerals correlates very well with abundance of gold.

Structure

Structure at the Vulture is fairly simple except for pre-mineral and post-mineral faulting. The Proterozoic sequence dips north 35° and is gently warped. The unconformably overlying Tertiary volcanic rocks dip about 15° east. The porphyritic quartz monzonite sill appears to be conformable to compositional layering and a structural zone marked by what has been called

AGE	SYMBOL	UNIT/THICKNESS (in mine area)	LITHOLOGY	ALTERATION/ MINERALIZATION
Quaternary	Qal	Alluvium (Qal) 0 - >150 m	Alluvium and colluvium derived from the rocks below. Desert pediment and flood wash gravels. Often immature, subgranular, poorly sorted. Includes pC granitic rock from > 13km NW.	Poorly lithified but locally cemented by caliche.
Tertiary	Tv	Volcanics (TV) 0 - ~150 m	Undifferentiated volcanics from gray-brown basalt flows through tan accretionary tuffs and multi-colored agglomerate and pyroclastics of intermediate composition, also trachyte dikes up to 10 m thick (particularly cutting the qp, below)	Generally devitrified and weathered, soft and porous.
Late Cretaceous	Kqp	Quartz porphyry (Kqp) 0 - ~20 m (for sill alone)	Beige, med. to coarse grained granite to quartz monzonite with quartz porphyroblasts (often up to 4mm dia.). Quartz is often pale greenish gray to milky white. Mica is mostly muscovite, some biotite. Occurs as a stock and as an apophysis cutting the mine area as a discontinuous sill-like body. Cut by massive quartz veins.	Includes white quartz veins with coarse euhedral pyrite, galena, chalcopyrite, and trace sphalerite, gold. Granite often silicified and impregnated with disseminated sulfides and gold.
Early Precambrian	p€	Precambrian (pC) > 2,000 m	Undifferentiated metavolcanic and metasedimentary sequence including amphibolitic schists (typically footwall to Vulture lode) quartz-sericite ± chlorite schists (hanging wall to lode) and possible meta-wacke, meta-siltite and meta-quartz-pebble conglomerate.	Generally barren except where in proximity to Kqp (above). Then silicified, sericitized, pyritized and gold mineralized up to 5 m into hanging wall and/or footwall. Displays upper greenschist to lower amphibolite facies, metamorphism.

Figure 3: Schematic stratigraphic section of the immediate Vulture Mine area, and explanation for Figures 4 and 5.

a "quartz pebble conglomerate" lies at its footwall. It is more convincingly interpreted as an intrusive breccia. It consists of subrounded clasts of quartz within a gray-brown, very fine grained, siliceous matrix that is probably silicified gouge.

The major explanation of fitfullness in the Vulture's production history is the post-mineral faulting. Two major sets of faults cut the occurrence into many fragments. The less troublesome are east-trending, south-dipping normal faults, each with displacement of 1 to 10 m. This is reflected in a washboard pattern to the stopes (Figure 5). The more severe problems relate to northwest-striking, steeply northeast-dipping normal faults with 3 to 200 m or greater displacements. About 150 m of Tertiary basalts, ash and agglomerate are preserved in a graben bounded by these faults, just east of the Vulture Mine. These faults are probably related to development of the Basin and Range Province.

Earliest mining between 1863 and 1879 proceeded reasonably smoothly down dip from surface outcrops of bonanza gold veins through to the 650 level. In 1879, however, the Talmadge fault, a Basin and Range normal fault with about 70 m of oblique slip, was encountered and confined mining from 1879 through 1888 to pillar robbing and cleanup until an extension was located across the fault and mined from 1908 to 1918, only to be lost again along the Astor fault at the 950 level. Only minor fault drag ore was found during exploration through the 1550 level. No additional vein extensions have been found, despite efforts in 1930 to 1932 which included some drilling and shaft sinking further east into the next suspected fault block.

Current Activity

Since 1984 the Vulture property, consisting of 14 patented claims and 460 unpatented lode and placer claims (about 23 km^2) has been under lease to A.F. Budge (Mining) Limited. The remaining tailings and the near surface, low grade material adjacent to the old pits have been evaluated by drilling. There are about 200,000 t of tails grading 1.3 g/t. The open-pitable, hard rock reserves are similar grade. There is also some limited placer potential with coarse and fine gold in the pediment gravels surrounding the Vulture Mine. Efforts to locate additional gold reserves are continuing.

Acknowledgments. The original opportunity to study the Vulture and share the results was provided by the late Ben F. Dickerson, III. Carole A. O'Brien is now representative of A.F. Budge on this and other projects. To both of them I owe gratitude for continued support of my work and permission to present these data. Geological views by many a visitor to the Vulture have helped immensely. That includes Stephen J. Reynolds and William A. Rehrig in particular. Most notably I thank Robert W. Hodder for his willingness to edit this paper and his ongoing assistance on the project.

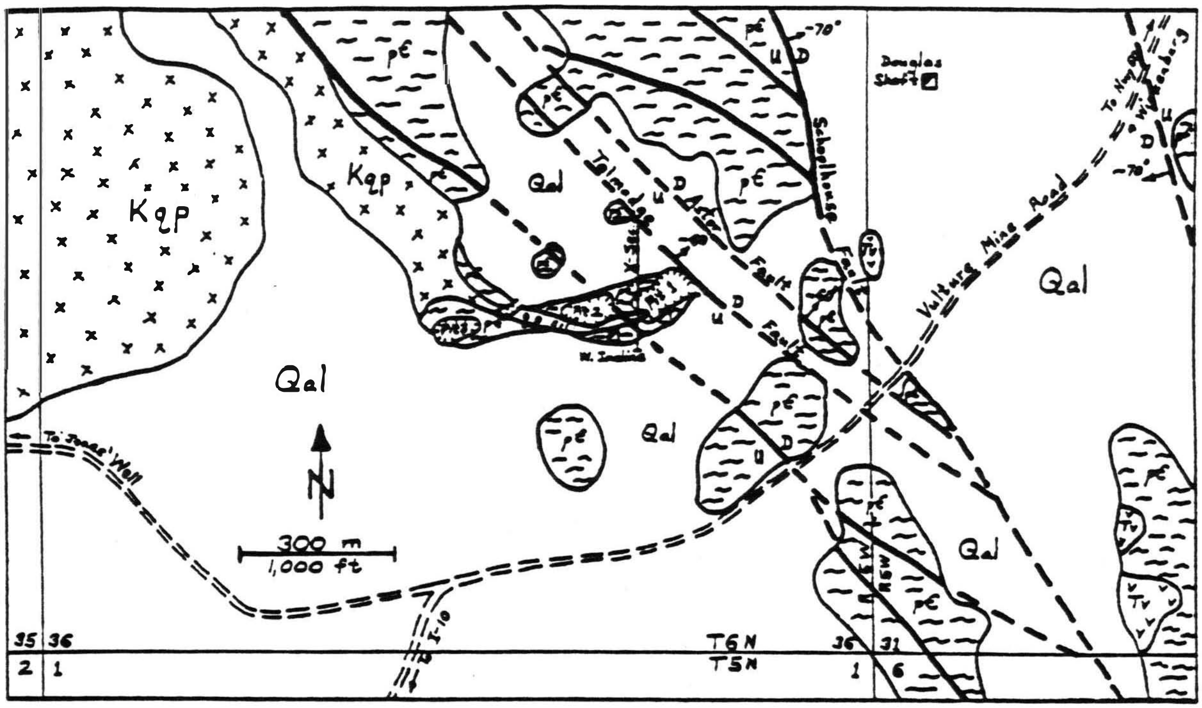

Figure 4: Sketch geologic map of the immediate Vulture Mine vicinity. See Figure 3 for geologic explanation. Note mining centered around apophysis of Kqp into pЄ sequence and cutting of the lode by NW-trending normal faults.

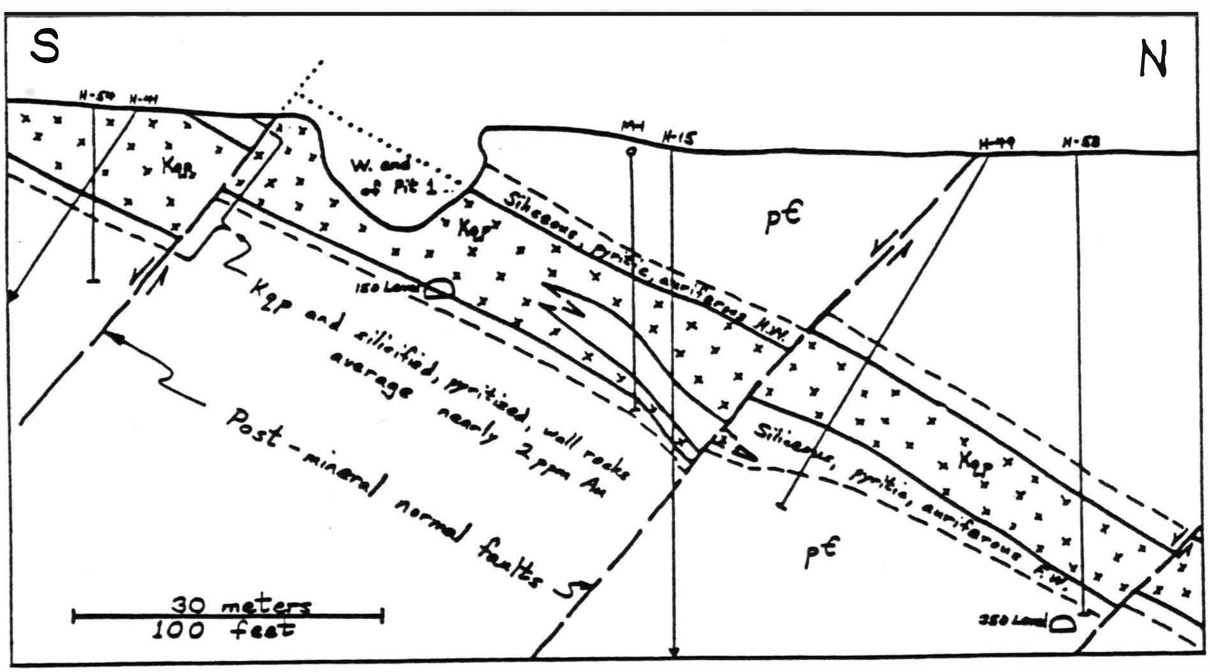

Figure 5: Vertical cross section, looking west. Note north-dipping Kqp sill and its silicified, auriferous envelope. Post-mineral faults offset lode.

References.

Dickie, Ernest R., 1942, "The Vulture Mine," Denver Equipment Co., Bull. No. M7-B13, 8 p.

Krueger, H.W., 1987, Letter communication of whole rock and muscovite separate isotope analyses and age determination, Aug. 31, 1987.

Metzger, O.H., 1938, "Gold Mining and Milling in the Wickenburg Area, Maricopa and Yavapai Counties, Arizona," US Bureau of Mines I.C. 6991, 78 p.

Rehrig, W.A., Shafiquallah, M., and Damon, P.E., 1980, "Geochronology, Geology, and Listric Normal Faulting of the Vulture Mountains, Maricopa County, Arizona," Ariz. Geol. Soc. Digest, Vol. 12, p. 89-110.

Smith, Duane A., 1972, "The Vulture Mine; Arizona's Golden Mirage," Arizona and the West, Vol. XIV, No. 3, Autumn, 1972, p. 231-252.

Tenney, James Brand, 1927-1929, "History of Mining in Arizona," Unpublished report to Ariz. Bur. Mines, p. 396-401.

Thompson, Arthur Perry, 1930, "Report on Vulture Mine, Maricopa Co., Arizona," Private, unpublished report for The Vulture Mining and Milling Company, Sept. 11, 1930, 37 p. plus maps, sections.

THE
Tonopah-Belmont Mine
MARICOPA COUNTY, ARIZONA

George B. Allen
Route 6, Box 32
Golden, Colorado 80403

William Hunt
10350 Andover Avenue
Sun City, Arizona 85351

The Tonopah-Belmont mine is a micromounter's paradise. An uncommon suite of base-metal oxides, carbonates, silicates, phosphates, arsenates, vanadates, sulfates, molybdates and chromates can be found at the mine. The abundance of species makes it an ideal introduction to the many mineral occurrences of the Big Horn Mountains.

INTRODUCTION

The Tonopah-Belmont mine is the second largest producer of metals in the aerially extensive Osborn Ag-Au district of Maricopa County in west-central Arizona. The primary property in the district is the U.S. mine, where a 1.4-million-ton orebody is now under production (Kerr, Dawson and associates, 1984). Mineralogically significant properties in the Osborn district include the Pack Rat, Moon Anchor and the Potter Cramer claims. The Pack Rat is the co-type locality for hemihedrite (Williams and Anthony, 1968), and the Potter Cramer claim is the type locality for wickenburgite. The Tonopah-Belmont mine is located in the southwest quarter of section 36, T4N, R7W, at the boundary between the Big Horn and Belmont Mountains of west-central Arizona. The mine is approximately 40 km south of Wickenburg. To get there drive south out of Wickenburg on the Vulture Mine road until the Tonopah-Aguila Road is encountered. From there continue south along a poorly maintained dirt road until Belmont Mountain, the host for the Tonopah-Belmont mine is in view. Then follow the obvious spurs toward the lone peak.

HISTORY

There are two conflicting accounts of the discovery of mineralization at Belmont Mountain. Ramsing (1957) reports the occurrence was discovered in 1904 and subsequently named the Belmont McNeal. Wilson (1967) reports that the discovery was made by George Dillar in 1907. In any event, the claims were sold in 1926 to the Tonopah-Belmont Company of Nevada which renamed the claims the Tonopah-Belmont mine. The Tonopah-Belmont company sank a 155-meter shaft and built a 50-ton bulk flotation plant (Ramsing, 1957). The mine was operated from that time until the Depression, at which time low metal prices forced closure. During the closure, some time between 1937 and 1939, a mine fire erupted. The rising hot gases from the fire traveled to the main adit level and along it to the old shaft which acted as a chimney. During the fire the roof of the tunnel melted to slag and some of the minerals were altered to a depth of 8 cm.

From 1941 until 1947 Ernest Dickie owned the mine. He extracted the high-grade pillars and reachable ore on each side of the shaft. Consequently the stopes caved up to the adit level and the shaft timbers collapsed.

The Arizona Bureau of Geology and Mineral Technology files report total historic production of 450,000 kg of copper, 4250 kg of silver and 240 kg of gold. Present mine workings consist of two steep inclines on the north side of Belmont Mountain, a 20-meter shaft on the south side which connects to a haulage adit, and numerous cuts and trenches which circumscribe Belmont Mountain.

GEOLOGY

West-central Arizona is a region of varied, highly deformed Proterozoic, Mesozoic and Tertiary crystalline and (rare) sedimentary rocks. Our understanding of the geologic framework for this region is a product of a renaissance of regional and detailed geologic studies of the past seven years (Reynolds, 1980; Rehrig and Reynolds, 1980;

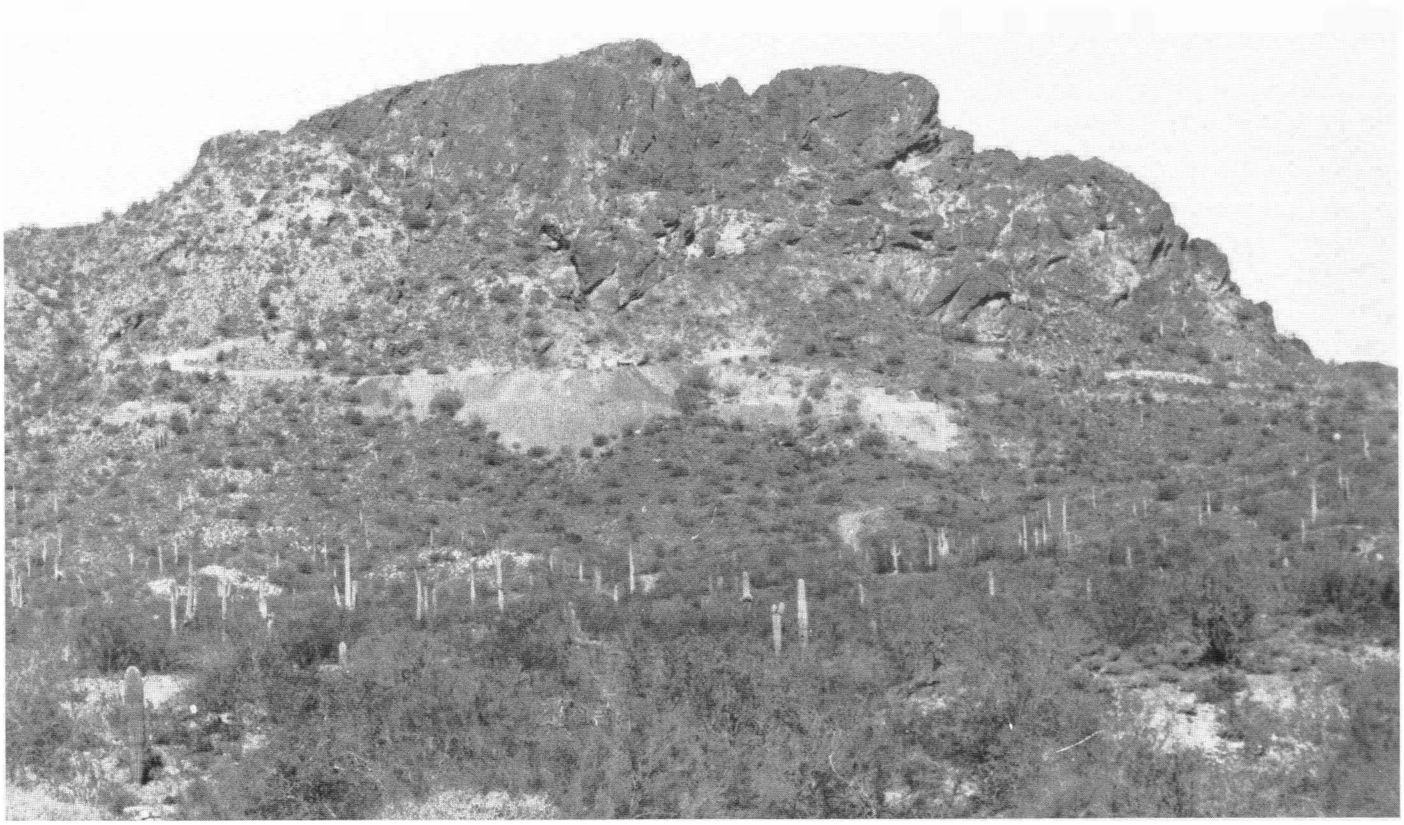

Figure 1. **Belmont Mountain; mine dumps at center.**

Rehrig *et al.*, 1980; Reynolds and Spencer, 1985; Hardey, 1984; Capps *et al.*, 1985a and 1985b). These works have established that the Harquahala Mountains to the west of the Big Horn Mountains and the White Tank Mountains to the southeast of the Belmont Mountains are metamorphic core complexes, raised segments of the middle crust which are bounded by low-angle normal faults. These faults are major structural discontinuities and are termed detachment faults. A detachment fault probably underlies the Big Horn and Belmont Mountains. Movement along the detachment fault and related faults in the upper plate is probably the cause of widespread tilting of the Tertiary rocks throughout the region.

Three major lithologic terrains crop out in the Big Horn and Belmont Mountains: (1) Proterozoic amphibolite, phyllite, shist, gneiss and granite, (2) Mesozoic monzonite to diorite intrusives, and (3) Cenozoic mafic and silicic volcanic rocks and rare clastic sedimentary rocks. The entire Big Horn-Belmont Mountains area is cut by and tilted along north to northwest-trending low to moderate-angle normal faults that in places are cut by east to northeast-trending strike-slip faults. Four mineral districts occur in the Big Horn-Belmont ranges: the Tiger Wash barite-fluorite district, the Big Horn gold district, the Aguila manganese district, and the Osborne silver-gold-base metal district. The Big Horn district is thought to be Laramide (early Tertiary) in age (Allen 1985). The other three districts are likely to be mid-Tertiary in age and of an interrelated genesis (Allen 1985).

The geologic setting of the Tonopah-Belmont mine is moderately complex. The mine is hosted in a structurally isolated block of Miocene rocks that are surrounded by Proterozoic phyllite on all sides except to the southeast where the Miocene block is in fault contact with mid-Tertiary Belmont granite (Capps *et al.*, 1985a). The oldest rocks in the mine are Proterozoic phyllites, which are laminated steel-gray when fresh and brown to tan when weathered. Typically the phyllite is fine-grained and consists of 10% quartz and 90% muscovite. The phyllite generally strikes northeast with highly varied dips that are generally steep. Unconformably overlying the phyllite is a 26 to 40-meter sequence of mid-Tertiary volcanic and volcaniclastic rocks.

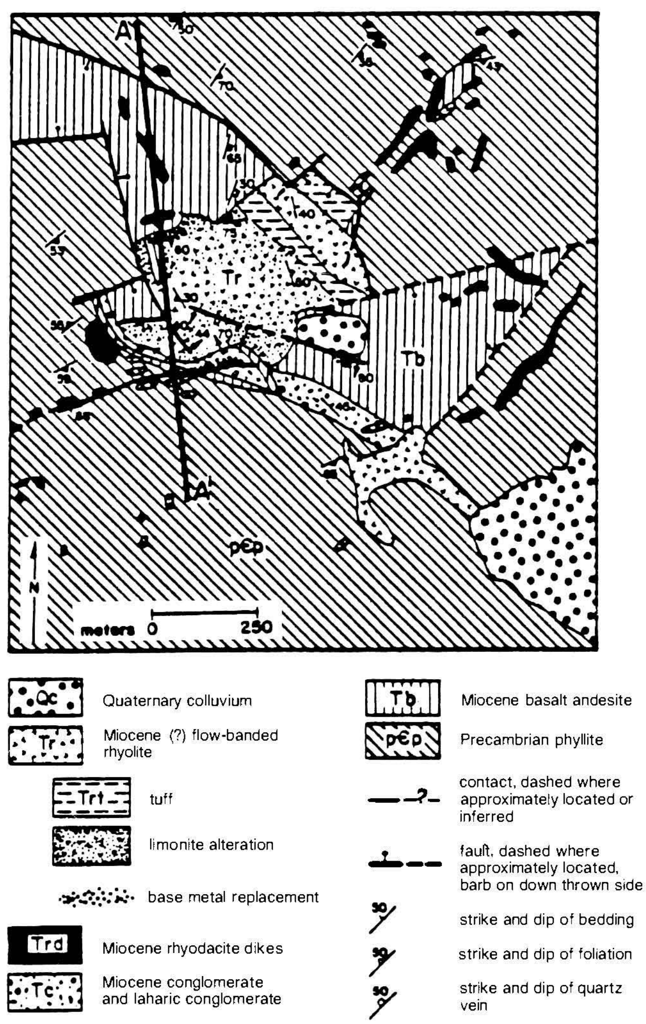

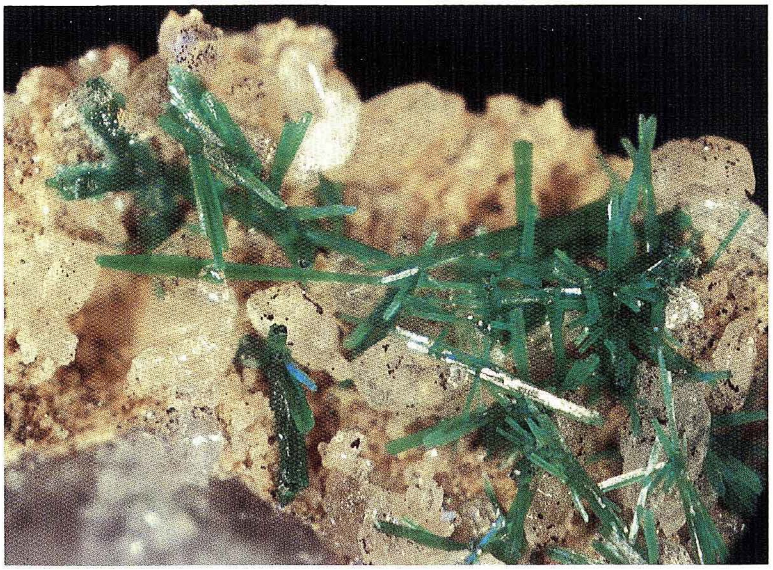

Clockwise from left:
Figure 2. **Wulfenite crystal, 3 mm.**
Figure 3. **Brochantite crystals to 2.6 mm.**
Figure 4. **Willemite sprays, 1.3 mm, on brochantite.**
Figure 5. **Caledonite crystals, 0.6 mm.**
Figure 6. **Linarite crystals, 1 mm.**
Figure 7. **Vanadinite crystal group, 3.5 mm, with descloizite.**
Figure 8. **Rosasite sphere, 3.5 mm.**
Figure 9. **Molybdofornacite crystals, 1 mm.**
All photos by William Hunt.

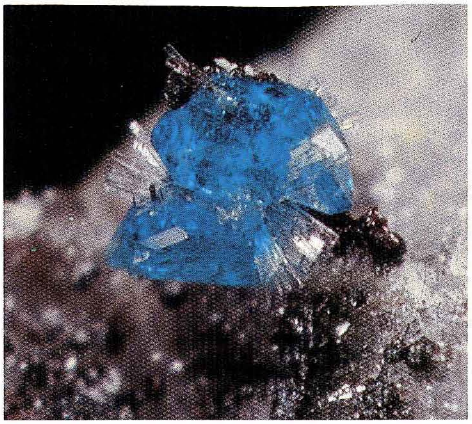

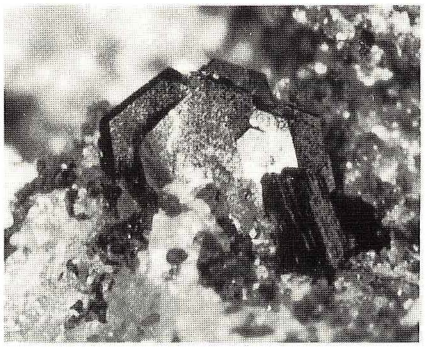

Figure 10. (above) **Plumbojarosite, 1 mm.**

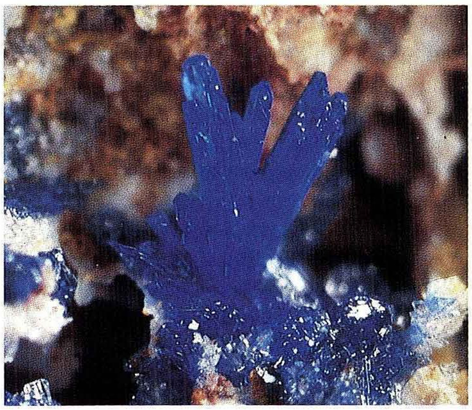

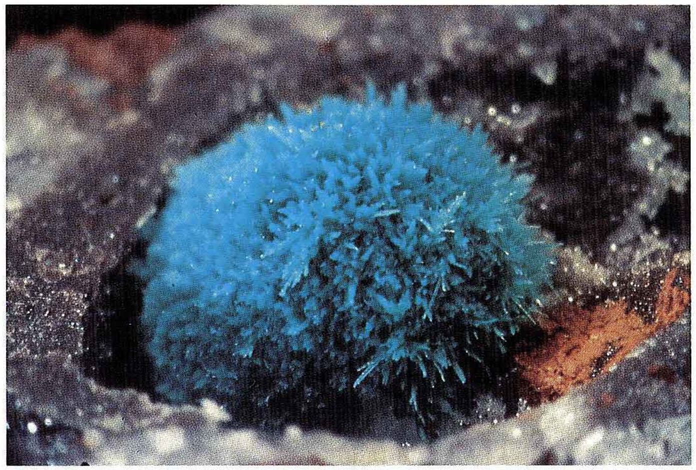

From bottom to top the sequence is, (1) 10 to 13-meter basalt flow, (2) 12 to 18 meters of dark gray to green laharic sedimentary rock that has abundant phyllite clasts, (3) a thin flow of basalt, (4) 31 meters of rhyolite and tuff along with a flow-foliated rhyolite intrusive named the Morning Star Rhyolite, and (5) rhyodacite dikes which intrude each of the units in the section.

The major structure of the area is a N40°W-striking, southwest-dipping, low-angle fault that drops out from 500 meters northwest of Belmont Mountain for 2 km to the southeast where the fault changes to a north strike and a west dip (Capps *et al.*, 1985a). The low-angle fault juxtaposes moderately northeast-dipping rocks in the hanging wall against the Proterozoic phyllite. This major fault is offset by east-northeast-striking cross faults that are loci of mineralization. The N75°E to N65°E-striking, southeast-dipping normal faults are the localizing structures of the south and north Tonopah-Belmont veins. A N20°W-striking, northeast-dipping normal fault cuts off both veins on the west end of Belmont Mountain. On the east end of Belmont Mountain the northern vein appears to die out whereas the southern vein is offset by a N70°W-striking, southwest-dipping normal fault. The structural relationships suggest that mineralization occurred during low-angle faulting, but did not continue after tectonism. The fact that the veins were cut off by a fault at the 130-meter level (AZBGMT Files) supports a syntectonism age of mineralization.

The north vein trends N70°E and dips 60°SW. It is exposed along strike for 120 meters, and ranges in thickness from 1 to 12 meters. The vein is mostly banded milky quartz with lesser copper carbonates as fracture fillings in a fault zone. The encompassing fault zone is at the contact between the basal Morning Star rhyolite flow or intrusion and a basalt flow. Whether the Morning Star unit is an intrusion or a flow determines the exact nature of the localizing contact. The character of this contact is obscured by the highly varied vertical flow foliations in the rhyolite, the absence of demonstrable offset on the north and south sides of the outcrop, and the unclear nature of the contact between the Belmont Mountain massif and the Morning Star tuff to the northeast.

The south vein trends N75°E, dips 80°NW, extends for 150 meters and varies from 2 to 10 meters in thickness. The south vein is localized at the contact of the basal laharic unit with the lowermost basalt, both of which are in the hanging wall of the steeply dipping normal fault of small displacement. This vein consists mostly of milky quartz breccia and replacement textures in contrast to the banded fracture-filling appearance of the northern vein.

Fluid inclusion studies were initiated with specimens from the Tonopah-Belmont veins, but a paucity of suitable calcite or quartz prevented acquisition of thermometric or compositional data. Studies on specimens from the geologically similar U.S. mine, however, were successful. Homogenization temperatures and freezing point depressions, which indicate the temperature and salinity of ore forming fluids, suggest temperatures and salinities ranging from 190° to 225° C and 8 to 14% total salt (Allen 1985).

MINERALS

Even though 46 minerals have been found at the Tonopah-Belmont mine, the micromount collecting potential has only begun to be probed. The fact that most of the underground workings are inaccessible in no way detracts from the collecting possibilities. Each of the identified species has come from the dump samples and all but three are found in euhedral microcrystals.

The large dump below the adit contains much barren rock but, with some searching, mineralized material can be found. Fortunately the small dump above the adit mostly consists of mineralized rock.

Outcrops peripheral to the old workings include 5 to 50-cm mineral veins that were ignored by the early miners. These small seams afford good specimens for those willing to break bedrock.

Table 1 lists and describes minerals found to date and their asso-

***Table 1.* Minerals found at the Tonopah-Belmont mine**

Species/Composition	Habit and Associations	Location
Anglesite $PbSO_4$	Mainly as a gray rind surrounding relict galena which is, in turn, surrounded by cerussite. There is a second generation of white, poorly crystallized material associated with linarite, brochantite, caledonite and leadhillite.	1, 2, 3
Aurichalcite $(Zn,Cu)_5(CO_3)_2(OH)_6$	Found sparingly as pearly blue-green blades with malachite and rosasite.	1, 2
Azurite $Cu_3(CO_3)_2(OH)_2$	Represented by malachite pseudomorphs after azurite to 6 mm.	8
Barite $BaSO_4$	Mainly as opaque white laths in quartz; also as brilliant, transparent, euhedral microcrystals to 1.5 mm, with descloizite.	1, 2
Brochantite $Cu_4(SO_4)(OH)_6$	Bright green microcrystals, acicular to prismatic, with linarite, caledonite, leadhillite and anglesite.	1, 2, 3
Calcite $CaCO_3$	Rare, opaque white rhombohedrons on willemite with hydrozincite.	1
Caledonite $Pb_5Cu_2(CO_3)(SO_4)_3(OH)_6$	Pale blue crystals to 2 mm with linarite, brochantite, leadhillite and anglesite	1, 2, 3
Cerussite $PbCO_3$	White crystalline crusts on anglesite rinds surrounding galena cores, also transparent euhedral crystals to 5 mm with brochantite.	1, 2
Chalcophanite $(Zn,Fe,Mn)Mn_3O_7{\cdot}3H_2O$	Found only in peripheral quartz veins outside the orebody, as striated rhombohedrons (with a brilliant *c* face) to 1.5 mm, with cryptomelane.	3
Chalcopyrite $CuFeS_2$	Weathered remnants, sometimes covered by covellite.	1, 2, 3
Chlorargyrite AgCl	Seen in a fragment of high grade ore with gold and willemite.	4
Chrysocolla $(Cu,Al)_2H_2Si_2O_5(OH)_4{\cdot}nH_2O$	Cavity fillings and pseudomorphs after an acicular mineral.	1, 2, 3, 5
Coronadite $Pb(Mn^{+4},Mn^{+2})_8O_{16}$	Pitch-like botryoidal incrustations with radial structure.	4

Covellite CuS	Iridescent purple coatings on chalcopyrite and sphalerite.	1, 2
Creaseyite $Pb_2Cu_2Fe_2Si_5O_{17}\cdot 6H_2O$	Pale green acicular crystals to 0.8 mm with plumbojarosite.	5
Cryptomelane $K(Mn^{+4},Mn^{+2})_8O_{16}$	Acicular crystals with chalcophanite, in peripheral quartz veins.	3
Descloizite $PbZn(VO_4)(OH)$	Sparingly as pale to dark brown crystals to 1.4 mm on barite and vanadite.	1, 2, 7
Epidote $Ca_2(Al,Fe)_3(SiO_4)_3(OH)$	Pale green microcrystals in basalt.	7
Galena PbS	Corroded cores mainly, but also in one small cavity as 0.1-mm cubes.	2
Goethite $FeO(OH)$	Thin iridescent to yellow velvety coatings.	1, 2, 3, 5
Gold Au	In high grade ore with gypsum.	4
Gypsum $CaSO_4\cdot 2H_2O$	"Ram's horn" habit.	4
Hematite Fe_2O_3	Bright red scales and botryoidal masses.	1, 8
Hemimorphite $Zn_4Si_2O_7(OH)_2\cdot H_2O$	Locally abundant as rosettes of 5-mm crystals with most of the secondary minerals.	1, 2, 3
Hydrozincite $Zn_5(CO_3)_2(OH)_6$	Pearly, matted crystals on one specimen with calcite and willemite.	1
Jarosite $KFe_3(SO_4)_2(OH)_6$	Pale to dark brown tabular crystals to 2 mm.	2, 5
Leadhillite $Pb_4(SO_4)(CO_3)_2(OH)_2$	Subhedral crystal crusts and also surface alteration coatings on cerussite, intimately associated with caledonite and linarite.	2, 3
Linarite $PbCu(SO_4)(OH)_2$	Subhedral crystal groups; occasional euhedral transparent blue crystals to 1.5 mm with brochantite, caledonite, anglesite and leadhillite.	1, 2, 3
Malachite $Cu_2(CO_3)(OH)_2$	Sprays of acicular crystals with rosasite; less abundant than brochantite.	2, 8
Mimetite $Pb_5(AsO_4)_3Cl$	Sparingly as opaque, yellow 0.5-mm pyramidal crystals with wulfenite, fornacite and willemite.	2, 3, 7
Minium Pb_3O_4	Bright red pseudomorphs after cerussite on willemite.	
Molybdofornacite $Pb_2Cu[(As,P)O_4][(Mo,Cr)O_4](OH)$	Pale to dark green euhedral crystals to 1.2 mm, and rosettes of subhedral microcrystals with willemite, wulfenite and pyromorphite.	2, 3, 6
Murdochite $PbCu_6O_{8-x}(Cl,Br)_{2x}$	Brilliant cuboctahedrons in a single willemite pocket.	1
Plattnerite PbO_2	Tufts of brilliant black acicular crystals in oxide ore.	1
Plumbojarosite $PbFe_6(SO_4)_4(OH)_{12}$	Pale to dark brown hexagonal scales, some coated by creaseyite, at one location.	5
Pyrite FeS	Represented only by pseudomorphs.	8
Pyromorphite $Pb_5(PO_4)_3Cl$	Colorless to pale green prismatic crystals, some tapered, to 2.5 mm with fornacite, vauquelinite and wulfenite.	2, 3, 4, 6
Quartz SiO_2	Mainly a gangue mineral but also as druses on secondary minerals.	1, 2, 3, 5, 6
Rosasite $(Cu,Zn)_2(CO_3)(OH)_2$	Balls of acicular crystals to 4 mm; blue to green.	1, 2, 3
Sphalerite ZnS	Only as remnants in weathered ore, sometimes coated with covellite	1
Sulfur S	On one specimen with gypsum and gold.	5
Vanadinite $Pb_5(VO_4)_3Cl$	Orange to red prisms to 5 mm, some with full or partial pyramidal terminations. Scarce on the south side of the mountain but plentiful on the north.	3, 6, 7
Vauquelinite $Pb_2Cu(CrO_4)(PO_4)(OH)$	Greenish brown to brown crystals to 2 mm in groups with willemite, wulfenite and pyromorphite. Much rarer than fornacite.	2, 3, 6
Willemite Zn_2SiO_4	Very plentiful as transparent, prismatic crystals to 3 mm, some tapered. Also as sprays of white acicular crystals.	1, 2, 3
Wulfenite $PbMoO_4$	Pale to dark orange tabular crystals to 8 mm with pyromorphite, mimetite, willemite, fornacite and vauquelinite.	2, 3
Zircon $ZrSiO_4$	Dark brown crystals, less than 0.05 mm, in andesite.	1

ciations. The numbers at the right-hand column are keyed to the list directly below and indicate where the minerals are found.

1—Large dump below the adit
2—Old dump above the adit
3—Outcrops above the old workings
4—Underground on the adit level
5—Dump on the north side of the mountain
6—Outcrops on the north side of the mountain
7—Prospects on the north side of the mountain
8—Prospects on the east side of the mountain

PARAGENESIS

The sequence of crystallization of the major phases, from early to late, is: sphalerite-pyrite-chalcopyrite-galena as primary sulfides plus gold; quartz as primary gangue. Aurichalcite, smithsonite, azurite, malachite and jarosite are secondary minerals. A detailed paragenitic study based on microcrystals indicates early pyrite-galena-chalcopyrite-sphalerite-gold-hematite-native silver-barite and quartz. A second generation of minerals include coronadite, goethite, covellite, anglesite, cerussite, brochantite, caledonite, leadhillite, linarite, aurichalcite, malachite, rosasite, chrysocolla, hemimorphite, pyromorphite, vauquelenite, molybdofornacite, wulfenite, mimetite, descloizite, jarosite and chlorargyrite. The final generation includes minor calcite and hydrozincite along with more abundant minium and gypsum.

The chemistry of the paragenesis suggests some overall patterns:

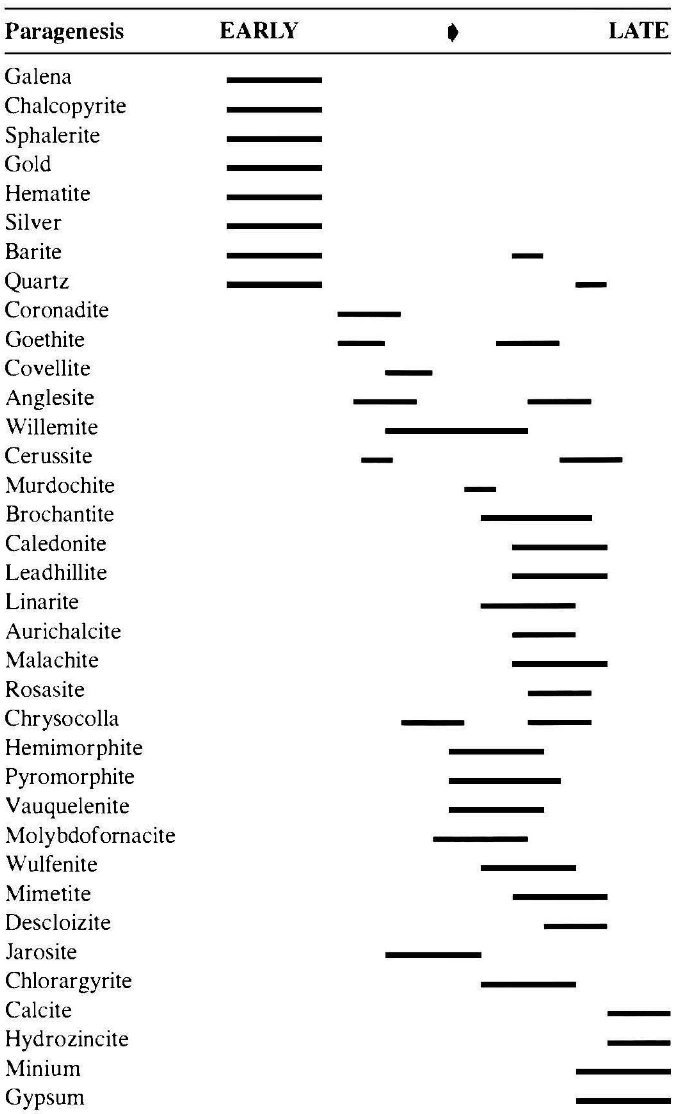

primary introduction of metals and sulfur resulting in an early sulfur-native element stability phase with barite-quartz gangue; a diverse episode of oxide, sulfate, carbonate and lesser silicate stability; an episode introducing the heavy elements phosphorus, arsenic, molybdenum and vanadium; and a final episode with oxide-sulfate and lesser carbonate stability.

As stated previously, complex variations in the water table and limited accessibility of the lower workings have prevented determination of a definitive paragenesis. The paragenetic chart below was worked out using only specimens from locations 1, 2 and 4. These locations are all on the same zone of mineralization.

DISCUSSION

The stratigraphic, structural and geochronological framework established by Capps *et al.* (1985 a and b), combined with the district-wide fluid inclusion data of Allen (1985) and the paragenetic data presented here, suggests an integrated geologic history for the Tonopah-Belmont mine mineral occurrence.

Mineralization at Belmont Mountain occurred between 21 and 16 million years ago during a period of widespread volcanism and block tilting. The lower age is constrained by radiometric determinations on biotite from the Morning Star Rhyolite host rock. The upper age is constrained by the age of the fault that cuts the Tonopah-Belmont vein at its eastern end. This fault is of a generation that regionally cuts 16 m.y. basalt. The mineralizing fluids that formed the Tonopah-Belmont deposit were probably dilute brines, having temperatures of 170° to 230° C. The range-wide similarity of fluid inclusions and widespread occurrence of potassium-metasomatized rocks (Allen 1985) suggests that these fluids were regional in distribution and manifest themselves only where local structures connect to deeper seated conduits. The mineralization at the Tonopah-Belmont mine may be a consequence of fluids rising along the conduits of the rhyolite vent at Belmont Mountain, and subsequent cooling and dilution as meteoric waters mixed with the hydrothermal fluids (Allen, 1985). The fluid inclusion data from the U.S. mine permits cooling and dilution as a mechanism of mineral precipitation.

The paragenetic sequence outlined combined with the historic record of a mine fire suggest five mineral-forming episodes: (1) an early base-metal sulfide, native precious metal, quartz, barite hypogene episode which was caused by dilution and cooling of hydrothermal waters by meteoric waters; (2) a series of oxide-silicate-hydroxide-carbonate-forming episodes as a consequence of fluctuating watertable levels; (3) a possible second phase of epithermally introduced elements expressed by the appearance of phosphates, arsenates, molybdates and vanadates; (4) a final dropping of the watertable and seasonal formation of calcite, hydrozincite, minium and gypsum as a result of descending perennial waters; and (5) an episode of high-temperature low-pressure mineral stability resulting from the late 1930's mine fire.

ACKNOWLEDGMENTS

Financial support for the geology section of this paper was provided by the Arizona Bureau of Geology and Mineral Technology as part of a 1985 range-wide study of the geology and mineral occurrences of the Big Horn and Belmont Mountains.

BIBLIOGRAPHY

ALLEN, G. B. (1985) Economic Geology of the Big Horn Mountains of West-Central Arizona. Arizona Bureau of Geology and Mineral Technology Open File 85-17, 140 p.

ANTHONY, J. W., WILLIAMS, S. A., and BIDEAUX, R. A. (1977) *Mineralogy of Arizona*. University of Arizona Press, Tucson, 255 p.

BEANE, R. E., and WILKINS, J. Jr. (1985) Thermal Regimes in the Detachment Fault Environment as Deduced From Fluid Inclusions (abs). Lunar and Planetary Science Conference, Sedona, Arizona.

(continued on page 207)

Notes from the Editor
(Continued from page 138)

with which the user may call up mineral formulas by name, or a list of minerals and formulas containing specified elements. It was being demonstrated in February at the Tucson Show and everyone who saw it was satisfactorily impressed. The program is called MINCAT; it consists of two diskettes and a manual, available for $99.99 from PC Geological Software Systems (Dept. of Earth Sciences, UNO, Lakefront, New Orleans 70148, Tel: (504) 286-6791).

Tonopah-Belmont mine
(Continued from page 144)

CAPPS, R. C., REYNOLDS, S. J., STIMAC, J. A., KORTMEIER, C. P., ALLEN, G. B., and SCOTT, E. A. (1985b) Preliminary Geologic Map of the Central Big Horn Mountains, West Central Arizona. Arizona Bureau of Geology and Mineralogy Technology Open File 85-16.

HARDEY, J. J. Jr. (1984) The Structural Geology, Tectonics and Metamorphic Geology of the Arrastre Gulch Window, South Central Harquahala Mountains, Maricopa County Arizona. M.S. Thesis, Northern Arizona University, Flagstaff, 79 p.

KERR, DAWSON and ASSOCIATES (1984) Report on the Big Horn property, Maricopa County, Arizona. Roddy Resources, Vancouver, B.C., 33 p.

RAMSING, F. C. (1957) Geologic Report on the Tonopah-Belmont Mine. Private report, 3 p.

REHRIG, W. A., and REYNOLDS, S. J. (1980) Geologic and geochronologic reconnaissace of a northwest-trending zone of metamorphic core complexes in southern and western Arizona. *in* Crittenden, M. D. Jr., *et al.* (eds.). Corderilleran metamorphic core complexes. *Geologic Society of America Memoir*, **153**, 131–157.

REHRIG, W. A., SHAFIQULLAH, M., and DAMON, P. E. (1980) Geochronology geology and listric normal faulting of the Vulture Mountains, Maricopa County, Arizona. *Arizona Geological Society Digest*, **12**, 89–110.

REYNOLDS, S. J. (1980) Geologic framework of west-central Arizona. *Arizona Geological Society Digest*, **12**, 1–14.

REYNOLDS, S. J. (1982) Multiple Deformation in the Harcuvar and Harquahala Mountains West-central Arizona. *in* Frost, E. G., and Martin, D. L., eds. *Mesozoic-Cenozoic Tectonic Evolution of the Colorado River Region*. San Diego, Cordilleran Publishers, 137–142.

REYNOLDS, S. J., CAPPS, R. C., KORTEMEIER, C. P., SCOTT, E. A., STIMAC, J. A., and ALLEN, G. B. (1985) Preliminary Geologic Map of the Belmont and eastern Big Horn Mountains, West Central Arizona. Arizona Bureau of Geology and Mineral Technology Open File 85-15, 25 p.

REYNOLDS, S. J., and SPENCER, J. E. (1985) Evidence for large-scale transport on the Bullard detachment fault, west-central Arizona. *Geology*, **13**, no. 5, 353–357.

SILLIMAN, B. (1866) On some mining districts of Arizona near the Rio Colorado, with remarks on the climate, etc. *American Journal of Science*, **41**, second series, 289–308.

WILKINS, J. Jr., and HEIDRICK, T. L. (1982) Base and precious metal mineralization related to low-angle tectonic features in the Whillis Mountains, California, and Buckskin Mountains, Arizona. *in* Frost, E. G., and Martin, D. L., eds. *Mesozoic-Cenozoic Tectonic Evolution of the Colorado River Region*. San Diego, Cordilleran Publishers, 182–204.

WILLIAMS, S. A. (1968) Wickenburgite, a new mineral from Arizona. *American Mineralogist*, **53**, 1433–1438.

WILLIAMS, S. A., and ANTHONY, J. W. (1980) Hemihedrite, a new mineral from Arizona. (abs) *American Mineralogist*, **53**, 1.

WILLIAMS, S. A., and ANTHONY, J. W. (1968) Hemihedrite, a new mineral from Arizona. *American Mineralogist*, **55**, 1088–1102.

WILLIAMS, S. A., and BIDEAUX, R. A. (1974) Creaseyite, a new mineral from Arizona and Sonora Mexico. *Mineralogical Magazine*, **40**, 227–231.

ECONOMIC GEOLOGY
OF THE BIG HORN MOUNTAINS
OF WEST-CENTRAL ARIZONA

by

George B. Allen

December 15, 1985

Arizona Bureau of Geology and Mineral Technology
Open-File Report 85-17

PREFACE

This study of the economic geology of the Big Horn Mountains was completed by George Allen in partial fullfillment of the requirements for an M.S. degree at the Department of Geosciences, University of Arizona. The study is intended to complement recent geologic mapping of the Big Horn and Belmont Mountains as part of the Cooperative Geologic Mapping Program (COGEOMAP), funded jointly by the Arizona Bureau of Geology and Mineral Technology and the U.S. Geological Survey. Preliminary geologic maps of the Belmont and eastern Big Horn Mountains have been released as AZBGMT Open-File Report 85-14 (Capps and others, 1985) and will be included in a Bureau Bulletin on the geology and mineral resources of the area (Reynolds and others, in prep.). This contribution by George Allen will be included as a chapter in the forthcoming bulletin, following review and editing by Bureau staff. The availability of this bulletin will be announced in a future issue of Fieldnotes, the Bureau's quarterly publication.

Dr. Stephen J. Reynolds
COGEOMAP Coordinator
Arizona Bureau of Geology
and Mineral Technology

LIST OF TABLES

ACKNOWLEDGMENTS

Financial support for this project was provided by the Arizona Bureau of Geology and Mineral Technology. Dr. Stephen J. Reynolds of the Bureau provided encouragement and guidance throughout the course of this study. Conversations with Chris Capps and Dr. Joaquin Ruiz greatly aided progress. Reviews by Dr. Joaquin Ruiz, Dr. Paul E. Damon, and especially, Dr. Stephen J. Reynolds greatly improved the manuscript. TRICON Mining Ltd. and Nicor Inc. provided geochemical assays. Parry Willard of TRICON provided a geologic map of the Pump Mine. Joy Mehulka of the Bureau drafted all of the figures.

LIST OF ILLUSTRATIONS

TABLE OF CONTENTS

ABSTRACT

The Big Horn Mountains are a geologically complex range that extends over 500 square km in west-central Arizona. Three major lithologic terranes outcrop: (1) Proterozoic amphibolite, phyllite, schists, gneiss, and granite; (2) Mesozoic monzonite to diorite intrusives; and (3) Cenozoic mafic to silicic volcanic rocks and clastic rocks. The entire area is in the upper plate of a detachment fault and, consequently, contains many low- to high-angle normal faults.

Each lithologic terrane has its associated mineral occurrences. The Big Horn district is exclusively hosted in the pre-Tertiary terrane. Most of its mineral occurrences are spatially related to the Late Cretaceous intrusive rocks. One occurrence, the Pump Mine, may be a metamorphic secretion deposit, and therfore, would be middle Proterozoic.

The vast majority of the mineral occurrences in the Big Horn Mountains are middle Tertiary in age and occur in three districts: the Tiger Wash barite-fluorite district; the Aguila manganese district; and the Osborne base and precious metal district. Fluid inclusions from Tiger Wash fluorite (T_h 120 to 210° C, NaCl wt. equivalent 17 to 18 percent not corrected for CO_2) and nearby detachment-fault- hosted Harquahala district fluorite (T_h 150 to 230° C., NaCl wt. equivalent 15.5 to 20 percent not corrected for CO_2) suggest cooling and dilution of fluids as they are presumed to evolve from the detachment fault into the upper plate. Mass-balance calculations suggest that the proposed evolution of fluids is sufficient to account for the observed tonnage of barite and fluorite. The Tiger Wash occurrences grade directly into calcite-gangue-dominated manganese oxides of the Aguila district. A wide

range of homogenization temperatures (T_h 200 to 370° C.), an absence of CO_2 and low salinities (NaCl wt. equivalent 1 to 2 percent) in the Aguila district calcite-hosted fluid inclusions argue for distillation of fluids during boiling or boiling of non saline-meteoric waters. Mass-balance calculations modeling the evolution of Ca and Mn during potassium metasomatism of plagioclase in basalt suggest that little if any influx of these cations is necessary to form the calcite-dominated manganese oxide tonnage observed. The Aguila district grades directly to the east into the base-metal and precious-metal occurrences of the Osborne district. Preliminary data describing geological settings, fluid inclusions, and geochemistry suggest that the Osborne district has a continuum between gold-rich to silver-rich epithermal occurrences. The gold-rich systems have dominantly quartz gangue, with or without fluorite, and are hosted in a variety of rocks, but are proximal to Precambrian phyllite or mid-Tertiary rhyolite. Fluid inclusions from two occurrences representative of the gold-rich systems spread across a minor range (T_h 190 to 230° C., NaCl wt. equivalent 17 to 23 percent not corrected for CO_2). Dilution of highly saline fluids is the inferred mechanism for precipitation of gold in the gold-quartz systems.

The silver-rich systems have dominantly calcite gangue with or without quartz, and are hosted in mid-Tertiary basalt. Calcite fluid inclusions from a representative high-silver occurrence display a wide range of homogenization temperatures and salinities (T_h 120 to 370° C., NaCl wt. equivalent 7 to 23 percent). Boiling and consequent neutralization of acidic solutions is the inferred mechanism for the silver-rich, calcite gangue systems.

A model inferring a regional fluid-flow regime and local sources of metals is proposed. Four possible regional and local causes of fluid flow in upper-plate detachment regimes are proposed: (1) regional elevation of geothermal gradients as a result of middle-crustal, lower-plate rocks rising to upper crustal levels: (2) meteoric water recharge along the southeast flank of the Harquahala antiform and consequent displacement of connate waters in the upper-plate of the Big Horn Mountains; (3) local emplacement of feeder stocks to rhyolitic flows: (4) and tilting of major upper-plate structural blocks.

INTRODUCTION

The Big Horn Mountains, and its contiguous range, the Belmont Mountains, extend over 500 square km in west-central Arizona (Figure 1). The most recent geologic map of Arizona (Wilson et al., 1969) delineates six crystalline units in the range; Proterozoic gneiss, Proterozoic schist, Proterozoic Granite, Cretaceous andesite, Cretaceous rhyolite, and Tertiary-Cretaceous rhyolitic intrusives. The range was also briefly described by Rehrig et al.(1980). They established the volcanics as middle Tertiary as opposed to the Cretaceous age inferred by Wilson. Furthermore, they noted that the volcanics in the eastern two thirds of the range are steeply to moderately tilted to the northeast and that the volcanics in the western third of the range are tilted to the west and southwest. From these relationships they inferred the range is dissected by listric normal faults.

The ensuing economic geology study is part of a joint U.S.G.S.-Arizona Bureau of Geology COGEOMAP project to gain a refined understanding of the geology and mineral occurrences of the Big Horn and Belmont Mountains. The resulting investigations (this volume) extensively details the stratigraphy and structure of the Big Horn and Belmont Mountains. Major amendments to the stratigraphy involve: the presence of Proterozoic granite in the western third of the range; the presence of an extensive Late Cretaceous monzonitic to granodioritic intrusive that has affinity to the Wickenburg Batholith of Rehrig et al. (1980); the presence of fluvial clastic rocks and laharic sedimentary rocks at the base of the Miocene section; the presence of mafic volcanics interspersed throughout the Miocene section; and the likelihood that the Belmont granite is mid-Tertiary (Reynolds et al.,

Figure 1. Location map for Big Horn Mountains mineral districts.

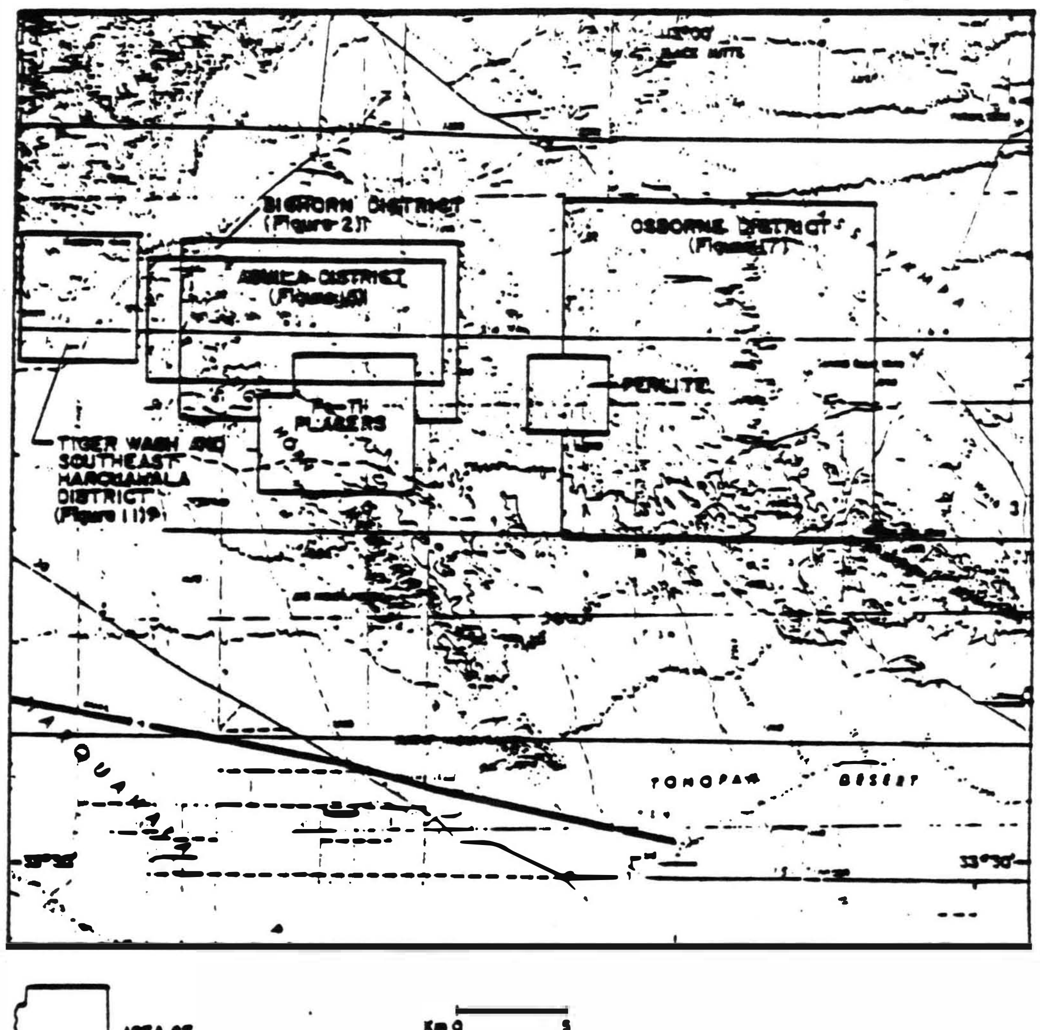

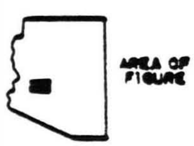

BIG HORN MOUNTAINS DISTRICT
LOCATION MAP

1985) in age as opposed to a Precambrian age (Wilson et al., 1957). Structural revelations are: the presence of major northeast-trending faults in the eastern half of the range that may have considerable strike-slip offset; and the existence of high-to moderate-angle faults cutting low-angle structures in the western extreme and in the south-central portion of the range. These latter relationships suggest multiple generations of normal faulting.

The great aerial extent of the range and the variety of terranes offers innumerable opportunities for economic geology studies. As a regional study, the emphasis here is to illuminate district-to-district disparaties and affinities, thereby establishing a metallogeny for the range. The geologic framework for establishing metallogeny is a product of the renaissance of regional and detailed geologic studies of the past five years in west-central Arizona (Coney and Reynolds, 1980; Reynolds, 1980; Reynolds et al., 1980; Rehrig and Reynolds, 1980; Rehrig, 1980; Reynolds, 1982; Richard, 1982; Reynolds and Spencer, 1985; Hardy, 1984; Capps et al., 1985). These works established the lower-plate detachment setting of the Harquahala Mountains on the western perimeter of the Big Horn Mountins. The southeast dip of the Bullard detachment fault on the western flank of the Big Horn Mountains suggests that the Big Horn Mountains are underlain by one or more detachment faults. The relationship between this major structural discontinuity, hydrothermal fluids, and mineral occurrences high in the upper plate has not been addressed. However, numerous investigations have been undertaken near immediately exposed detachment surfaces (Coney and Reynolds, 1980; Wilkins and Heidrick, 1982; Berg et al., 1982; Spencer and Welty, 1985; Van Nordt and Harris, 1985,; and Beane and Wilkins, 1985). These investigations mostly describe mineral occurrences in the Colorado

Trough area at deep levels of exposure in detachment terranes. One avenue of this study was to obtain homogenization temperatures and freezing point depressions on fluid inclusions from precious-metal occurrences on the Harquahala detachment fault and compare them to fluid inclusions from Middle Tertiary occurrences high in the upper plate and at extensive distances away from the exposed detachment fault. Similarly, establishment of the diverse character of middle Tertiary occurrences that run in a west-east transect from the Harquahala Mountains to the Belmont Mountains would place preliminary constraints on the character of detachment contemporaneous middle Tertiary fluid flow. Hewett (1964) discusses the phenomena of lateral and assumed vertical zonation of barite-fluorite-manganese-precious metal-base metal occurrences. In this paper evidence is presented to refine and delimit Hewett's model of epithermal zonation.

The virtual spatial coincidence of the Big Horn gold district with the Aguila manganese district, merits clarification. By analogy with other gold-quartz vein districts in Central Arizona, and, presumably, on the basis of its spatial coincidence with the middle Tertiary manganese mineralization, Keith et al. (1983) argued that the Big Horn district is of middle Tertiary age. Welty et al. (1985) further this inference by noting that the proximity of the Harquahala detachment fault suggests that the gold veins could be a detachment-related occurrence. Welty et al. (1985) suggest some of the Big Horn occurrences may be Laramide because they have associated northeast-trending silicic dikes.

BIG HORN DISTRICT

Introduction

The Big Horn district is located in the northwest quarter of the Big Horn Mountains (Figure 1), but includes one outlier in the north-central part of the range. The district is a northeast-trending swath of prospect pits, shafts, and inclines. The historic production of the Big Horn district is reported as; 2,800 oz. gold, 1000 oz. silver, 26,300 lbs. copper, and 6000 lbs. lead (Keith et al., 1983).

The Big Horn district is one of five basement-hosted, gold-quartz-vein districts in Maricopa County, and one of thirty-three in the state. Until recently, the age and mode of origin of these deposits had received little attention. An absence of demonstrably associated Phanerozoic rocks and a dearth of radiometric data from gangue minerals inhibits age designations. Rehrig and Heidrick's (1972) study of late Phanerozoic vein and fracture trends provided a first comprehensive tool for metallogeny. Davis (1981) established the evolution of strain through time for southeast Arizona and adjacent areas, thereby establishing a valuable framework for relating fracture and intrusive trends to episodes of mineralization. Dreier (1985) specifically studied the orientation of mineralized veins from the Late Cretaceous through the Tertiary, thereby allowing age constraints to be placed on late Phanerozoic veins without radiometric age determinations. Keith et al. (1983) used these criteria, radiometric age determinations of mineralization-related rocks, and geologic settings to produce a metallogenic map of Arizona, where they infer a mid-Tertiary age for the Big Horn district and for all of the basement-hosted gold deposits.

Welty et al. (1985) detailed criteria from literature reviews that are the basis for age designations, and, in some cases, further inferences that conflict with Keith et al. Welty et al. (1985) refined the category of basement-hosted, probable mid-Tertiary gold deposits by lithotectonic distinctions. They note that fifteen of the thirty-three deposits are related to mid-Tertiary detachment terranes. Further, they distinguish a category of microdiorite-dike-related deposits. Eleven of the the thirty-three basement-hosted deposits are spatially related to microdiorite dikes. By analogy to detailed geochronologic work on microdiorite-related deposits in the South Mountains (Reynolds, 1984), these deposits are mid-Tertiary as well. Welty et al. (1985) classification leaves seven basement hosted districts of equivocal lithotectonic setting and age. These are the Big Horn, Vulture, Cave Creek, Winifred, Gila Bend, Pikes Peak, San Domingo, and Sunrise. In view of the current interest in gold exploration, an understanding of these central Arizona gold districts would be an important aid to exploration. This study was undertaken to characterize the Big Horn district geologic setting to constrain its age.

Geologic Setting

Reynolds et al. (this volume) describe the geology of the northwest and west-central Big Horn Mountains. Proterozoic rocks constitute about two thirds of the encompassing Big Horn district. The oldest Proterozoic rocks are schist and gneiss which outcrop in the geographic center of the district and account for about half of the total outcrop. These schists are typically fine-grained amphibolites with 35 to 60 percent amphibole, 35 to 60 percent feldspar and up to 5 percent quartz. The gneissic-textured amphibolites have ptygmatic veinlets and

Figure 2. Selective outcrop map for the Big Horn gold district. Individual prospects are described in Table 1.

SELECTIVE OUTCROP MAP OF THE BIG HORN DISTRICT

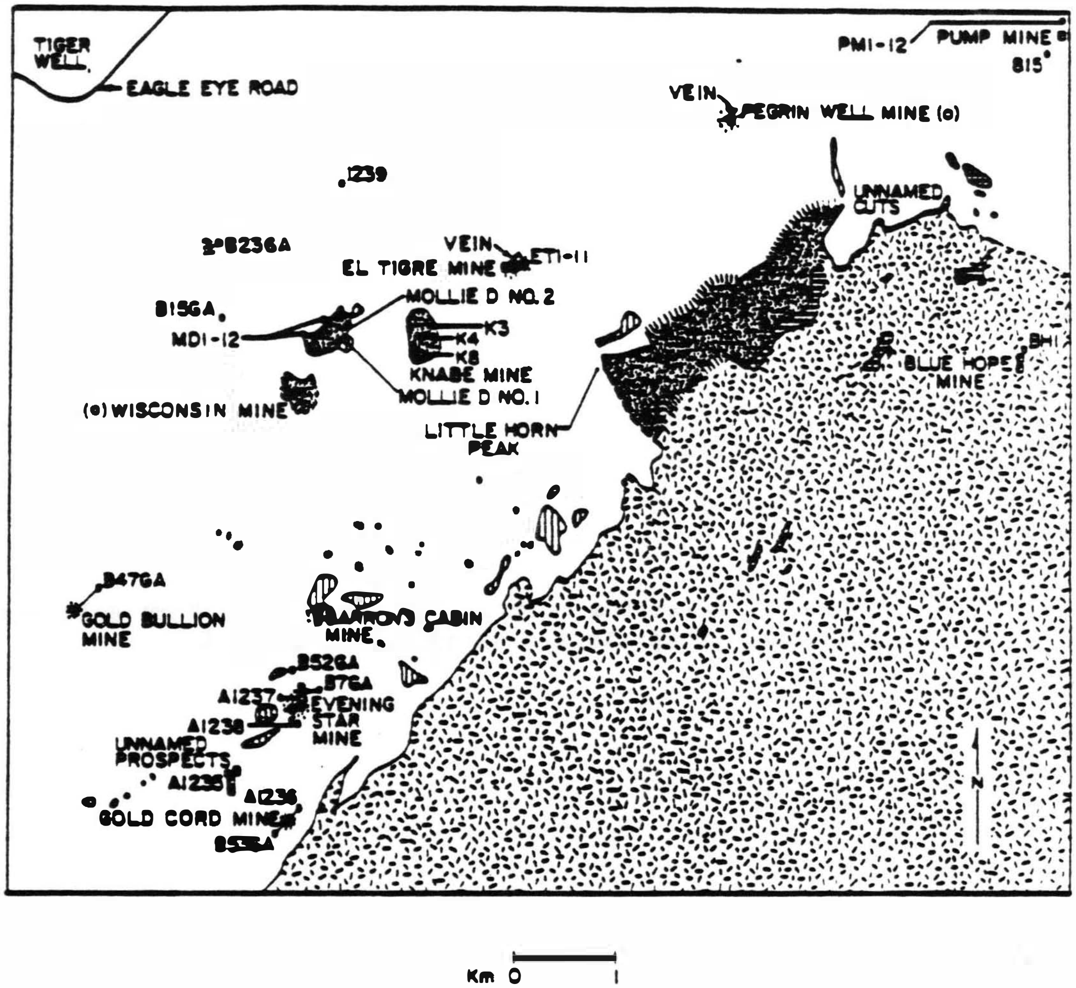

Late Cretaceous quartz diorite to diorite intrusives

Late Cretaceous aplitic monzonite intrusives

Late Cretaceous granodiorite to monzonitic intrusion

Late Cretaceous intrusives and commingled Precambrian crystalline rocks

contact, dashed where approximately located

fault, dashed where approximately located

gradational contact

iron oxide stain

shaft or incline

•A1234 sample location

veins of medium-grained to pegmatitic granite. Intruding these is a Proterozoic medium-grained biotite granite which accounts for one third of the total outcrop. The granite has 60 to 80 percent feldspar, 15 to 25 percent quartz, and 12 to 20 percent biotite. The biotite is commonly weathered to chlorite. Ridge-tops of the district expose coarse-grained to pegmatitic granite pods with up to 10 percent muscovite. The granite has sporadically developed, widely occurring mylonitic fabrics. The contacts between the granite and the older Proterozoic rocks are typically gradational.

Fine-grained monzodioritic to dioritic intrusions make up about one percent of the total outcrop (Figure 2). These intrusions are frequently northeast-aligned exposures or have related northeast-trending dikes. These intermediate composition intrusives are highly varied : 45 to 75 percent plagioclase; 15 to 30 percent biotite or amphibole, but not both; and 0 to 10 percent quartz. Rarely, some dikes have potassium feldspar. These rocks are not mylonitized, and, as discussed in the REE section, are assumed to be Late Cretaceous relatives of the batholithic granodiorites.

The remaining twenty percent or so of the outcrop is composed of the undifferentiated dark gray, brown, and red, vesicular to massive multi-flows of the mid-Miocene Dead Horse basalt. The basalt rests unconformably on the basement and is porphyritic to aphyric. The porphyritic basalts contain 5 to 20 percent phenocrysts ranging form 2 to 10 percent olivine, 2 to 15 percent clinopyroxene, 2 to 5 percent plagioclase, and trace to 3 percent orthopyroxene (Capps et al., 1985). In many places the basalt is brecciated and veined with calcite.

The Proterozoic schists and gneisses are intensely folded. Crystalloblastic foliation attitudes vary greatly, but northwest to east-west strikes with consistent moderate to steep northeast to north dips are typical. In the east-central part of the district the major gradational contact between the Proterozoic metamorphic rocks and the fine- to medium- grained granite trends N35°W. The linearity of this contact suggests it is a Proterozoic tectonic structure. The Proterozoic granite has rare, local mylonitic fabrics, which, in the Big Horn district, have no consistent trend.

The middle Tertiary structures are locally complex. Minor structures are typically north- to north-northwest-striking, high-angle normal faults. The major structures of the district are N40°W-striking, low- to moderate-angle normal faults. In places, strike-slip movement in tear faults is suggested by horizontal slickensides and apparent displacement. Apparent shingling of low-angle faults in the Lion's Den Mine area suggest at least two generations of normal faulting.

Character of Mineralization

Mineral occurrences of the Big Horn district are gold-rich, basement-hosted, narrow-quartz-pods and veins that are commonly associated with northeast-trending, Late Cretaceous, intermediate-composition intrusives, and commonly have sericitic alteration. Table 1 summarizes the geology of individual prospects. The ensuing sections describe the geology of occurrences that display the variety in the character of the Big Horn district.

The El Tigre Mine

The El Tigre mine is in the northwest part of the range, 1.6 Km northwest of Little Horn Peak (Figure 2). The El Tigre mine is the premier gold producer of the district, accounting for over 80 percent of

Table 1. Big Horn Gold District.

PROSPECT	LOCATION	PRODUCTION/ DEVELOPMENT	HOST	STRUCTURE/ GEOMETRY	MINERALOGY/ GEOCHEMISTRY
Barron's Cabin	NW 1/4 Sec 8 T4N R9W, Big Horn 15'.	Unknown.	Precambrian granite and Late K diorite (?).	Unknown. Assumed to be pods and veins.	Unknown. Mineralization is spatially related to a qtz. diorite intrusion.
Blue Hope	NE 1/4 Sec 31 T5N R8W, Big Horn 15'.	No production. Small pits.	Late K monzodiorite.	Pods of indistinct orientation.	Abundant chrysocolla and lesser malachite. Biotite in Late K host monzodiorite is chloritized.
Dead Horse	NE 1/4 Sec 15 T5N R8W Aguila 15'.	No production. One 13 m deep shaft to level. Three trenches ave. 9m long.	Late K granodiorite.	Pods and indistinctive veins. Overall mineralization appears to be east-west aligned. Minor mineralization is localized along a N52E, 80SE structure.	Chrysocolla is abundant. Some chalcocite cores to chrysocolla. Extensive iron oxide staining. Some greasey green mica. Sericite is common. Mineralization is commonly ass.-ociated with qtz flooding.

El Tigre	SW 1/4 Sec 27 T5N R9W, Big Horn 15'.	Approx. 2300 oz. Au, 150 oz. Ag, and 700 lbs. Cu from 9500 tons. 3 shafts: one 15m, the others approx. 60m deep. Total of 250m of workings.	Gabbro and granite pegmatite.	Two qtz lenses, 1.5 to 2m wide and app. 25 m long. Attitude is app. N35E 30NW. A N45W-striking SW- dipping low-to mod. angle flt. cuts the vns. at the west end. A similar normal flt. is inferred to cut the veins on the NE.	Milky quartz gangue dominates. Area is iron oxide stained. Some jarosite, some Mn oxide staining at depth. Native gold is rare. Qtz. diorite intrusive spatially associated with vein has limonite after pyrite.
Evening Star	SW 1/4 Sec 7 T4N R9W, Big Horn 15'.	A small amount of Au, Ag, Cu, and Pb were produced. A 21m shaft an a 60m incline. Principle vein opened by cuts over 0.8 km strike length.	Precambrian granite gneiss.	Veins and pods. Northernmost vein oriented N10E 60SW to to N10W 55NW.	Iron-oxide-stained quartz vein. Pod at the west end of main shaft has propable alunite, wulfenite, trace mimetite, and probable cuprite.
Gold Bullion	NW 1/4 Sec 12 T4N R9W, Big Horn 15'.	No production. 9m deep shaft	Precambrian granite.	Pod that appears to have an east-west alignment. Up to 1 km east of shaft, limonite after py. is along east-trending slickensides in slightly mylonitized Precambrian granite.	Quartz vein breccia with some possible felsite dike material host specular hematite, minor calcite, and chrysocolla. Some limonite after pyrite boxworks.

Gold Cord	NE 1/4 Sec 18 T4N R9W, Big Horn 15'.	No production. Single 25m deep shaft and scattered pits.	Precambrian granite.	Pod of indistinct orientation.	Hematite-stained grey to white qtz. Trace chrysocolla. Some limonite after pyrite boxwork.
Knabe	NE 1/4 Sec 33 T5N R9W, Big Horn 15'.	No production. Four pits.	Precambrian (?) granite and Late K diorites.	Pods of indistinct orientation. Spatially associated diorite dikes have a vaguely arcuate outcrop pattern.	Quartz pods host iron-oxide staining and some limonite after pyrite. Pods are associated with large, coarse sericite making up to 20% of surrounding rocks. Argillic alteration of encompassing granite is common.
Mollie Davenport	NW 1/4 Sec 33 T5N R9W, Big Horn 15'.	No production. Shaft approx 40m deep. Haulage adit approx 80m long.	Precambrian granite and schist and Late K monzodiorite.	Indistinct pods that appear to have NE trends.	Iron-oxide staining proximal to qtz. pods which outcrop 0.2 to 0.3 km SW of the main shaft. Some sericitic alteration. Mineralization is associated with felsite and monzonitic to dioritic intrusives.

Pegrin Well	SE 1/4 Sec 23 T5N R9W, Aguila 15'.	No production. 9m long incline in collapsed workings. 10m long open cut.	Precambrian granite and gneiss.	9 to 12m X 1.5 to 2.5m vein oriented N62E, 60SE.	Iron-oxide staining in qtz. vein is proximal to felsite dike. Some limonite after py. Sericite is common.
Pump or Purple Pansey	NE 1/4 Sec 19 T5N R8W, Aguila 15'.	Approx. 200 oz. Au, 50oz. Ag, 150 lbs Cu, from 2277 tons suspected production. 3 shafts cut main vein: 90m, 50m, and 25m. Pits extend over 1200m.	Precambrian amphibolite, phyllite, mylonitic granite.	1200m long vein or and shear zone that ranges from 0.1 to 2.5m wide. SE half trends east-west, dips 40 to 55N. NW portion trends N40 to 60W, and dips 30 to 45 NE. Vein is cut off by NNW-trending, west-WSW-dipping low- to moderate-angle normal flt.	Intensley iron-oxide stained, yellow greasey qtz. vein and hosting metamorphic rocks. Chlorite is common.
Wisconsin	SE 1/4 Sec 32 T5N R9W, Big Horn 15'.	No production. Shaft approx. 20m and adit approx 11m. No production. Shaft approx. 20m and adit approx 11m.	Precambrian granite and Late K granitoids.	Pod with indistinc trend. Possibly of NE trend.	Iron-oxide staining of quartz vein. Specularite is in small cavities. Sericite is app. 1% of enclosing host rock.

Figure 3. Geologic cross section of the northwest-facing open cut of the El Tigre mine.

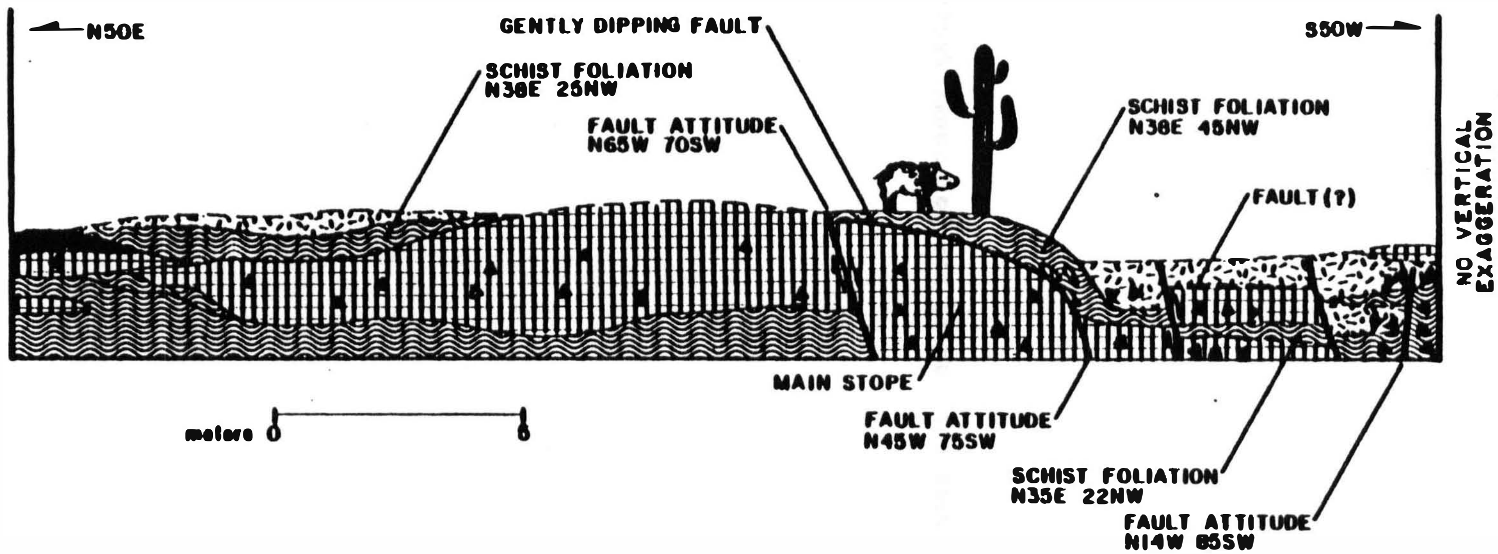

GEOLOGIC CROSS SECTION OF THE NORTHWEST-FACING OPEN CUT OF THE EL TIGRE MINE

TKmd	Cretaceous - Early Tertiary(?) mafic dike		breccia
TKq	Cretaceous - Early Tertiary(?) bull quartz vein		contact, dashed where approximately located
pCg	Precambrian foliated granite		fault, with arrows showing offset
pCgs	Precambrian gneiss and schist		surface dashed where approximate

Figure 4. Geologic map of the El Tigre mine.

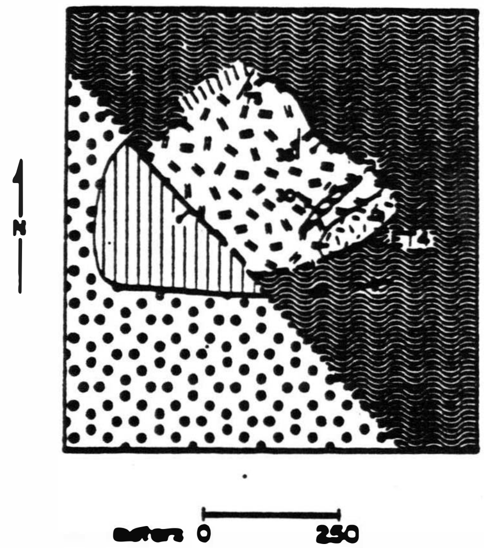

GEOLOGIC MAP THE EL TIGRE MINE

QTg	Late Tertiary - Quaternary gravels
Tb	Miocene basalt
TKq	Cretaceous - Early Tertiary milky quartz vein
TKd	Cretaceous - Early Tertiary quartz diorite
pЄ-TKgp	Precambrian or Cretaceous - Early Tertiary gabbro and pegmatite
pЄsgg	Precambrian schist, gneiss and granite
	contact, dashed where approximately located
	gradational contact
	fault, dashed where approximately located, dotted where concealed, barb on down thrown side
	vertical foliation
	strike and dip of foliation

the district's production. The workings consist of a single, open incline that is approximately 74 meters deep, two levels of development, a large, northwest-facing open-cut (Figure 3), and numerous prospect pits.

The El Tigre vein is hosted in a moderately complex assemblage of crystalline rocks (Figure 4). The oldest rocks are intensely deformed Proterozoic schists with gneiss bands and granitic pods. These rocks are intruded by an assemblage of coarse-grained to pegmatitic granite and gabbroic pegmatites. The gabbro contains pyroxenes up to 5 cm in diameter and is locally foliated. The granitic pegmatite is not foliated.

The youngest intrusive unit at the mine is a medium- grained, equigranular quartz diorite whose contact to the gabbro-pegmatite assemblages trends northeast. The quartz diorite is gossan stained and the feldspars are slightly argillically altered. The quartz diorite is considered to be younger than the schist complex and the gabbro-pegmatite assemblage because the quartz diorite lacks foliation and has a relatively "fresh" appearance. A second criterion, whose systematics are discussed separately, the coincidence of the REE pattern of a sample from the quartz diorite (ET 1) with the pattern of the 70.1 Ma regional granodiorite (Reynolds et al., this volume), argues for a Late Cretaceous age for the quartz diorite intrusive at the El Tigre. The crystalline rocks are overlain by Miocene Dead Horse basalt and poorly to moderately sorted Late Tertiary-Quaternary gravels.

The structural geology of the El Tigre mine is relatively simple. The El Tigre vein itself trends N40°E 30° NW and is along a fault or shear zone (Figure 3). Slickensides striae and mullions plunge down the dip. A regional structure, the Little Horn Peak fault, trends N50 °W and has a low to moderate southwest dip. The fault drops moderately dipping mid-Tertiary basalt down against the Proterozoic rocks and cuts off the El Tigre vein on its southwest end. The El Tigre vein is similarly cut off to the northeast by an inferred structure that is presumably sympathetic to the Little Horn Peak fault.

The El Tigre vein outcrops along strike for 30 m and is 2 m thick over a 3 to 5 m length. To either side of this bulge, the vein thins down significantly (Figure 3). The major lens is paralleled by several smaller ones and is discordant to Proterozoic foliation. The vein material is brecciated, iron-oxide-stained bull quartz that locally contains native gold. At depth, specularite, limonite, and manganese oxides are abundant. The wall rocka have spotty, moderately intense alteration.

A single doubly polished slide of milky quartz was made from vein material. Fluid inclusions of greater than 5 microns are rare and difficult to find. Most of the inclusions are less than 3 microns. The inclusions are simple two phase, vapor-liquid inclusions and range from 8 to 20 percent vapor (avereage of 12 percent vapor). None of the inclusions homogenized when heated to 400° C. Presumably the inclusions would either homogenize at higher temperatures or would never homogenize because the small size metastably inhibits homogenization. The small size of the inclusions precluded reasonable expectations of achieving freezing point depressions, and so no attempts were made.

Assays (Table 2) from a number of different sources were plotted to characterize metals from the Big Horn district (Nicor files, 1985; Tricon files, 1984; this study). Plots display fairly tight clustering of the El Tigre assays (Figures 5, 6, and 7). The relative homogeneity of

Figure 5. As vs. Au assay plot for selective prospects of the Big Horn district. Each assay is from high grade dump or vein material from the repective mine. Pump mine and Molly Davenport assays courtesy of TRICON Mining.

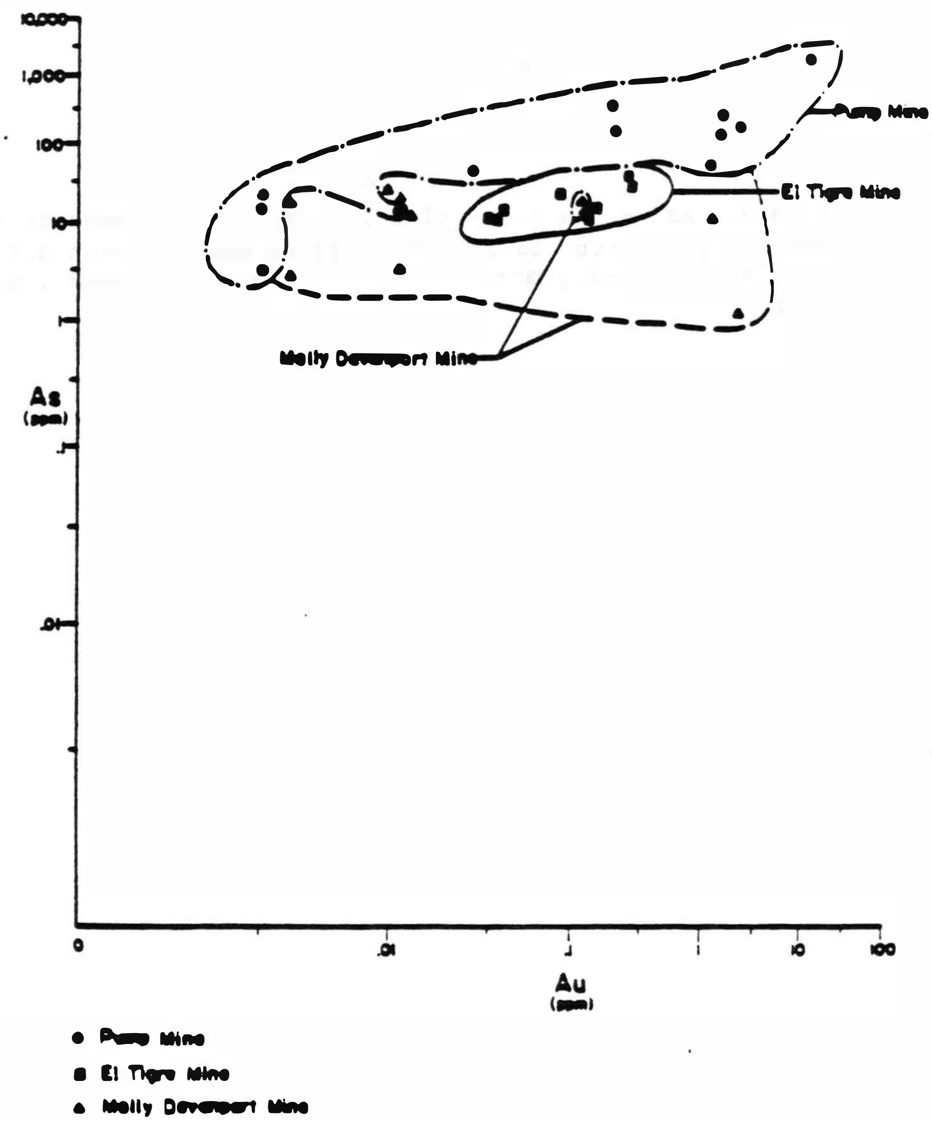

10,000
1,000
100
10
1
.01
As
(ppm)
0
.01
.1
1
10
100
Au
(ppm)
El Tigre Mine
Molly Davenport Mine

Figure 6 Ag vs. Au plot for selective prospects from the Big Horn district. Each assay is from high grade dump or vein material from the repective mine. Pump mine and Molly Davenport assays courtesy of TRICON Mining.

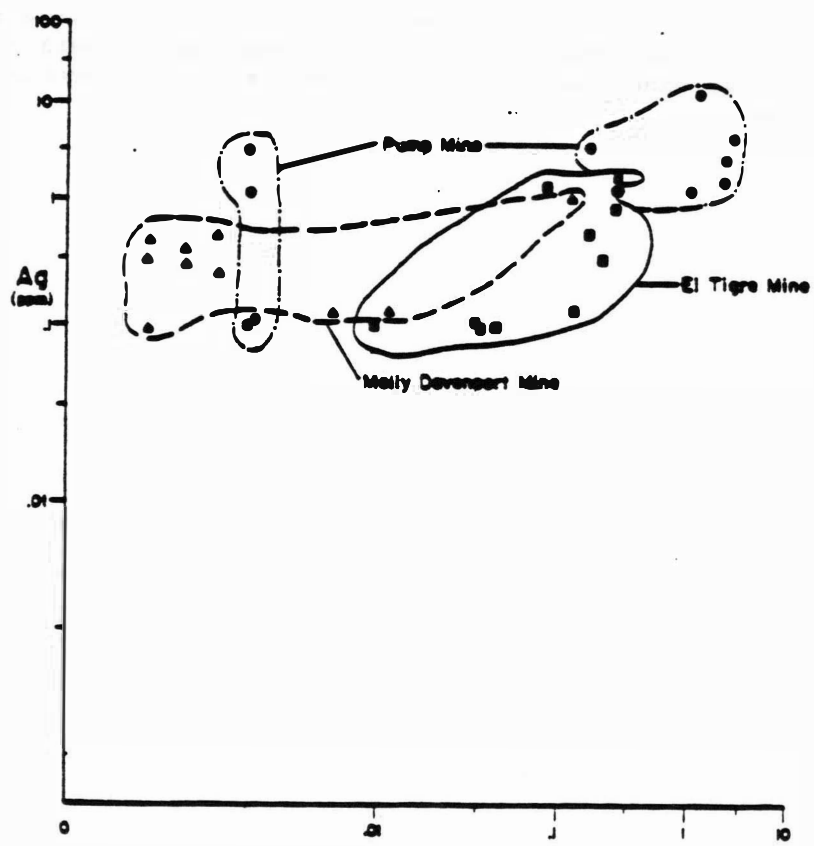

● Pump Mine

■ El Tigre Mine

▲ Molly Davenport Mine

Figure 7. Pb vs. Au plot for selective prospects from the Big Horn district. Each assay is from high grade dump or vein material from the repective mine. Pump mine and Molly Davenport assays courtesy of TRICON Mining.

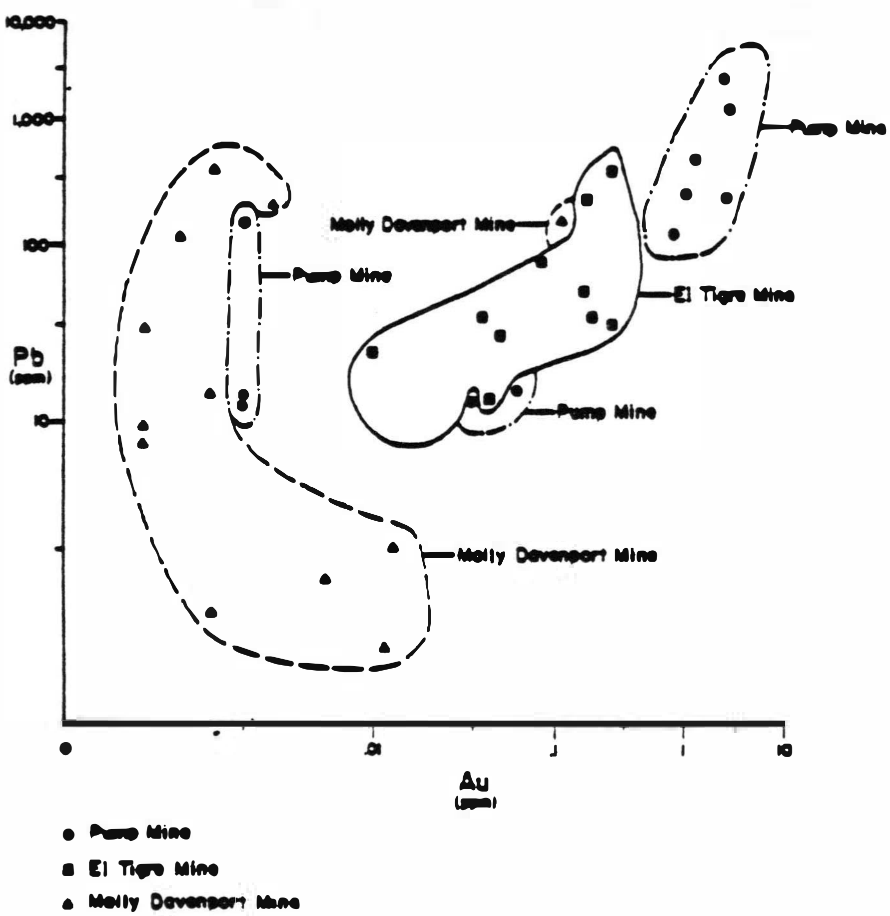

10,000
1,000
100
10
Pb
(ppm)
Pump Mine
Molly Davenport Mine
El Tigre Mine
Pump Mine
Pump Mine
Molly Davenport Mine
0
.01
.1
1
10
Au
(ppm)
Pump Mine
El Tigre Mine
Molly Davenport Mine

Table 2. Metal assays are from high grade dump grab samples. High grade samples were taken to illuminate anamalous metals and are not intended to represent ore grades. Samples locations are on district location maps.

Table 2. Precious and Base Metal Assays

Sample	Au	Ag	Pb	Zn	Cu	As	Sb
B53GA	23.99	19.88					
B15GA	0.09	2.4					
B52GA	0.01	1.4					
B47GA	0.46	3.0					
B7GA	0.26	30.0					
B23GA	< 50	<0.5	96	200	26	68	22
BH1	<50	5.5	38	130	96	<5	0.8
K3	<50	<0.5	32	270	130	5	1.0
ET4	<50	<0.5	34	69	290	12	0.5
Dead Horse	0.03	3.2					
Pegrin Well	0.16	0.8					
K4	<0.2	0.2					
Wisconsin	3.5	0.2					
Mollie D.	<0.02	0.2					
Mollie D.	<0.02	0.4					
ET1	0.09	2.0	87	123	30	37	2
ET2	0.435	2.4	543	653	60	44	2
ET3	0.21	0.7	32	106	20	13	2
ET4	0.425	0.9	50	170	38	61	2
ET5	0.250	0.5	55	277	53	24	2
ET6	0.18	0.2	70	400	65	17	2
ET7	0.055	0.1	26	154	82	13	2
ET8	0.065	0.1	45	128	61	23	2
ET9	0.055	0.1	57	228	77	15	2
ET10	0.010	0.1	33	124	65	27	2
A1235	3.3	23	10,000	4700	15,000		
A1236	6.8	20	90	250	75		
A1237	0.17	2.6	1400	100	930		
A1238	<0.02	1.4	110	55	290		
PM1	0.005	5.1	273	256	317	12	
PM2	0.005	1.3	17	86	20	28	
PM3	1.61	10.2	691	615	4797	277	
PM4	1.040	1.4	375	60	473	136	
PM5	3.350	2.9	4326	1376	406	113	
PM6	4.400	2.5	1363	188	2099	576	
PM7	0.970	0.2	139	596	390	87	
PM8	0.05	0.1	26	163	42	10	
PM9	3.9	4.0	334	140	523	218	
PM10	0.075	0.1	27	148	38	14	
PM11	0.005	0.4	21	99	32	12	
PM12	56.00	10.0	23,442	1249	4129	4925	
MD1	0.115	1.1	282	99	64	24	2
MD2	0.002	0.7	32	236	32	12	2
MD3	0.003	0.5	51	451	51	9	2
MD4	0.003	0.6	43	272	43	2	2
MD5	0.002	0.1	19	20	19	20	2
MD6	0.004	0.4	24	23	24	10	2
MD7	0.016	0.2	10	6	10	10	2
MD8	0.008	0.2	29	28	29	15	2
MD9	0.002	0.5	26	16	26	179	2

MD10	0.004	0.7	83	67	83	9	2
MD11	0.004	0.1	40	48	40	37	2
MD12	0.006	0.2	115	371	115	41	2
BH110	<1						
Rainbow	<0.02	<.2					
Rainbow X.	<0.02	0.2					
Weldon	0.04	47					
Snowball	0.05	0.4					
Alaska	1.3	1.4					
Paleoz.	<0.02	0.02					
Paleoz.	0.41	1.2	25	140	4400		
Black Q.	<0.02	1.0					
Black Nug.	0.05	<0.2					
Apache	0.04	<0.2					
Valley V #1	<0.02	3.4					
Valley V #2	0.03	0.4					
Fugatt	<0.02	3.2					
B23GA	5.5	>4000	270				
Scott	<0.02	3.4					
XR3	0.32	13	330	270	270	7	2.2
Well	0.05	0.6					
Black Dia.	0.83	2.8	55	40	205	90	<2
Black Dia.	0.06	6.2	200	305	950	20	<2
A-1811	1.6	62	13,500	16,000	10,500	20	4
A-1812	3.1	>350	17,000	24,000	89,000	220	16
XR12	<0.05	0.5	160	360	22	22	2.3
XR13	2.1	1000	24,000	8600	120,000	980	58
A-1816	1.9	3.4	245	155	1300	40	2
A-1817	1.1	1.4	170	70	800	<10	<2
A-1818	0.86	1.4	60	65	740	30	2
A-1819	8.5	2.4	15	100	1450	30	<2
XR1	1.9	7.0	2600	99	9500	53	3.4
XR9	170	0.5	130	32	330	15	1.0
A-1823	0.96	1.2	20	110	5500		
A-1242	0.34	0.6	51,000	1500	75		
A-1243	0.05	5.8	64,000	1400	120		
A-1244	<0.02	3.6	26,000	105	25		
XR11	0.03						

the ratios suggests a single mineralizing event.

The Knabe Mine

The Knabe Mine is located in northwest part of the range. The mine is approximately 2 km west of Little Horn Peak. No mineral production has been documented from the property and development is limited to three prospect pits, three-meter deep drill holes, and some bulldozer scrapings adjoining the pits.

The oldest rocks in the Knabe area are the same schists and gneisses that are found 1.6 km to the north at the El Tigre mine (Figure 8). The metamorphic rocks are intruded by a granite which hosts mineralization and is locally highly fractured. The granite is typically medium-grained, but locally pegmatitic. Biotite constitutes up to 4 percent of the granite, and is commonly altered to chlorite. Limonite after pyrite is common in fractures. Muscovite is common in the limonitic zones where it occurs as clots and composes up to 10 percent of the rock volume. Quartz-eye porphyry texture also commonly occur in alteration zones. The granite is argillically altered in mineralized zones. It is unclear from field relations whether the granite is Proterozoic, Late Cretaceous, or an assemblage of both. At the boundaries of the granite, in areas immediately surrounding the Knabe pit, are porphyritic, limonitic diorite dikes of varied orientations. Their outcrop pattern suggests they are border phases. This interpretation would make the main granite more likely to be late Cretaceous than Proterozoic becauae the REE pattern of dioritic dikes is exactly coincident with the REE pattern of the 70.1 Ma granodiorite (Figure 10). Alternatively, dikes that are spatially associated with mineralization could postdate the biotite granite. The total area of

Figure 8. Geologic map of the Knabe mine.

N

meters 0 250

GEOLOGIC MAP OF THE KNABE MINE AREA

TKf	Cretaceous – Early Tertiary felsite dike
TKd	Cretaceous–Early Tertiary fine-grained diorite dike
pЄg	Precambrian iron-oxide-stained medium-grained granite
pЄsgg	Precambrian schist, gneiss and granite
	iron-oxide alteration
xb	percent biotite present
ym	percent muscovite present
	contact, dashed where approximately located
	gradational contact
	strike and dip of crystalloblastic foliation
	manganese prospect
	shaft

alteration does not exceed 200 square meters and occurs in numerous patches. Mineralization is mostly expressed as iron-oxide staining in granite adjacent to dioritic dikes. Outcrops in the northwesternmost prospect pit have up to 20 percent limonite after pyritohedral pyrite. The feldspars of the host granite are 50 percent argillically altered. Coarse sericite is abundant in the mineralized zones, but was not observed outside of the immediate Knabe area's granite.

The Pump Mine

The Purple Pansey or Pump Mine is located in the northern end of the range. The mine has produced a small amount of gold and consists of three major shafts and numerous pits. In 1984, TRICON Minerals of Vancouver tried a heap leaching operation which left a small ore pile near the main road. The following discussion is based on mapping by P. Willard, TRICON Minerals (1984).

The country and host rocks are medium-grade metavolcanic and meta-intrusive rocks. The meta-intrusive rocks are intensely mylonitized near the vein. The Pump is coincident with the westernmost occurrence of sericite schist in the Big Horn Mountains (Reynolds et al, this volume). Mineralization occurs in a 1440-m-long quartz vein of highly varied thickness (Figure 9) The quartz vein is in a shear or fault zone that ranges from 15 cm to 2 m in thickness. The southern half of the vein trends N80°E to N80°W, dips 40°, and cuts crystalline rocks that have a N65°E, 45°NW attitude. At its west end, the vein bends to the north, probably in response to drag on a mid-Tertiary low- to moderate-angle fault. Metzger (1938) reports iron, copper, lead, and zinc oxide at the surface with their respective sulfides at depth. Epidote is a pervasive gangue. Wulfenite and an unidentified yellow mineral (massicot ?) were found on a dump west of the main road. Metal-ratio plots display a bimodal distribution for Pump Mine gold values (Figures 6,7 and 8). The larger population is distinctly higher than representative Big Horn district gold occurrences at the El Tigre and Molly Davenport Mines. The second, smaller population is typical of the district. In comparison with the El Tigre and Moly Davenport mines, the metal plots also point to higher arsenic values for the larger of the two Pump populations.

The Pump mine is distinctive from the other mines within the Big Horn district for the following reasons; (1) the absence of Late Cretaceous rocks, (2) the presence of silicic metavolcanic hosts, (3) the east-west and northwest strikes, (4) the rough coincidence of mineralization with crystalloblastic foliation, (5) the apparently elevated arsenic values, (6) the presence of abundant epidote, and (7) and the great linear extent of the Pump Mine. The general attributes of the Pump are permissive of a metamorphic origin as proposed by Boyle (1979) for the Archean occurrences of Canada.

The Dead Horse Prospect

Dead Horse prospect is located at the northernmost headwaters of Dead Horse Wash. No production is known from the prospect. Development consists of short trenches and a vertical shaft, which is 15 m deep that serves a level of unknown extent. The country rocks and host are pegmatitic and aplitic varieties of the regional Late Cretaceous monzonitic to granodioritic intrusives. The biotites of the monzonite are conspicuously fresh. Mineralization is localized in quartz pods of indistinct orientation, but iron-oxide staining is roughly aligned east-west and covers an area 100 m by 7 m. There is also a mineralized

Figure 9. Geologic outcrop map of the Pump mine (modified after mapping by P. Willard of TRICON Minerals, 1984).

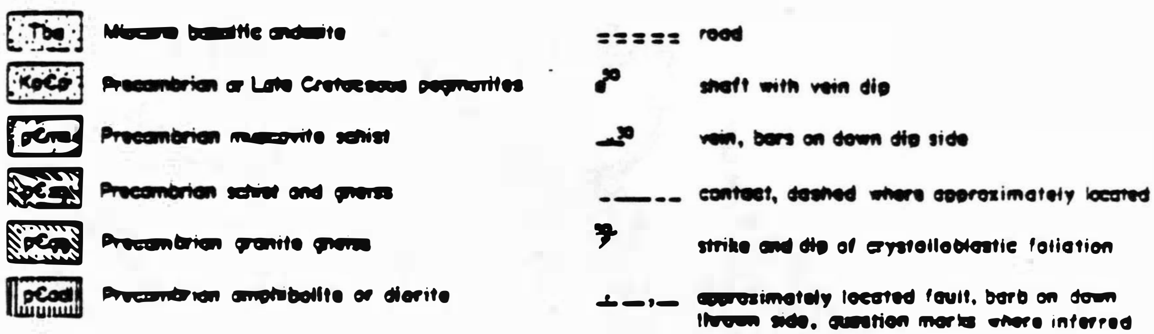

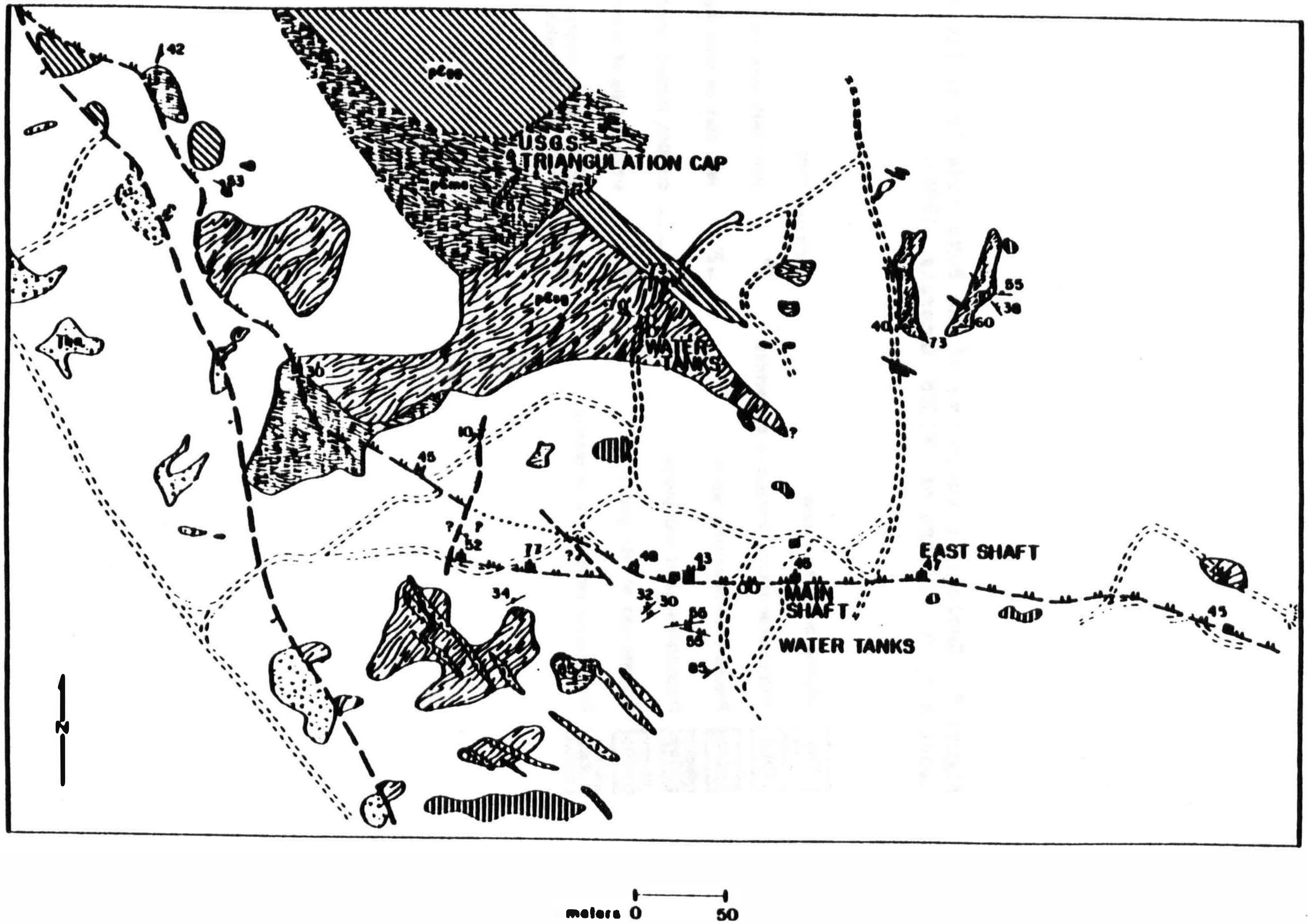

GEOLOGIC OUTCROP MAP OF THE PUMP MINE

Figure 10. Chondrite normalized REE plot of mid-Tertiary volcanics, ore related intrusives (K3, ET 4, B23GA), and the Late Cretaceous granodiorite. Leedey chondrite used for normalization (Masuda et al., 1973). The Belmont Granite and the Beer Bottle rhyolite Eu assays are below detection limits of 0.2 ppm and 0.4 ppm respectively. Those limits were arbitrarely choosen to depict the unknown concentration for the REE plots. Capps et al. and Reynolds et al. (this volume) provide descriptions and age determinations respectively for the Belmont Granite and Big Horn suite rocks.

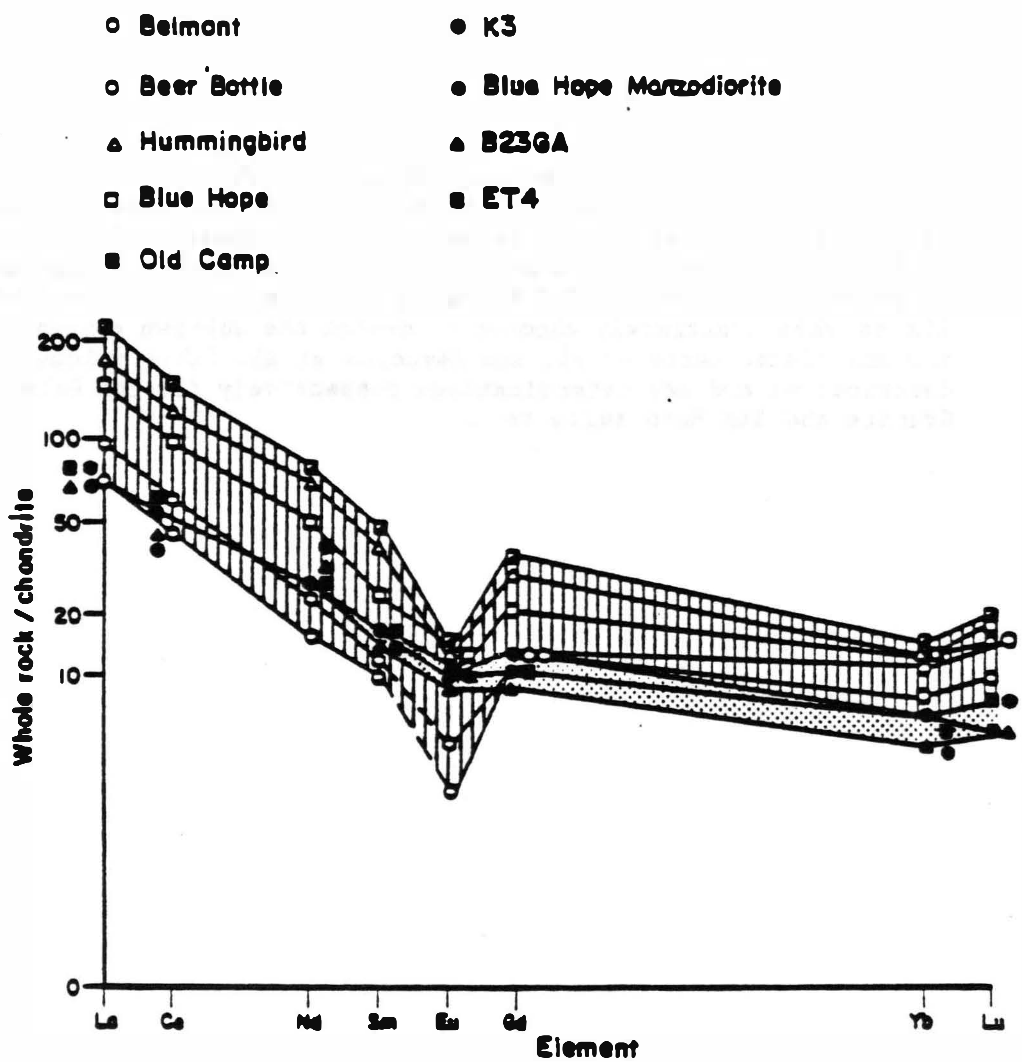

REE PLOT OF BIG HORN MOUNTAIN IGNEOUS ROCKS

Table 3. Trace element assays are mostly from altered but not replaced host rock material from various prospects. Sample locations are keyed to district maps. XR13 is a sample of vein replacement material from the Tonopah-Belmont mine.

Table 3. Trace Elements.

Sample	SC	CR	MN	FE	CO	NI	SE	BR	RB	SR	MO
XR1	3.5	240	92	9.1%	<5	14	<10	<5	<100	<1000	10
K3	15.0	10	840	7.3%	19	18	<10	<5	260	290	<1
XR3	12.0	70	870	2.4%	5	15	<10	<5	<100	<1000	<1
Blue Hope	8.4	300	960	4.2%	11	21	<10	<5	200	830	<1
B23GA	15.0	200	4300	5.0%	12	34	<10	<5	180	300	<1
ET4	8.1	300	560	4.5%	6	20	<10	<5	160	790	<1
XR9	3.0	190	350	36%	<5	<5	<10	<5	<100	<1000	10
XR12	4.3	200	92	1.2%	<5	6	<10	<5	250	70	<1
XR13	<0.5	80	40	3.8%	100	11	<10	<5	<100	<1000	20

	CD	CS	Y	ZR	NB	BA	LA	CE	ND	SM	EU
XR1	<2	<2				<0.1%	15	35	10	1.7	0.5
K3	<2	24	<10	140	30		23	55	20	4.1	0.9
XR3	<2	<2				8000	2	8	<10	1.3	0.9
Blue Hope	<2	3	10	160	10		28	61	20	3.8	0.9
B23GA	<2	9	10	120	20		24	44	20	3.7	0.8
ET4	<2	4	<10	160	20		31	58	20	4.1	1.1
XR9	<2	<2				<1000	3	8	<10	<0.5	<0.5
XR12	2	3	50	210	20		76	142	60	9.9	1.1
XR13	2	<2				<1000	1	8	<10	1.2	<0.5

	YB	LU	HF	TA	W	TH	U
XR1	1.7	0.2	2	<2	470	4	<5
K3	1.5	0.2	4	<2	<10	3	<5
XR3	1.5	0.2	<1	<2	40	1	<5
Blue Hop	1.5	0.3	6	<2	<10	8	<5
B23GA	1.0	0.2	3	<2	20	2	<5
ET4	1.5	0.3	5	<2	<10	7	<5
XR9	<0.2	<1	<2		1900	3	<5
XR12	4.0	0.7	8	<2	<10	12	14
XR13	<0.5	<0.5	<1	<2	20	<1	19

structure that trends N52°E 80°SE. Sericite and green mica are both common. Chrysocolla is abundant in vein material. Chrysocolla rims on remnant chalcocite cores also occur in dump material. An assay of highly altered, chrysocolla- bearing monzonite yielded 0.03 ppm Au and 3.2 ppm Ag. The Dead Horse prospect is noteworthy because it is exclusively hosted in the Late Cretaceous plutonic rocks, thereby suggesting that the Big Horn district mineralization cannot exclusively be the result of Proterozoic events.

REE Data

To constrain the age of Big Horn mineralization REE assays were obtained from three mineralized intrusives that are spatially related to Big Horn district prospects, the regional Late Cretaceous intrusives, the Belmont Granite, and four of the major mid-Tertiary silicic flow units. These data show a distinctive bimodal pattern (Figure 10). The Big Horn district assays all cluster tightly together with chondrite-normalized La/Tb averaging 6.41 and ranging from 5.07 to 6.83. The silicic flows and their inferred relation, the Belmont Granite (Reynolds et al., this volume), have a lower average chondrite-normalized La/Tb of 6.34 and a greater range of 4.14 to 7.98. These data make it highly unlikely that Big Horn district mineralization is related to mid-Tertiary volcanism. The strong similarity of the REE pattern of altered Big Horn district intrusives with that of the regional granodiorite suggest they are comagmatic, and therefore, the Big Horn district is a product of Late Cretaceous plutonic events.

Summary

Four styles of mineralization occur in the Big Horn district: (1)

northeast-trending quartz-veins with associated intermediate intrusive rocks; (2) indistinct quartz-pods without associated intermediate intrusive rocks; (3) Late Cretaceous intrusive-hosted chrysocolla bearing quartz-pods, (4) and a metavolcanic and meta-intrusive hosted linearly extensive quartz vein. The vast majority of the occurrences are the northeast-trending quartz-vein and pods with associated intermediate rocks. The intrusives range in composition from monzonite to diorite and typically contain limonite after pyrite. These deposits have low Ag/Au ratios (average of historic production 5). Their alteration consists of limited argillic and sericitic halos with abundant iron-oxide staining.

The second category of occurrences is represented by minor prospects bounding the western perimeter of the district. The Gold Bullion mine, the Gold Cord mine, and location B15GA are quartz pods of indistinct orientation and without spatially related intrusives. These prospects have quartz with limonite after pyrite, jarosite, and rare copper carbonates. Prospect B15GA has sphalerite, malachite, wulfenite, and probably barite.

Three occurrences differ from the majority of the prospects. Numerous characteristics distinguish the Pump mine. It is longer than any other vein in the Big Horn district, and it trends east-west and northwest in contrast to the typical northeast trends. In addition, it is not proximal to intermediate-composition intrusives, and it is hosted and roughly conformable to an amphibolite-sericite schist sequence. Furthermore, assays suggest the Pump may have two populations of gold, arsenic and lead values; one of which is consistent with values considered typical for the district, whereas the other has higher gold and arsenic values. The Dead Horse prospect and the Blue Hope mine constitute a fourth, somewhat, distinctive style of Big Horn district mineralization. Both are hosted in Late Cretaceous granitoids in indistinct quartz pods and veins. Chrysocolla is the dominant metal phase, and sericite is the characteristic alteration.

Discussion

Lithologic and structural relationships combined with a matching of REE patterns of associated igneous rocks to that of the 70.1 Ma regional granitoid suggest that most of the Big Horn district is related to the evolution of the regional intrusives. The structural evidence is manifold, if somewhat oblique. The consistent discordance of the veins with Proterozoic foliation argues that the mineralization postdates the main pulse of metamorphism. The documented occurrence of gold-quartz veins that are discordant to metamorphic fabric but are still roughly contemporaneous with metamorphism (Colvinel et al., 1984) renders discordance only permissive evidence for a post-metamorphism chronology. The prevalence of northeast attitudes, in the light of the regional deformation history (Rehrig and Heidrick, 1976; Davis, 1981; Dreier, 1985), lends further structural support to a Late Cretaceous origin for most of the Big Horn district. The fact that mineralization associated igneous rocks are unlikely to be mid-Tertiary and the fact that the mid-Tertiary Little Horn Peak fault cuts off the El Tigre vein both argue that the district is pre-Miocene. Eliminating Proterozoic metamorphism metallogeny and Miocene volcanic metallogeny makes a Laramide age preferred, if for no other reason, for lack of another gold-quartz vein metallogeny. A fourth, alternative, metallogenic setting is that the district is related to the Proterozoic biotite granite. P. Anderson (personal communication, 1985) suggests that quartz veins similar to those in the Big Horn district are found surrounding the Proterozoic Crazy Basin batholith in southern Yavapai County. The completely barren nature of the Proterozoic granite in the Big Horn Mountain and the absence of mineralized apophyses argues against this intrusive as the progenitor of the Big Horn occurrences.

The Dead Horse prospect and the Blue Hope mine are chrysocolla-dominated, quartz pods and veins that are hosted in the Late Cretaceous granitoid. Their close association with the Late Cretaceous granitoid suggests they are associated with the evolution of the granitoid.

The Pump mine alone eludes Late Cretaceous affinity. The fact that the vein does not have the characteristic northeast trend, but instead has a east-west general trend argues against a Late Cretaceous affinity. A Proterozoic age is permitted by the fact that the vein is nearly coincident with crystalloblastic Proterozoic foliation, the apparent arsenic anomaly, and the interpretation that the occurrence is hosted in a metavolcanic sequence. These characteristics roughly correspond to Boyle's (1979) model for metamorphic secretion deposits. It is unclear whether the extensive length of the vein supports or detracts from the secretion model.

TIGER WASH DISTRICT

Introduction

The barite-fluorite prospects of the extreme western end of the Big Horn Mountains are here named the Tiger Wash district. The Tiger Wash District is one of 60 distinct mid-Tertiary barite occurrences that lie in a northwest-trending belt running from Cochise through Mohave County (Hewett, 1964). The greatest producer of these districts was the Granite Reef Mine near Phoenix which produced 300,000 tons (Stewart and Pfister, 1960). Vein systems surrounding the Plomosa Mountains, 150 kilometers west of the Big horns, constitute the greatest single concentration of barite veins in Arizona (Stewart and Pfister, 1960). This study of field relations and fluid inclusion characteristics of the Tiger Wash and the adjacent east Harquahala district has been undertaken to place preliminary constraints over fluid-flow dynamics from the Bullard detachment fault into the upper plate. To achieve this the project was expanded to include reconnaissance study of the geology of the eastern Harquahala district prospects (Table 4).

The Tiger Wash district consists of several occurrences of barite mineralization with some development and a minor fluorite prospect. The only published description of the Tiger Wash occurrences is by Stewart and Pfister (1960) who report production of 600 tons from the Princess Ann group. Currently, these prospects heve a deep open cut adjacent to a bulldozer-scraped area. The White or Blue Bird claims, the other developed occurrence, contain four contiguous unpatented claims that were established in 1950. Developments include a 65 m long haulage adit, and numerous open cuts.

Geologic Setting

The Tiger Wash District occurs in a sequence of Miocene mafic volcanic flows that overlie and are interbedded with arkosic sandstone and conglomerate, which locally rests unconformably on Precambrian crystalline rocks. The Miocene volcanic-sedimentary sequence is in the upper plate of the Bullard detachment-fault which is buried beneath the recent gravels of Tiger Wash (Figure 11). The Miocene sequence dips west toward the detachment fault at moderate angles and is displaced along low-angle normal faults. The mafic volcanic-sedimentary sequence of the Tiger Wash district correlates with the Dead Horse basalt member of the Big Horn volcanics (Capps et al., 1985). The Dead Horse basalt occurs near the base of the Tertiary section. In the Tiger Wash district, a generalized stratigraphic sequence from bottom to top is: (1) 35 m of arkosic conglomerate with mostly Precambrian crystalline clasts; (2) 90 m of aphyric basalt flows intercalated with fine- to medium-grained arkose beds that are as thick as 25 m; (3) 3 m of partially welded biotite tuff; and (4) 105 m of basalt flows that cap the sequence.

An outcrop of Paleozoic limestone, quartzite, and dolomite hosts a small fluorite prospect one kilometer south of the Princess Ann group. The Paleozoic rocks dip gently to the northeast, and are cut by numerous minor faults. The exposed sequence, from top to bottom, includes the following: 16 m of quartzite; 2m of limestone; 1 m limonite bearing phyllite; 23 m of quartzite with interbedded siliceous limestone; and 23 m of brown dolomite that grades into blue-grey limestone.

Structural Setting

The Tiger Wash barite-fluorite district is in the upper plate of the

Table 4. Tiger Wash District.

PROSPECT	LOCATION	PRODUCTION/ DEVELOPMENT	HOST	STRUCTURE/ GEOMETRY	MINERALOGY/ GEOCHEMISTRY
Paleozoic Block	SW 1/4, Sec 4 T4N R10W Lone Mtn. Mtn 15'.	No production or development.	Limestone.	Mineralization is in pods along a NW-trending, SW-dipping low angle fault.	Fluorite is in massive veins up to 12cm thick. Fluorite is mostly green with some purple. There are minor inclusions of chalcpy. in fluor. Chrysocolla and poss. turq. are present. Limestone host has silicic, sericiti and dolomitic alteration.
Princess Ann claims	NW 1/4, NE 1/4 Sec 4 T4N R10W Lone Mtn. 15'.	100 tons production in 1930. Present development includes a single open cut and a 30m X 60m scrapped area.	Basalt.	Deposit is veins that extend over 600m. Largest vein is 6m wide. Vein along major cut is on N55W 35NE fault.	About 5% of vein material is green and purple fluorite. USBM (Stewart and Pfister, 1960) assay: 53% barite; 15.6% fluorite; 1.7% calcite.

Unnamed prospect	Center NW 1/4 Sec 35 T5N R10W Lone Mtn. 15'.	No recorded production or development.	Basalt and arkose.	Veinlets and breccia clasts extend for 0.4 km along N65W to N55W 30NE fault. Most barite is in footwall arkose, althought some is in hanging wall basaltic andesite.	No fluorite.
White Rock claims	SW 1/4, NW 1/4 Sec 35 T5N R10W Lone Mtn. 15'.	No recorded production development consists of a 60m long haulage adit and open cuts.	Arkosic conglomerate and basalt.	Anastomozing veins ranging from 3cm to 1m are subparallel blades. Fluorite ave. 0.3 cm Barite extends over 15 to 20m wide by 60m long area. Veins are localized along E-W-trending, low-angle, normal faults.	Veins ave. 6cm and are mostly massive with lesser rosettes and single cubes which are mostly clear to straw yellow, rarely, purple. USBM assay: 86.5 % barite: 7.7% fluorite: 3.4% calcite.

Table 5. Eastern Harquahala District.

PROSPECT	LOCATION	PRODUCTION/ DEVELOPMENT	HOST	STRUCTURE/ GEOMETRY	MINERALOGY/ GEOCHEMISTRY
Alaska Mine	SE 1/4 Sec 33, T5N R10W, Lone Mtn. 15′	No recorded production but 30m X 10m X 3m tailing pile indicates some production. Numerous dozer cuts extend over 1 acre. App. 12 new drill holes on road.	Chloritic breccia.	Disseminated mineraliz..	Vein material is milky qtz. and white calc. Hematite staining of chlor. brecc. is common. Dump mater. has chryso-colla coat-ings.
Rainbow Mine	NW 1/4 Sec 7, T4N R10W, Lone Mtn. 15′.	No recorded production. Dozer cuts extend over 30m X 20m area. 25m X 11m X 6m stockpile rests beside south edge of cuts.	Chlorit. granite.	Quartz veins and pods, ave 2cm thick of irregular direction.	90% of dump material has hematite stain. Spec-ularite is common. Some purple fluor. and massive white barite. Trace chrysocolla.

Rainbow Mine Extension	Cent. Sec 6, T4N R10W, Lone Mtn. 15′.	No recorded production. Development is on 60m diameter hill that is completely scraped.	Chloritic, mylonitic schist and highly iron oxide stained, mylon. granite.	Disseminated mineraliz.	Specularite common. Pervasive py. ave. 0.1 mm. Limo. aft. py up to 2mm common. Native gold.
Snowball Mine	SE 1/4 Sec 29 T5N R10W, Lone Mtn. 15′.	No recorded production. Prospected area is extensive, consisting of many open cuts and scraped areas. Evidence of recent explor. activity.	Chloritized schist.	Fluorite miner. is in N60 to N75W 30 to 70N fault Up to 8m thick and app. 660m long.	Fluorite is abundant. Mostly grn. Black Calc. abun. but less comm. Limonite, hematite, and barite minor.
Weldon Mine	NW 1/4 Sec 7, T4N R10W, Lone Mtn.	No recorded production. Two inclines that are roughly 20m deep.	Qtzite. Qtzose. metaseds.	15 cm to 1m thick vein coincident with crystalloblastic foliation. Exposed for 30m along strike.	Quartz and fluorite, in places euhedral Limo. aft. py. common. Specularite abundant. Crysocolla rare. Paragen: cpy,fl,qtz, spec,bar, calc.

Figure 11. Location map for the Tiger Wash and eastern Harquahala districts showing the Bullard-detachment-fault (from unpublished mapping by S. Richard, 1984).

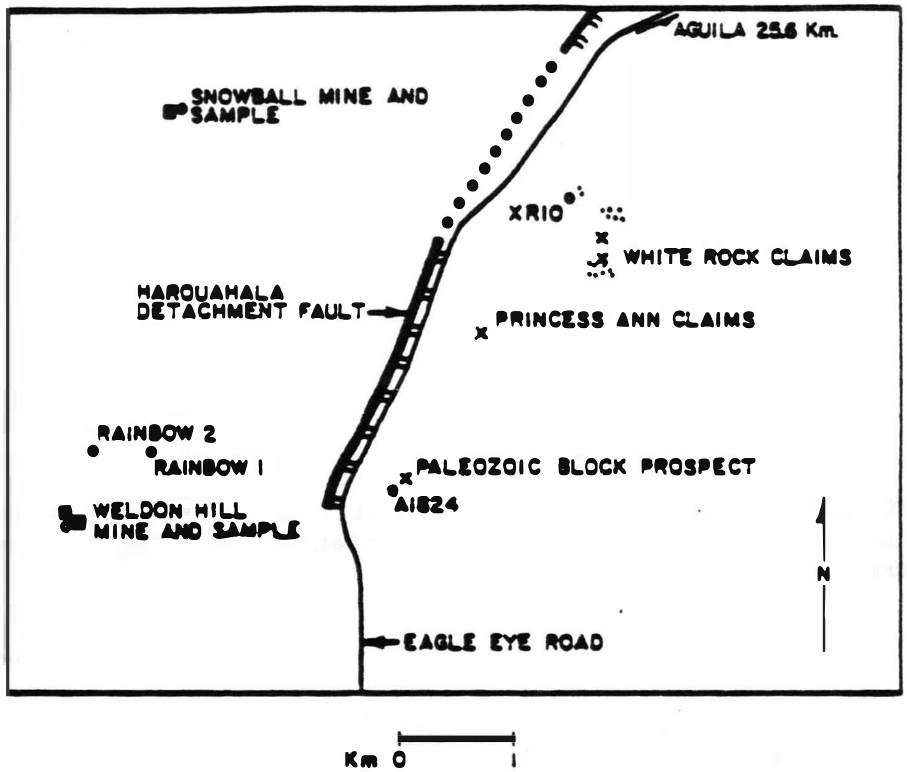

LOCATION MAP OF THE TIGER WASH BARITE–FLUORITE DISTRICT AND EASTERN HARQUAHALA DISTRICT

Harquahala detachment fault, dotted where concealed, hatchures on upper plate (from Richard, 1985)

mine

x prospect

sample location

undeveloped barite mineralization

Figure 12. Geologic map of the northern portion of the Tiger Wash district.

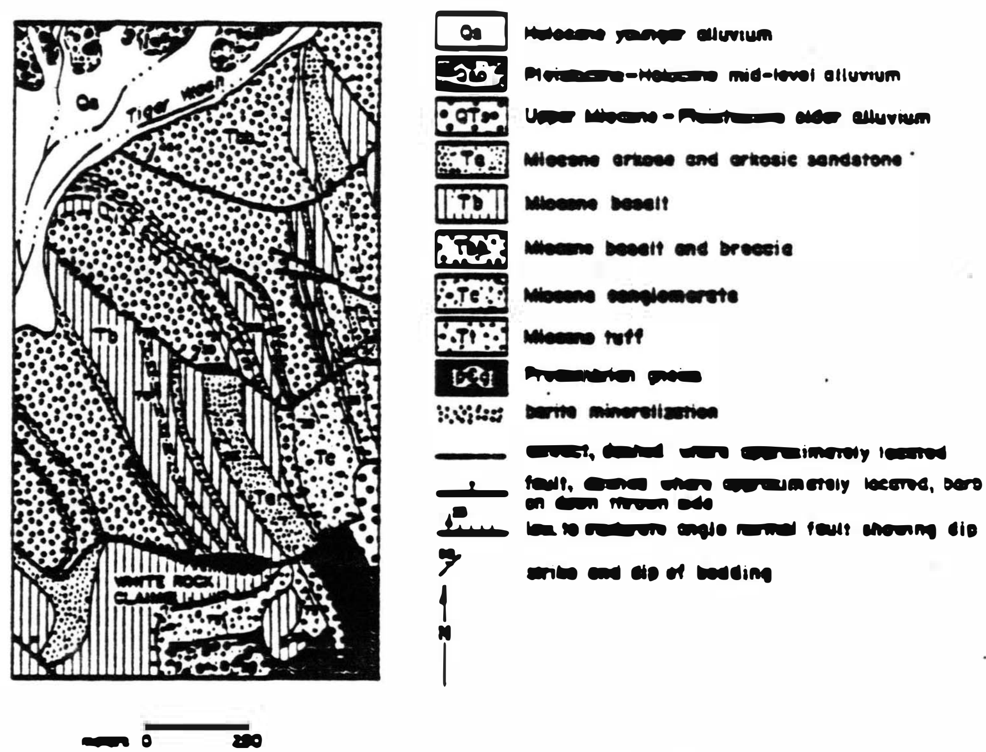

GEOLOGIC MAP OF THE NORTHERN
PORTION OF THE TIGER WASH BARITE-FLUORITE DISTRICT

Bullard detachment fault (Rehrig and Reynolds, 1980; Reynolds, 1982). The detachment fault is sporadically exposed through the gravels 0.1 to 1 kilometer west of the district (Figure 11). Upper-plate non-mylonitic volcanic and sedimentary rocks dip 45° to the west and discordantly abut into the detachment fault, which overlies highly deformed lower-plate Precambrian, Paleozoic, and Mesozoic rocks. To the north and northeast of the barite-fluorite mineralization, the Miocene section gradually bends toward the northwest strikes and dips become much more erratic. Listric faults, spaced 0.5 to 1 km apart, are probably responsible for the variation in attitude. The strike of these faults systematically varies from north-south at the southernmost barite prospect to N50°W at the northernmost occurrence (Figure 12). The dips remain moderate. The systematic change in the strike of the bedding and listric faults may be the result of large-scale drag folding along the detachment fault, such as describe elsewhere (Reynolds, 1982: Reynolds and Spencer, 1985). The Paleozoic section on average strikes N65°W and dips 35°NE. Minor faulting complicates the structure at the southern extreme of the Paleozoic block. Alteration and minor brecciation along bedding planes in the central part of the block suggest some bedding-plane displacement. In places the quartzite unit is brecciated along the margins of the block. Inferences from regional geology and attributess specific to this block strongly suggest a megabreccia origin and permit speculation that the block maybe triply allocthonous (Reynolds et al., this volume).

Structural Control Over Mineralization

The three barite-fluorite occurrences of the district are all localized on or near faults (Figure 12). The Princess Ann claims are directly above and to the east of the Bullard detachment fault and are localized along a fault that strikes N55°W and dips 30°NE. This occurrence is more vein-like than the less productive White Rock claims and the adjacent, unnamed occurrences to the north. The White Rock and nearby unnamed occurrences are all localized along low-angle normal faults, with mineralization occurring both in the hanging wall and footwall. Where the exposure is most clear, the hanging wall is the preferred locus of barite mineralization and basaltic andesite is the preferred host. The occurrence to the north of the White Rock claims displays arkose host for barite breccia.

Mineralization in the Paleozoic Block is also localized along structures. The fluorite pods at the southern end of the block are localized along a N45°W-striking, southwest-dipping, low-angle fault. A zone of limonite after pyrite exists along a possible low-angle, bedding-plane fault in the northern one third of the Paleozoic block.

Paragenesis

Barite, fluorite, and calcite are the only phases noted by Stewart and Pfister (1960) in the Princess Ann and the White Rock claims. This author never observed calcite directly associated with barite mineralization in the district, but fluorite was consistently seen to exists both as a vug filling in barite and to be completely encased in barite at the Princess Ann and White Rock claims. These observations suggest that either barite preceded fluorite and a phase of barite mineralization followed, or the phases co-precipitated. The mineral occurrence immediately north of the White Rock claims has barite only. The Paleozoic block has fluorite with less than 10 percent calcite, minor chrysocolla, and some possible turquoise. There are also small metallic blebs in fluorite that may be chalcopyrite. The relationship of the fluorite to the calcite is undetermined, but the chalcopyrite (?) presumably preceded the fluorite, and the copper silicate and phosphate evolved after fluorite. The absence of dissolution textures or observed crosscutting veins permits the inference that all of the phases precipitated in a narrow time frame.

Fluid Inclusion Studies

Fluid inclusion studies were undertaken on fluorite collected from five prospects in the Tiger Wash and eastern Harquahala districts (Figure 11). Cleavage slivers of fluorite were used for all of the inclusion studies. Homogenization temperatures, freezing point depressions, and preliminary crushing experiments were done to characterize the ore-forming solutions. A major pitfall in working with fluorite is the likelihood of stretching during heating or cooling (Bodnar, and Bethke, 1984). Two procedures were employed to guard against stretching. First, all of the homogenization determinations were made before any freezing was done because freezing is more likely to stretch an inclusion than heating (Bodnar and Bethke, 1984). Secondly, when freezing determinations were run, some of the freezing runs were immediately coupled with homogenization determinations to see if the homogenization temperature was anomalously higher than the previously characterized population. Also, homogenization and freezing point depressions were commonly done two or more times on each inclusion. Although the sum of these precautions does not eliminate the possibility of systematic error, the absence of any evidence of stretching from these cross checks is reassuring.

Fluid inclusions from all of the prospects are liquid-vapor inclusions, commonly with a third gas phase present. All of the samples displayed two styles of inclusions. Fluid inclusions from the Princess Ann prospect consist of solitary inclusions that are primary and extended arrays that are pseudosecondary. The primary inclusions are generally spheroids and less commonly have rectilinear outlines. They range in size from 10 microns to 100 microns and are typically 30 microns. On average, they have 11 percent vapor, most of which is assumed to be water. Many of the the inclusions have faint double annuli, reflecting the likely presence of a third phase. The pseudosecondary inclusions are characterisitically smaller than the primary inclusions. These inclusions range from 5 microns to 30 microns. The pseudosecondary inclusions are generally spheroidal. Their arrays do not cut across the primary inclusions. The pseudosecondary inclusions average about 11 percent vapor. However, the trace of a second annulus is much less common in these secondary-appearing inclusions.

The fluid inclusions from the White Rock prospect are not markedly different from those at the Princess Ann. One distinction is that the pseudosecondary inclusions more commonly have rectilinear outlines than do the secondary inclusions from the Princess Ann. The White Rock pseudosecondary inclusions are also smaller, on average, than those from the Princess Ann. There are many arrays of 3 micron and smaller pseudosecondary inclusions in the White Rock samples. A second distinction is that the White Rock fluid inclusions average 9 percent vapor as opposed to the 11 percent total vapor for the Princess Ann inclusions. Although the second annulus is as ill-defined in the White Rock samples as in the Princess Ann, many of the primary inclusions, and some of the pseudosecondary inclusions appear to have a third phase.

The fluid inclusions from the Paleozoic block fluorite are similar in character to the aforementioned populations, but they tend to be larger. Their size ranges up to 200 microns. The distinction between the primary and pseudosecondary inclusions is more marked than it is with the fluorite from the two barite prospects. The vapor fraction ranges from 9 to 12 percent, and a slight second annulus is generally evident.

Fluorite from the Snowball and Weldon mines of the eastern Harquahala district were selected for fluid inclusion study. Fluid inclusions from the Snowball Mine (Figure 11) are large (averaging 40 microns, varying from 20 to 120 microns), commonly necked, and very abundant. They have an average of 8 percent water vapor and nearly all show a slight second annulus of a third phase. The majority of these inclusions are presumed to be pseudosecondary. A small percentage of the inclusions are solitary and, for that reason are assumed to be primary. The Weldon Mine inclusions are descriptively similar to the Snowball fluid inclusions except that the average vapor volume of the assumed primary inclusions is 11 percent. The pseudosecondary inclusions from the Weldon Mine can also be distinguished from their correlaries at the Snowball on the basis of vapor percentage. The Weldon Mine pseudosecondary inclusions typically have 5 to 8 percent vapor.

A total of 137 homogenization temperatures and 26 freezing-point depressions were determined for the Tiger Wash district. The results (Figure 13) show distinct clustering of the homogenization temperatures. The plotted temperatures are not pressure corrected. Estimation of the overlying column of rock during the mid-Tertiary suggests 0.3 to 0.5 km burial. Since conditions of <3.8 mole percent CO_2 and 20 percent NaCl require less than 20 temperature correction for pressures at 200° C. (Roedder, 1984), a temperature correction for pressure is not needed. The homogenization temperatures for the Princess Ann and White Rock claims range from 135° to 190° C with a few isolated determinations extending the range from 123° to 200° C. Fluid inclusions from the fluorite prospect on the Paleozoic block have homogenization temperatures that are distinct from the Princess Ann and White Rock barite-fluorite prospects homogenization temperatures. The fluorite temperatures narrowly cluster from 190o to 210° C (Figure 13).

Fifty homogenization temperature determinations on fluorite were made from the Snowball and Weldon mines of the eastern Harquahala district material. Between the two mines there is a distinct bimodal distribution (Figure 13). The Snowball Mine displays a range from 160° to 190° C with a few determinations in the 200° to 220° C range. In contrast, the bulk of the Weldon Mine homogenizations cluster from 200° to 230° C around a peak of 210° to 220° C.

The salinities (Figure 14) are total NaCl equivalent calculated from freezing-point depressions using the equation from Potter et al. (1978). The raw data is presented and not corrected for possible CO_2 content because the numerous uncertainties over the species and volume of possible CO_2 in these inclusions. Collins (1979) and Hedenquist and Henley (1985) discuss the important controls that non-water phases, and CO_2 in particular, have over freezing point depression. To determine the extent of CO_2 in the Tiger Wash fluid inclusions, a number of samples were cooled to minus 96° C. No clathrates formed and no double melting point was observed. The large size of the observed inclusions (greater than 100 microns) makes it seem unlikely that the clathrates

Figure 13. Histograms of homogenization temperatures from range wide fluid inclusion locations. Determinations are not pressure corrected. Fluid inclusion host minerals are as follows: Eastern Harquahala district, fluorite; Tiger Wash district, fluorite; Aguila district, calcite; Osborne district; the US mine, fluorite, the Contact mine, amythestine quartz, the Scott mine, calcite. Small, single blocks indicate a single determination. Large blocks indicate a number of determinations that fall within a 5° C range.

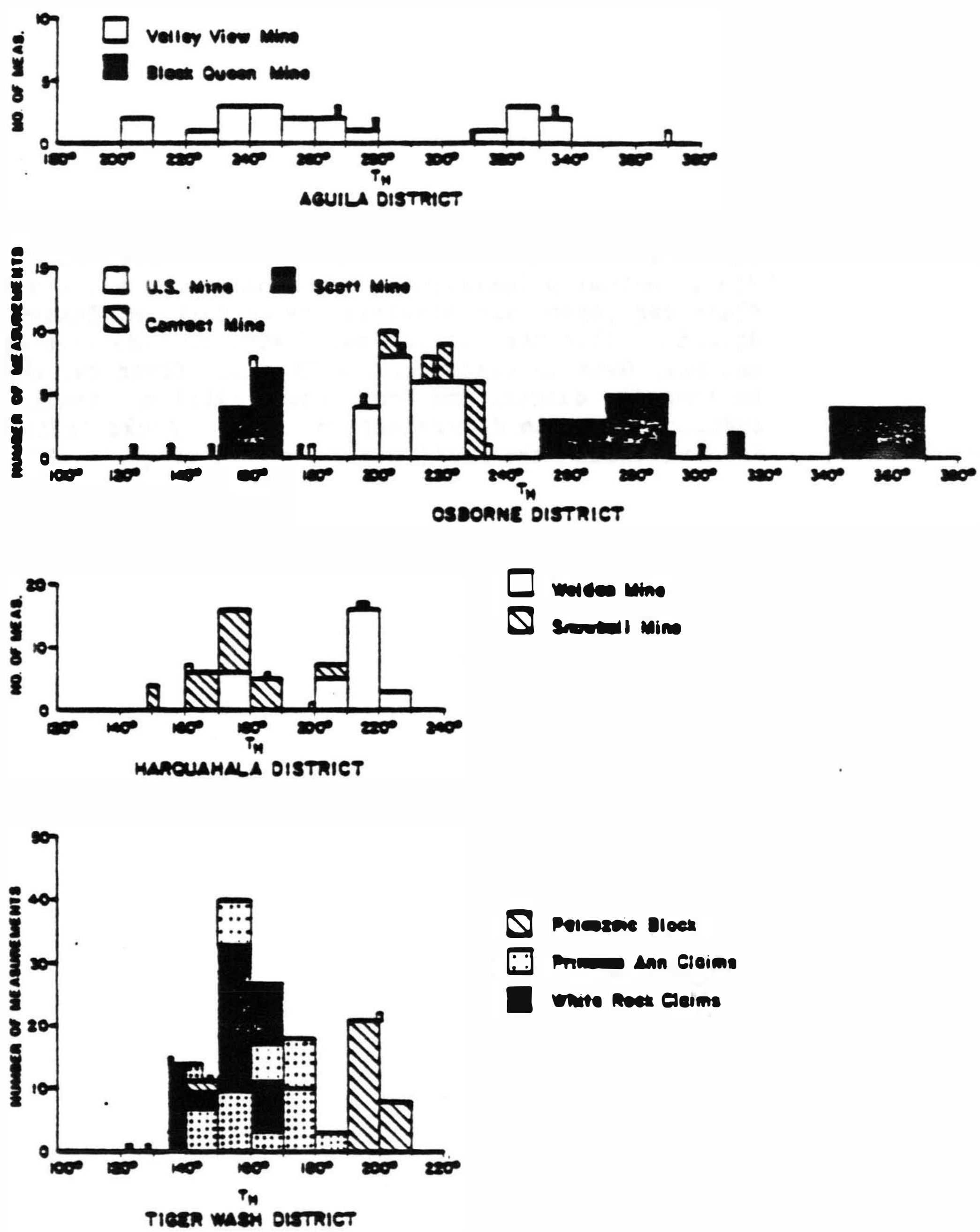

HISTOGRAMS OF HOMOGENIZATION TEMPERATURES FROM FLUID INCLUSIONS

Figure 14. Histograms of weight percent NaCl equivalence of fluid inclusions from the Big Horns. Salinities are not corrected for CO_2 content or probable high potassium proportion. Fluid inclusion host minerals are as follows: Eastern Harquahala district, fluorite: Tiger Wash district, fluorite; Aguila district, calcite: Osborne district, the US mine, fluorite; the Contact mine, amythestine quartz; the Scott mine, calcite. Small, single blocks indicate a single determination. Large blocks indicate a number of determinations that fall within a 5° C range.

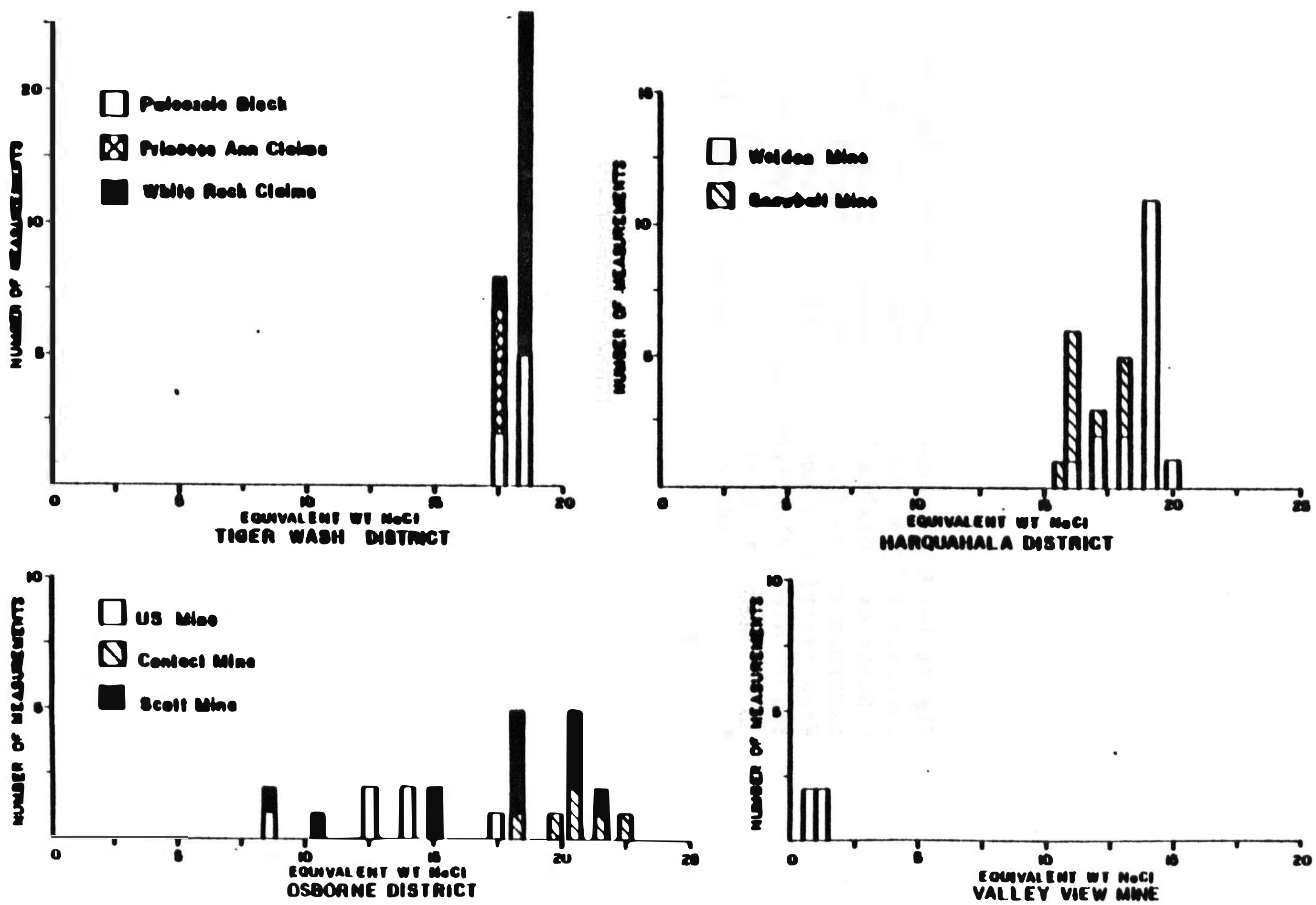

HISTOGRAMS OF WEIGHT PERCENT NaCl EQUIVALENT OF FLUID INCLUSIONS were missed. Alternatively, it is assumed either that the CO_2 content is too low to allow clathrate formation, or that the annulus on the water vapor bubbles is from another phase. Preliminary crushing experiments with both glycerine and kerosene indicated the presence of both CO_2 and methane, or possibly, a more complex hydrocarbon.

A total of 41 freezing-point depression measurements were obtained from the Tiger Wash district fluorites (Figure 14). The salinities cluster tightly at 17 to 18 percent. Twenty seven freezing-point depression measurements were obtained from the eastern Harquahala district prospects. The NaCl equivalents of the Snowball Mine range from 16 to 18 percent. The NaCl equivalents for the Weldon Mine range from 16 to 20 percent.

The fluid characteristics from the Snowball Mine are not notably different from those of the barite-fluorite prospects in the Tiger Wash district. The uncertainties over compressible gas content render the absolute value of the NaCl equivalent of unknown significance. The fact, however, that the NaCl equivalents are high, 17 to 18 percent, and all cluster tightly together remains notable. The nearly identical salinities suggest all of these occurrences evolved from the same hydrothermal system. The high NaCl equivalents for an epithermal deposit, even when corrected for as much as 7 percent CO_2 which would require a 50 percent salinity correction of the average NaCl equivalent to 12 percent, places the Tiger Wash-forming hydrothermal solutions at the extreme end of salinities for epithermal systems (Roedder, 1984). The high salinities suggest either a magmatic, metamorphic, or basinal brine component to the fluids responsible for Tiger Wash district mineralization (Beane and Wilkins, 1985).

Hypothetical Mechanisms for Barite-Fluorite Mineralization

Holland and Malinin (1979) outlined likely mechanisms for barite and fluorite precipitation. Viable mechanisms for fluorite precipitation include an increase in salinity, decrease in temperature, increase in pH, and mixing of fluorine-bearing solutions with calcium-rich solutions. Viable mechanism to precipitate barite include decreased total NaCl, decreased temperature, and mixing of connate brines with hydrothermal solutions.

A comparison the fluid characteristics and styles of mineralization of the detachment-hosted deposits in the Harquahala district to those of the Tiger Wash district permits testing the assumption that the heat source for upper-plate mineralization is the elevated geothermal gradients of the middle-crustal, lower-plate rocks. By assuming fluid flow from the detachment surface into the upper plate, the differences in fluid characteristics between the zones serves to model the efficacy of mineral-precipitation mechanisms.

In comparing the characteristics of the Weldon Mine fluorite fluid inclusions to those of the Tiger Wash district, a weak case can be made for a salinity gradient, but a fairly significant temperature gradient can be inferred from the homogenization temperature differences between the areas. The clustaring of the Weldon homogenization temperatures around 215° C contrasts with the Paleozoic-block, fluorite homogenization temperatures that cluster around 195° C and even more markedly so with those of the White Rock claims that cluster at 155° C. The data suggest a 60° C temperature differential between the precious metal detachment hosted fluorite gangue and fluorite from 5 km to the northwest.

Efficacy calculations based on this 60° temperature difference, thermochemical data from Richardson and Holland (1979), and the assumption that the White Rock prospects have a total of 100 tons of fluorite that was deposited from 2 molal NaCl solutions, yield a flow rate of 150,000 liters/year for 100,000 years as the necessary volume to deposit 100 tons. The 1 to 2 percent total salinity difference between the Weldon and the White Rock claims is too small to be significant in view of the extensive uncertainties of these calculations. In any case, a decrease in salinity causes dissolution of fluorite, not precipitation, thus rendering salinity change an unlikely cause of fluorite precipitation in the Tiger Wash district. None of the observations made for this study can constrain the possibility of a change in pH as control over fluorite precipitation. The fourth of the viable mechanisms for fluorite precipitation that Holland and Malinin (1979) discuss is the mixing of fluorite-rich waters with calcium-rich waters. Some geologic evidence can constrain the possible influence of this mechanism. The occurrence of the White Rock claims (Figure 12) at the fault contact between calcium-basalt on the hanging wall and arkosic conglomerate in a lower footwall allow for rising fluorine rich solutions mixing with fluids in equilibrium with the upper calcium-rich basalt.

The difference in fluid characteristics from the Weldon Mine to the White Rock prospects can also be used to test the viability of mechanisms for barite precipitation. Using the thermochemical data from Blount (1977) and the assumption of 2 molal NaCl solutions, a 900 ton barite deposit can be generated by means of the 60° C difference at a rate of 350,000 liters of hydrothermal fluid per year for 100,000 years. Using the 2 percent weight NaCl equivalent difference from the

Weldon Mine to the White Rock, and assuming the fluids were at 200° C and 500 bars, Blount's (1977) data shows a rate of 350,000 liters hydrothermal fluid/year for 100,000 years would also yield the 900 tons of barite. None of the research engaged here lends direct bearing on the mixing model for barite deposition. The suggestion that detachment-related, high-salinity fluids may have a basinal brine component, (Beane and Wilkins, 1985) coupled with the observation that the mineral deposition is roughly contemporaneous with volcanism, permits, but does not prove, mixing of hydrothermal fluids with basin brines.

A Model for Barite-Fluorite Mineralization

The precise chronology of mineralization with respect local faulting and detachment faulting remains elusive. The absence of bedded deposits, which one might expect if the mineralization completely preceded faulting, makes a completely pre-deformation origin unlikely. The presence of barite clasts in fault breccia at the northernmost of the occurrences places an upper age bracket on mineralization, and demonstrates that at least some of the mineralization was contemporaneous with faulting. The east-northeast to northeast offset of the Tiger Wash prospects from the Weldon mine is consistent with the sense of offset along the Bullard detachment. If the fluids flowed up into the upper plate and the Tiger Wash occurrences are the upper-level expressions of the Weldon mine mineralization, then the mineralization occurred before the final 4 to 8 kilometers of offset along the Bullard detachment.

The hydrothermal gradient implied in drawing a source line from the Weldon Mine in the Harquahala district through the Paleozoic-block fluorite prospect to the Princess Ann prospect and beyond to the White

Rock claims suggests an evolution of fluids. Schematically, the fluids start as fluorine and barium rich at 220° C, then flow northeast toward the Paleozoic block where a cooling of 15° C causes precipitation of fluorite and minor sulfides. Further flow to the Princess Ann prospect is attended by a 25° C temperature drop and a slight dilution of 1 to 2 weight percent NaCl, whereupon barite and fluorite are deposited. Temperature drops centered on the low-angle faults of the White Rock area cause further barite and fluorite deposition. The fluid is thereafter so depleted in fluorine that only barite precipitates upon further cooling in the northernmost prospects. If one allows for cooling as the only mechanism for fluorite precipitation and cooling coupled with dilution for barite precipitation, fluids take 150,000 and 175,000 years respectively to account for an estimated 1000 tons of 10 percent fluorite and 90 percent barite.

AGUILA DISTRICT

Introduction

The Aguila manganese district, located in the western and west-central Big Horn Mountain, ranks as the second greatest producer of manganese in Arizona. Production was 186,117 lb. (Welty et al. 1985). At the present-day price of 70 cents per pound of manganese, production from the Aguila district is valued at $32,000,000, which is thirty times the value of Bighorn gold district production and ten times the value of Osborne district production.

Previous Investigations

The individual mine geology, development status, and production history of the Aguila district are described in Jones and Ransome (1919), Wilson and Butler (1930), and Farnham and Stewart (1958). These authors focused on ore-body geometries, localizing structures, and major features of host lithologies and paragenesis. Their work is the basis for the individual prospect tabulation (Table 6). The early workers did not address the relationship of the mineralization to district-wide or regional structures. This present study was directed at understanding the influence of regional structures and host-rock types on mineralization.

Welty et al. (1985) characterized the district mineralization and state that the abundance of manganese prospects hosted in mid-Tertiary volcanics requires that mineralization be mid-Tertiary or younger. They did not discuss the possible relationship to detachment events.

Geologic Setting

The regional setting of the Aguila district is the same as the Big

Figure 15. Outcrop map of Dead Horse basalt, structures, and mine locations for the Aguila manganese district. Assays from individual prospects (Table 2) are from high grade dump samples. Individual prospects are described in Table 6.

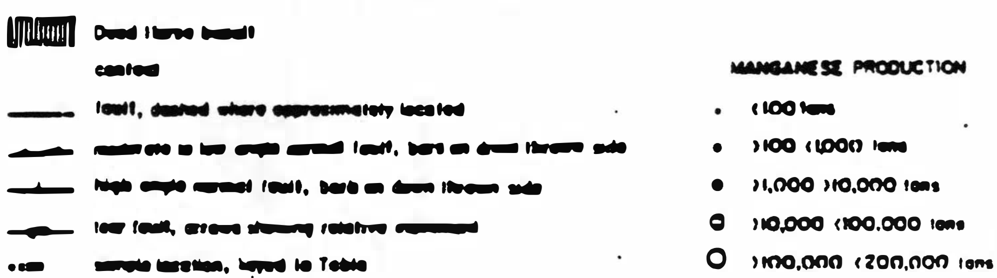

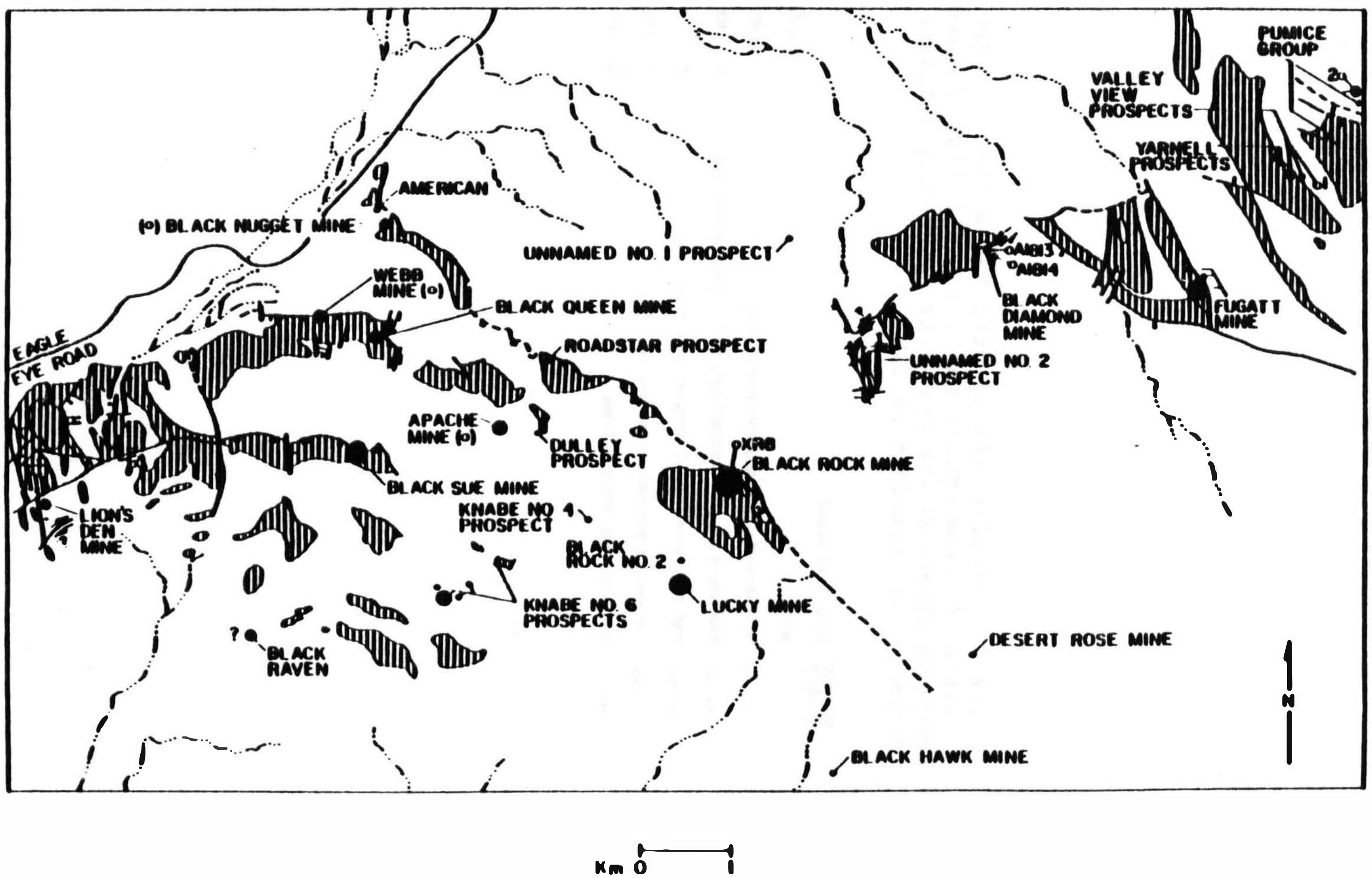

MAP OF THE AGUILA MANGANESE DISTRICT

Table 6. Aguila Manganese District.

PROSPECT	LOCATION	PRODUCTION/ DEVELOPMENT	HOST	STRUCTURE/ GEOMETRY	MINERALOGY/ GEOCHEMISTRY
American	SE 1/4 Sec 19, T5N R9W, Aguila 15'.	Small. Pits and open cuts.	Basalt.	3 vein fracture zones ranging from 1 to 5m wide and seperated by intervals of 60 to 150m. West vein is 50m long, central vein is 60m, east vein is 150m long. Veins strike north and dip steeply westward.	Commoon Mn oxides.
Apache	SE 1/4 Sec 10, T5N Big Horn 15'.	Total of 320 tons ave. 22.8 % Mn. 8m long incline of unk. depth, 22m sq. open pit.	Precambrian granite.	Two veins. One 24m long, 1 to 1.5 m wide, the other 120m X 1 to 1.5m. Both strike north with steep dips The east vein dips to the east (?), the west vein dips to the west.	Pyrolusite and and some psilomelane. Calcite is major gangue.

Black Bart (Lucky)	SW 1/4 Sec 32, T5N R 9W, Big Horn 15′.	Small production. Shallow pits and cuts along 60m X 1.5m vein.	Precambrian granite.	Many veins with 30 to 210m of seperation between them. The most extensive vein is 60 X 1 to 1.5m. Each strikes due north and dips steeply westward.	Mn oxides with calcite and quartz.
Black Crow	SE 1/4 Sec 10, T5N R8W, Aguila 15′.	Small. Three shafts: 3m, 16m and 22m deep.	Precambrian granite and gneiss.	2 veins of unknown orientation.	Mn oxides (?)

Black Diamond (Kat Head)	SW 1/4 Sec 24, T5N R9W, Aguila 15'.	Small production. Shallow open cuts and pits. Most extensive is 16m long, about 1m wide, and 2 to 3m deep.	Basalt.	2 veins approx. 60m apart. East vein is 90m long X 0.6 to 1.5 m wide. West vein outcrops only for 15m and is 0.6 to 1.2m wide. Both strike NE and dip to the NW.	Pyrolusite and and some psilomelane.
Black Hawk	NW 1/4 Sec 10, T4N R9W, Big Horn 15'.	Production assumed to be minor. Development consists of scattered open pits.	Late Cretaceous monzonite.	Veins of short extent and presumed NW strike.	Mn oxides.
Black Queen	NW 1/4 Sec 29, T5N R9W, Aguila 15'.	8600 tons ave. 21.53% Mn. 1.5 to 15m X 246m X 30m deep cut.	Precambrian granite and schist.	Zone about 240m long and 1.5 to 15m wide. Veins in zone strike north to NNE and dip steeply to the west and east. A series of east- to WNW-trending faults offset the zone. Veins are in the hanging wall of an extensive low angle fault.	Pyrolusite and psilomelane. Abundant calcite.

Black Raven	NW 1/4 Sec 1, T4N R10W, Big Horn 15'.	500 tons ave. 23% Mn. Development status unknown.	Late Cretaceous monzonite.	10 or more veins. Some extend for 60 to 90m. Thicknesses range from 0.3m to 2.5m. Attitudes vary greatly. Most are either north tending and steeply westward dipping or east striking and moderately south dipping.	Pyrolusite, manganite psilomelane. Abundant calcite.
Black Rock	NE 1/4 Sec 34, T5 R9W, Big Horn 15'.	158,566 tons ave. 19.82% Mn from 1956 through 1959. Open 270m in diameter and 110m deep. And many adits.	Basalt and tuff.	Manganese is localized betw. NW striking moderately NE dipping normal faults. Mine is at the top of the Dead Horse section in the hanging wall of the regional Little Horn Peak fault.	Psilomelane pyrolusite manganite, calcite, a qtz. Anthony and others (1977) report Ramsdellite.

Black Rock #3	SW 1/4 Sec 34, T5 R9W, Big Horn 15′.	Several hundred tons. Shallow pits and open cuts. Largest cut is 33m X 1m X 2m.	Basalt and tuff.	Vein at least 30m long X 0.7 to 1.5m wide. Unknown orientation.	Mn oxides (?).
Black Sue	SE 1/4 Sec 30, T5N R9W, Big Horn 15′.	9100 tons. 100 X 70m and 27 X 12 X 6m workings.	Basalt and tuff.	Fracture zone 105m X 60 to 12m wide. NW striking and south dipping. Localized at the top of the Dead Horse section in the hanging wall of an east striking, moderate- to low- angle south dipping normal fault.	Pyrolusite calcite, and quartz.

Desert Rose	SW 1/4 Sec 2, T4N R9W, Big Horn 15'.	No production. 16 X 9 X 9m pit.	Basalt.	Fault or fracture zone trending N10E 55SE. East side appears to be down.	Mn oxides.
Dulcey	SW 1/4 Sec 28, T5N R9W, Big Horn 15'.	Production not differentiated from the Apache. 24 X 10 X 1.5m open cut.	At the fault between Precambrian granite and basalt.	Vein 23m X 0.8 to 1.2 m. North strike with presumed east dip.	Pyrolusite some psilomelane and calcite.
Fugatt	NW 1/4 Sec 19, T5N R8W, Aguila 15'.	7,500 plus tons. 100 X 65m open pit.	Basalt.	Veinlets and irregular masses in sheared and brecciated Mn. Extent is 330 X 60 to 90m wide. Zone is NW striking and steeply SW dipping. Zone is at the top of the Dead Horse section in the hanging wall of an extensive NNW striking SW-dipping moderate- to low- angle normal fault.	Pyrolusite psilomelane, magnetite, limonite, and abundant calcite.

Knabe #4	SE 1/4 Sec 33, T5N R9W, Big Horn 15'.	12,000 tons low grades screened to yield 1000 to 2000 tons of screened material ave. 17%. Mn. Overall 370m square open pits.	Precambrian (?) Granite.	Two fracture zones. East zone is 18 X 32m. West is 50 X 6 to 9m. Both strike to the north and dip steeply to the west.	Pyrolusite, calcite, and quartz.
Knabe #6	S 1/2 Sec 32, T5N R8W, Big Horn 15'.	1000 tons 9% Mn. 25 X 16m open pit.	Precambrian granite.	Shear or breccia Pyrolusite, zone 30 X 10 to calcite and 16m wide. North trending.	Pyrolusite, calcite, and quartz.
Lion's Den	NE 1/4 Sec 25, T5N R10W, Lone Mtn. 15'.	600 tons. 12 X 3 X 3m open cut and incline. 3m deep open cut.	Basalt. and tuff.	Breccia zones 30m X 3 to 7m. Zone strikes to the north. Zone is in hanging wall of a north-trending steeply easterly dipping normal fault.	Mn oxide calcite, and iron oxide.

Pumice	SW 1/4 Sec 16, T5N R8W, Aguila 15′.	Several hundred tons of low grade. Open cuts and shallow incline shaft.	Basalt. and Sugarloaf rhyolite.	Veins and breccia zones. Major features are four veins ranging from 0.8 to 1.8m in thickness. One occurrence had irregular seams outcropping over 600m.	Pyrolusite, manganite, calcite, and quartz.
Roadside	NW 1/4 Sec 28, T5N R9W, Big Horn 15′.	Small. 10 X 3 X 2m cut.	Basalt.	Two fracture zones. West zone is 30 X 1 to 2m. East zone is 90 X 6 to 9m. Both trend north.	Pyrolusite and calcite.
Sambo Aguila	SW 1/4 Sec 36, T5N R8W, Aguila	4300 tons plus at 39% Mn ave. grade. 30 X and 3 shafts 3 to 7m deep.	Basalt. and tuff.	Over 10 fracture zones. The most extensive zone is 30 X 15m. The zones trend north.	Pyrolusite, manganite, psilomelane, and calcite.
Unnamed #1	SW 1/4 Sec 23, T5N R9W, Aguila 15′.	No production. Minor pits.	Precambrian granite.	Unknown geometry and orientation.	Mn oxides.
Unnamed #2	NE 1/4 Sec 25, T5N R9W, Big Horn 15′.	No production. Minor pits.	Tuff.	Unknown geometry and orientation.	Mn oxides (?).

Valley View	NW 1/4 Sec 20, T5N R8W, Aguila 15'.	1300 tons estimated. Open cuts.	Basalt.	Four veins 30 to 60m apart. The major vein is the Valley View which extends for over 330 m and ranges from 0.3 to 3m in thickness. All of the veins strike east-west and dip steeply to the south.	Manganite, pyrolusite psilomelane, and abundant calcite. Hewitt (1964) reports fluorite and barite and an assay yielding 2.9 oz. Ag/ton and 15% Pb.
Webb	SE 1/4 Sec 19, T5N R9W, Aguila 15'.	Several 1000 tons of low grade. 30 X 6 X 6m incline.	Basalt	Two fractured zones 24m apart. Northern zone is 45m X 6m. Southern zone is 20 X 5 to 6.5m. Both are east-west trending and south dipping. Zones are in the hanging wall of an extensive moderate to low angle normal fault with the same attitude as the zones.	Pyrolusite, some psilomelane and calcite.

Yarnell	NE 1/4 Sec 20, T5N R8W, Aguila 15′.	Production not differentiated from the Valley View. Open cuts.	Basalt.	Veins are the western extension of the Valley View veins. Orientations are the same as Valley View.	Assumed to be same as the Valley View.

Horn district.

Geology of the Manganese Deposits

A generalized description of the manganese occurrences is as follows (Farnham and Stewart, 1958):

> The individual deposits range from narrow veins, with small but enriched ore shoots, to wide shear and breccia zones of lower grade material. The chief manganese minerals are the common oxides, usually occurring as a mixture of pyrolusite, psilomelane, wad, and manganite. The gangue is composed largely of calcite, quartz: and unreplaced fragments of wall rock.

The individual occurrence descriptions are summarized in Table 6.

Host Rocks

Manganese mineralization occurs in the Proterozoic granite, Late Cretaceous monzodiorite, and Miocene Dead Horse basalt and tuff. Seven occurrences are in the Proterozoic granite, two are in the Late Cretaceous monzodiorite, eleven occurrences are in the basalt, and two are in mid-Miocene tuff. Many of the basalt-hosted occurrences include minor amounts of biotite tuff. Ninety-three percent of the total production was from deposits hosted in basalt. The remaining fraction of production came from occurrences hosted in Proterozoic (MRDS,1983).

Structural Relations to Mineralization

The Aguila district is coincident with a regional antiform described by Rehrig et al. (1980). All of the manganese occurrences are localized along tectonic structures, and none are strataform. Nearly all of the production tonnage was localized at the top of the Miocene section proximal to regional north-northwest-striking, northeast and southwest-dipping, low- to moderate- angle, normal faults (Figure 15). The easternmost occurrences, in the Pumice group, are localized along roughly east-west striking, south-dipping structures. Individual manganese pods are localized along minor high-angle normal faults. The cross section of the south- facing wall of the Black Rock mine, the major producer of the district, illustrates the localization of manganese pods along small scale structures (Figure 16). The two largest mines, the Black Rock and the Fugatt, are localized at minor inflections in the fault traces. The Proterozoic-hosted occurrences are almost exclusively localized along north-trending, steeply west-dipping, fractures or, possibly, faults. The Desert Rose mine, hosted in Late Cretaceous monzodiorite, is along a structure that strikes N10°E and dipe 55°SE structure.

Timing of Mineralization

Well-exposed geologic relations in the Black Rock pit constrain the timing of mineralization with respect to regional detachment events. The pit floor of the Black Rock mine (Figure 16) is Proterozoic schist and gneisses, whereas the pit walls are Miocene basalt. The contact between the two units is the Little Horn Peak normal fault which strikes N30°W, and dips 20°SW (Reynolds et al., this volume). Mineralization does not extend into the footwall, so mineralization probably started after the onset of faulting. The presence of manganese minerals smeared along minor faults suggests that the mineralization was, in part, pre-faulting. The overall fissure filling and vein character of the mineralization, however, makes it unlikely that mineralization was entirely pre-faulting because one would expect some strataform manganese occurrences if pre-faulting manganese precipitation had occurred. Since translation along low-to moderate-angle faults in the upper plates of detachment regimes is contemporaneous with detachment faulting, and the

Figure 16. Geologic cross-section of the south-facing wall of the Black Rock mine.

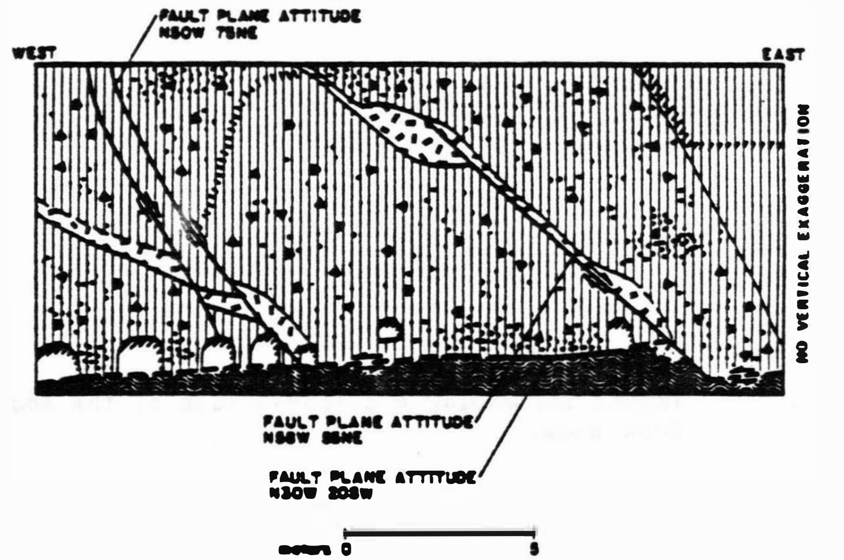

GEOLOGIC CROSS SECTION OF THE SOUTH FACING WALL OF THE BLACK ROCK MINE

- Miocene (?) arkose dike – sill
- Miocene (?) silicic dike
- Tbab Miocene (?) basaltic andesite
- p€c Precambrian crystalline rocks
- contact
- fault, dashed where approximately located, arrows showing relative displacement
- adit
- breccia
- manganese oxide mineralization

mineralization appears to be contemporaneous with faulting, the mineralization is contemporaneous with middle Tertiary detachment faulting.

Paragenesis

All of the Aguila district occurrences, except for the Valley View prospects at the eastern end of the district, consist of manganese oxides in a gangue of calcite, and, less commonly, quartz. Psilomelane and pyrolusite are the most abundant manganese minerals, but manganite is locally present. Ramsdellite, a rare manganese oxide, is found only at the Black Rock Mine (Anthony et al., 1977). Hewett (1972) implies that most of the manganese oxides are hypogene and contemporaneous with calcite. No relationship was established between quartz and the rest of the suite. The Valley View Mine displays layers of barite and fluorite crystals that alternate with black calcite (Hewett, 1964). The sequence of deposition in a well-exposed vein was: manganese oxides followed by fluorite, barite, and calcite (Hewett, 1964). Hewett (1964) notes that manganese mineralization hosted in mafic volcanics is ubiquitously associated with three-quarters to wholesale replacement of plagioclase by adularia.

Fluid-Inclusion Studies

To characterize ore-forming fluids, fluid-inclusion homogenization temperatures and freezing point depressions were determined from calcite that is associated with manganese oxides in the the Black Queen and Valley View prospects were selected. Fluid inclusions from both prospects are jagged or elongate in outline and contain liquid plus vapor. The Black Queen inclusions average 20 microns in their largest diameter and ranged from 9 to 12 percent in vapor content. The Valley View inclusions average 7 microns in their largest diameter and have a considerable range in vapor volumes, from 3 to 18 percent. No double menisci are found in either set of fluid inclusions. Therefore, there is probably little to no CO_2.

The difficulty of finding suitable inclusions permitted homogenization determinations only on four inclusions from the Black Queen and nineteen from the Valley View mine. The determinations are spread from 200° to 340° C with a gap from 280° to 310° C and a solitary determination at 370° C (Figure 13). No inclusione from the Black Queen mine were found suitable for freezing-point depression determinations. Four inclusions from the Valley View Mine yielded freezing point depressions that all clustered around 1 to 2 percent NaCl equivalent (Figure 14). The wide range of homogenization temperatures combined with the anomalously low salinities suggest the solutions were boiling at the time of deposition of calcite. The paucity of the data and the necked appearance of the inclusions place these conclusions in question.

Genesis of the Aguila District

A few generalities about the Aguila district emerge from field relations and observations of paragenesis, mineralogical, and alteration (Hewett, 1964, 1972). The Aguila occurrences are calcite-dominated, hypogene, manganese-oxide, vein deposits, which are hosted at the top of a mafic volcanic flow sequence along steep local structures that are ancillary to extensive regional low- to moderate-angle normal faults. A hot springs origin is indicated by the following: (1) modern analogs to Aguila-like, manganese vein systems (Hewett, 1964): (2) the location of most of the occurrences at the top of the Miocene section: (3) and the fluid-inclusion characteristics.

Boiling of the fluids in the western and west-central portion of the Big Horn Mountains was probably facilitated by the highly fractured character of the basalts. The high fracture density might be a result of fracturing during the formation of the Big Horn Mountains' antiform. In the Midway Mountains of southeastern California, manganese vein occurrences are found in fensters above antiforms in the underlying detachment-fault (Berg et al., 1982). If the antiform described by Rehrig et al. (1980) is a reflection of an arch in the detachment surface, a relationship may exist between rugousities in underlying detachment surfaces, fracture density in upper plate rocks, and consequent permeability.

The source of the manganese and of the hydrothermal fluids in the hot springs is more problematic. Most studies of hotsprings deposits reveal a dominantly meteoric origin for the fluids (White, 1980), but place few constraints on the origin of metals. Hewett's (1964) observation of potassium metasomatism ubiquitously associated with mafic-volcanic-hosted manganese occurrences and the presence of intense K-metasomatism in the Big Horn Mountains (Reynolds et al., this volume) suggest a genetic model solely dependent on K-rich, CO_2-bearing solutions reacting with mafic volcanics.

Mass-balance calculations indicate that alteration of 20 percent of the total plagioclase in the basalt of the western Big Horn Mountains to adularia can account for all of the calcite observed and some of the manganese. The generation of calcite is a consequence of cation exchange of potassium for calcium, consequent supersaturation of fluids with calcium, and concurrent immiscibile separation of CO_2 during boiling. The manganese is presumed to evolve during K-metasomatism of plagioclase because adularia contains between 2 and 10 times less manganese than intermediate plagioclase (Wedepohl, 1969-1978). Calcite, amounting to twelve percent of the total volume of basalt in the western Big Horn Mountains and one seventh the total manganese produced (12,500,000) are evolved if one assumes the following: an average content of 10 ppm Mn in adularia, 60 ppm Mn in plagioclase, 29 percent plagioclase in basalt (Turner et al., 1979), sufficient CO_2 in the fluids to generate $CaCO_3$, and that 20 percent of the plagioclase in 2.8 Km cubed (estimated total volume of basalt in the western Big Horn Mountains) is altered to adularia.

These calculations, all their uncertainties notwithstanding, demonstrate that the observed alteration of plagioclase to adularia can account for commonplace calcite gangue and some of the manganese. Although none of this study constrains the alteration of amphibole and pyroxene, the reaction of these minerals with alkali-rich solutions presumably could account for much of the manganese without having to resort to initially manganese-bearing solutions. If this model is correct, and the solutions were K-rich, then these solutions may have had a brine character prior to boiling, and therefore would be affine to the Tiger Wash hydrothermal fluids.

OSBORNE DISTRICT

Introduction

The Osborne district is a group of approximately twenty Pb-Zn-Ag-Au-Cu occurrences that cluster in a north-northeast trend in the east-central and eastern Big Horn Mountains (Figure 17). The Osborne district is one of twenty-five middle Tertiary base-metal districts in Arizona (Keith et al., 1983). Of these districts twenty two are Pb-Zn-Ag dominant and three are silver-dominant with lesser Pb and Zn. The Ag-dominant districts are the source of the vast majority of the dollar value from the middle Tertiary base-metal districts. The Osborne district ranks eighth in terms of present day value of production from these middle Tertiary districts (Welty et al., 1985). The district produced 1,369,000 lbs. Cu,7,710,000 lbs. Pb, 500 lbs. Zn, 13,000 oz. Au, and 195,000 oz. Ag (Keith et al., 1983).

Mid-Tertiary base-metal districts can be subdivided into those districts that are hosted in tilted volcanics and those that are not. The distinction is noteworthy in two regards. First, two of the three silver-dominated districts are in nontilted volcanics, and the third, Mineral Hill, is hosted in Pinal Schist. Therefore, the silver-rich mid-Tertiary base-metal deposits are not located in detachment terranes. Secondly, of the districts hosted in tilted volcanic rocks, the Osborne ranks third in present day value of historic production.

Geologic Setting

The oldest rocks in the district are Proterozoic rocks that consist of phyllite and schist in the eastern half of the district and are dominantly amphibolite with some gneisse and meta-granitoid in the western portion of the district (Capps et al. 1985). There is also a single occurrence of gabbro that is assumed to be Proterozoic. The northwest portion of the district has extensive outcrops of Late Cretaceous granitoids that are typically sphene-bearing granodiorite. Unconformably overlying these units are the lower and middle Miocene Big Horn volcanics, which are 1000 to 3500 m thick and are the predominant outcropping rocks of the central Osborne district. The basal unit of the Miocene sequence ranges from a coarse sandstone and conglomerate to laharic sedimentary rocks. These basal clastic rocks are overlain by basalt and basaltic andesite flows and pyroclastic rocks of the Dead Horse basalt member. Overlying and interlayered with the Dead Horse basalts are a series of rhyolite to rhyodacite flows of the Old Camp and Hummingbird Springs rhyolites. These flows, along with the overlying Mine Wash andesite, Sugarloaf rhyolite, Moon Anchor andesites, and Beer Bottle rhyolite outcrop in the central portion of the district. The eastern portion of the district has Morning Star rhyolite as the basal silicic flow instead of the Old Camp rhyolite. Rocks younger than the Big Horn volcanics include middle to upper Miocene landslide-type megabreccias, sedimentary breccias and fanglomerates, Middle Miocene Hot Rock basalt, and various generations of alluvium.

The middle Tertiary structures in the Osborne district are complex (Reynolds et al, this volume). The major structures are regionally extensive N25°W-to N45°W-striking, dominantly southwest-dipping, moderate-to low-angle normal faults. A set of N20°E- to N80°E-striking faults of apparent strike-slip displacement, offset or otherwise terminate the low-to moderate-angle normal faults. Three to four kilometers of strike-slip offset is suggested by the outcrop pattern along the N45°E-trending fault that dissects the north-central portion

Figure 17. Osborne district prospect location map. Individual prospect descriptions are found in Table 7.

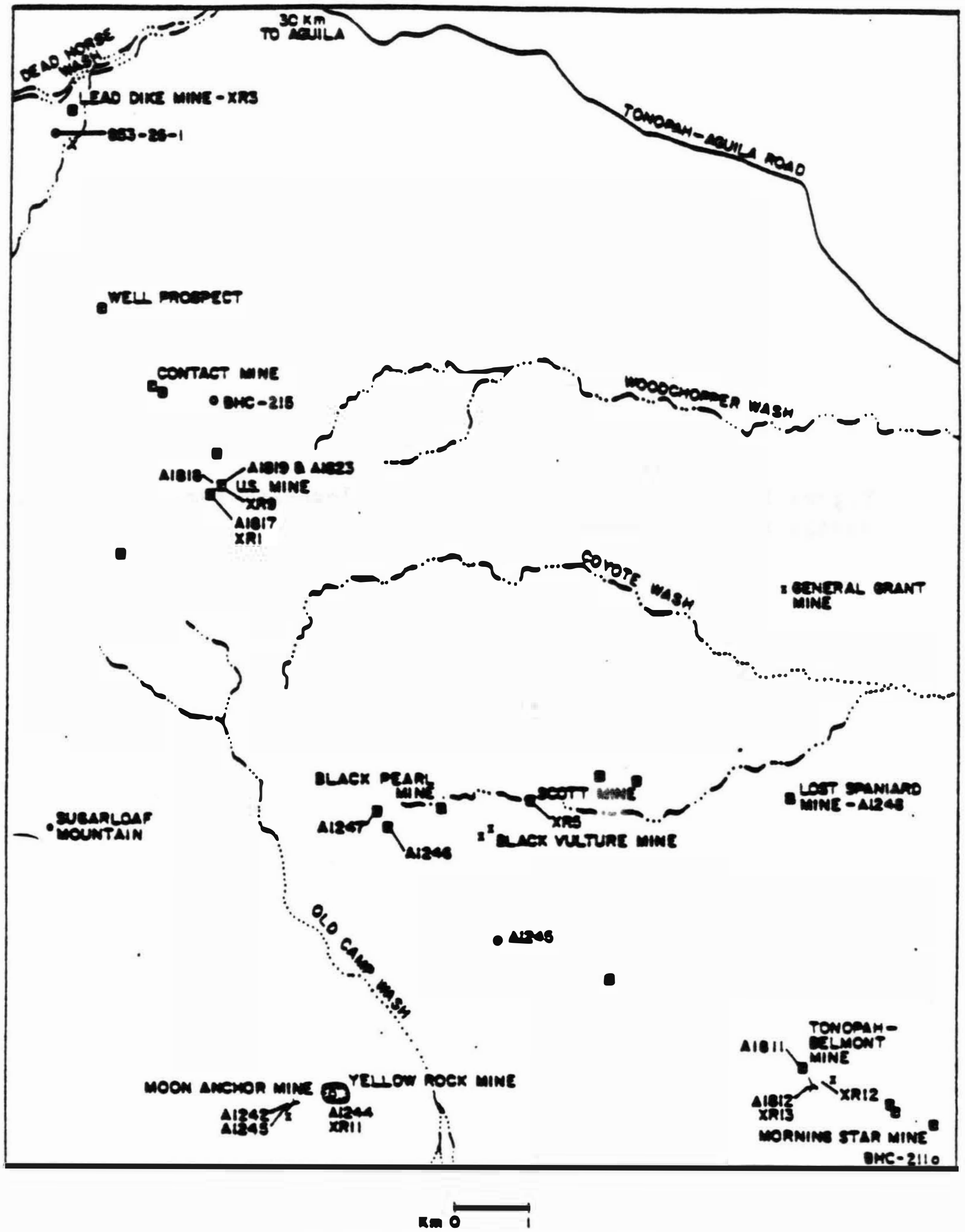

OSBORNE DISTRICT LOCATION MAP

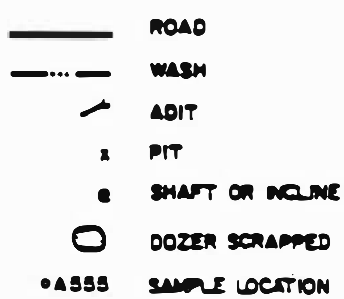

Table 7. Osborne District.

PROSPECT	LOCATION	PRODUCTION/ DEVELOPMENT	HOST	STRUCTURE/ GEOMETRY	MINERALOGY/ GEOCHEMISTRY
Black Pearl Mine	NW 1/4 Sec 20 T4N R7W, Belmont Mts. 15'.	No prod., one shaft and some pits.	Basalt. Also limo. aft. py-bearing, iron-oxide-stained, 10 X 6m plug..	Vein. 2 to 3m wide. Exposed for 4m at incline. Extends sporatic-ally for 120m. Trends N35W 70NE.	Main incline has specularite, calcite vein-ing and quartz veining with black calcite in the core.
Black Vulture Mine	NW 1/4 Sec 21 T4N R7W, Belmont Mts. 15'.	No prod., minor work-ings.	Basalt.	Unknown.	Mn oxides, calcite, hema-tite, and manganite.
Contact Mine	NW 1/4 Sec 31 T5N R7W, Big Horn Mts. 15'.	No record-ed produc. Two shafts, an adit, and scatt-ered open cuts over 0.4 km vn strike length.	Gneiss. Pods of garnet-bearing peg. Fine-grained mafic dikes spatially associated w/ mineral-ization.	Vein trace-able for 2 km. ranges up to 2m wide. Attitude ranges from N30 N50W, varied dips, typically moderate angles.	Vein of amythest up to 1.5 m. wide. Chrysocolla is common.

General Grant Mine	NE 1/4 Sec 11 T4N R7W Belmont 15'.	No prod. One adit, infilled pits, and trench	Hummingbird Springs rhyolite and andesite.	210 to 240m long X 45 to 60m wide zone of breccia-appears to to NW. Dip is unclear.	Limonite aft. py in calcite veinlets. 1 to 2 cm irregular veinlets. Basalt is propylitically altered.
Lead Dike Mine	NE 1/4 Sec 21, T4N R7W Aguila 15'.	No prod. One 8m, one 24m shaft. Cuts and pits.	Late K sphene-bearing grano-diorite.	6 m-long breccia-dike zone trending N8W 74NE at main shaft. Sporatic out-crops show vein system extends for at least 90m in the immediate area.	Galena and cerrusite on main dump. Some amytheat. At pit 65m SE of main shaft is minor crys-ocolla and possible barite.
Lost Spaniard Mine	NW 1/4 Sec 24, T4N R7W, Belmont Mts. 15'.	No prod. One 30m shaft. One adit.	Hummingbird rhyolite and basaltic andesite. Precambrian or Belmont granite as country rock.	Vein in fault zone w basaltic andesite on HW and Old Camp rhyolite on FW. Vein-fault trend N65E 30NW.	Unusual mineral suite (Anthony et al., 1977.). Ajoite, cerrusite, creaseyite, croicite, hemihedrite, hydro-cerrusite, laumontite, masicot, minium, duftite phoenicochroite, shattuckite, vaulque-linite, wickenburgite, galena, chalcopyrite, bornite, cerrusite, malachite, azurite, qtz. fluor.

249

Moon Anchor Mine	SW 1/4 Sec 31 T4N R7W Big Horn Mts. 15'.	Small prod. 16 X 7m room driven. 30 X 8 X 2 m pit.	Morning Star rhyolite and basalt.	N35E 30 striking vein along fault. Estimated size of pod is 15 X 9 m.	Unusual mineral suite (Anthony et al., 1977). Beudantite, fornacite, mimetite, ajoite, alamosite, phoenicochroite, wickenburgite, quartz, and possible fluorite. Probable new species now at the Smithsonian (Bill Hunt, personal communication).
Morning Star Mine	NW 1/4 Sec 6 T3N R7W Belmont Mts. 15'.	31 tons. One shaft 120m deep another 28m. 30m open cut betw. inclines.	Basalt and Old Camp rhyolite.	Vein is 1.3 m X 30 m. Trending N80E 30 NW at west end and N70E 60NW at east end.	Quartz, chalcopy., copper carbonates. Ore reportedly had 31% carbonates (AZBGMTF).
Morning Star Extension	SW 1/4 Sec 36 T4N R7W Belmont Mts. 15'.	No prod. 30m shaft.	Basalt.	Dike is 10 X 30m. Trend is N20W 65NE along apparent fault.	No visible mineralization.
Scott Mine	NW 1/4 T4N R7W Belmont Mts.	17 tons oz/ton. 30m shaft.	Basalt.	Vein 1 X 33m. Trends N70W 65NE at shaft. Iron oxide stained 20m west of shaft trends N60W 90.	Black calcite is has probable minium. Pyrite, chrysocolla, and probable rhodocrosite.

88

Tonopah-Belmont Mine	SW 1/4 Sec 36 T4N R7W Belmont Mts. 15'.	50,000+ tons. 100,000+ oz Ag. 8000+ oz Au. 1 mill.+ lbs. Cu. 3 inclines to 120m depth. Many surf.	Basaltic andesite, laharic sedimentary rocks, and Morning Star rhyolite.	North vein 1 to 12m wide 120m long, trends N70E 60SW. South vein 2 to 10m wide, 150m long, trends N75E 80NW.	Unusual mineral suite (Anthony et al., 1977). See text. High graded dump sample shows significant enrichment in Cu, Pb, Zn, Au. Ag, As, Cd, and Sb. Co and U are somewhat enriched. Extensive argillic alt.
US Mine	NW 1/4 Sec 1 T4N R7W Big Horn Mts. 15'.	4200 plus tons prod. at 0.141 oz Au/ton and 0.755 Cu. Two shafts, one 20m adit, many pits. 565,000 tons at 0.09 oz Au/ton now blocked out.	Beer Bottle rhyolite, laharic sedimentary rocks, and basaltic andesite.	North breccia-vein zone is 5 to 25m wide and traceable for 200m. It trends due north, and is vertical. The south vein zone varies 5 to 25m and extends for 300m. Trends due north to N40E. 90 to NW	Quartz and fluorite are major gangue. Amytheat is rare. Specularite and malachite are common. Azurite rare. Galena, sphalerite, and chalcopy. reported at depth. High-graded dump sample indicates anomalous Cu and Au. Slight enrichment in Ag, W. and Pb. Gold is reported as native.
Well Prospect	NW 1/4 Sec T5N R7W Big Horn Mts. 15'.	No prod. Two major pits along vein. One is 2m deep.	Late K monzonite and aplitic monzonite.	Veins and indistinct pods At 15' map shaft vein trends N20W 50 to 75SW. 50m north of main shaft is 2.5 X 11m vein.	Milky qtz and fluor. Abundant iron-oxide staining.

Yellow Rock Mine	SW 1/4 Sec 31 T4N R7W Big Horn Mts. 15'.	No prod. currently under devel. App. 30m X 60m scraped area.	Basaltic andesite.	Veinlets and two larger veins. Vein at adit is 0.5m wide, trending N20 to 30E 28SE. Hosting flow trends N48W 50NE.	Black calcite is major gangue. Chrysocolla is widespread but not abundant. Rare green fluorite.

108

of the district through the US mine. The presence of an extensive fenster in the southern portion of the district, with high-angle normal faults cutting the upper plate, suggests at least two distinct episodes of middle Tertiary faulting.

Characterization of Mineralization

Beyond the fact that the occurrences are base-metal dominant, fracture or fault localized, and epithermal in character, the Osborne district prospects have few unifying attributes (Table 7). The occurrences can be grouped by several classifications based on differences in host rock types (silicic vs. mafic rocks), trends of localizing structures (north to northwest vs. east-west), or gangue suites (calcite vs. quartz plus or minus fluorite). Generally, the calcite-dominated, mafic-rock-hosted occurrences have a Pb-Ag metal suite, whereas, the quartz-dominated, silicic-rock-hosted occurrences have a Cu-Au-Pb-Zn-Ag metal suite. The mafic-rock-hosted occurrences cluster from unnamed locale A1247 in the west through the Lost Spaniard mine seven kilometers to the east (Figure 17). These occurrences include calcite- and quartz-dominated gangue systems. The cluster of occurrences from the US mine northwest to the Lead Dike mine includes most of the prospects localized along north-northwest-trending structures. These prospects are mostly quartz-dominated and include both mafic- and silicic hosts. To illustrates the variety of mineral occurrences in the Osborne district, the geology of major mines is described below. Individual occurrence descriptions are summarized in Table 7.

The US Mine

The US mine is located near the head of Woodchopper Wash. The

Figure 18. Geologic cross section and map of the US mine.

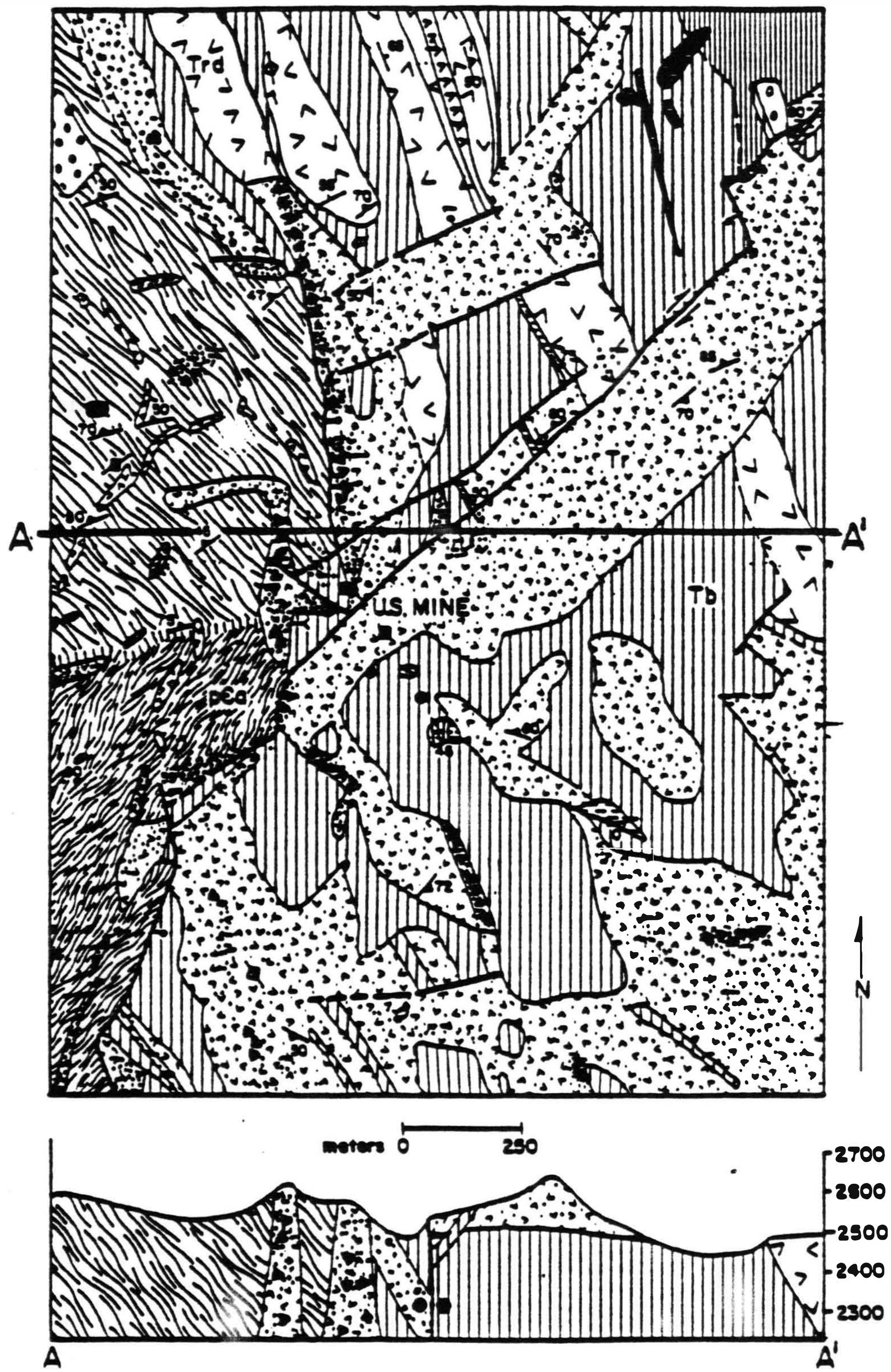

GEOLOGIC MAP AND CROSS SECTION OF THE U.S. MINE

Figure 18. Geologic cross section and map of the US mine.

Quaternary alluvium

Tertiary rhyolite

Tertiary andesite

Tertiary rhyolite

Tertiary rhyodacite

Tertiary basaltic andesite

Tertiary rhyodacite

Tertiary laharic clastics

Precambrian gabbro

Precambrian gneiss

Precambrian amphibolite

Fe + argillic alteration

Breccia

Strike and dip of foliation

Strike and dip of beds

Fault, barb on downthrown side, arrows show lateral motion

Gradational contact

Contact

THIS PAGE

INTENTIONALLY BLANK

prospects cover a north-trending ridge top that contains the most conspicuously iron-oxide-stained rocks in the Big Horn Mountains. Roddy Resources Inc. of Vancouver, B.C. currently controls the property, which consists of ten patented and twelve unpatented claims (Balik, 1985). The property contains two 150 m-deep shafts with crosscuts at the 30 m and 60 m levels. There is also a 30 m adit at the north end of the property. 4,500 tons of dump ore with grades of 0.128 oz Au/ton and 0.5 to 0.75 percent Cu were milled in 1943 (Belik, 1985). In 1961, 133 tons of ore averaging 0.091 oz Au/ton and 2.01 percent Cu were shipped (Belik, 1985). Roddy Resources reports blocking out 565,000 tons of ore at 0.09 oz Au/ton. The geologic setting of the mine is complex. Two, or possibly three, Proterozoic units occur in the western third of the mine area (Figure 18). A medium-grained amphibolite crops out in the southwestern portion of the area. In gradational contact with the amphibolite is a medium-grained to porphyritic gneissic granite. The gneissic granite is commonly mylonitized and inter-tongued with lenses of amphibolite. A small outcrop of tourmalinite (70 percent tourmaline in a milky quartz matrix) exists in the gneissic-granite, but does not have a metamorphic fabric. Consequently, its age is unclear.

Unconformably overlying the basement is 3 to 30 m of greenish, to purplish, laharic sedimentary breccia. Interlayered throughout the Miocene sequence are the mafic flows of Dead Horse basalt. They have highly varied thicknesses and are of discontinuous lateral extent. The flows are purplish-grey or reddish, and generally aphyric, but locally contain clinopyroxene or biotite. The oldest silicic flow unit in the Miocene sequence are grey rhyodacite flows and related dikes and tuffs of the Old Camp member. The unit consists of multiple flows that typically have 8 to 12 percent plagioclase phenocrysts, 2 to 3 percent biotite, and zero to 3 percent quartz. Overlying the Old Camp member, in the northeast corner of the mapped area, is a locally mappable varient of the Dead Horse basalt. The unit consists of red clinopyroxene-bearing dikes and derivative, immature, sedimentary rocks. Lying in angular unconformity over the remainder of the Miocene package are the intensely flow-foliated flows of the Beer Bottle rhyolite. In the US mine area the flows have 5 to 12 percent potassium feldspar phenocrysts, 3 to 5 percent quartz phenocrysts, and, commonly, 1 to 3 percent limonite after pyrite crystals that are usually less than 1 mm in diameter.

The structural setting of the US mine, with a few important distinctions, ascribes to the outline established in the overall geologic setting. In contrast to the regional setting where north-northwest-trending normal faults predominate and northeast-trending structures are of subordinate significance, northeast-trending structures are the loci of major displacement, and north-trending, instead of north-northwest-trending structures, are the secondary loci of displacement (Figure 18). The north- to north-northwest-trending faults appear to be moderate- to high-angle normal faults. These faults dip to the west in the northern quarter of the mapped area, and to the east in the southern three quarters of the mapped area. The northeast-trending faults consistently crosscut the north-trending faults and appear to be right-lateral, strike-slip faults in the southern half of the mapped area, where they have large offsets, and left-lateral faults in the northern part of the area. The northeast-trending faults that offset a block of Beer Bottle rhyolite north of the center of the map are likely to be normal faults with some strike-slip displacement. The major northeast-trending, strike-slip fault that transverses the center of the area demonstrates at least 0.5 km of offset when the immature laharic unit is projected back from the US mine shaft to its companion outcrop in the southwest corner of the map.

Mineralization at the US mine centers on two vertical quartz-veined breccia zones that are offset along a northeast-trending fault. The northern zone varies in thickness from 5 to 25 m and can be traced for 200 m along strike. The southern zone varies similarly in thickness and can be discontinuously traced for 300 m (Kerr et al., 1984). Aerial photographs demonstrate that the US mine is in the northern third of a zone of iron oxide-staining that extends in a north-south trend for over 10 km.

Mineralization occurs as veins and stockworks of quartz at the Proterozoic-middle Tertiary unconformity. In dump material, replacement textures are more prevalent than open-space fillings, but both occur. The ore-grade material is hosted in Beer Bottle rhyolite intrusive dikes, and to a much lesser extent, in the basal laharic sedimentary rocks (Figura 18). The northern ore body is in the hanging wall of a high-angle normal fault of unknown displacement. The fact that the laharic sedimentary rocks are in depositional contact with gneissic granite directly to the north of the mineralized zone suggests that the displacement along the high-angle fault is minimal. The outcropping slickenside planes bounding the ore zone may be a consequence of dike intrusion and rather than true tectonic displacement. Ore-grade material blocked out in the southern zone is more discontinuous, but is also hosted in dikas of Beer Bottle rhyolite, and, to a lesser extent, in basalt.

Iron-oxide staining and argillic alteration extend for up to 0.25 km to the east of the ore zones into the adjacent Beer Bottle Rhyolite. The alteration is much more subdued in the Proterozoic rocks to the west of the main ore zones and in the basalt to the south of the US mine shaft. The Beer Bottle rhyolite has sporatic argillic alteration and limonite-staining throughout the US Mine area. A single multi-element assay of dump material shows the ore to be markedly enriched in Cu and Au and slightly enriched in Ag, W, and Pb (Table 3, XR1 and XR2). Dump material from the US Mine shaft area consists of completely replaced Beer Bottle rhyolite that is now earthy hematite, jarosite, octahedral fluorite,and specularite. Fluorite constitutes a considerable percentage of the gangue and fluorite veins locally occur to 10 cm thicknesses. The most intensely miner-alized rocks have copper carbonates, oxides, and silicates that locally range up to 5 to 10 percent by volume (Belik, 1985). The gold occurs as native gold (Belik, 1985). Inaccessibility of the workings prevented establishing if a sulfide suite still exists, and, therefore, what its paragenesis might be. Observation of the cross-cutting and mutually enclosing relationships of fluorite, specularite, and quartz reveal that they mutually cross-cut each other.

On the assumption that fluorite fluid inclusions are representative of ore-forming conditions at the US mine, homogenization temperatures and freezing point depression temperatures were determined. Fluid inclusions are water liquid-vapor type. and are very abundant in the US Mine specimens. About half of them are sigmoidal and half have angular profiles. Rare inclusions have negative tetrahedral shapes. The inclusions range in their largest diameter from 8 to 50 microns. Vapor bubble volume does not greatly vary and averaged around 10 percent. All of the bubbles had traces of double menisci which are assumed to be a third phase. Preliminary crushing experiments in glycerine revealed some evolution of gas which is presumed to be CO_2. No clathrates were observed upon freezing. Twenty-nine homogenization temperatures were determined (Figure 13). They cluster in a range from 190° to 225° C. One determination was at 235° C. Seven freezing point depressions were determined (Figure 14). These are recorded in NaCl weight equivalents as calculated from Potter (1977), and are not corrected for potential CO_2. The freezing point depressions occur in three groups that range from 8 to 14 percent NaCl equivalent. If a CO_2 correction for 7 percent CO_2 were imposed on the NaCl equivalents, the NaCl equivalents would range from approximately 5.5 to 9.5 percent NaCl weight equivalent (Collins, 1979).

Fluid inclusions in amethyst from the nearby Contact mine were similarly studied to test the assumption that the fluorite from the US mine is representative of fluids at the time of mineralization. Contact mine inclusions are very similar in their morphology to inclusions from US mine fluorite. Seventeen homogenization temperatures were determined. They are coincident in their temperature range with the US mine fluorite homogenizations (Figure 13). Six freezing-point depressions were determined (Figure 14). These were plotted identically to the procedure for other inclusion suites. The NaCl weight equivalents range from 17 to 25 percent. Correction for 7 percent CO_2 (a maximum for non-clathrating CO_2) yields 11.5 to 14.5 percent NaCl equivalent.

Data presented above establish important constraints over the chronology of mineralization in relation to structural history and over the character of mineralizing fluids. The presence of mineralization in the Beer Bottle rhyolite limits the ore forming event to post-emplacement of the Beer Bottle rhyolite, latest Miocene silicic flow, dated at 16.4 Ma (Reynolds et al., this volume). The fact that the Beer Bottle rhyolite lies in angular unconformity over earlier tilted flows argues that mineralization occurred after most of the deformation. The prevalence of vertical to sub-vertical veins throughout the district also argues for a post-tilting chronology. The offsetting of the ore body by splinter faults off of the major northeast-trending strike-slip fault further constrains the timing to prior to the last movement along faults synchronous with the eruption of the Big Horn volcanic. Regional mapping (Capps et al., 1985) suggests that the displacement along the northeast-trending fault is on the order of three to four kilometers. The fact that mineralization is only offset 0.25 km supports the inference that mineralization occurred prior to the end of tectonism.

The fluid inclusion data from both the US mine and the Contact mine display consistent homogenization temperatures, and, even when corrected for possible CO_2, consistently elevated salinities. The consistency of homogenization temperatures from two different gangues that were 1.5 km apart suggest temperature and pressure homogeneity over extended distances. The elevated salinities necessitate a non-meteoric fluid component. The relatively diluted salinities of the US mine in contrast to those of the Contact mine may be interpreted as a function of gradual influx of meteoric fluids over time at the potentially longer lived, US mine system. Alternatively, the salinitiy differences may reflect variation in CO_2 content which exaggerates freezing point depressions (Collins, 1979).

The Tonopah-Belmont Mine

The Tonopah-Belmont mine is located in the eastern part of the Big Horn Mountains and at the west end of the Belmont Mountains (Figure 17). Recorded production from the mine spans from 1926 to 1957, and consists of approximately 1 million lbs. of Cu, 150,000 oz Ag, and 8500 oz Au (AZBGMTfiles). The only current source of activity at the mine is from mineral collectors exploiting the unusual supergene suite found at the mine (Anthony et al., 1977). Mine workings consist of two steep inclines on the north side of Belmont Mountain, a 20 m adit on the south side of Belmont Mountain, a glory hole opening from stopes to the adit, and numerous open cuts circumscribing Belmont Mountain. The workings are reported to have extended to the 125 m level where the ore is faulted off (AZBGMTfiles).

The geologic setting is moderately complex (Figure 19). The mine is hosted in a structurally isolated block of Miocene rocks that are surrounded by Proterozoic phyllite on all sides except to the southeast where the Miocene block is in fault contact with mid-Tertiary (?) Belmont Granite (Capps et al., 1985). The oldest rocks in the mine area are Proterozoic phyllites, which are laminated, steel-grey when fresh, and brown to tan where weathered. Typically the phyllite is fine-grained and consists of 10 percent quartz and 90 percent muscovite. The phyllite generally strikes northeast with highly varied dips that are typically steep. Unconformably overlying the phyllite is a basalt flow that is 10 to 13 m thick. Overlying the earliest basalt flow is a 12 to 18 m of laharic sedimentary rock that is dark grey in outcrop and green-tinted in fresh specimens. The unit has 30 percent subangular phyllite clasts that range from 1 mm to 1.5 cm in diameter.

Rounded quartz pebbles constitute 3 percent of the clasts. Overlying the laharic unit is a flow of basalt that also overlies the Morning Star rhyolite (Capps et al., 1985a). In the mine area the earliest Morning Star rocks are the flow-foliated flows or intrusions that form Belmont Mountain. Phenocryst content is less than 1 percent feldspars that are argillically altered. These rhyolites are commonly brecciated, silicified and slightly to moderately iron-oxide stained. Limonite after pyrite cubes that average 0.1 mm in diameter typically make up 0.1 to 1 percent of the rock. On the northeast end of Belmont Mountain, in uncertain stratigraphic relation to the Belmont Mountain flow-foliated rhyolite, is a sequence of Morning Star tuffs and flow-foliated rhyolite flows. From bottom to top, the sequence is as follows: (1) 6 m of flow foliated, fragmented aphyric rhyolite with 0.3 percent limonite after pyrite and iron oxide stain; (2) 3 m of punky, nonlithic, very fine-grained aphyric tuff of moderate induration, and bearing 0.5 percent, 0.5-mm-on-a-side, cubes of limonite after pyrite cubes: (4) 2.5 m of white and pink moderately-indurated lithic tuff with 40 percent aphyric silicic flow volcanic fragments whose average size is 1 cm: the tuff beds are 3 to 5 cm thick with a trace of limonite after pyrite; (5) 10 m of lithic tuff-bearing 40 to 55 percent aphyric silicic lithic fragments and 5 percent basalt fragments: (6) 11 m of blocky flow-foliated rhyolite with 0.5 percent quartz phenocrysts that average 1mm in diameter, and limonite after pyrite that constitutes 0.8 percent, and averages 0.5 mm in diameter. Rhyodacite dikes that have up to 7 percent plagioclase phenocrysts and sparse quartz phenocrysts intrude the entire sequence, including the youngest basalt flow. The precise extent of the rhyodacite intrusive period is unclear.

Figure 19. Geologic cross section and map of the Tonopah-Belmont mine.

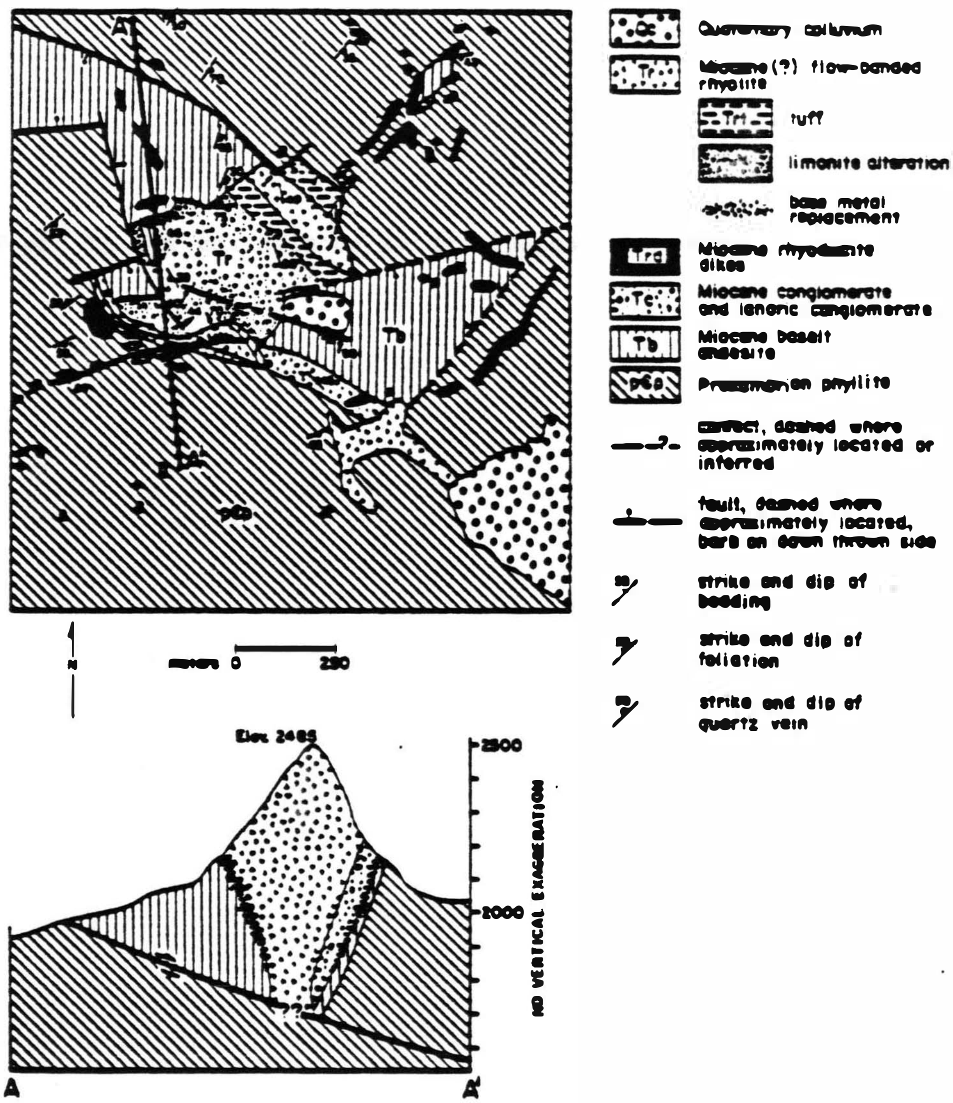

GEOLOGIC MAP AND CROSS SECTION OF THE TONOPAH BELMONT MINE

The major structure of the area is a N40°W-striking, southwest-dipping, low-angle fault that outcrops from 0.5 km northwest of Belmont Mountain for 2 km to the southeast where the fault changes to a north strike and a west dip (Capps et al. 1985). The low- angle fault juxtaposes moderately northeast-dipping rocks in the hanging wall against the Proterozoic phyllite. This major fault is offset by east-northeast-striking cross faults that are loci of mineralization (Figure 19). The N75°E- to N65°E-striking, southeast-dipping normal faults are the localizing structures of the south and north Tonopah-Belmont veins. A N20°W-striking, northeast-dipping normal fault cuts off both veins on the west end of Belmont Mountain. On the east end of Belmont Mountain the northern vein appears to die out whereas the southern vein is offset by a N70W-striking, southwest-dipping normal fault. The structural relationships suggest that mineralization occurred during low-angle faulting, but did not continue after tectonism. The fact that the veins were cut off by a fault at the 130 m level (AZBGMTfiles) supports a syn-tectonism age of mineralization.

The north vein trends N70°E 60°SW, is exposed along strike for 120 m of strike length, and ranges in thickness from 1 to 12 m. The vein is mostly banded milky quartz with lesser copper carbonates as fracture fillings in a fault zone. The encompassing fault zone is at the contact between the basal Morning Star rhyolite flow or intrusion and a basalt flow. Whether the Morning Star unit is an intrusion or a flow determines the exact nature of the localizing contact. The character of this contact is obscured by the highly varied vertical flow foliations in the rhyolite, the absence of demonstrable offset on the north and south sides of the outcrop, and the unclear nature of the contact between the Belmont Mountain massif and the Morning Star tuff to the northeast. The south vein trends N75°E, dips 80°NW, extends for 150 m, and varies from 2 to 10 m in thickness. The south vein is localized at the contact of the basal laharic unit with the lowermost basalt, both of which are in the hanging wall of a steeply-dipping normal fault of small displacement. This vein has mostly milky quartz breccia and replacement textures in contrast to the banded, fracture filling appearance of the northern vein.

Two assays (Table 3, XR12 and XR13), one from slightly iron-oxide-stained Morning Star rhyolite, and the other from high-grade vein material reveal significant enrichment in Cu, Pb, Zn, Au, Ag, As, Cd, and Sb. Cobalt and U are also somewhat anomalous. W. Hunt (personal communication, 1985) reports the presence of 33 phases in the ore: aurichalcite, barite, brochantite, caledonite, cerussite, chalcophanite, chrysocolla, coronadite, covellite, cresseyite, cryptomelane, descloizite, epidote, fornacite, galena, goethite, garnet, hemimorphite, jarosite, lepidochrosite, linarite, malachite, massicot, minium, murdochite, plumbojarosite, pyromorphite, rosasite, tenorite, vanadinite, vauquelenite, willemite, and wulfenite. This author also found sphalerite and calcite. A preliminary paragenesis, of major phases, from early to late is: sphalerite-pyrite-chalcopyrite-galena as primary sulfides, quartz as primary gangue, and aurichalcite, smithsonite, azurite, malachite-calcite, and jarosite as supergene minerals. A single whole-rock analyses of the Morning Star rhyolite (Table 8, XR12, K_2O is 9.99 percent) suggests that the host rocks are potassium metasomatized. A single slide of quartz with sphalerite and copper carbonates was examined for fluid inclusions. The quartz has myriad small inclusions. A couple of two phase, liquid and vapor water inclusions, of workable size were found. They averaged around 5 microns in size. None of the inclusions homogenized at temperatures up to 350° C. It is presumed that the small size of the inclusions metastabily prevented homogenization.

The Scott Mine

The Scott Mine is located eastern Big Horn Mountains. Reported production is from the years 1942 through 1949 when approximately 12,000 lbs. Pb, 500 lbs. Zn, and 100 oz Ag were produced (AZBGMT files). There is a single 30-m-deep shaft. There are also two recently drilled exploration holes of unknown depth.

The Scott Mine is in a topographic basin that has poor exposures. The surrounding terrane is mostly calcite-veined Dead Horse basalt, and lesser Morning Star rhyolite (Capps et al., 1985). The basin is bounded by circuit normal faults on its west, north and east sides. The southern basin margin may also be fault bounded. The Scott Mine is hosted in Dead Horse basalt. Mineralization occurs as a 32 m long vein that ranges from 1 to 2.5 m wide, and varies from a N55°W strike, and 80° NE dip at its southeast end to a N70°W strike and 65°NE dip at its northwest end. The vein is cored by 10 to 40 cm of black calcite and contains outer vein selvages of banded quartz that is 0.5 m thick. Typical dump material is 30 percent black calcite and 70 percent highly altered basalt. The black calcite has a orange mineral found in calcite cleavages that is presumed to be minium. There are small crystals of pyrite in quartz veinlets from dump material of basaltic andesite breccia. Minor chrysocolla and probable rhodocrosite also occur. Two assays of high-grade dump samples assays, one for Pb, Zn and Ag, the other for Ag and Au, suggest the prospect is significantly enriched in

Pb and Ag, but not anomalously enriched in Au or Zn.

Vying on the assumption that the Pb- and Ag-bearing anomalous black calci is paragenetically contemporaneous with the metal phases, fluid inclusion homogenization temperatures and freezing point depression determinations were obtained from calcite. The inclusions are two-phase, liquid-vapor type, that display no evidence of a third phase. The inclusions are commonly dendritic in profile, appear to be necked, and are found in rhombohedral cleavages. One quarter of the inclusions deemed suitable for thermometry are angular in profile and three quarters are spheroidal. The inclusions range in their largest diameter from 10 to 20 microns. Thermometry procedures outlined in earlier sections were followed for these determinations. Thirty-eight homogenization temperatures were obtained. They range from 125° to 370° C and cluster in three groups: from 150° to 170° C, from 250° to 290° C, and from 340° to 370° C (Figure 13). Twelve freezing-point depression determinations ranged from 8 to 22 NaCl weight percent equivalent (Figure 14). The small size of the sample population prevents distinct clusterings from being identified. The wide distribution of both the homogenization temperatures and the freezing point depressions, however, are permissive of a boiling interpretation for the genesis of the calcite. Thermodynamic constraints (Drummand and Ohmoto, 1985) also suggest boiling as a likely genesis for hydrothermal calcite.

Volcanic Enrichment Factors

Assays for fifty-three elements were obtained for four of the major silicic Big Horn volcanic units in order to see if any of the rhyolites are anomalously enriched in base or precious metals, and, therefore, could be a preferred ore host or source. Ratios of elements analyzed

Figure 20. Volcanic enrichment factors plotted as earliest silicic mid-Tertiary eruptive (Morning Star rhyolite) over the latest mid-Tertiary silicic eruptive (Beer Bottle rhyolite). Elements without bars mean both assays were below detection limits. Bars with arrows mean the depleated rock's assay was below detection limits. Where bars are of equal length for each assay, the assays are of equal value.

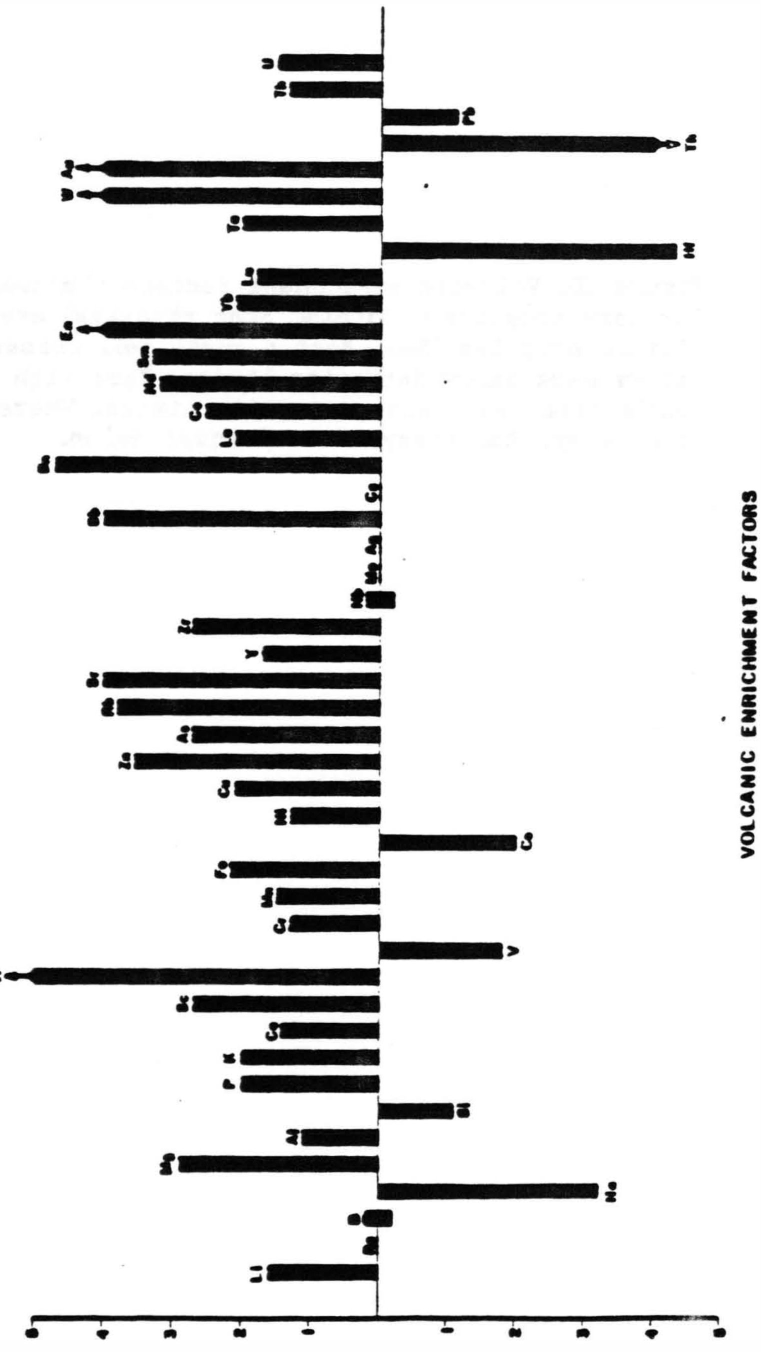
VOLCANIC ENRICHMENT FACTORS

from a pristine sample of Morning Star rhyolite, the earliest silicic eruptive, divided by analyses of pristine Beer Bottle Rhyolite, the latest silicic eruptive were plotted as volcanic enrichment factors to constrain whether concentration of metals early or late in the eruptive history of the volcanics has any relationship to host-rock systematics or chronology-chronology of mineralization (Figure 20). The plot shows enrichment of Cu-Zn-As-Au and W in the earliest eruptive. Pb is enriched in the latest, and Ag assays were below detection limits for both.

Osborne District Summary

Osborne district mineral occurrences display a variety of gangue suites, vein orientations, metal suites, and especially, host rock types. Mineralizations occurs in Proterozoic amphibolite, Late Cretaceous granodiorite, Miocene laharic conglomerate, Miocene Dead Horse basalt Miocene Morning Star Rhyolite, Miocene Old Camp volcanics, and Miocene Beer Bottle rhyolite. Limited geochemical data suggest there are two metal suites that correlate to the two major gangue suites. The gangue suite of quartz plus or minus fluorite correlates to the Cu-Au-Pb-Zn-Ag metal suite, and the gangue suite of black calcite plus or minus quartz correlates to the Pb-Ag metal suite. Vein orientations vary widely, but there is a weak correlation between east-west strikes and the calcite-dominated occurrences at the Valley View group and the Scott lead mine. The Black Pearl mine, the only other calcite-dominated occurrence has a different orientation.

The most obvious overall correlation between these criteria is that the Cu-Au-Pb-Zn-Ag suite is dominantly in the quartz-fluorite occurrences, which are mostly hosted in rhyolites or at the lower contact between rhyolite and the basal laharic sedimentary rocks or basalt. An exception is the Contact mine, which is proximal to the basal Tertiary contact, but is hosted in gneiss, muscovite granite, and a mafic dike. The Well mine is also an exception because it is hosted in Late Cretaceous Granodiorite. The Pb-Ag occurrences also elude systematic correlation of descriptive criteria. However, three of the five Pb-Ag occurrences (The Scott Lead, the Black Pearl, and the Yellow Rock) all occur in basalt and have predominantly black calcite gangue. The Valley View mine, discussed previouly in the Aguila distruct, is exceptional because it is a Pb-Ag-rich manganese occurrence hosted in Sugarloaf rhyolite.

Osborne District Discussion

The fact that most of the Osborne district occurrences are hosted in mid-Tertiary volcanics, along mid-Tertiary structures, and in a discrete north-northwest trending belt, argue for a mid-Tertiary metallogenesis for the entire district. The absence of mineralization that is extensively offset by faults, and the good exposures of slightly offset mineralization in Beer Bottle Rhyolite at the US mine suggest mineralization occurred up until the latest moderate-angle normal fault displacements, approximately 16 Ma (Reynolds et al., this volume). The absence of mineralization in the latest high-angle normal faults makes it unlikely that mineralization continued beyond 16-15 Ma. The presence of mineral occurrences along low-angle structures in the Morning Star Rhyolite at the Moon Anchor mine places a lower time bracket of 21 Ma (radiometric date of Morning Star, Reynolds et al., this volume) on mineralization. The fact that the mineralization is along low-angle faults lends support to this maximum age of mineralization because the low-angle normal faults are likely to be originally formed moderate- to high-angle normal faults that have been rotated to more gentle dips by continued extension. (Reynolds et al., this volume). The constraining of Osborne mineralization to the middle Miocene indicates that the hydrothermal events were contemporaneous with extensive translation of the Big Horn Mountains during middle Tertiary detachment-faulting as documented by Reynolds and Spencer (1985).

The probable contemporaniety of diversely hosted occurrences and the clustering of the district in a north-northwest trend suggests a regionally extensive hydrothermal system was active. The local variation in gangue and metal suites, therefore, may be a function of various of degrees equilibration between the hydrothermal fluids and host rocks. The volcanic enrichment factors lend support to the inference that mineralization is not directly related to the emplacement of specific volcanic flows. The predominant concentration of metals in the earliest flows would lead one to expect that if mineralization were solely related to the emplacement of flows, then mineralization would be restricted to the earliest flows and structures. The fact that the only known ore body in the district occurs in the latest eruptive argues against important influence of local flow's trace element content over mineralization. The high salinities of fluid inclusions selectively studied from the district also support the notion that fluids are regional in character and not local meteoric fluids.

Different mechanisms of mineral precipitation also appear to control metal suites. The relatively high sulfide character (in contrast to the calcite-dominated occurrences) of the US mine and Tonopah-Belmont mine suggest that bisulfide complexing of gold (Barnes, 1979) may have been significant for the gold-rich occurrences. The wide range of salinity values in the US mine fluorites suggests dilution as the mechanism of gold precipitation for these systems. In contrast, the base-metal rich systems, like the Scott Lead mine, seem to be relatively low-sulfide systems. Theoretical studies suggest that base-metals travel as chloride complexes (Barnes, 1979). The preponderance of calcite and permissive evidence of boiling at these occurrences argue that the chloride-complexed, base-metals precipitated as base-metal minerals when the CO_2 buffer was destroyed during boiling (Drummand and Ohmoto, 1985).

Interrelationship of Middle Tertiary Districts

Diverse sets of data suggest that the Harquahala precious metal, the Tiger Wash barite-fluorite, the Aguila manganese, and the Osborne base and precious metal districts have an interrelated genesis. The most provocative evidence is the tight spatial overlap of the four districts. The Harquahala district precious-metal and fluorite occurrences end within two kilometers of the westernmost Tiger Wash occurrence (Figure 11). The westernmost manganese-calcite is 0.3 km west of the easternmost barite occurrence, the White Rock claims. The Aguila district is devoid of base-metal values until its easternmost extent, at the Valley View claims (Figure 13), where assays run as high as 2.9 oz Ag/ton and 15 percent lead (Hewett, 1964). The precise chronological relationshipe between these districts is not obvious. The localization of each of these districts in middle Tertiary structures, in conjunction with K-Ar chronology, brackets them all between Early and Middle Miocene. Host-rock relationships permit mineralization to have begun after the emplacement of the earliest volcanic flows in each respective section. The presence of manganese in the Sugarloaf rhyolite at the Pumice claims (Figure 13) suggests some manganese mineralization occurred after 19.6 Ma (Reynolds et al., this volume). The presence of Osborne district mineralization in the highest silicic flows requires that some Osborne district mineralization postdates the 16.4 Ma Beer Bottle rhyolite (Reynolds et al. this volume). These brackets imply that mineralization is progressively younger to the east.

Limited fluid-inclusion data from each district present provocative similarities. The apparent absence of secondary inclusions from each district argues against important multiple phases of mineralization. The coincidence of homogenization temperatures and freezing-point depressions from occurrences lacking evidence of boiling furthers this inference. The pervasively high salinities found in all inclusions that lack evidence of boiling is suggestive evidence for a similar provenance of fluids for each district. Roedder (1984) reports that the NaCl weight equivalents (salinities) of epithermal occurrences are generally low, ranging from 0 to 5 percant; 12 percent is considered to be the extreme of typical epithermal occurrences. The salinities throughout the Big Horn Mountains and in the Harquahala district are mostly above 12 percent, even if one accounts for the maximum possible exaggeration by CO_2 clathrating. These salinities suggest that either some unknown process is concentrating alkalis throughout the range or that all of the fluids have a non-meteoric character, and therefore, may have a similar origin.

The observation of widespread K-metasomatism presents another attribute, which, along with the fluid-inclusion data, suggest affinity of range-wide hydrothermal fluids. Rehrig et al. (1980) established the presence of high-K rocks in the adjacent Vulture Mountains, and Capps et al. (this volume) present similar evidence for widespread, albeit, sporatic, K-metasomatism of the Big Horn volcanics (Table 8). The potassium enrichment of Late Cretaceous granodiorite near the Blue Hope mine (Table 8) qualitatively illustrates the extent of K-metasomatism. If the model presented for generation of manganese occurrences by K-metasomatism model is accepted, then the observation of calcite veining in Dead Horse basalts from the easternmost barite occurrence all the way through the easternmost Osborne occurrence further illustrates the extent of metasomatism and its important spatial association in each

Figure 21. Schematic cross section through the mid-Tertiary mineral districts of the Big Horns. Big arrow represent high salinity, CO_2-bearing fluids. Small arrows represent meteoric waters. The meteoric fluids flowing down the detachment are shown driving connate waters toward the east.

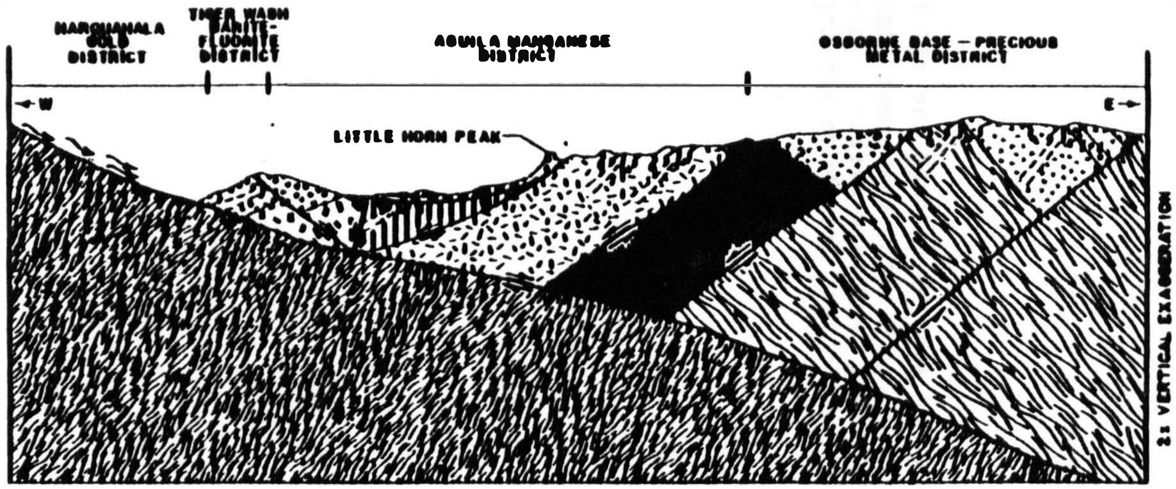

SCHEMATIC CROSS SECTION OF THE BIG HORN MOUNTAINS

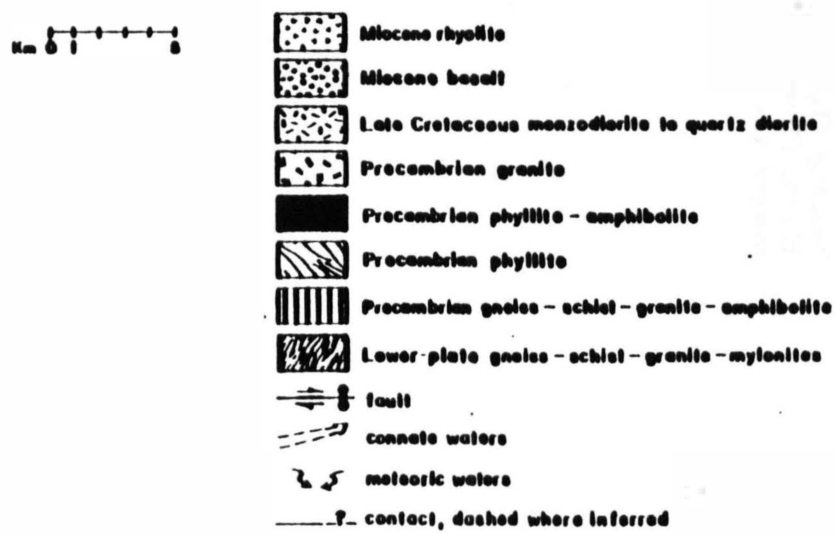

127

Table 8. Whole rock analyses are from widely seperated sample location of the same unit. They are displayed to qualitatively demonstrate the widespread occurrence of potassium metasomatism in the region. The upper assay of the pairs is a relatively pristine sample. The lower assay or assays are potassium metasomatised. The lower assay from the basalts is probably not K-metasomatised. The sample locations and rock types are as follows: 853-26-1, S 1/2 Sec 13, T5N R8W, Aguila 15', Blue Hope, N 1/2 Sec 31, T5N R8W, Big Horn 15', both are Late Cretaceous Granodiorite; BH-56, S 1/2 Sec 22, T5N R8W, Aguila 15', 72-60, N1/2 Sec 24 (Rehrig et al., 1980), T7N R6W, Vulture Mountains 15', both are mid-Miocene basaltic andesite; BHC-211 S 1/2 Sec 6, T3N R7W, Belmont Mts. 15', Beer Bottle rhyolite, BHC-215 S 1/2 Sec 30, T5N R7W, Big Horn 15', Old Camp rhyolite, and XR12, W 1/2 Sec 36, T4N R7W, Belmont Mts. 15', Morning Star rhyolite.

Table 8. Potassium-Metasomatized Rocks

Sample Unaltered-*Altered	SIO2	AL203	CAO	MGO	NA20	K20	FE203	MNO
853-26-1	66.7	15.5	3.51	1.56	3.73	3.87	3.66	0.06
*Blue Hope	65.5	15.8	2.96	1.77	3.20	5.03	4.18	3.20
BH-56	49.0	15.4	11.2	9.08	2.66	0.77	8.88	0.14
72-60	59.8	14.3	6.40	4.54	2.92	1.84	2.38	0.10
BHC-211	77.3	12.2	0.33	0.08	4.36	4.45	0.81	210ppm
*BHC-215	71.2	13.9	0.28	0.29	1.61	9.58	1.70	620ppm
*XR12	74.0	12.6	0.26	0.17	0.30	9.99	1..7	40ppm

Sample	TIO2	P205	CR203	LOI	SUM	RB	SR	Y	ZR	NB	BA
853-26-1	0.42	0.13	0.01	0.62	100.0	150	590	10	160	10	1010
*Blue Hope	0.41	0.14	0.03	3.39	100.4	200	830	10	160	10	2290
BH-56	1.00	0.42	0.03	1.47	100.2	30	760	20	110	20	440
72-60	0.80	—	—	—	—	—	—	—	—	—	—
BHC-211	—	0.03	130ppm	0.54	100.0	120	10	30	60	40	110
*BHC-215	0.32	0.06	62ppm	0.93	100.1	290	80	40	300	30	1420
*XR12	0.22	0.04	0.02	0.70	99.7	250	70	50	210	30	1380

district.

Although the major differences in the character of the middle Tertiary districts suggests different ore-forming conditions, a few occurrences suggests nearly identical ore-forming conditions existed in distinct districts. The character of the important US mine deposit and the gold occurrences on the Bullard detachment fault both suggest that CO_2-bearing, Au, Ag, Cu, Si, Fe, and F enriched fluids precipitated minerals at temperatures between 160° to 230° C, under low f_S and high f_{O2}. The solutions probably differed in their alkali and base metal content. The Bullard fluids were probably Ca-rich, K-poor, and depleted in Pb and Zn, whereas the US mine fluids were probably K-rich, Ca-poor, and enriched in Pb and Zn. The silver-lead-rich, calcite-gangue-dominated character of the Valley View prospects in the Aguila district and the Scott Lead and Black Vulture prospects of the Osborne district suggest that CO_2-bearing fluids enriched in Ag, Pb, and possibly Zn, precipitated metals under low f_s, very high f_{O2}, boiling conditions.

A Model for Middle Tertiary Districts
of the Big Horn Mountains

Mineralization in the Harquahala district, the Tiger Wash district, the Aguila district, and the Osborne district is a result of intense local thermochemical changes precipitating metals that were probably locally derived from host rocks proximal to the site of the mineral occurrences. The fluids originally were high-K, CO_2-bearing solutions of basinal brine (?) origin which were mobilized throughout the upper-plate of a detachment fault. Fluid-flow associated with the formation of specific mineral occurrences may be driven by one or more of the following: regional and local geothermal gradients, topographically controlled fluid regimes, and tilting of upper-plate structural block (Figure 21).

Controls over thermal and hydrologic gradients for the eastern Harquahala and Tiger Wash districts are: (1) the initially elevated temperatures of brines compared to meteoric water (Beane and Wilkins, 1985); (2) tilting of upper-plate blocks and consequent gravity-driven fluid-flow; and (3) regionally elevated geothermal gradients as a result of middle- to lower-crustal rocks rising to upper-crustal levels (Spencer and Welty, 1985). Beane and Wilkins (personal communication, 1985) invoke basinal brine solutions as the detachment-fault-related, ore-forming fluids to account for the high salinities, commonplace CO_2, local methane, and high fluid-inclusion homogenization temperatures of lower-plate fluid inclusions. They believe that the fluids had to be thermally elevated before interacting with the hot lower-plate rocks because they believe lower-plate rocks are not hot enough to account for the 200° to 300° homogenization temperatures. The mineral occurrences of the eastern Harquahala district are probably the result of local thermal gradients directly above the Bullard detachment fault. The overlying column of rock, and probable depth of mineralization was probably the Tiger Wash Miocene section, which is approximately 1 km thick. Presumably, the gold-copper-rich (plus or minus fluorite) character of the Harquahala occurrences is a reflection of metal scavenging from lower-plate amphibolite and granite. The barite-fluorite occurrences of the Tiger Wash district are presumed to be a consequence of cooling and dilution of fluids that flowed up from the hot lower plate. The barite-fluorite occurrences probably formed 0.3 to 0.5 km below the paleo-surface. The source of the ionic species is unconstrained, but preliminary speculation is warranted. The presence of sulfides in the eastern Harquahala district, and the likelyhood that these fluids flowed into the overlying Miocene volcanics points to the lower-plate as a source of SO_4. The common presence of fluorite in the Bullard detachment-hosted occurrences similarly suggests F originated from the lower-plate rocks. Isotopic studies on similar occurrences suggest Ca is derived from the fluorite-hosting basalts (Ruiz et al., 1985). Presumably, the Ba was derived from the arkoses and arkosic conglomerates which are proximal to the occurrences.

The hydrologic regime of the Aguila district may have been a consequence of: (1) meteoric waters recharging off of the southeastern flank of the Harquahala Mountains antiform, and, subsequently, driving K-rich, CO_2-bearing, connate waters to the east, down into the Big Horn Mountains upper-plate; and (2) gravity driven, downward, fluid-flow as a consequence of tilting of upper-plate blocks and subsequent heating of the water at the hot, lower-plate rocks. Leach et al. (1983) postulate a meteoric recharge system for the Mississippi Valley ore-forming fluids. They envisioned the foreland of the Ouachita Mountains as a recharge area driving basinal brines to the north. The presence of a relatively thick sequence of fluvial sedimentary rocks at the west end of the Big Horn Mountains suggests surface waters may have been recharged there. The rapid mid-Tertiary extension rates, and consequent tilting of upper-plate rocks, may account for some gravity driven fluid-flow. When the fluids reach the high heat-flow from the lower-plate a hydrothermal cell would be set up. Upon encountering the Miocene basalts, high in the upper- plate (approximately 0.3 km from the surface), the K-rich fluids reacted with Ca-bearing phases in the basalt, thereby, evolving Ca and Mn. Concurrent boiling, as a result of released pressure in fracture and fault zones, caused co-precipitation of calcite and manganese oxides.

Thermal and hydrological regimes for the Osborne district are much more difficult to constrain than those for the eastern Harquahala, Tiger Wash, and Aguila districts. Significant flushing of connate waters by meteoric waters is unlikely because of the large distance from the proposed Bullard recharge zone, and the fact that Osborne occurrences are generally not localized along major structures. Instead, elevated thermal gradients attendant to the emplacement of high-level-rhyolite-feeder dikes, and gravity driven fluid-flow (outlined above) are presumed to be the causes of fluid-flow in the Osborne district.

Local emplacement of high-level, rhyolite, feeder stocks is assumed to be the major control over the genesis of gold-rich occurrences (US mine, and Tonopah-Belmont mine) in the Osborne district. Presumably, high-K, CO_2-bearing fluids were mobilized as a consequence of stock emplacement. The longest-lived systems extensively equilibrated with country rocks, and, during the thermal decline of the systems, precipitated base- and precious-metals in response to cooling and dilution. The dilution of the ore-bearing fluids is a result of the influx of meteoric fluids. The widespread occurrence of breccia at the US mine suggests boiling may also have contributed to metal precipitation.

Because precipitation of metals in the Pb-Ag-rich occurrences of the Osborne district occurred predominantly in a major north-northwest-trending fracture zone that extends for over 12 km, and not along the regional normal faults which are assumed to be through-going to a underlying detachment fault or faults, it is unlikely that major faults influenced mineralization. Consequently, the model for gravity-induced fluid-flow is preferred in explaining the majority of the Osborne district occurrences. Flow up into the upper-plate structural blocks presumably allowed cation exchange of the K-rich fluids with the Ca-rich host rocks thereby causing the fluids to be saturated with Ca. The highly fractured character of the hosting basalts caused boiling and consequent precipitation of calcite. The sudden drop in f_{CO2} caused destabilization of base-metal chloride complexes and consequent base-metal precipitation. The base-metal character of the fluids is assumed to be a result of leaching of metals from the metavolcanic-Proterozoic basement. The fact that manganese oxides are sparingly present suggests the f_{O2} of the fluids was significantly lower than the f_{O2} of the Aguila district fluids.

APPENDIX: INDUSTRIAL MINERAL RESOURCES

Magnetitic Alluvium

Approximately 6,000 acres of alluvial plain have been located by Fred R. Brown of Picacho as a large magnetite placer deposit in the Big Horn Mountains... The alluvial area comprises parts of secs 9, 10, 14, 15, 16, 17, 19, 20, 21, 22, 23, 27, 28, 29, 30, and 32, T4N, R9W... The magnetite placer area starts about 17 miles south of the town of Aguila, just east of the Aguila Tonopah road.

Titaniferous magnetite occurs in alluvium and stream gravels reportedly ranging from a few feet to more than 100 feet. The magnetite with minor amounts of ilmenite makes up 3 to 7 percent of the alluvium; parts of the deposit contain as much as 10 percent magnetite.

Benefication tests made by lessees in 1961, including screening and megnetic seperation, yielded concentrates containing 65 to 69 pecent iron and 0.3 to 0.8 percent titania. The area has been prospected by scattered pits 10 and 15 feet deep. (Harrier, 1964).

Perlite

Outcrops of the Sugarloaf rhyolite in Sec 10, 11, 14, and 15, T4N R8W, Big Horn Mts. 15' have an unassessed amount of perlite (MRDS).

REFERENCES

Anthony, J.W., Williams, S.A., and Bideaux, R.A., 1977, Mineralogy of Arizona: Tucson, University of Arizona Press, 255 p.

AZBGMT files (Arizona Bureau of Geology and Mineral Technology Files).

Barnes, H.L., 1979, Solubility of ore minerals, in Barnes, H.L. ed., Geochemistry of Hydrothermal Ore Deposits (2d ed.): New York, John Wiley & Sons, p. 404-454.

Beane, R.E., and Wilkins, J. Jr., 1985, Thermal Regimes in the Detachment Fault Environment as Deduced From Fluid Inclusions [abs.]: Sedona, AZ., Lunar and Planetary Science Conference.

Belik, G.D., 1985, Preliminary economic evaluation of the Big Horn Gold

Prospect, private report prepared for Roddy Resources Inc.: Vancouvar, B.C., 15 p.

Berg, L., Leveille, G., and Geis, P., 1982, Mid-Tertiary detachment faulting and manganese mineralization in the Midway Mountains, Imperial County, California, in Frost, E.G., and Martin, D.L. eds., Mesozoic-Cenozoic tectonic evolution of the Colorado River Region, California, Arizona, Nevada: San Diego, Cordilleran Publishers, p. 299-311.

Blount, C.W., 1977, Barite solubilities and thermodynamic quantities up to 300 degree C and 1400 bars: Ame. Mineral., v. 62, p. 942-957.

Bodnar, R.J., and Bethke, P.M., 1984, Systematics of stretching of fluid inclusions I: Fluorite and sphalerite at 1 atmosphere confining pressure: Econ. Geol., v. 79, p.141-162.

Boyle, 1979, The Geochemistry of Gold and its deposits: Geologic Survey of Canada, Bulletin 280, 584 p.

Capps, R.C., Reynolds, S.J., Stimac, J.A., Kortemeier, C.P., Allen, G.B., and Scott, E.A., 1985, Preliminary geologic map of the Belmont and eastern Big Horn Mountains, West-Central Arizona: Arizona Bureau of Geology and Mineral Technology Open File 85-15, 25 p.

Carmichael, I.S.E., Turner, F.J., and Verhoogan, J., 1974, Igeneous Petrology: New York, McGraw-Hill, p.33.

Collins, P.L.F., 1979, Gas Hydrates in CO2-bearing fluid inclusions and the use of freezing data for the estimation of salinity: Econ. Geol., v. 74, p. 1435-1444.

Colvinel, A.C., Andrews. A.J., Cherryl, M.E., Durocher, M.E., Fyon, A.J., Lavigne, Jr., M.J., MacDonald, A.J., Soussan Marmontl, Poulson, K.H., Springer, J.S., and Troop, D.G., 1984, An integrated model for the origin of Archean lode gold deposits: Ontario Geological Survey, 100 p.

Coney, P.J., Reynolds, S.J., 1980, Cordilleran metamorphic core complexes and their uranium favorability: U.S. Dept. of Energy, 627 p.

Davis, G.H., 1981, Regional strain analysis of the superposed deformations in southeast Arizona and the eastern Great Basin: Arizona Geological Society Digest, v. 14, p. 155-172.

Denton, T.C., and Kumke, C. A., 1949, Investigation of the Snowball Fluorite Deposit, Maricopa Count, Arizona: U.S. Bureau of Mines Report of Investigation 4540, 15 p.

Dreier, J., 1985, Regional tectonic control of epithermal veins in the western United States and Mexico: Arizona Geological Society Digest, v 15, p. 28-53.

Drummand, S.E., and Ohmoto, H., 1985, Chemical evolution and mineral deposition in boiling hydrothermal systems: Econ. Geol., v. 80, p. 126-147.

Farnham, L.L., and Stewart, L.A., 1958, Manganese deposits of western Arizona: U.S. Bureau of Mines Information Circular 7843, 87 p.

Hardy, J.J.,Jr., 1984, The structural geology, tectonics, and metamorphic geology of the Arrastre Gulch Window, south-central Harquahala Mountains, Maricopa County, Arizona (M.S. thesis): Flagstaff, Northern Arizona University, 99 p.

Hedenquist, J.W., and Henley, R.W., 1985, The importance of CO_2 on freezing point measurements of fluid inclusions: evidence from active geothermal systems and implications for epithermal ore deposit: Econ. Geol., v. 80, p. 1376-1406.

Hewett, D.F., 1964, Veins of hypogene manganese oxide minerals in the southwestern United States. Econ. Geol., v.59., p. 1429-1472.

Hewett, D.F., 1972, Manganite, hausmannite, braunite: features, modes of origin. Econ. Geol., v. 67, p. 83-102.

Hewett, D.F., and Fleischer, M., 1960, Deposits of the manganese oxides, Econ. Geol., v. 55., p 1-55.

Holland, H.D., and Malinin, S.D., 1979, The solubility and occurrence of non-ore minerals, in Barnes, H.L. ed.: New York, Geochemistry of Hydrothermal Ore Deposits, John Wiley & Sons, p. 461-508.

Jones, E.L., and Ransome, F.L., 1920, Deposits of manganese ore in Arizona: in Ransome, F.L. and Burchard, E.F., eds. Contributions to Economic Geology, U.S.G.S. Bulletin 710, p. 135-143.

Keith, S.B., Gest, D.E., DeWitt, E., Woode-Toll, N., and Everson, B.A., 1983, Metallic mineral districts and production in Arizona: Arizona Bureau of Geology and Mineral Technology Bulletin 194, 58 p., scale 1:1,000,000.

Kerr, Dawson, and Associates, 1984, Report on the Big Horn property, Maricopa County, Arizona, U.S.A.: Roddy Resources, Vancouvar, B.C., 33 p.

Leach, D.L., Viets, J.G., Rowan, L., Appalachian-Ouachita orogeny and Mississippi Valley-type lead-zinc deposits [abs]: GSA Abstracts and Programs, v. 16, p. 572.

Masuda, A., Nakamura, N., and tanaka, T., 1973, Fine structures of mutually normalized rare-earth patterns of chon drites: Geochim. et Cosmochim. Acta, v.37, p. 239-248.

Metzger, O.H., 1938, Gold mining and milling in the Wickenburg Area, Maricopa and Yavapai Counties, Arizona: U.S. Bureau of Mines Information Circular, no. 6991, 78 p.

MRDS (Mineral Resource Data System), 1983: U.S. Geological Survey.

Potter, R.W., Clynne, M.A., and Brown, D.L., 1978, Freezing point depressions of aqueous sodium chloride solutions: Econ. Geol., v. 73, p., 284-285.

Roedder, E., 1984, Fluid inclusions: Reviews in mineralogy, Amer. Miner., v. 12, 644 p.

Rehrig, W.A., Shafiqullah, M., and Damon, P.E., 1980, Geochronology, geology, and listric normal faulting of the Vulture Mountains, Maricopa County, Arizona: Arizona Geological Society Digest, v. 12, p.89-110.

Rehrig, W.A., and Reynolds, S.J., 1980, Geologic and geo- chronologic reconnaissance of a northwest-trending zone of metamorphic core complexes in southern and western Arizona, in Crittenden, M.D., Jr., et al., eds., Cordilleran Metamorphic Core Complexes: Geologic Society of America Memoirs 153, p. 131-157.

Rehrig, W.A., and Heidrick, T.L., 1972, Regional fracturing in Laramide stocks of Arizona and its relationship to porphyry copper mineralization: Econ. Geol., v. 67, p. 198-213.

Reynolds, S.J., 1980, Geologic framework of West-Central Arizona: Arizona Geological Society Digest, v. 12, p.1-14.

Reynolds, S.J., 1982, Multiple deformation in the Harcuvar and Harquahala Mountains, west-central Arizona, in Frost, E.G., and Martin, D.L. (eds.), Mesozoic-Cenozoic tectonic evolution of the Colorado River Region: San Diego, Cordilleran Publishers, p. 137-142.

Reynolds, S.J., 1985, Geology and geochronology of the South

Mountains, central Arizona: Arizona Bureau of Geology and Mineral Technology Bulletin 195, 61 p., scale 1:24,000.

Raynolds, S.J., Spencer, J.E., and Richard, S.M., 1983, A field guide to the northwestern Granite Wash Mountains west-central Arizona: Arizona Bureau of Geology and Mineral Technology Open-File Report 83-24, 9 p.

Reynolds, S.J., and Spencer, J.E., 1984, Geologic map of the Aguila Ridge-Bullard Peak area, eastern Harcuvar Mountains, west-central Arizona: Arizona Bureau of Geology and Mineral Technology Open-File Report 84-4, scale 1:24,000.

Reynolds, S.J., and Spencer, J.E., 1985, Evidence for large - scale transport of the Bullard Detachment fault, West-Central Arizona, Geology, v. 13, no.5, p. 353-357.

Reynolds, S.J., Scott, E.A., and O'Haire, R.T., 1985, A Fluorite Bearing Granite, Fieldnotes: Ariz. Bureau of Geol. and Min. Tech., v.15, no.2, p.3-5.

Reynolds, S.J., Capps, R.C., Allan, G.B., Stimac, J.A., Kortemeier, K. P., Spencer, J.E., and Scott, E. ., in preperation, Geology and mineral resources of the Big Horn and Belmont Mountains: Arizona Bureau of Geology and Mineral Technology.

Richardson, C.K., and Holland, H.D., 1979a, The solubility of fluorite in hydrothermal solutions, an experimental study: Geochim. et Cosmochim. Acta., v. 43, p. 1313-1325.

_______, 1979b, Fluorite deposition in hydrothermal systems: Geochim. et Cosmochim. Acta, v. 43, p. 1327-1335.

Ruiz, J., Kesler, S.E., Jones, L.M., 1985, Strontium isotope geochemistry of fluorite mineralization associated with fluorite-rich igneous rocks from the Sierra Madre Occidental, Mexico: possible exploration significance: Econ. Geol., v. 80, pp. 33-42.

Spencer, J.E., and Welty, J.W., 1985, Possible controls of base and precious metal mineralization associated with Tertiary detachment faults in the Lower Colorado River Trough, Arizona and California, Geology, in press.

Stewart, L.A., and Pfister, A.J., 1960, Barite deposits of Arizona: U.S. Bureau of Mines Report of Investigation 5651, 89 p.

Van Nordt, S.D., and Harris,M., 1985, Geology and mineralization of the Picacho Gold Prospect, Imperial County, California: Arizona Geological Society Digest, v. 15, p. 175-187.

Welty, J.W., Spencer, J.E., Allen, G.B., Reynolds, S.J., and Trapp., R.A., 1985, Geology and production of middle Tertiary Mineral districts in Arizona, Arizona Bureau of Geology and Mineral Technology Open File report 85-1.

Wedepohl, K.H., executive director, 1969-1978, Handbook of Geochemistry 2 vols: New York, Springer, 25-D-12 and 13.

Wernicke, B., 1981, Low-angle normal faults in the Basin and Range Province: nappe tectonics in an extended orogen: Nature, v. 291, p. 645-648.

White, D.E., 1980, Active geothermal systems and hydrothermal ore deposits: Econ. Geol., 75th anniversary volume, p. 392-423.

Wilkins, J. Jr., and Heidrick, T.L., 1982, Base and precious metal mineralization related to low-angle tectonic features in the Whipple Mountains, California and Buckskin Mountains, Arizona, in Frost, E.G., and Martin, D.L., eds., Mesozoic-Cenozoic tectonic evolution of the Colorado River Region, California, Arizona, and Nevada: San Diego, Calif., Cordilleran Publishers, p. 182-204.

Wilson, E.D., Moore, R.T., and Pierce, H.W., 1957, Geologic map of Maricopa County, Arizona: Arizona Bureau of Mines, scale 1:375,000.

Wilson, E.D., and Butler, G.M., 1930, Manganese ore deposits in Arizona: Arizona Bureau of Mines Bulletin 127, 107 p.

Wilson, E.D., Moore, R.T., and Cooper, J.R., compilers, 1969, Geologic map of Arizona Arizona Bureau of Mines and U.S. Geological Survey, Scale 1:500,000.

MAPS

THIS PAGE

INTENTIONALLY BLANK

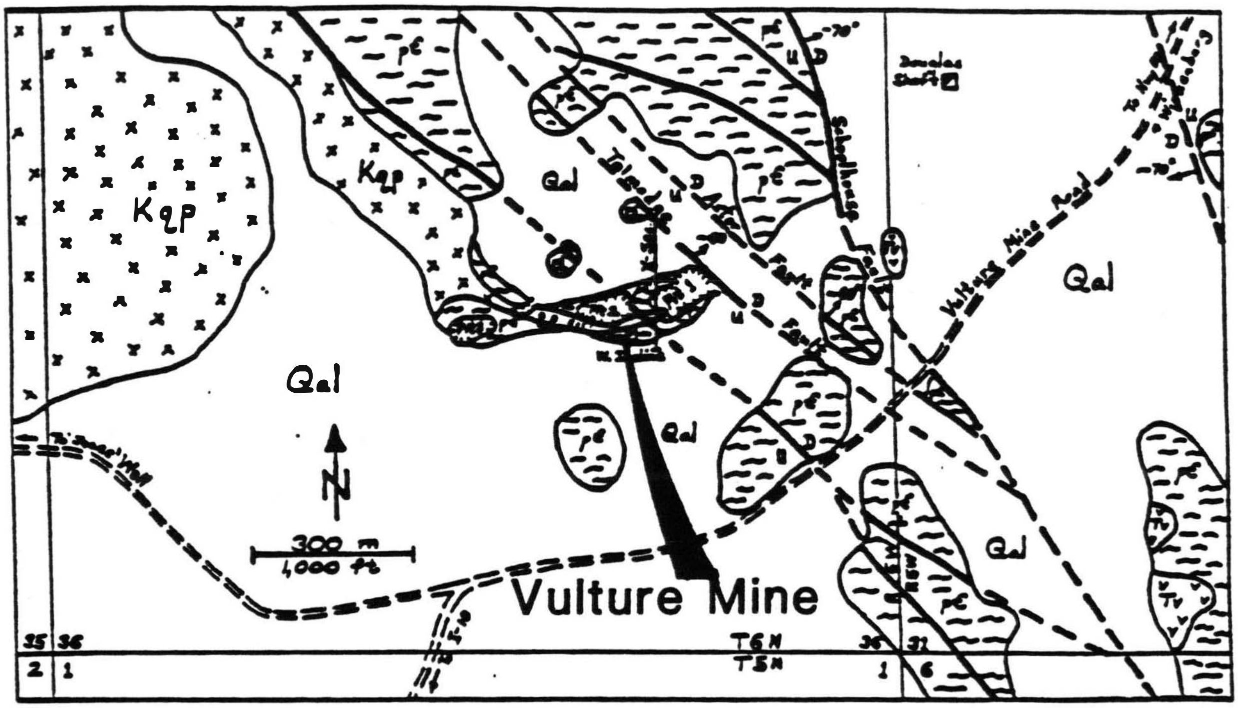

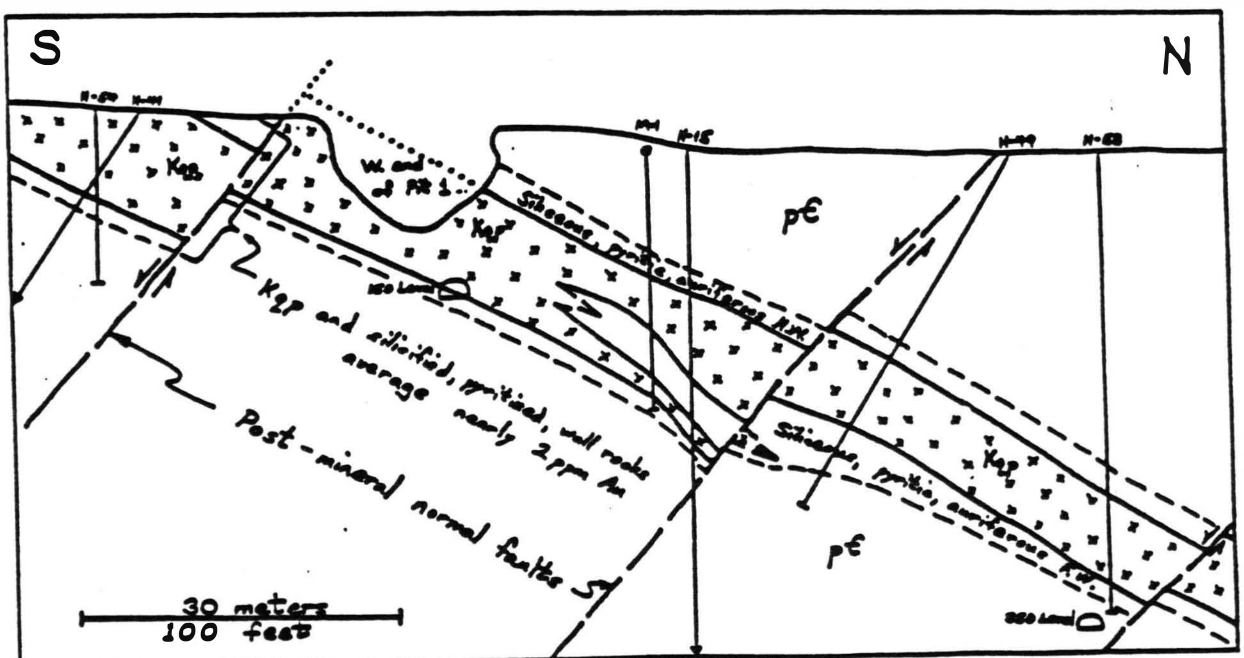

from White (1988)

VULTURE MINE GEOLOGY

Map 1

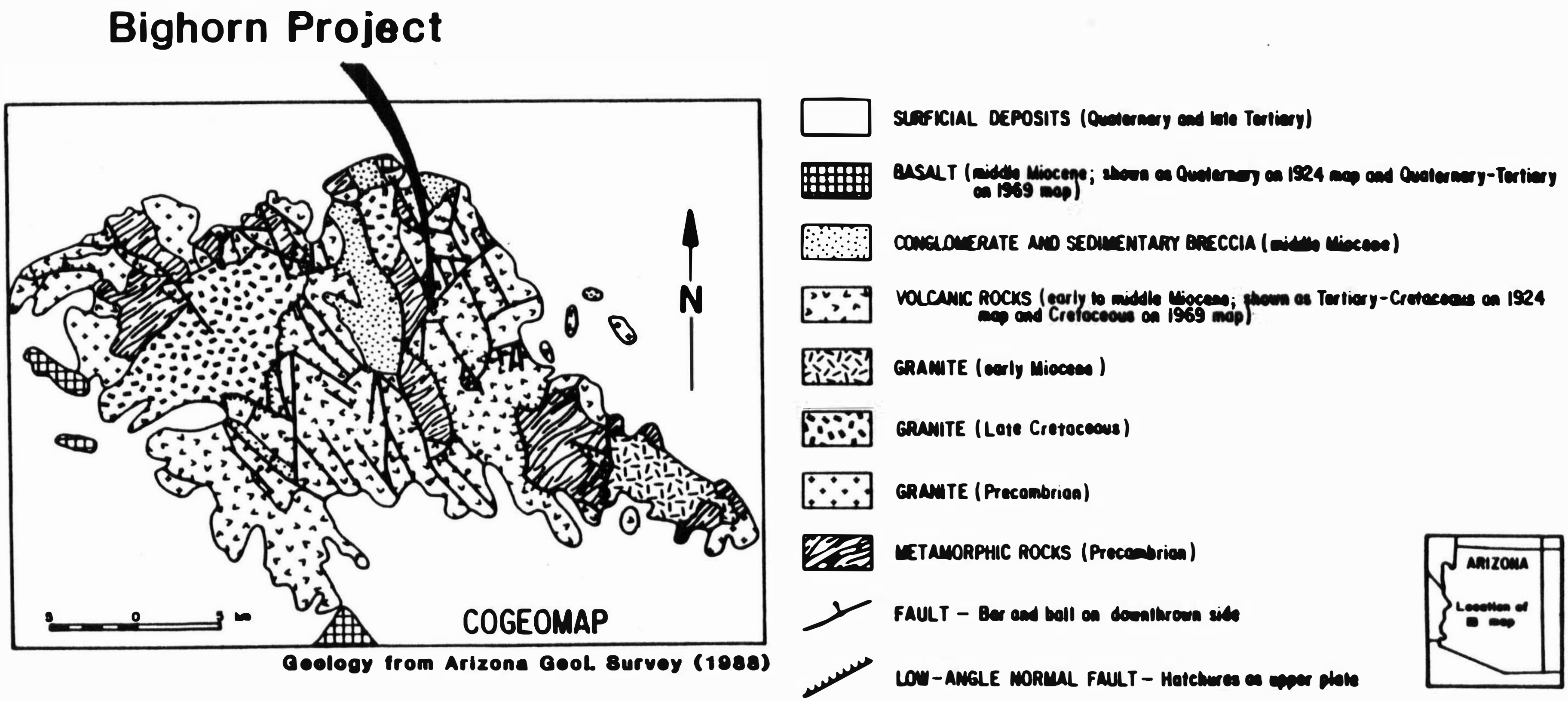

Geology from Arizona Geol. Survey (1988)

BIGHORN MOUNTAINS

Map 2

BIGHORN PROJECT GEOLOGY

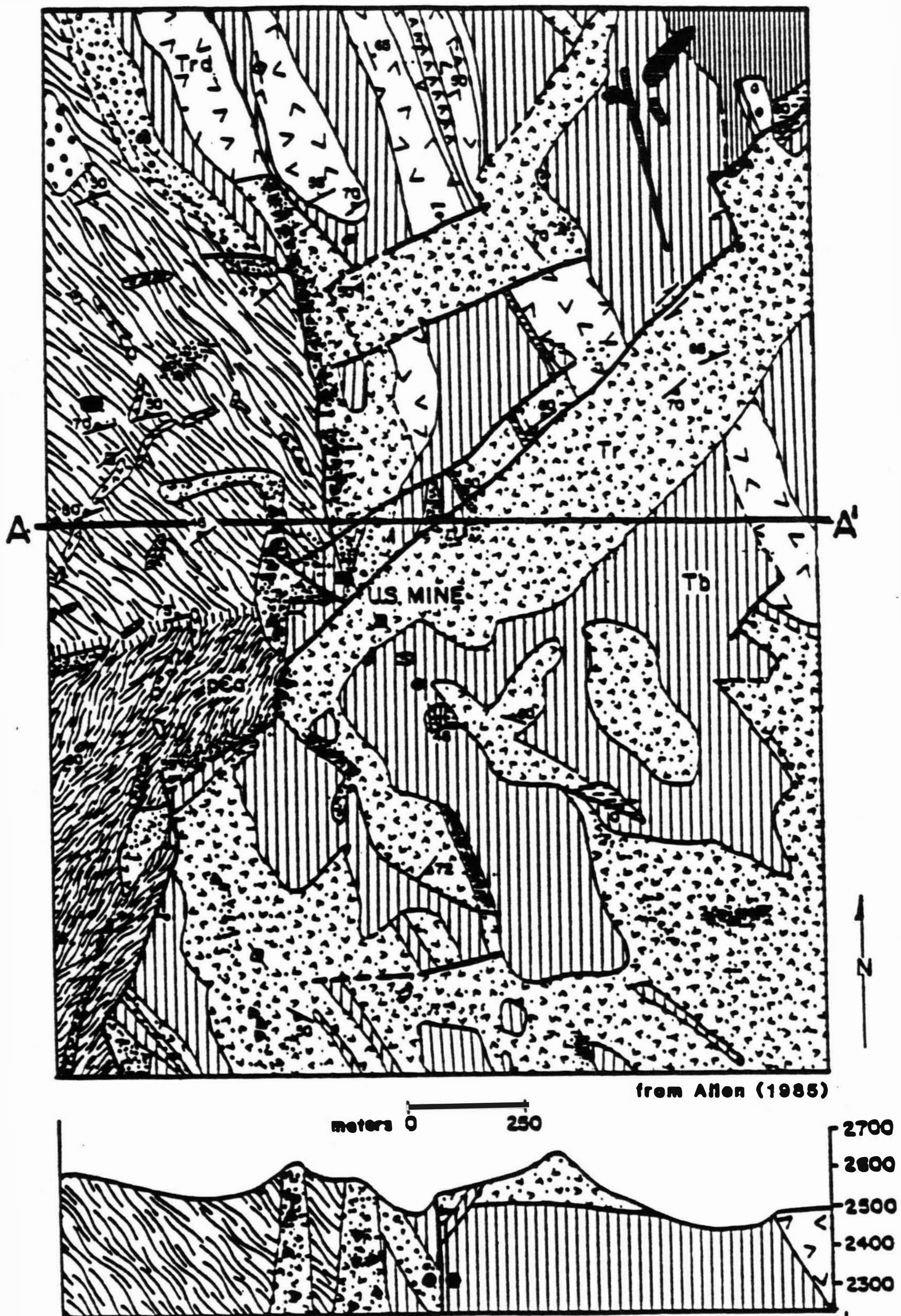

from Allen (1985)

Map 3

GEOLOGIC MAP AND CROSS SECTION OF THE U.S. MINE

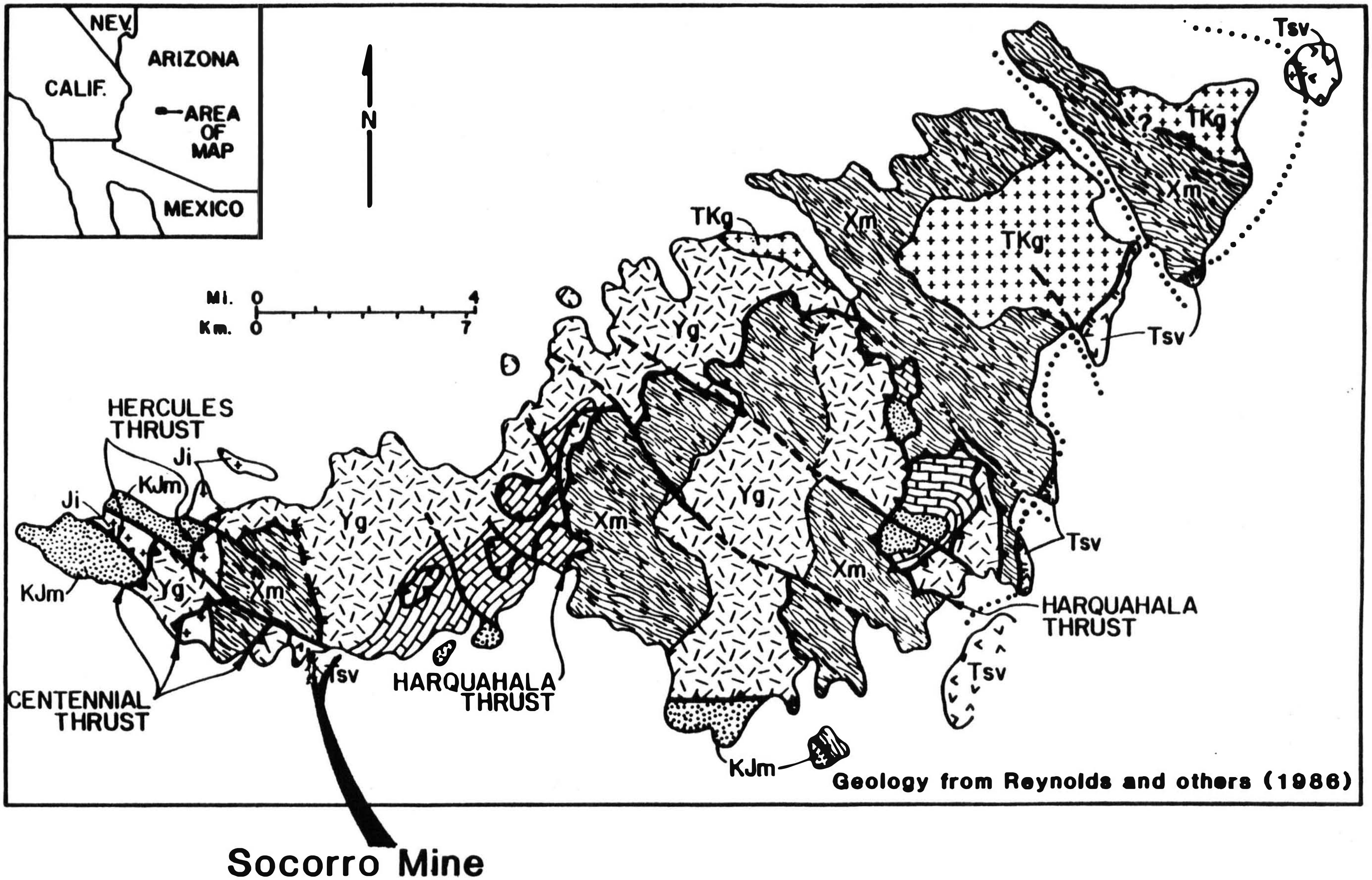

HARQUAHALA MOUNTAINS

Map 4

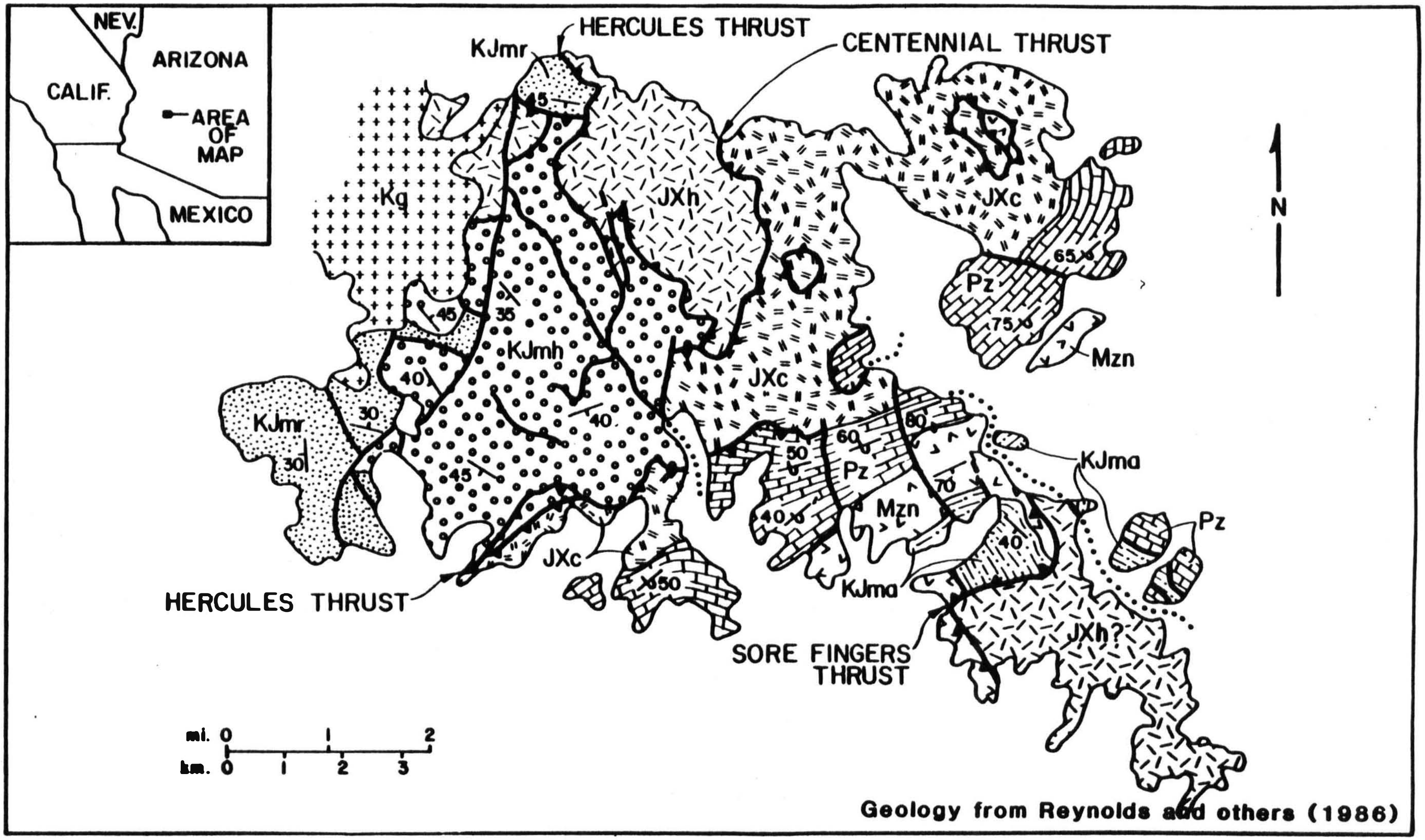

LITTLE HARQUAHALA MOUNTAINS

Map 5

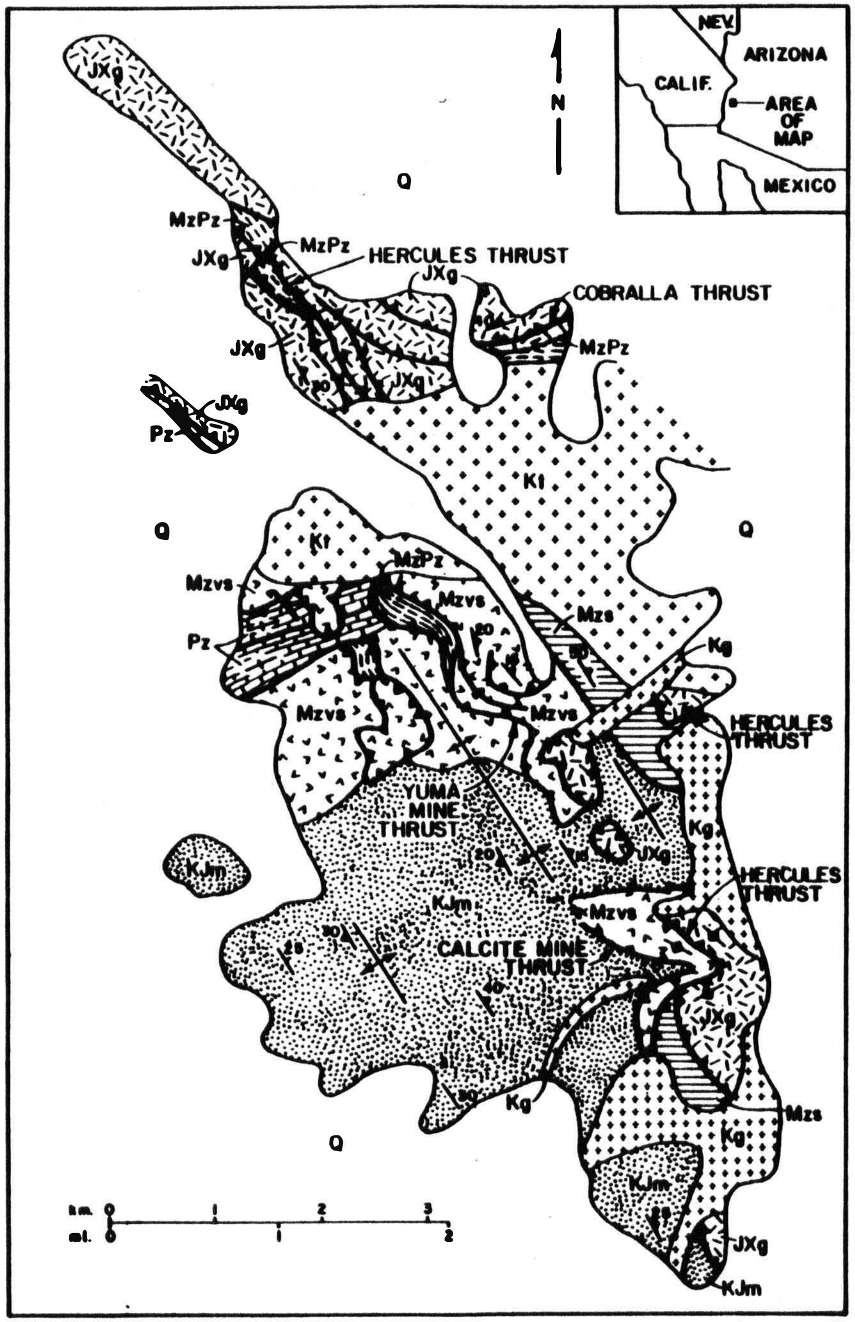

Geology from Reynolds and others (1986)

Q	Quaternary surficial deposits
Kg	Upper Cretaceous Granite Wash Granodiorite
Kt	Upper Cretaceous Tank Pass Granite
KJm	Cretaceous or Jurassic McCoy Mountains Formation
Mzvs	Mesozoic volcanic and sedimentary rocks
Mzs	Mesozoic sedimentary rocks
MzPz	Mesozoic and Paleozoic sedimentary rocks
Pz	Paleozoic sedimentary rocks
JXg	Jurassic granitic rocks and Proterozoic metamorphic and granitic rocks
	contact
	fault
	thrust fault or shear zone
	antiform
30	strike and dip of bedding
40	strike and dip of foliation or cleavage

GRANITE WASH MOUNTAINS

Map 6

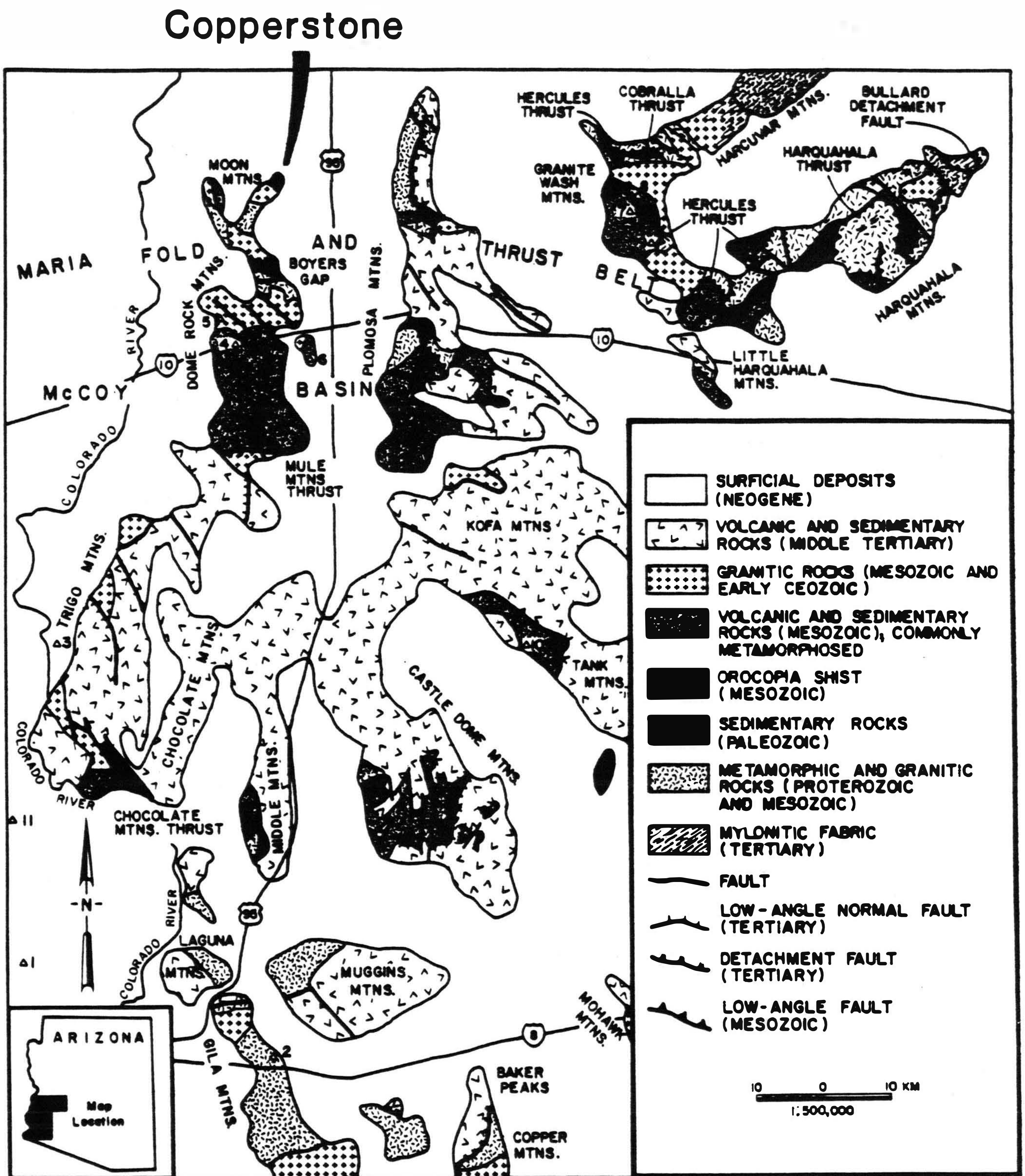

Geology from Arizona Geol. Survey (1988)

GEOLOGY - SOUTHWESTERN ARIZONA

Map 7

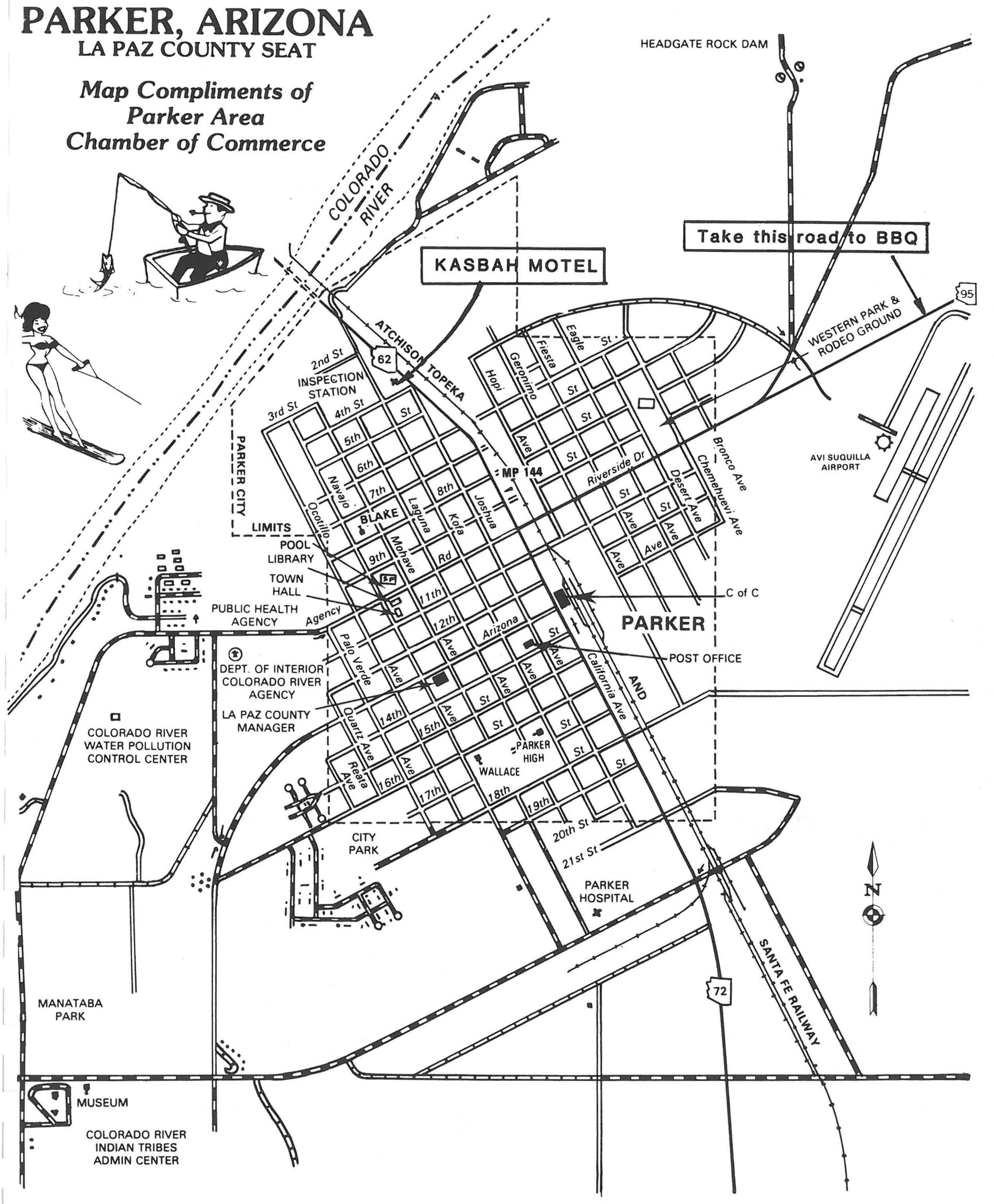
PARKER, ARIZONA
LA PAZ COUNTY SEAT
Map Compliments of Parker Area Chamber of Commerce
COLORADO RIVER
KASBAH MOTEL
Take this road to BBQ
HEADGATE ROCK DAM
WESTERN PARK & RODEO GROUND
95
AVI SUQUILLA AIRPORT
ATCHISON TOPEKA AND SANTA FE RAILWAY
62
2nd St
INSPECTION STATION
3rd St
4th St
5th
6th
7th
8th
9th
11th
12th
14th
15th
16th
17th
18th
19th
20th St
21st St
PARKER CITY LIMITS
Hopi
Geronimo
Fiesta
Eagle St
Ave
St
Riverside Dr
Bronco Ave
Chemehuevi Ave
Desert Ave
MP 144
Navajo
Ocotillo
BLAKE
Laguna
Kofa
Joshua
Mohave
Rd
POOL
LIBRARY
TOWN HALL
PUBLIC HEALTH AGENCY
Agency
C of C
PARKER
Arizona
POST OFFICE
California Ave
Palo Verde
DEPT. OF INTERIOR COLORADO RIVER AGENCY
LA PAZ COUNTY MANAGER
Quartz Ave
Reata Ave
PARKER HIGH
WALLACE
COLORADO RIVER WATER POLLUTION CONTROL CENTER
CITY PARK
PARKER HOSPITAL
72
N
MANATABA PARK
MUSEUM
COLORADO RIVER INDIAN TRIBES ADMIN CENTER

Parker, Arizona - *Some Hi-Lites*

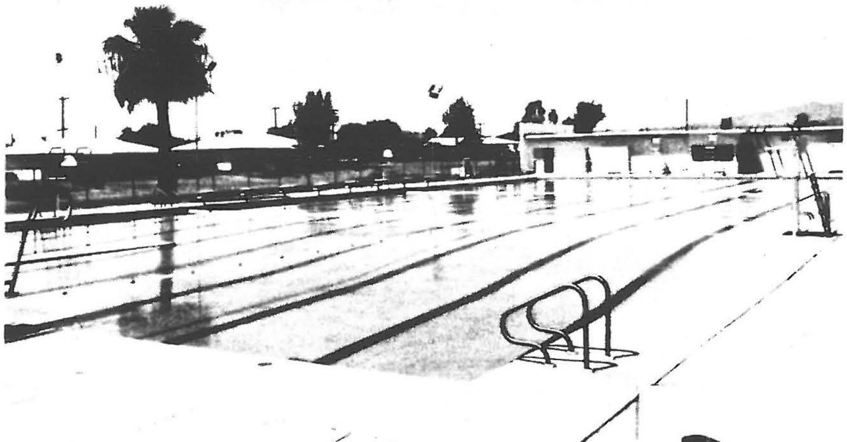

The Town of Parker Olympic size swimming pool is located on Agency Road and Navajo Avenue and is used each year for the Special Olympics Swim meet. Swimming lessons and special programs are a regular part of the summer months. The pool is complimented by Pop Harvey Park on the corner of Agency Road and Mohave Avenue, with a nice picnic area for our many visitors as well as local residents. The Parker Library is located across the street.

New in the area, the Moovalya Plaza Shopping Center is located on Az. 95 (Riverside Drive) just south of the Airport turn-off. Many large firms are located in the Center as well as a number of specialty shops. The Moovalya Plaza Shopping Center is located on Colorado River Indian Tribes Reservation under long term lease.

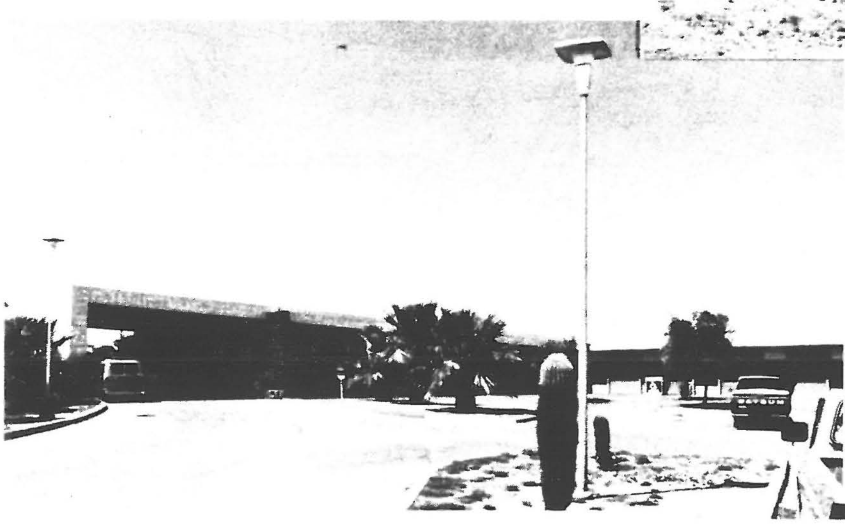

Parker Community Hospital, a 39 bed full service acute care hospital is located on Mohave Road just south of Az. 95-72 (California Avenue). The Parker Community Hospital is a District hospital and is operated under a governing board of 15 local residents from the area the hospital serves. PCH employs approximately 100 people, in addition to Physicians.

The Joshua Street Mall, located directly across the street from the Parker Post Office, on Joshua Street, between Arizona Avenue and 14th Street, features a number of specialty shops, beauty shop, laundromat, fast food, video games, western and childrens shops, camera and film, prescription and drug centers, insurance and others. Conveniently located to the downtown area, with plenty of parking area.

"RIVER FEVER" .... *Catch It!!*

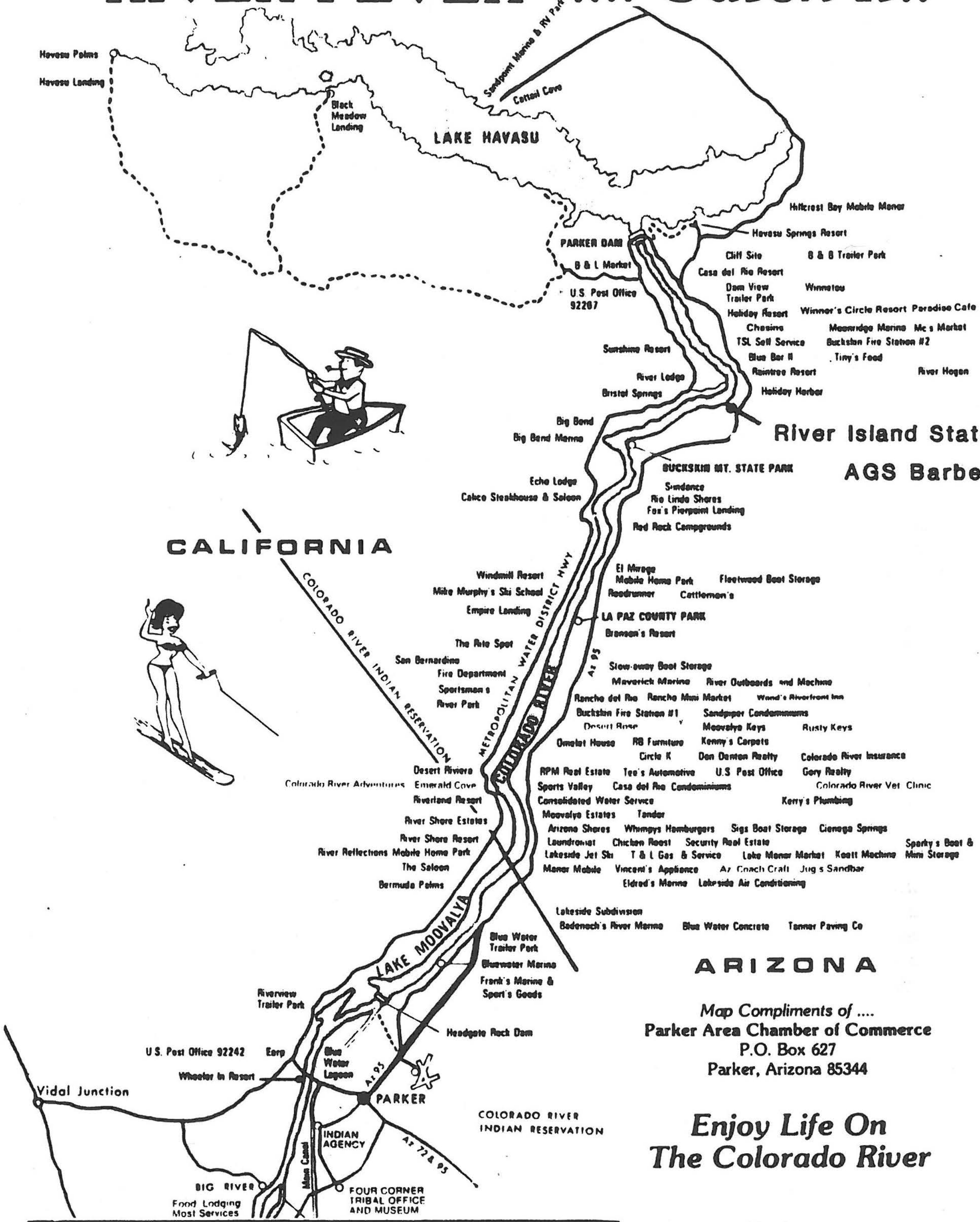

Map Compliments of ....
Parker Area Chamber of Commerce
P.O. Box 627
Parker, Arizona 85344

Enjoy Life On The Colorado River

Visit Us Soon!! We're Not Far Away.

Mileage to the Parker Area:

Orange County	240
Los Angeles	250
Las Vegas	190
Phoenix	170

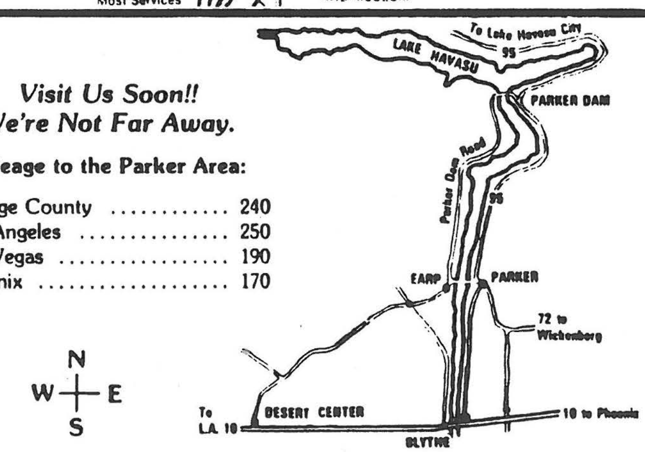

- Hunting
- Fishing
- Family Boating
- Frogging
- Swimming
- Picnicking
- Rock Hunting
- Boat Racing
- Camping
- Water Skiing
- Road Racing
- Retirement Living
- Square Dancing

River Island Unit Facilities

* 22 Campsites with Water
* 8 Tent Sites without Hookups
* Shower and Rest Room Facilities
* Sanitary Dump Station
* Boat Launch Area
* Group Day Use Area with Fire Pit
* Shaded Ramada for Group Use
* River Island Market - Groceries, Tackle, Fishing Licenses and Swimwear

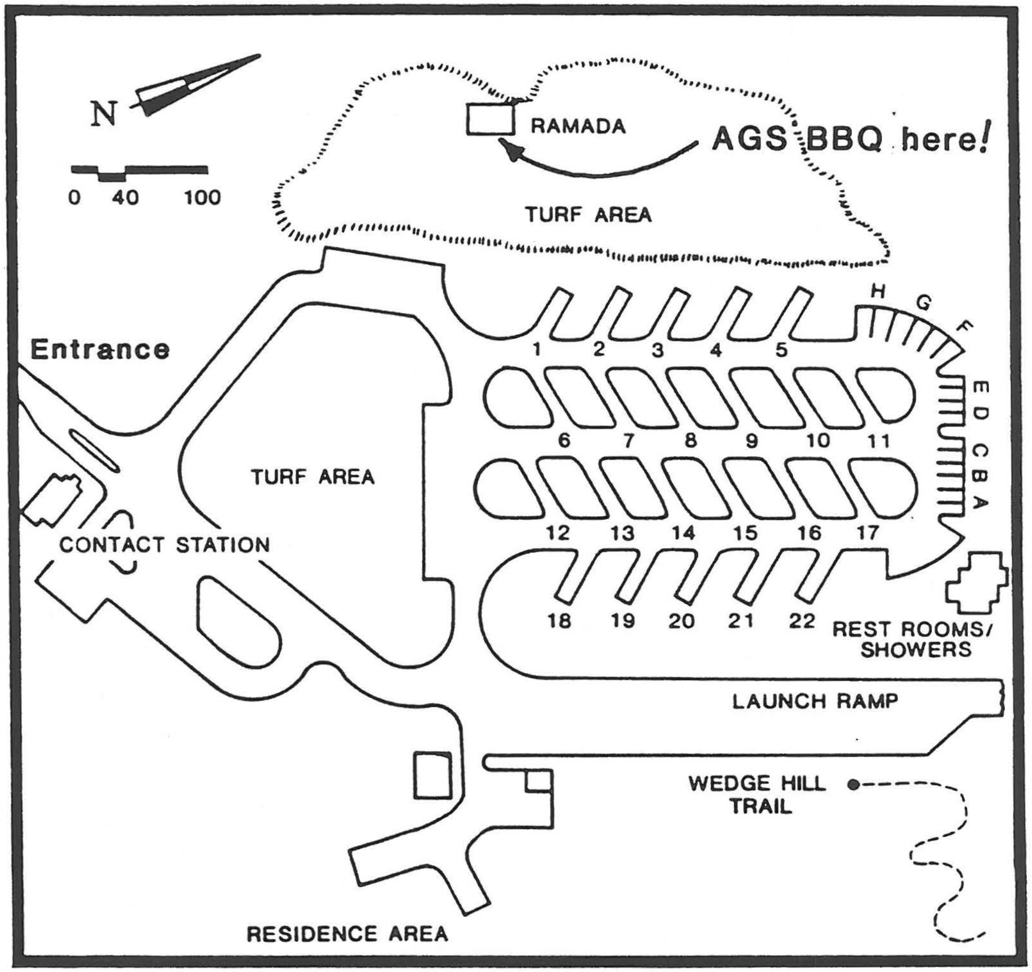

FIELD TRIP

HANDOUTS

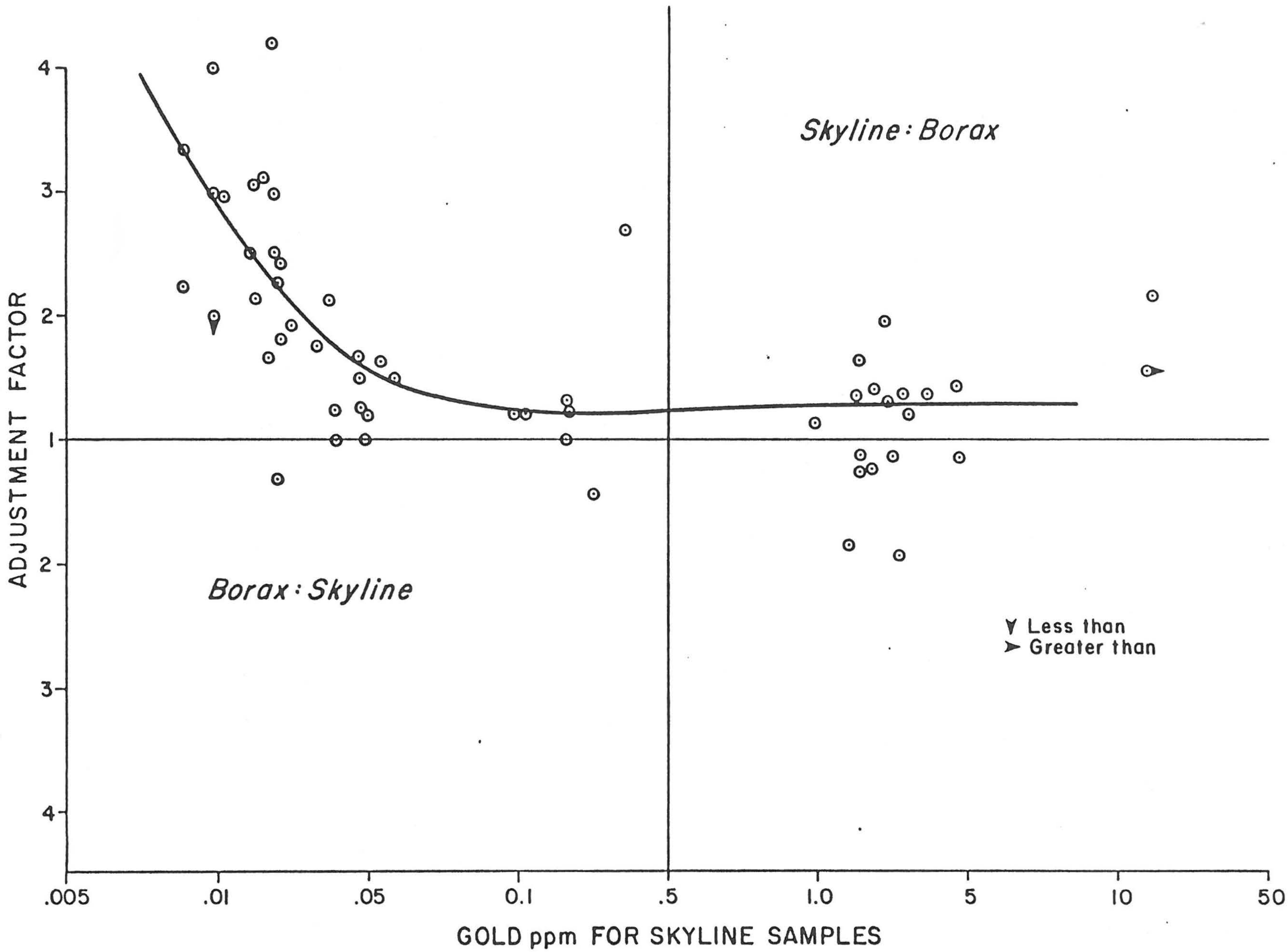

Figure 32. Variation diagram showing factors to adjust Skyline Laboratory atomic absorption data to U.S. Borax Laboratory fire assay data.

The depth of Block D, which contains Hill 2462, was taken as 450 feet with the additional 100 feet added because of higher elevations in the hill. Plan dimensions of Block F were taken from the maps and the vertical dimension of 20 feet was taken from intercepts in the GH-1 drill hole and from estimated heights of stopes within the old Socorro Mine workings. All of the above information is summarized in Table 15.

Total gold content, gold grade, and dollar value of gold within each block was calculated according to three models (Table 15). The first calculation (Model 1) assumed a conservative model where average gold values derived from Skyline Laboratory's analytical data were assumed to represent true surface values and do not increase with depth. The second model (Model 2) assumed that the Skyline Laboratory analytical data is systematically low by a factor of 1.3 (See section on Verification of Gold Grade), and that there was no increase in grade with depth. The third and most optimistic model (Model 3) assumed the average gold values from Skyline Laboratory were low by a factor of 1.3 and therefore had to be adjusted upward as in Model 2 and also assumed the gold grades increased with depth by a factor of 2 (See section on Possible Variations of Gold Content with Depth).

Dollar values for all models in Table 15 were calculated at a gold price of $450/oz. Gold contents and dollar values at various gold prices for various combinations of blocks and economic models are shown in Table 16. From present data the silver content within the Socorro Reef gold anomaly is too low to be of economic interest (Table 17). The total indicated silver value for all blocks within the Socorro Reef gold anomaly is only $2,300,000; this is 79 times less than the dollar value of gold. The above numbers for silver assumed a gold:silver ratio of 1.77 over the Socorro Reef gold anomaly and a gold:silver price ratio of 45:1.

Model 1 is clearly the most conservative of the three models and probably is too conservative because of the analytical technique used to obtain the gold values. Model 2 is perhaps the most realistic of the three models given what is <u>currently</u> known about the Socorro Reef gold anomaly. If it is assumed (and this is a sizeable assumption) that the SAD-1 drill hole represents a fair test of gold grades with depth, then a significant increase in depth from surface values is not predicted. The SAD-1 drill hole data is reinforced with the induced polarization (IP) data, which suggests the sulfide-bearing material is fairly evenly distributed throughout the quartzite portion of the Socorro Reef gold anomaly and does not increase with depth.

However, there are substantial reasons to question the Model 2 assumptions. First, one drill hole is probably not representative. Second, as outlined in the previous section on Variations in Gold Content with Depth, gold grades within the SAD-1 drill hole do increase slightly with depth. The lower 100 feet of the hole averaged 0.0155 oz gold/Ton based on 40 5-foot composite samples of drill cuttings, whereas surface samples within Block C average 0.0123 oz gold/Ton based on 44 samples. This latter number is very close to the average grade (0.012 oz gold/Ton) for 40 composite samples from the upper 100 feet of the SAD-1 drill hole.

Table 15: Gold Grade and tonnage information for various gold-bearing blocks within the Socorro Reef gold anomaly

ECONOMIC PARAMETERS	BLOCK						
	A	B	B high grade	C	D	E	F
Map Dimensions (feet)	250 x 200	725 x 275	725 x 130	550 x 250	940 x 325	875 x 500	250 x 375
Depth extension (feet)	350	350	350	350	450	350	20
Number of surface samples	14	64 (.023)	37 (.035)	44 (.0123)	41	23	9 (.0144)
Number of subsurface samples	-	16 (.012) (from adit)	16 (.012) (from adit)	40 (.0138) (from SAD-1)	-	-	11 (.23)
Number of surface and subsurface samples	14	80	53	84	41	23	23
Average gold grade from subsurface and surface data (oz/ton)	.0041	.021	.028	.013	.0113	.0056	.138
Standard deviation (oz/ton)	.006	.0415	.0491	.0166	.0156	.0114	.284
Tonnage (short tons)	1,458,000	5,815,000	2,749,000	4,010,000	11,456,250	12,760,000	156,250
Total gold content (oz)	5,978	122,115	76,972	52,130	129,453	71.456	21,562
Dollar value (@ $450/oz)	2,690,000	54,952,000	34,637,000	23,458,000	58,354,000	32,155,000	9,703,000
	* (1.84)	(9.45)	(12.60)	(5.85)	(5.09)	(2.52)	(62.20)
RECALCULATION OF ABOVE ASSUMING GOLD GRADE ADJUSTMENT FROM BORAX DATA (Model 2)							
Average gold grade of all data (oz/ton)	.0053	.0273	.0363	.016	.0147	.0073	.179
Total gold content (oz)	7,727	158,750	99,789	64,160	168,403	73,148	27,969
Dollar value (@ $450/oz)	3,477,150	71,437,000	44,905,000	28,872,000	75,781,000	41,917,000	12,586,000
	* (2.38)	(12.28)	(16.34)	(7.20)	(6.61)	(3.28)	(80.68)
RECALCULATION OF ABOVE ASSUMING INCREASE IN GOLD GRADE WITH DEPTH (Model 3)							
Average gold grade of lower 1/2 of block (oz/ton)	.0106	.0546	.0726	.032	.0294	.0146	
Tonnage of lower 1/2 of block	729,000	2,907,500	1,374,500	2,005,000	5,728,125	6,380,000	
Gold content of lower 1/2 of block	7,700	150,700	99,800	64,200	168,400	93,200	
Average gold grade of upper 1/2 of block (oz/ton)	.0041	.021	.028	.013	.0113	.0056	
Tonnage of upper 1/2 of block	729,000	2,907,000	1,374,500	2,005,000	5,728,125	6,380,000	
Average gold grade of entire block (oz/ton)	.008	.0409	.0543	.024	.022	.011	
Gold content of upper 1/2 of block (ounces)	3,900	79,400	49,500	32,100	84,200	46,600	
Total gold content of block (ounces)	11,600	238,100	149,300	96,200	252,600	139,800	
Dollar Value (@ $450/oz)	5,215,000	107,000,000	67,000,000	43,000,000	113,000,000	63,000,000	
	* (3.57)	(18.40)	(24.37)	(10.72)	(9.86)	(4.94)	

* Number in parenthesis is gold value in dollars per ton.

Table 16: Gold content and Dollar value combinations of various blocks

ECONOMIC PARAMETERS	B + C Model 1	B + C Model 2	B + C Model 3	B + C + D Model 1	B + C + D Model 2	B + C + D Model 3
Tonnage (millions of short tons)	9.825	9.825	9.825	21.281	21.281	21.281
Gold Grade (oz/ton)	.018	.023	.034	.0143	.0184	.0276
Gold Content (oz)	174,245	222,910	334,300	303,698	391,313	586,900
Dollar Value						
@ 400/oz	70,000,000 * (7.12)	89,000,000 (9.06)	134,000,000 (13.64)	121,000,000 (5.71)	157,000,000 (7.40)	235,000,000 (11.08)
@ 450/oz	78,000,000 * (7.94)	100,000,000 (10.18)	150,000,000 (15.27)	137,000,000 (6.46)	176,000,000 (8.30)	264,000,000 (12.45)
@ 500/oz	87,000,000 * (8.85)	111,000,000 (11.30)	167,000,000 (16.99)	152,000,000 (7.17)	195,000,000 (9.20)	293,000,000 (13.82)
@ 600/oz	105,000,000 * (10.69)	134,000,000 (13.64)	201,000,000 (20.46)	182,000,000 (8.58)	235,000,000 (11.08)	352,000,000 (16.60)

ECONOMIC PARAMETERS	B+C+D+F Model 1	B+C+D+F Model 2	B+C+D+F Model 3	A+B+C+D+E+F Model 1	A+B+C+D+E+F Model 2	A+B+C+D+E+F Model 3
Tonnage (millions of short tons)	21.437	21.437	21.437	35.655	35.655	35.655
Gold Grade (oz/ton)	.0152	.0192	.0284	.0113	.0144	.0213
Gold content (oz)	325,260	412,875	608,462	402,694	513,750	759,862
Dollar Value						
@ 400/oz	130,000,000 * (6.06)	165,000,000 (7.69)	243,000,000 (11.33)	161,000,000 (4.51)	205,500,000 (5.76)	304,000,000 (8.61)
@ 450/oz	146,000,000 * (6.81)	185,000,000 (8.63)	273,000,000 (12.73)	181,000,000 (5.08)	231,000,000 (6.48)	342,000,000 (9.59)
@ 500/oz	162,000,000 * (7.56)	206,000,000 (9.61)	304,000,000 (14.18)	201,000,000 (5.64)	257,000,000 (7.21)	380,000,000 (10.66)
@ 600/oz	195,000,000 * (9.10)	247,000,000 (11.52)	365,000,000 (17.03)	242,000,000 (6.79)	308,000,000 (8.64)	456,000,000 (12.79)

* Number in parenthesis is gold value in dollars per ton.

Table 17: Economic data for silver within the Socorro Reef Gold Anomaly

ECONOMIC PARAMETERS	Block						
	A	B	B high grade	C	D	E	F
Gold grade (oz/Ton)	.0041	.021	.028	.013	.0113	.0056	.138
Silver grade (oz/Ton)*	.0023	.012	.016	.0073	.0064	.0032	.078
Tonnage (short ton)	1,458,000	5,815,000	2,749,000	4,010,000	11,456,000	12,760,000	156,250
Total Silver (oz)	3,353	69,780	43,984	29,273	73,139	40,370	12,182
Dollar Value (@ 10./oz)	33,534	697,800	439,840	292,730	731,390	403,700	121,820

Total Silver in dollars
$2,291,000

* Calculated assuming a gold:silver ratio of 1.77 (based on 1904-1934 Socorro Mine production)

Third, the induced polarization (IP) data discussed in the geophysics section is not resolved enough to identify small tonnage zones (about 200,000 tons or less) that contain higher sulfide-bearing zones which are presumably more gold rich, even though the method does generally identify a zone of moderately intense, apparent polarization within the quartzite-granite blocks. Fourth, Model 2 assumes that no high-grade, bonanza pockets are present within Blocks A-E. Even one bonanza pocket, like the one encountered in the 'Castle Garden' stope within the Bolsa Quartzite at the Harquahala Mine in the Little Harquahala Mountains, would substantially increase the overall gold content of the Socorro Reef gold deposit. As outlined in the previous section on Variation in Gold Content with Depth, there are substantial geologic reasons (by analogy with the high-grade material within the Golden Eagle thrust at the old Socorro Mine) to expect an increase in gold content with depth towards the Golden Eagle thrust. The presence of high-grade bonanza pockets, the presence of intermediate-tonnage, moderate-grade gold zones (0.08 to 0.12 oz/ton), and the overall increase in grade with depth are all taken into consideration in Model 3. Because the removal of the large tonnages that are involved would considerably dilute the effect of bonanza pockets and moderate-tonnage, higher grade zones, the overall factor by which the grade can be reasonably expected to increase above surface grades is taken to be a factor of two or double the known surface grades. This increase is projected for the lower one half or the lower 175 feet of Blocks A-E. Economic aspects of Models 1, 2, and 3 are shown in Tables 15 and 16.

The summation of all data for Blocks A-F (Table 16) reveals that in the moderately anomalous portion of the Socorro Reef gold anomaly there is an indicated tonnage of 35.6 million tons with an average grade (using Model 3 assumptions) of 0.0213 oz gold/Ton. At $450/oz, and using Model 3 assumptions, this amounts to a total of $342,000,000 of gold with a gold value of $9.59/Ton. It is clear from Tables 15 and 16, however, that the average gold grade quoted above is not evenly distributed over all blocks; within the moderately anomalous granite and quartzite blocks, Blocks B, C, D, and F have substantially higher grades and constitute an attractive gold target with an indicated 21.4 million tons of potential gold ore. Of these, Blocks B and C are the most economically attractive.

From the existing data the Blocks with the most potential for mining are Blocks B, C, and F and a 'high-grade' subblock within Block B containing an indicated 2.75 million tons comprises the most attractive possibility. With Model 2 assumptions, the indicated surface grade for this subblock is 0.036 oz gold/Ton, which is comparable to gold grades of cyanide heap leach properties in Nevada that were operating in 1979 (See Table 18). With Model 3 assumptions for this higher grade subblock of Block B, the average indicated gold grade for this ground increases to 0.054 oz gold/ton, which is very close to the grade of most of the properties listed in Table 18. Obviously, Block B should be given the highest priority for confirmation drilling. Several larger tonnage targets within the Socorro Reef gold anomaly are also attractive, particularly a 9.8 million ton block that comprises Blocks B and C. This block of ground contains $100,000,000 of gold (using Model 2 assumptions) or $150,000,000 of gold (using Model 3 assumptions) (See Table 16). The 0.034 oz/Ton grade of this block (using Model 3 assumptions) is similar to the grades of producing properties at Windfall, Cortez, and Gold Acres

Table 18: Comparison of Socorro Reef with other disseminated, low-grade gold deposits in the western United States

Deposit	Tons (short)	Gold Grade (oz/ton)	Gold Content Dollars/ton (@ $450./oz)	Mining Costs Dollars/ton (pre-tax)	Recovery Method	Reference
Ortiz, New Mexico	6,841,000	.053	23.85	9.84 (mid-1981 total mining, processing and administrative cost)	Cyanide Heap-Leach	Hickson (1981)
Carlin, Nevada	9,370,000 (1965-77 Production)	.32	144.07	37.20 (Nov. 1981)	Milling	Mining Record (Nov. 1981)
Bootstrap, Nevada		.063 #1 heap .028 #2 heap		1.67 direct (1979) costs	Cyanide Heap-Leach	McQuiston & Shoemaker (1980)
Cortez, Nevada	422,000 tons/year	.036	16.20	1.22 (1979)	Cyanide Heap-Leach	McQuiston & Shoemaker (1980)
Gold Acres, Nevada	907,000 tons/year	.036	16.20	1.22 (1979)	Cyanide Heap-Leach	McQuiston & Shoemaker (1980)
Round Mtn, Nevada		.06	27.00	5.32 (1979 direct and administrative)	Cyanide Heap-Leach	McQuiston & Shoemaker (1980)
Windfall, Nevada	220,000 tons/year	.028	12.60	3.93 (1980 mining and processing costs)	Cyanide Heap-Leach	McQuiston & Shoemaker (1980)
Socorro Reef, AZ						
B+C+D+F Model 3	21,437,000	.0284	12.73			
B+C+D+F Model 2	21,437,000	.0192	8.63			
B+C Model 3	9,825,000	.034	15.27			
B+C Model 2	9,825,000	.023	10.18			

in Nevada (Table 18). Grade continuity and a slight increase in grade

with depth for Blocks B and C have already been tested to some degree by the SAD-1 drill hole in Block C. If Block D is added to the Block B and C package, the indicated tonnage increases to over 21 million tons and (using Model 3 assumptions) contains $264,000,000 of gold at $450/oz. However, mining costs within Block D would be substantially higher because of the additional waste material that would have to be removed from Hill 2462 to gain access to the mineralized quartzite block. Thus, drilling confirmation should be acquired first for Blocks B and C. The high-grade ground within Block F is too low in tonnage to justify an open cut mine by itself. However, high grade portions of this ground could be blended with lower grade rock in Blocks B and C to obtain higher and more evenly distributed gold grades for recovery purposes. Blocks A and E, while containing about 14 million tons of gold-bearing material, do not contain high enough grades to justify drilling confirmation at this time.

From Table 18 it can be seen that pre-tax operating costs per ton for various, recently operating, open-cut gold mines in the southwestern U.S. are substantially lower than the overall dollar value of gold content per ton of ore mined by at least a factor of 3. As can be inferred from the table this factor can be considerably influenced by the price of gold, so that one would like the difference between actual gold content and cost of mining to be as high as possible. It should be noted that the Windfall Mine, which has the lowest grade of the operating properties in Table 18, closed in 1981 when the price of gold fell below $350/oz, but is expected to open soon as the price of gold has now been consistently above $400/oz. Therefore, the difference between gold content and pre-tax operating costs at Socorro Reef gold deposit should consistently be greater than 2.5 to 1 before the Socorro Reef gold deposit could be brought into profitable production. At a gold price of $450/oz a 2.5 to 1 ratio of gold value to cost of production seems viable for Blocks B, C, D, and F using Model 3 assumptions, for Blocks B and C using Model 3 assumptions, for Block B using either Model 2 or Model 3 assumptions, and for the 'high-grade' subblock within Block B using Model 1, 2, or 3 assumptions. Thus, based on present data, Block B at the surface is comparable to producing, open-cut, heap-leach, gold operations elsewhere and could be brought into production if drilling confirmed the surface grades to depth. Blocks B and C could be brought into production if drilling substantiates Model 3 assumptions or if the price of gold increases to and remains above $550/oz. Thus, about 10 million tons of ground within the Socorro Reef gold deposit is commercial pending drilling confirmation of Model 3 assumption, and is commercial as it stands if the price of gold increases to and remains over $550/oz and mining costs do not escalate.

Conclusions and Recommendations

Geologic, geochemical, and geophysical data presented in Part II strongly suggest the inference that the Socorro Reef gold anomaly is the surface expression of a large-tonnage, low-grade, disseminated gold deposit. Economic evaluation of all available surface data using optimistic, but reasonable, geologic assumptions (Model 3) suggest that about 760,000 ounces of gold (0.0213 oz of gold/Ton) are contained within 35.6 million tons of gold-bearing material in six blocks (Figure 26). At a gold price of $450/oz the above material contains $342,000,000 of gold. Under present economic conditions about 10 million tons of gold-bearing rock in Blocks B and C are commercial pending drilling confirmation of gold grades with depth. The estimated value of gold in the 10 million ton block using Model 3 assumptions is about $150,000,000. If economic conditions improve slightly, that is, if the price of gold increases to and remains over $500/oz, then another 11 million tons of gold-bearing rock can be added to the 10 million tons described above and the net worth of the Socorro Reef gold deposit would increase to about $293,000,000.

It is recommended that drilling priority be given to Blocks B and C with the objective of confirming and hopefully increasing gold grades in ground beneath surface exposures of these blocks. A fair test of these blocks would consist of five shallow drill holes (fully cored) of 500 feet each to obtain subsurface information on gold grades beneath Blocks B and C. At a cost of $20/foot this amounts to about $50,000 of drilling. Supportive geochemical work should consist of gold, silver, and tungsten assays for every 10-foot interval of core; this amounts to approximately $2750.00 of analytical work. Some of the holes should be angled across the width of the exposed gold anomaly in order to obtain information about gold grades in representative cross sections. At this time, no new surface information is required because abundant data has already been obtained from previous surface sampling programs conducted by the various major mining companies. The recommended drilling work can be done by Socorro Mining Corporation under my supervision or by one of the major mining companies currently interested in the property. This work could easily be done within six to nine months of the lease date. It is recommended that the confirmatory drilling be done as soon as possible by either Socorro Mining Corporation or a mining company lease-partner, because the economic climate is becoming increasingly favorable for development of low-grade, disseminated gold deposits. With many major mining companies now directing their exploration programs toward such targets, the Socorro Reef gold deposit is now a prime exploration target.

Acknowledgments

The entire report presented herein was prepared within three and one-half weeks, a considerable achievement. Completion of this report would have been impossible without the cooperation and support of several people who spent many overtime hours doing word processing, editing, drafting, collating, layout, typing, etc. These people deserve special mention. Susan Angelon, in particular, organized and supervised most of the graphic design, layout, and drafting for the text with its many plates, figures, and gatefolds. She was ably assisted by Chris Smith and Susanne Baker who drafted many of the figures and plates and by Thelma J. MacArthur (Mac) who spent many overtime hours providing superb hand coloring for all of the figures and plates. Jan Wilt, one of my colleagues helped with the word processing and provided invaluable editorial assistance and last minute assembly help. Pat Pileggi did an admirable job of word processing, which also included many hours of overtime. Supplemental typing help was also provided by Christine Dodson. Finally, Socorro Mining Corporation is gratefully acknowledged for its support during the entire Socorro Reef gold project. With a little more perseverence, Socorro Reef could well become a profitable gold mine.

List of References

Hickson, R. J., 1981, Heap leaching practices at Ortiz Gold Mine, Santa Fe County, New Mexico: Soc. Min. Eng. of AIME, Preprint No. 81-347, 14p.

Keith, S. B., and Reynolds, S. J., 1980, Geochemistry of Cordilleran metamorphic core complexes; Chapter 4, in Coney, P. J., and Reynolds, S. J., eds., Uranium favorability of Cordilleran metamorphic core complexes: Dept. of Energy (DOE) report GJBX-80-

Keith, Stanley B., Reynolds, Stephen J., and Richard, Stephen M., 1981, Laramide thrust-fault sandwich in the Salome region, west-central Arizona, in Keith, S. B., and others, eds., Low-angle tectonic phenomena between Tucson and Salome, Arizona: Arizona Bureau of Geology and Mineral Technology, Open-file Report 81-2, 114 p.

Keith, Stanton B., 1978, Index of mining properties of Yuma County, Arizona: Ariz. Bureau of Geology and Mineral Technology, Bull. 192, 185 p.

Laskey, S. G., and Webber, B. N., 1949, Manganese resources of the Artillery Mountains region, Mohave County, Arizona: U. S. Geol. Survey Bull. 961, 86 p.

McQuiston, J. R., and Shoemaker, R. S., 1980, Gold and silver cyanidation plant practice, v. 2: AIME, 263 p.

Rehrig, W. A., and Reynolds, S. J., 1980, Geologic and geochronologic reconnaissance of a northwest-trending zone of metamorphic core complexes in southern and western Arizona: Geological Soc. of America Memoir 153, p. 131-157.

Reynolds, S. J., 1980, Geologic framework of west-central Arizona: Arizona Geological Soc. Digest, v. 12, p. 1-16.

Reynolds, Stephen J., 1982, Multiple deformation in the Harcuvar and Harquahala Mountains, west-central Arizona, in Frost, E. G., and Martin, D. L., eds., Mesozoic-Cenozoic tectonic evolution of the Colorado River region, California, Arizona, and Nevada: Cordilleran Publishers, San Diego, CA, p. 137-142.

Reynolds, Stephen J., Keith, Stanley B., and Coney, Peter J., 1980, Stacked overthrusts of Precambrian crystalline basement and inverted Paleozoic sections emplaced over Mesoaoic strata, west-central Arizona: Arizona Geological Society Digest, v. 12, p. 45-51.

Richard, Stephen M., 1982, Preliminary report on the structure and stratigraphy of the southern Little Harquahala Mountains, Yuma County, Arizona, in Frost, E. G., and Martin, D. L., eds., Mesozoic-Cenozoic tectonic evolution of the Colorado River region, California, Arizona, and Nevada: Cordilleran Publishers, San Diego, CA, p. 235-244.

Shackelford, T. J., 1980, Tertiary tectonic denudation of a Mesozoic-early Tertiary(?) gneiss complex, Rawhide Mountains, western Arizona: Geology, v. 8, p. 190-194.

Shafiqullah, M., and others, 1980, K-Ar geochronology and geologic history of southwestern Arizona and adjacent areas: Arizona Geological Society Digest, v. 12, p. 201-260.

Varga, R. J., 1976, Stratigraphy and superposed deformation of a Paleozoic and Mesozoic sequence in the Harquahala Mountains, Arizona: unpub. M.S. thesis, Tucson, Univ. of Arizona, 61 p.

Varga, Robert J., 1977, Geology of the Socorro Peak area, western Harquahala Mountains: Arizona Bureau of Geology and Mineral Technology, Circular 20, 20 p.

Wilson, E. D., 1960, Geologic map of Yuma County, Arizona: Tucson, Arizona Bureau of Mines, scale 1:375,000.

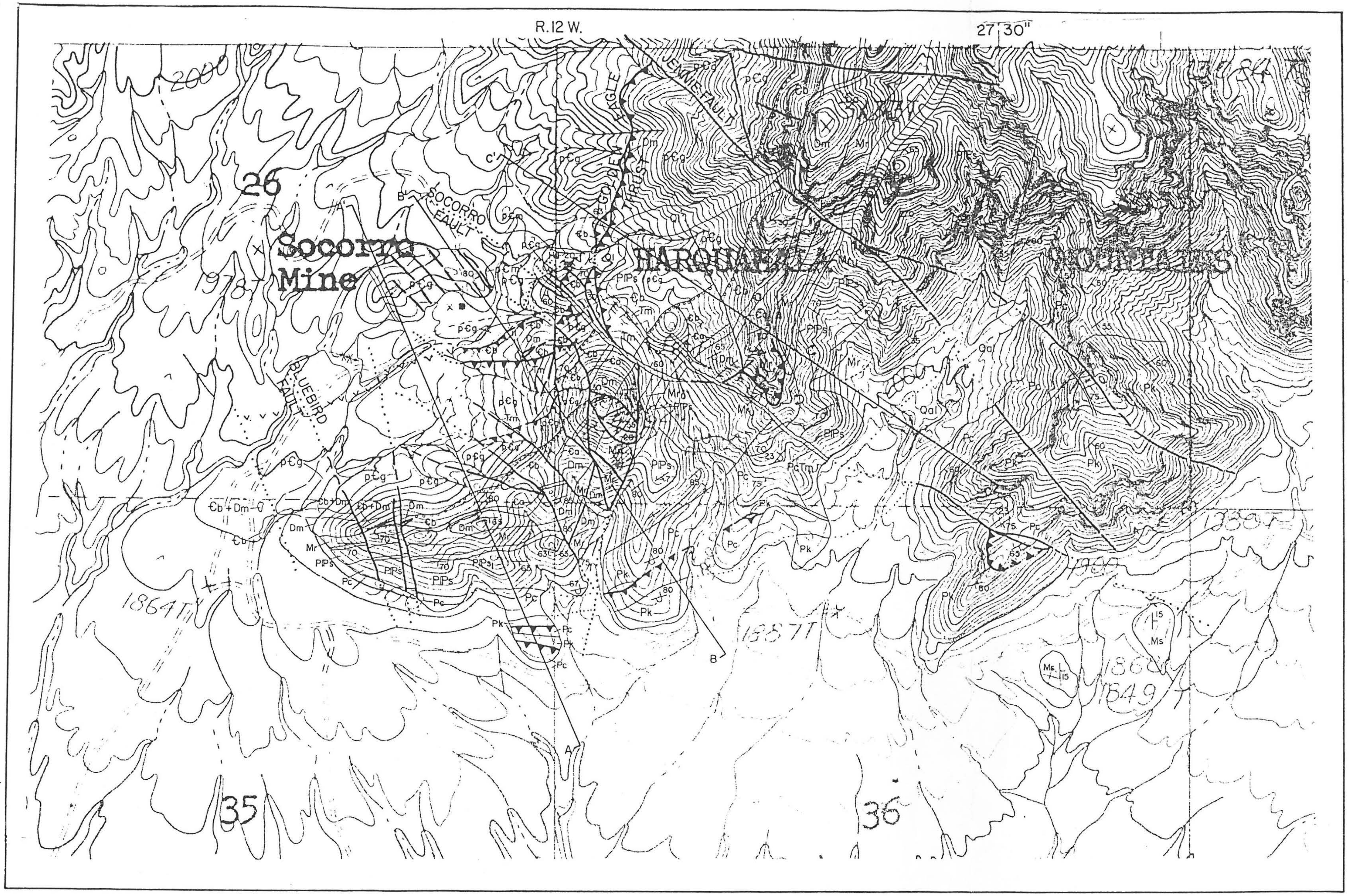

EXPLANATION

ROCKS

Hd	Mine dump
Qal | Ql	Qal-surface alluviums; Ql-landslide and/or debris flow materials
Tm	microdiorite dikes
Ms	undifferentiated clastic sedimentary rocks
Pk	Kaibab Formation
Pc	Coconino Formation
PIPs	Supai Formation
$PIPs_l$	Supai Formation-lower red shale member
Mr | Mr_u	Mr-Redwall Formation; Mr_u-upper cherty carbonate member of Redwall Formation
Dm	Martin Formation
Ꞓa	Abrigo Formation
Ꞓb	Bolsa Quartzite-small circles show basal conglomerate
pꞒg	porphyritic biotite granite (probably 1.4 b.y. old); locally contains K-feldspar megacrysts
pꞒm	alaskitic muscovite granite (probably 1.4 b.y. old)

STRUCTURE

80 — lithological contact; dashed where approximated, dotted where concealed, dip shown where measured

65 — faults dashed where approximated, dotted where concealed, dip shown where measured

15 — thrust fault (barbs on upper); dashed where approximated, dotted where concealed, dip shown where measured

trace of anticline showing plunge where observed

trace of shallowly inclined or recumbent fold showing plunge where observed

60 strike and dip of bedding

60 strike and dip of overturned bedding

N

GEOLOGIC MAP OF THE SOCORRO REEF GOLD ANOMALY, WESTERN HARQUAHALA MOUNTAINS YUMA COUNTY, ARIZONA

500 0 500 1000 Feet

Scale 1" = 500'

CONTOUR INTERVAL - 20 feet

Portion of Preliminary 7.5' Lone Mtn. Quad

NOVEMBER 1982

by STANLEY B. KEITH